COALBED GAS ORIGIN AND DISTRIBUTION

IN THE SOUTHEASTERN ILLINOIS BASIN

Dariusz Strąpoć

Coalbed gas origin and distribution in the southeastern Illinois Basin
Dariusz Strąpoć

Accepted by the Graduate Faculty, Indiana University, in partial fulfillment of the
requirements for the degree of Doctor of Philosophy

Doctoral Committee:

_____

Arndt Schimmelmann, Ph.D. (co-chair)

_____

Maria Mastalerz, Ph.D. (co-chair)

_____

Flynn Picardal, Ph.D. (Minor Advisor)

_____

Erika Elswick, Ph.D.

October 19th, 2007

Abstract

Coal seams worldwide contain biogenic methane that in some coal basins forms easily accessible and large amounts of coalbed methane (CBM). Economically important biogenic CBM occurs not only in coals of low rank but also in higher rank coals where uplift and brine dilution initiated microbial methanogenesis. Distributions and compositions of gases in biogenic systems are governed by numerous factors including salinity, microbe-accessible porosity, and coal permeability. In contrast, thermogenic gas systems are primarily controlled by coal rank and depth. Determination of gas origin is, therefore, critical for a successful exploration strategy.

This study employs geochemical, stable isotopic, and microbiological techniques to investigate the distribution and the origin of coalbed gases in the southeastern Illinois Basin. Our results suggest that high permeability and shallow (100-250 m) depths of Indiana coals allowed their inoculation with a methanogenic microbial consortia, thus leading to widespread and abundant microbial methane generation along the eastern marginal part of the Illinois Basin. Consequently, high volatile bituminous C Indiana coals with a vitrinite reflectance $R_o \sim 0.6\%$ contain significant amounts of coal gas (~3 cm^3/g, 96 scf/t) with $\geq$ 97 vol.% of microbial methane. In contrast, deeper (>300 m) and more mature (high volatile bituminous A) coals in a tectonically active zone in the western Kentucky part of the basin contain gases of distinctly thermogenic origin.

Enrichment experiments and phylogeny of the microbial community responsible for generation of coalbed methane in the Indiana part of the Illinois Basin imply that coal organic matter was biodegraded by a complex microbial consortium to form simple molecules, such as H_2 and CO_2, that fuel methanogenesis. 16S rRNA analyses of both *in-*

situ microbial communities and methanogen enrichments indicate that *Methanocorpusculum* is the dominant genus responsible for biogenic CBM formation.

Table of contents

List of Figures

Fig. 4. Carbon isotopic differences between individual methane measurements and the weighted mean value for each canister (based on off-line data from six desorption canisters from which gas was vented on daily basis). The weighted mean is represented by the horizontal zero line. Thick horizontal lines represent average values for three desorption intervals. The average $\delta^{13}C$ value for the 33 to 66% desorption interval (grey rectangle) most closely approximates the overall weighted mean value (zero line).

Fig. 5. $\delta^{13}C_{CH4}$ values for coal sample II-3/5. Desorbed gas volumes were measured, sampled, and vented only six times, allowing at least seven days of equilibration between consecutive measurements. Dotted line represents weighted mean $\delta^{13}C$ value of the entire methane volume.

Fig. 6. Changes of $\delta^{13}C_{CO2}$ versus changes in CO_2 content (A) and versus $\delta^{13}C_{CH4}$ (B) during coal gas desorption from coal sample V-3/1. Numbers in brackets indicate the percent of total CO_2 desorbed at the time of sampling. Dashed lines guide the eye along paths of desorption.

Fig. 7. A - Histogram depicting the timing of midpoint gas desorption from 31 canisters using Illinois Basin Pennsylvanian coals; B – Dependence of timing of desorption mid-point on the total desorbed gas (final volume, obtained when desorption ceases, usually after three months) for 19 canisters using Seelyville coal. The solid line is a 2nd order polynomial regression.

Fig. 8. Relationships between measured cumulative gas volumes after 5 or 10 days of desorption and total desorbed gas. These relationships can be used to predict total gas volume via extrapolation of shorter-term initial desorption measurements. The data are based on over 30 canister samples from Illinois Basin Pennsylvanian coals.

Fig. 9. Changes in $\delta^{13}C$ of CH_4 over the first two weeks of coal gas desorption from coals of various maturities. Rectangular fields represent ranges of data (R_o and $\Delta\delta^{13}C$) provided in the literature.

Fig. 10. Genetic classification of coalbed gases with three distinguishable fields, according to Smith and Pallasser (1996). The filled diamond (♦) indicates the average for Seelyville coal gas. Symbol size relates to the typical analytical error. The rectangle around the symbol relates to the expected desorption-related isotopic variance in $\delta^{13}C$ of CH_4 and CO_2.

Chapter 4

Fig. 1. Study area: (a) map of Springfield Coal Member depth; (b) East-West stratigraphic profile across Illinois Basin (along line indicated in Fig. 1a) with 52x vertical exaggeration; (c) map of vitrinite reflectance R_o of Springfield Coal Member overlain by major tectonic structures in southeastern Illinois Basin (after Greb et al., 1992; Hower et al., 2005). Dashed lines distinguish counties: S – Sullivan, K – Knox, G – Gibson, U – Union, W – Webster.

Fig. 2. Litostratigraphic column of Pennsylvanian in the Indiana part of Illinois Basin, with positions of sampled coal beds indicated (modified from Mastalerz and Harper, 1998).

Fig. 3. Major gas components of coalbed gases in SE Illinois Basin; coals are listed in stratigraphic sequence according to Fig. 2.

Fig. 4. Compound specific isotopic data for Indiana and Kentucky coalbed gases. (a) and (b) show δ^{13}C values, and (c) and (d) show δD values of hydrocarbons plotted against the reciprocal carbon numbers of methane to butane according to Chung et al. (1988). The same δ^{13}C and δD data are cross-plotted for Indiana (e) and western Kentucky (f). The inserted legend in (f) is valid for symbols in all parts of Fig. 4. Section (b) also plots data from hydrous pyrolysis artificial maturation experiments that generated thermogenic end-member gases from Indiana coals. Therefore we compare artificial and natural thermogenic gases generated from the same coals. δD$_{i\text{-}C4}$ values were plotted for coals where δD$_{n\text{-}C4}$ values were unavailable due to microbial degradation of *n*-butane (see Table 3).

Fig. 5. Carbon isotopic shifts of residual methane and CO_2 from crushed coals in comparison with gases that were desorbed from coal core segments. Residual gases tend to be enriched in ^{13}C.

Fig. 6. The solid line demarcates the maximum expected thermogenic gas potential in relation to coal maturity (after Meissner, 1984). The dashed line suggests additional early thermogenic gas generation (Schimmelmann et al., 2006). The ellipse with hachure indicates the observed thermogenic gas content in coals from the studied area of western Kentucky. The upper oval outlines the observed coalbed gas content of less mature Indiana coals.

Fig. 7. Graphic stable isotopic gas classifications of Indiana and Kentucky coalbed gases and gases from hydrous pyrolysis experiments: (a) natural gases from this study; (b) natural gases from this study cross-plotted isotopically according to Whiticar (1996); (c) Indiana coalbed gases from this study cross-plotted isotopically according to Whiticar et al. (1986) where ellipses enclose typical ranges of values for microbially generated gases. Additionally one data point from hydrous pyrolysis is plotted to highlight significant difference between $\alpha_{CO2-CH4}$ values of microbial (via CO_2-reduction) and thermogenic generation of methane.

Fig. 8. Indiana coal bed-associated waters are isotopically similar to modern regional meteoric water but are distinctly different from Mississippian and Pleistocene environmental waters. Data sources: [1] Craig (1961), Rozanski et al. (2003); [2] Stueber and Walter (1994); [3] McIntosh and Walter (2005); [4] McIntosh et al. (2002).

Fig. 9. Gas alteration diagrams. (a) Ratio of vol. % of C_2 over C_3 versus isotopic difference between C_2 and C_3 depicting the biodegradation of C_3 and the increase in $\Delta^{13}C_{C3-C2}$. We assume that C_2 is not subject to significant alteration. The asterisks * identify values for thermogenic gases that were calculated according to Berner and Faber (1988). (b) Increasing $\delta^{13}C_{C3}$ values with decreasing remaining fraction of C_3 suggest preferential microbial alteration of $^{12}C_3$. Samples with the highest C_2 and C_3 concentrations presumably reflect the initial concentrations prior to alteration; α values represent preference for biodegradation, for example $^{12}C_3H_8$ over $^{13}C^{12}C_2H_8$. (c) A comparison of average data for Springfield and Seelyville coalbed gases from Indiana and western Kentucky suggests preferential microbial C_3-alteration in Indiana.

Chapter 5

Fig. 1. Study area and gas properties: (a) eastern margin of the Illinois Basin showing the depth of Seelyville Coal. (b, c, d) Relatively low variability of all parameters. $C_1/(C_2+C_3)$ decreases towards the depocenter of the basin (indicated by a black star on panel a), where more early thermogenic C_{2+} hydrocarbons might have been generated.

Fig. 2. Fig. 1. Study area and gas properties: (a) eastern margin of the Illinois Basin showing the depth of the Seelyville Coal and the locations studied; (b) variation in gas

content in the Seelyville Coal; (c) slight decrease towards basin's depocenter of $C_1/(C_2+C_3)$ ratio; (d) low variability of $\delta^{13}C_{CH4}$.

Fig. 3. Geochemical classification of Indiana's coal gas origin (Strąpoć et al., 2007a). This graph plots all samples from the entire study area. Plotted data from production wells are limited to the most recent March 2007 measurements. Gases are dominated by methane of microbial origin via CO_2-reduction. Gases from wells INS-P8 and INS-P9 are characterized by exceptionally low $\delta^{13}C_{CO2}$ values, probably due to microbial methane oxidation.

Fig. 4. Coalbed gas properties and coal depth: data points from the entire study area. (a) Carbon stable isotopic signatures pointing to microbial methanogenesis. (b) The ratios of methane over the sum of ethane and propane indicate that propane biodegradation occurs over the entire depth range of coal occurrence. (c) The concentration of total gas in coal does not depend on depth.

Fig. 5. Total gas contents across three coal cores from which consecutive 30 cm core sections generated contiguous gas desorption data. Y-axis numbers represent successive 30 cm core sections counting from the top of each coal bed. Top and bottom sections of cores tend to contain more gas than middle sections.

Fig. 6. Total gas contents in all 30 cm coal core sections plotted according to their relative positions within coal beds counting from the top in each location. Middle sections of coal cores tend to contain less gas than top and bottom sections.

Fig. 7. Gas geochemical parameters of continuously sampled and desorbed coal cores of Seelyville Coal (INS-1 and INS-3) and Springfield Coal (ING-2). Y-axis numbers represent successive 30 cm core sections counting from the top of each coal bed. Desorbed gases from cores INS-1 and INS-3 express more distinctly microbial isotopic signatures in their top and bottom sections (in direction of the arrows). Top and bottom sections also contained larger gas concentrations (see Figure 5) suggesting slightly higher microbial methanogenic activity in top and bottom coal sections.

Fig. 8. Methane adsorption isotherms of the Seelyville Coal in Indiana from four locations determined via volumetric adsorption. Star symbols represent theoretical values of gas adsorption capacity (AC) of a particular coal at its reservoir pressure. Matching

values of AC and measured total gas contents (MGC, obtained using desorption canisters) for each location suggest coal saturation with coal gases.

Fig. 9. Maceral composition (volume %, mmf – on mineral matter free basis) of coals from all core sections versus total gas content desorbed from coals. No correlation is evident between maceral composition and total gas content.

Fig. 10. Geochemical coalbed gas data from seven Indiana CBM production wells that have been sampled every nine months. Well INS-3 was also sampled during the original drilling. Most wells exhibit slight increases in $C_1/(C_2+C_3)$ and CH_4/CO_2 over time (dashed arrows). Decreasing values of CH_4/CO_2 in the oldest wells INS-P8 and INS-P9 (dotted arrow) suggest production-induced microbial oxidation of methane.

Chapter 6

Fig. 1. Map showing the extent of the Seelyville Coal in the Illinois Basin. The sampling site is located in the eastern marginal zone of the basin. It is a coal gas producing well from a depth of 105 m. The dotted and dashed lines represent the southernmost extents of the most recent Pleistocene glaciations. The arrows indicate the inferred direction of melt water influxes during inter- and post-glacial periods.

Fig. 2. SEM pictures of methanogenic enrichment filtered on a 0.22 μm membrane; a) predominantly spherical cells with diameters of ≤0.5 μm; b) close up of three typical 0.4 μm spherical cells, most likely *Methanocorpusculum parvum*.

Fig. 3. Microbial diversity in the coalbed waters from coal gas-producing well INS-P11, the Seelyville Coal, depth 105 m. The tree was created using neighbor joining method, substitution method: p-distance, bootstrap 3000 replicates generated using MEGA 3.1 software (32); * - among the archaeal clones, 54 coalbed water clones and all enrichment clones were almost identical, therefore each group is represented by one clone.

Fig. 4. Distribution of archaeal intact polar membrane lipids (IPLs) in the methanogenic enrichment sample dominated by close relatives of *Methanocorpusculum parvum*. GDGT – glycerol dialkyl glycerol tetraether; PG – phosphatidylglycerol; DMAPT - (N,N-dimethyl)-aminopentanetetrol; TMAPT – (N,N,N-trimethyl)-aminopentanetetrol; 1G, 2G, 3G – glycosyl (mono, di, tri); A – archaeol; * - tentatively identified derivative of the original compound (e.g. TMAPT-A) with similar fragmentation pattern and 14 *da* higher

mass. [1] PG-GDGT, [2] 1G-GDGT-PG, [3] 2G-GDGT-PG, [4] 3G-GDGT-PG, [5] 2G-GDGT-DMAPT*, [6] 2G-GDGT-DMAPT, [7] PG-GDGT-DMAPT.

Fig. 5. Proposed mechanisms of stepwise biodegradation of organic matter in coal, annotated with microbes found in clone library and capable of performing indicated processes: (i) defragmentation of coal geomacromolecular structure predominately by fermentation targeted at oxygen-linked moieties and oxygen containing functional groups; this process detaches some of the oxygen-linked aromatic rings, generates some short organic acids; (ii) anaerobic oxidation of available aromatic and aliphatic moieties, derived from coal defragmentation or from dispersed oil present in coal in small quantities; major product of this process is CO_2; (iii) fermentation of products available from of step 1 to H_2, CO_2, and acetate; (iv) methanogenesis utilizing H_2 and CO_2 wins the competition with homoacetogenesis and generates the terminal product of OM degradation – CH_4; additionally excess of acetate may get recycled to H_2 and CO_2 by syntrophic oxidation and further fuel up methanogenesis. The brown area represents a droplet of oil. The molecular model of coal after (47). For more detailed environmental functions of listed microbes see Table 2.

Fig. 6. Free energy dependence on the substrate and product availability of microbial reactions in average measured Indiana coals *in-situ* conditions (salinity 3.11 g/L, temperature 17˚C, pressure 10.5 atm, H^+ 10^{-8} M, $H_{2,aq}$ $3.8 \cdot 10^{-8}$ M, CH_3COO^- $4.3 \cdot 10^{-6}$ M, $CH_{4,aq}$ $1.5 \cdot 10^{-2}$ M, and HCO_3^- $1.7 \cdot 10^{-2}$ M). The data points represent *in-situ* conditions in three coal gas-producing wells within 5 km from each other. Lines represent -15 kJ of available free energy, a minimum required to generate 1 mol of ATP (50), for each microbial reaction. The arrows indicate conditions, under which given reaction will be more exergonic than the required minimum. * - based on the reactions as written (see Table 1).

Chapter 7

Fig. 1. Model of the geological history of coal beds in the Indiana part of the Illinois Basin in terms of environmental parameters that are important for the productivity of subsurface micro biota. Initial sterilization of coal occurred at 90˚C when small amounts of thermogenic gas were generated (red line); at the same time, about 8 wt.% oil was

generated that remained dispersed in the coal. A – a temperature below 60°C was a necessary requirement for life of complex microbial community. B – a relatively shallow depth of 0.3 km allowed increased influx of meteoric water. C – inter/post glacial fresh water influx diluted coalbed brines to chlorinities that were tolerable for microbes. D – onset of microbial biodegradation of early thermogenic C_{2+} hydrocarbons, coal-derived oil, and coal organic matter, along with associated methanogenesis.

List of Tables

Chapter 3

Chapter 4

Chapter 5

Table 1. Properties of Seelyville and Springfield coal core sections from boreholes in eastern Indiana; V – vitrinite, L – liptinite, I – inertinite, mmf – mineral matter free, as rec. – as received, scf/t – standard cubic feet per ton, st. dev. – standard deviation, n.d. – not determined.

Table 2. Concentration and isotopic parameters of coal gases desorbed from fresh cores, eastern Indiana. N_2 not determined; C_1 – methane, C_2 – ethane, C_3 – propane, i-C_4 – *iso*-butane, n-C_4 – n-butane, n.d. – not determined.

Table 3. Concentration and isotopic parameters of produced coal gases, eastern Indiana; III – production from the Seelyville Coal, V – from the Springfield Coal, III+V – single well penetrates and produces gas from both coal seams. N_2 not determined, start of production given in month/year format, n.d. – not determined.

Table 4. Physicochemical and isotopic parameters of co-produced coalbed waters, eastern Indiana; b.d.l. – below detection limit, III – production from the Seelyville Coal, V – from the Springfield Coal, III+V – single well penetrates and produces gas from both coal seams.

Chapter 6

Table 1. Microbial reactions taken into consideration as potentially occurring in Indiana coal beds; chemical formulas, standard free energies, and *in-situ* free energies; [&] - calculated for average concentrations obtained for the area: H^+ 10^{-8} M, $H_{2,aq}$ $3.76 \cdot 10^{-8}$ M, CH_3COO^- $4.3 \cdot 10^{-6}$ M, $CH_{4,aq}$ $1.5 \cdot 10^{-2}$ M, and HCO_3^- $1.7 \cdot 10^{-2}$ M; the $\Delta G°_{P,T}$ and ΔG represent the values for the reactions as written.

Table 2. Species related to clones from clone library of the coal water-environmental sample, their environmentally known biodegradation targets, and potential *in-situ* functions of related clones in the coal bed environment.

CHAPTER 1

Introduction

1.1. Objectives of the study

The main objectives of this study were the assessment of the origin and extent of the occurrence of coal gas in the Indiana part of the Illinois Basin. The basin expresses a gradient of thermal coal maturity causing the generation of biogenic and/or thermogenic coalbed gases depending on coal properties and geologic setting. Relatively shallow eastern Illinois Basin coals in Indiana with low maturity (vitrinite reflectance R_o ~0.6%) contain significant resources of coalbed methane (CBM) (Drobniak et al., 2004; Mastalerz et al., 2004). Important questions about these relatively immature coals center on (i) the amount of biogenic CBM that contributes to bulk coalbed gas, and (ii) biogeochemical controls of modern CBM generation. With regard to higher maturity coals in the southern part of the Illinois Basin, we hypothesize that past tectonic and hydrothermal activities (Hower and Gayer, 2002; Rowan et al., 2002) triggered thermogenic gas generation in western Kentucky where R_o ranges from 0.7 to 0.8%.

This study documents variations in gas composition and isotopic signatures in two Pennsylvanian coal beds in Indiana, the Springfield Coal Member of the Petersburg Formation and the Seelyville Coal Member of the Dugger Formation. The use of stable isotope ratios in CBM exploration requires a practical and reasonably fast method for desorbing and sampling of gas. Coal from freshly drilled cores is typically placed in desorption canisters (Gas Research Institute, 1995) from which desorbed gas is subsequently sampled for isotopic analysis. Desorption from coal proceeds over weeks and months, with gas yields decreasing exponentially over time and desorbed gases expressing isotope fractionation. In this study, we quantify gas speciation and isotopic fractionation along sequential desorption of methane and CO_2 from high-volatile,

2

bituminous coal expressing a narrow range of maturity from R_o 0.54 to 0.64% vitrinite reflectance.

We sampled coals and gases from these two coal beds from multiple locations at various subsurface coal depths. In each case, the entire thickness of a coal seam was sampled using multiple desorption canisters and resulting in exhaustive data coverage. The resulting overall data set allows us to contrast the regional range of variations in gas characteristics against the variability that can occur among multiple samples across a coal seam in a single location. Furthermore, our CBM production time-series data provide insight into the compositional and isotopic variability during ongoing gas production.

Additional goals of this study were to document presence and speciation of methanogenic Archaea in the Illinois Basin coals, and to explore the complexity of the entire microbial consortia in terms of metabolic functions in biodegradation. Several lines of evidence point to a biogenic origin of coalbed gas along the eastern margin of the Illinois Basin (Strąpoć et al., 2007; Ch. 4). In this study we take a phylogenetic, geochemical, and culturing approach to the understanding of microbial processes of subsurface biodegradation of organic matter leading to the formation of subsurface methane accumulations of economic importance, with special emphasis on the terminal process of methanogenesis.

1.2. Study area

The depocenter of the asymmetric, spoon-shaped Illinois Basin is located in the southeast (see Ch. 4, Fig. 1a). The basin is an intracratonic structural depression that accumulated sediments of shallow marine origin (up to 3500 m, 530 to 280 Ma; see Ch.

4, Fig. 1b) during Cambrian to Pennsylvanian time. The post-Paleozoic history of the basin was dominated by erosion, and more recently included northern glacial loading. Only the very southeastern part of the basin in western Kentucky was subjected to intense tectonic activity along the Rough Creek and Pennyrile Fault systems. Tectonic activity began in the early Paleozoic as an east-west extension of the abandoned Reelfoot Rift zone (see Ch. 4, Fig. 1c) (Macke, 1995) and continued throughout basin-filling. Vertical translocations at the Rough Creek Graben and an increased geothermal gradient locally caused a relatively greater present-day coal depth of ~400 m and higher coal maturity (R_o ~0.7 to 0.8%; see Ch. 4, Fig. 1a, c).

Pennsylvanian coal-bearing sediments in the Illinois Basin reach 750 m in thickness. Pennsylvanian lithostratigraphy is characterized by relatively thin and laterally extensive units relating to deposition during multiple transgressions and regressions. The depositional environment has been recently described as mainly nearshore to marginal marine characterized by tidal coastal plains (Kvale et al., 2004), although it was formerly thought to have been coal swamps developing on deltaic platforms (Roseman Wright, 1977). Our study focuses on the Springfield and Seelyville Coal Members in the southeastern Illinois Basin that are commercial CBM targets (Solano-Acosta et al., 2005) (see Ch. 4, Fig. 2) ranging in thickness from 0.7 to 1.6 m and from 0.4 to 1.6 m, respectively. Average coalbed gas contents, on a raw basis (moisture and mineral matter included), range from 2.0 to 3.0 cm^3g^{-1} in the Springfield Coal Member and from 2.2 to 4.6 cm^3g^{-1} in the Seelyville Coal Member (Mastalerz et al., 2004). The Springfield and Seelyville coals in Indiana are located at typical depths of between 60 and 200 m (Mastalerz et al., 2004), and have high-volatile bituminous C and B rank throughout the

state, with an average R_o ~0.56% for the Springfield Coal (Hower et al., 2005) and 0.60% for the Seelyville Coal (Drobniak et al., 2004). The stratigraphically equivalent coal beds in western Kentucky feature increased R_o from 0.7 to 0.8% and rank as high-volatile bituminous A coals.

1.3.   Methodology

The determination of the origin of coalbed methane in the Indiana part of the Illinois Basin coals was carried out using variety of approaches. Coal gases were classified in terms of molecular and stable carbon and hydrogen isotopic compositions using gas chromatography oxidation/pyrolysis compound-specific isotope ratio mass spectrometry (GC-ox/pyr-IRMS) utilizing a custom made inlet system GASIS (Henning et al., 2007) for accomodating variable gas sample sizes. Our versatile GASIS inlet system can be applied to a variety of gas samples, including mixtures of gases containing hydrogen and/or carbon with individual component concentrations higher than 10 ppm (e.g. natural gases including coalbed (Strąpoć et al., 2007) and shale gases, pyrolysis gases, atmospheric gases, head space gases from microbial incubations). The GASIS inlet system conveniently allows the user to obtain relative gas concentrations and isotopic data for multiple gas species over a wide range of concentrations in a single GC-ox/red-IRMS run. The user can target individual parameters for specific sample types by varying (i) sampling loop sizes, (ii) the timing of injections and back-flushes within the run, and (iii) the GC program over a wide temperature range. Precise measurements of H_2 concentration in coal gas were performed using a Peak Performer 1 (PP1) Gas Analyzer

(Peak Laboratories, LLC, California) equipped with a Reducing Compound Photometer (RCP) at the University of Bremen in Dr. Hinrichs' laboratory.

Coalbed water that was co-produced with CBM at commercial gas wells in Indiana was analyzed in terms of its chemistry using inductively coupled plasma-atomic emission spectroscopy (ICP-AES) with a Perkin Elmer Optima 3000 ICP spectrometer at the National Energy Technology Laboratory (NETL), Pittsburgh, PA by Dr. Hedges. Physicochemical properties of co-produced coalbed waters were analyzed at the coalbed gas production wells with a multi-functional probe YSI 600XL (Yellow Springs Instruments, Inc., Yellow Springs, Ohio). Hydrogen and oxygen stable isotopic compositions of coalbed waters were analyzed using a Delta Plus XP stable isotope mass spectrometer with on-line peripherals (H-Device for δD_{H2O} and Gas Bench for $\delta^{18}O_{H2O}$, manufactured by ThermoFinnigan, Bremen, Germany). Intact polar lipid (IPL) biomarkers from coalbed waters were analyzed using high-performance liquid chromatography mass spectrometry (HPLC-MS) with a ThermoFinnigan LCQ Deca XP Plus ion-trap mass spectrometer (ThermoFinnigan, Bremen, Germany) with an electrospray ionization (ESI) interface (Dr. Hinrichs' laboratory, University of Bremen, Germany). Acetate concentrations were analyzed by IRM-LC/MS using a ThermoFinnigan Surveyor HPLC coupled to a ThermoFinnigan Delta Plus XP irMS via the Finnigan LC IsoLink interface (Dr. Hinrichs' laboratory, University of Bremen, Germany). The microbiological studies, including methanogenic enrichments were performed in Dr. Flynn Picardal's microbiological laboratory in the School of Public and Environmental Affairs, Indiana University, Bloomington. The DNA extraction and phylogenetic study was conducted in cooperation with Penn State University in Dr.

Macalady's laboratory. Detailed descriptions of methodologies and materials are provided in the following chapters.

1.4. Importance of molecular and stable isotopic compositions for studying the origin of gas

Empirical compositional and isotopic classifications for discerning different origins of natural gases (e.g., Schoell, 1983; Chung et al., 1988; Whiticar, 1999) have been applied to coalbed gases in various basins (e.g., Scott et al., 1994; Smith and Pallasser, 1996; Ahmed and Smith, 2001; Hoşgörmez et al., 2002; Katz et al., 2002; Aravena et al., 2003; Faiz et al., 2003; Thielemann et al., 2004). Frequently used diagnostic parameters are (i) the ratio of methane to the sum of ethane and propane $C_1/(C_2+C_3)$ (i.e., gas wetness; Bernard et al., 1978), (ii) carbon $\delta^{13}C_{CH4}$ and hydrogen δD_{CH4} isotopic compositions of methane (Schoell, 1980; Whiticar et al., 1986), and (iii) the carbon isotopic difference between CO_2 and methane $\Delta^{13}C_{CO2-CH4}$ (Smith and Pallasser, 1996; Strąpoć, 2007). Typical diagnostic values for thermogenic versus microbial gases are, respectively: (i) $C_1/(C_2+C_3)$ ratios of <15 versus >1000, (ii) $\delta^{13}C_{CH4}$ values of >-50‰ versus <-55‰ (i.e., more ^{13}C-enriched versus more ^{13}C-depleted), and (iii) $\Delta^{13}C_{CO2-CH4}$ values of <40‰ versus >55‰. In addition, plotting of compound-specific $\delta^{13}C$ values of methane C_1 to butane C_4 hydrocarbon gas components against the reciprocal carbon number (Chung, 1988) is useful for discriminating thermogenic from biogenic gases, whereby only thermogenic C_1 to C_4 plot along a straight line. The $\delta^{13}C_{CH4}$ value of mixtures of microbial and thermogenic methanes shifts towards more negative

7

values with the addition of microbial methane. Selective biodegradation of hydrocarbon gas components can cause enrichment in ^{13}C in residual C_3 and n-C_4 (Katz et al., 2002).

1.5. Significance of subsurface microbiology in organic matter degradation

Worldwide occurrences of methane accumulations with microbial isotopic signatures in coals (Scott et al., 1994; Thielemann et al., 2004), shales (McIntosh et al., 2002), biodegraded oils (Bekins et al., 2005; Milkov and Dzou, 2007), ocean floor sediments (Newberry et al., 2004), and municipal landfills (Huang et al., 2002) imply that widespread subsurface microbial communities are capable of biodegrading complex organic matter (OM). A common terminal step of organic matter degradation in anoxic subsurface environments is methanogenesis (Zengler et al., 1999; Salminen et al., 2006; Waldron et al., 2007), a metabolism unique to methanogenic Archaea.

Coal is an extremely OM-rich rock (> 50%) and could be considered very attractive for microbial biodegradation. However, coal is a solid rock, often dominated by recalcitrant, partially aromatic and largely lignin-derived macromolecules which tend to be chemically stable. The rate-limiting step of coal biodegradation is the initial fragmentation of the partially aromatic, geomacromolecular, polycyclic, lignin-derived network of coal. It has been found that lignin degradation can be achieved by extracellular enzymes used by fungi and some microbes (Crawford et al., 1983; Fakoussa and Hofricher, 1999). It has been also shown that up to 40 wt. % of coal can be enzymatically dissolved using extracted microbial hydrogenases (Scott et al., 1994). Furthermore, there are known microbial species capable of anaerobic degradation of methylated and ethylated aromatic compounds (Coates et al., 2001; Jothimani et al.,

2003; Townsend et al., 2004; Chakraborty et al., 2005) or even polycyclic aromatic hydrocarbons (PAHs, Coates et al., 1997; Chang et al., 2002; Christensen et al., 2004; Meckenstock et al., 2004).

Methane generation from coal by microbial consortia has been documented earlier. It has been shown that microflora present in water leached from coal mines can generate methane (Thielemann et al., 2004). Furthermore, a methane-generating consortium extracted from coal was observed to grow on low volatile bituminous coal as a sole carbon source (Shumkov et al., 1999). Microbial communities may also target the dissipated bitumen/oil droplets generated from coal. Long-chain *n*-alkanes, the main constituents of non-biodegraded oil, can be anaerobically utilized by microbes (Zengler et al., 1999; Sei et al., 2003; Hostettler, 2004). Even small quantities of *n*-alkanes in the form of dispersed oil in coal may possibly serve as a preferred target for microbial biodegradation.

This study implies that widespread subsurface biodegradation and methanogenesis in OM-containing geologic formations can provide significant amounts of energy supply − methane. We will show that the crucial factors for microbial gas generation are habitable temperature, salinity, permeability, and contact with ground waters to dilute brines and provide the microbes (both methanogens and a consortia of coal OM degraders) to inoculate the coal beds. Observations from this research can pave the way to extended exploration for subsurface microbial methane reserves within shallow crustal rocks (i.e. coals and shales) of many sedimentary basins.

References

Ahmed, M., Smith, J.W., 2001. Biogenic methane generation in the degradation of eastern Australian Permian coals. Organic Geochemistry 32, 809-816.

Aravena, R., Harrison, S.M., Barker, J.F., Abercrombie, H., Rudolph, D., 2003. Origin of methane in the Elk Valley coalfield, southeastern British Columbia, Canada. Chemical Geology 195, 219-227.

Bekins, B.A., Hostettler, F.D., Herkelrath, W.N., Delin, G.N., Warren, E., Essaid, H.I., 2005. Progression of methanogenic degradation of crude oil in the subsurface. Environmental Geosciences 12, 139–152.

Bernard, B.B., Brooks, J.M., Sackett, W.M., 1978. Light hydrocarbons in recent Texas continental shelf and slope sediments. Journal of Geophysical Research 83, 4053-4061.

Chakraborty, R., O'Connor, S.M., Chan, E., Coates, J.D., 2005. Anaerobic degradation of benzene, toluene, ethylbenzene, and xylene compounds by *Dechloromonas* strain RCB. Applied and Environmental Microbiology 71, 8649–8655.

Chang, B.V., Shiung, L.C., Yuan, S.Y., 2002. Anaerobic biodegradation of polycyclic aromatic hydrocarbon in soil. Chemosphere 48, 717-24.

Christensen, N., Batstone, D.J., He, Z., Angelidaki, I., Schmidt, J.E., 2004. Removal of polycyclic aromatic hydrocarbons (PAHs) from sewage sludge by anaerobic degradation. Water Science and Technology 50, 237-44.

Chung, H.M., Gormly, J.R., Squires, R.M., 1988. Origin of gaseous hydrocarbons in subsurface environments: Theoretical considerations of carbon isotope distribution. Chemical Geology 71, 97-104.

Coates, J.D., Woodward, J., Allen, J., Philp, P., Lovley, D.R., 1997. Anaerobic degradation of polycyclic aromatic hydrocarbons and alkanes in petroleum-contaminated marine harbor sediments. Applied and Environmental Microbiology 63, 3589–3593.

Coates, J.D., Chakraborty, R., Lack, J.G., O'Connor, S.M., Cole, K.A., Bender, K.S., and Achenbach, L.A., 2001. Anaerobic benzene oxidation coupled to nitrate reduction in pure culture by two novel organism. Nature 411, 1039-1043.

Drobniak, A., Mastalerz, M., Rupp, J., Eaton, N., 2004. Evaluation of coalbed gas potential of the Seelyville Coal Member, Indiana, USA. International Journal of Coal Geology 57, 265–282.

Faiz, M., Hendry, P., 2006. Significance of microbial activity in Australian coal bed methane reservoirs – a review. Bulletin of Canadian Petroleum Geology 54, 261-272.

Fakoussa, R.M., Hofrichter, M., 1999. Biotechnology and microbiology of coal degradation. Applied Microbiology and Biotechnology 52, 25-40.

Gas Research Institute, 1995. A guide to determining coalbed gas content. Gas Research Institute, 1995, GRI-94/0396.

Henning, M.J., Strąpoć, D., Lis, G.,Sauer, P., Fong, J., Schimmelmann, A., Pratt, L.M., 2007. Versatile inlet system for on-line compound-specific δD and δ^{13}C GC-c/pyr-IRMS analysis of gaseous mixtures. Rapid Communications in Mass Spectrometry 21, 2269-2272.

Hostettler, F.D., 2004. Methanogenic biodegradation of *n*-alkanes and *n*-alkylated cyclohexanes and benzenes in the oil spill long-term study site at Bemidji, MN. GSA 2004 Denver Annual Meeting (November 7–10, 2004), Paper No. 248-6.

Hoşgörmez, H., Yalçin, M.N., Cramer, B., Gerling, P., Faber, E., Schaefer, R.G., Mann, U., 2002. Isotopic and molecular composition of coal-bed gas in the Amasra region (Zonguldak basin – western Black Sea). Organic Geochemistry 33, 1429-1439.

Hower, J.C., Gayer, R.A., 2002. Mechanisms of coal metamorphism: case studies from Paleozoic coalfields. International Journal of Coal Geology 50, 215-245.

Hower, J.C., Mastalerz, M., Drobniak, A., Quick, J.C., Eble, C.F., Zimmerer, M.J., 2005. Mercury content of the Springfield coal, Indiana and Kentucky. International Journal of Coal Geology 63, 205-227.

Huang, L.-N., Zhou, H., Chen, Y-.Q., Luo, S., Lan, C.-Y., Qu, L.-H., 2002. Diversity and structure of the archaeal community in the leachate of a full-scale recirculating landfill as examined by direct 16S rRNA gene sequence retrieval. FEMS Microbiology Letters 214, 235-240.

Jothimani, P., Kalaichelvan, G., Bhaskaran, A., Selvaseelan, D.A., Ramasamy, K., 2003. Anaerobic biodegradation of aromatic compounds. Indian Journal of Experimental Biology 41, 1046-67.

Katz, B.J., Narimanov, A., Huseinzadeh, R., 2002. Significance of microbial processes in gases of the South Caspian basin. Marine and Petroleum Geology 19, 783-796.

Kvale, E.P., Mastalerz, M., Furer, L., Engelhardt, D.W., Rexroad, C.B., Eble, C., 2004. Atokan and early Desmoinesian coal-bearing parasequences in Indiana, U.S.A. In: Paschin, J.C., Gastaldo, R.A. (Eds.), Sequence Stratigraphy, Paleoclimate, and Tectonics of Coal-bearing Strata. American Association of Petroleum Geologists, Studies in Geology 51, 71-88.

Macke, D.L., 1995. Illinois Basin Province. In: Gautier, D.L., Dolton, G.L., Takahashi, K.I., and Varnes, K.L. (Eds.), National Assessment of United States Oil and Gas Resources - Results, Methodology, and Supporting Data: U.S. Geological Survey Digital Data Series 30 (064).

Mastalerz, M., Drobniak, A., Rupp, J., Shaffer, N., 2004. Characterization of Indiana's coal resource: availability of the reserves, physical and chemical properties of the coal, and present potential uses. Indiana Geological Survey Open-File Study 04-02, July 2004.

McIntosh, J.C., Walter, L.M., Martini, A.M., 2002. Pleistocene recharge to midcontinent basins: effects on salinity structure and microbial gas generation. Geochimica et Cosmochimica Acta 66, 1681–1700.

Meckenstock, R. U., Griebler, C., Safinowski, M., 2004. Anaerobic degradation of polycyclic aromatic hydrocarbons. FEMS Microbiology Ecology 49, 27-36.

Milkov, A.V., Dzou, L., 2007. Geochemical evidence of secondary microbial methane from very slight biodegradation of undersaturated oils in a deep hot reservoir. Geology 35, 455-458.

Newberry, C.J., Webster, G., Cragg, B.A., Parkes, R.J., Weightman, A.J., 2004. Fry diversity of prokaryotes and methanogenesis in deep subsurface sediments from the Nankai Trough, Ocean Drilling Program Leg 190. Environmental Microbiology 6, 274-287.

Roseman Wright, C., 1977. Depositional history of the Pennsylvanian System in the Illinois Basin – A summary of work by Dr. Harold R. Wanless and associates. In: Palmer, J.E., Dutcher, R.R. (Eds.), Depositional and Structural History of the Pennsylvanian System of the Illinois Basin. Part 2: Invited Papers, 21-26. Ninth International Congress of Carboniferous Stratigraphy and Geology, May 26 to June 1, 1979.

Rowan, E.L., Goldhaber, M.B., Hatch, J.R., 2002. Regional fluid flow as a factor in the thermal history of the Illinois basin: Constraints from fluid inclusions and the maturity of Pennsylvanian coals. American Association of Petroleum Geologists Bulletin 86, 257-277.

Salminen, J.M., Hänninen, P.J., Leveinen, J., Lintinen, P.T.J., Jørgensen, K.S., 2006. Occurrence and rates of terminal electron-accepting processes and recharge processes in petroleum hydrocarbon-contaminated subsurface. Journal of Environmental Quality 35, 2273-2282.

Schoell, M., 1980. The hydrogen and carbon isotopic composition of methane from natural gases of various origins. Geochimica et Cosmochimica Acta 44, 649–661.

Schoell, M., 1983. Genetic characterization of natural gases. American Association of Petroleum Geologists Bulletin 67, 2225–2238.

Scott, C.D., Woodward, C.A., Scott, T.C., 1994. Use of chemically modified enzymes in organic solvents for conversion of coal to liquids. Catalysis Today 19, 381-394.

Sei, K., Sugimoto, Y., Mori, K., Maki, H., Kohno, T., 2003. Monitoring of alkane-degrading bacteria in a sea-water microcosm during crude oil degradation by polymerase chain reaction based on alkane-catabolic genes. Environmental Microbiology 5, 517–522.

Shumkov, S., Terekhova, S., Laurinavichius, K., 1999. Effect of enclosing rocks and aeration on methanogenesis from coals. Applied Microbiology and Biotechnology 52, 99-103.

Smith, J.W., Pallasser, R.J., 1996. Microbial origin of Australian coalbed methane. American Association of Petroleum Geologists Bulletin 80, 891–897.

Solano-Acosta, W., Mastalerz, M., Rupp, J.A., Strąpoć, D., Schimmelmann, A., 2005. Coal-bed gas potential in Pennsylvanian coal beds of Indiana. Proceedings of the 2005 International Coalbed Methane Symposium, Tuscaloosa, Alabama, May 2005, Paper No. 0526, CD edition.

Strąpoć, D., Mastalerz, M., Eble, C., Schimmelmann, A., 2007a. Characterization of the origin of coalbed gases in southeastern Illinois Basin by compound-specific carbon and hydrogen stable isotope ratios. Organic Geochemistry 38, 267-287.

Thielemann, T., Cramer, B., Schippers, A., 2004. Coalbed methane in the Ruhr Basin, Germany: a renewable energy source? Organic Geochemistry 35, 1537–1549.

Townsend, G.T., Prince, R.C., Suflita, J.M., 2004. Anaerobic biodegradation of alicyclic constituents of gasoline and natural gas condensate by bacteria from an anoxic aquifer. FEMS Microbiology Ecology 49, 129–135.

Waldron, P.J., Petsch, S.T., Martini, A.M., Nüsslein, K., 2007. Salinity constraints on subsurface archaeal diversity and methanogenesis in sedimentary rock rich in organic matter. Applied and Environmental Microbiology 73, 4171–4179.

Whiticar, M.J., Faber, E., Schoell, M., 1986. Biogenic methane formation in marine and freshwater environments: CO_2 reduction vs. acetate fermentation – isotope evidence. Geochimica et Cosmochimica Acta 50, 693–709.

Whiticar, M.J., 1999. Carbon and hydrogen isotope systematics of bacterial formation and oxidation of methane. Chemical Geology 161, 291-314.

Zengler, K.., Richnow, H.H., Rosselló-Mora, R., Michaelis, W., Widdel, F., 1999. Methane formation from long-chain alkanes by anaerobic microorganisms. Nature 401, 266-269.

CHAPTER 2

Versatile inlet system for on-line compound-specific δD and δ¹³C GC-ox/red-IRMS analysis of gaseous mixtures*

Mark Henning [1], Dariusz Strąpoć [2], Grzegorz P. Lis [3],
Peter Sauer [2], Jon Fong [2], Arndt Schimmelmann [2], Lisa M. Pratt [2]

[1]Inertia Oil & Gas, LLC, Evansville, IN 47708, USA
[2]Department of Geological Sciences, Indiana University, Bloomington, IN 47405, USA
[3]Department of Geological Sciences, University of Saskatchewan, Saskatoon, S7N 5E2, Canada

Abstract

Compound-specific δD and $\delta^{13}C$ analyses of gas mixtures are useful indicators of geochemical and environmental factors. However, the relative concentrations of individual components in gas mixtures (e.g., H_2, CO_2, methane, ethane, propane, *i*-butane, *n*-butane) may vary over several orders of magnitude. The determination of hydrogen and carbon compound-specific stable isotope ratios requires that the hydrogen and carbon dioxide produced from each separated component has a concentration adjusted to match the dynamic range of the stable isotope mass-spectrometer. We present a custom-built gas sampling and injection system (GASIS) linked with a Delta Plus XP mass-spectrometer that provides flexibility, ease of operation, and economical use of small gas samples with wide ranges of analyte concentrations. The overall on-line GC-ox/red-IRMS (Gas Chromatography – oxidation/reduction – Isotope Ratio Mass Spectrometry) system consists of (i) a customized GASIS inlet system and (ii) two alternative reactors, namely an oxidative Cu-Ni-Pt reactor at 950 ºC for production of CO_2 and a reductive graphitized Al_2O_3 reactor at 1420 ºC for production of H_2. In addition, the system is equipped with (iii) a liquid nitrogen spray-cooling unit for cryo-GC-focusing at -20 ºC, and (iv) a Nafion® dryer for removal of water vapor from product CO_2. The GASIS inlet system's three injection loops allow flexibility in the volume of injected analyte gas (e.g., from 0.06 μL to 500 μL) in order to measure reproducible δD and $\delta^{13}C$ values for gases at concentrations ranging from 100% down to 10 ppm. We calibrate our GC-ox/red-IRMS system with two isotopically distinct methane references gases that are combusted off-line and characterized using isotope ratio dual-inlet IRMS.

15

2.1. Introduction

Stable carbon and hydrogen isotopic compositions of hydrocarbon gases (C_1 through C_5) vary widely due to strong isotopic effects associated with biological and abiotic physicochemical processes. Patterns of isotopic variability have shed light on classification of natural gas mixtures (Schoell, 1983), sources and sinks of atmospheric methane (Quay et al., 1999; Miller et al., 2002), environmental contaminants (Ward et al., 2000), and bacterial metabolism (Morasch et al., 2001; Valentine et al., 2004). Early work on the isotopic composition of hydrocarbon gases (Schoell, 1983; Quay et al., 1991) was labor intensive, requiring oxidation or reduction in sealed tubes, vacuum-line purification of large samples, followed by dual-inlet IRMS. Significant improvement in sample size requirements and automation were achieved with the development of gas chromatography isotope ratio mass spectrometry (GC-IRMS) in which GC effluents are either combusted (oxidized) to CO_2 for $^{13}C/^{12}C$ analysis (GC-ox-IRMS; Hayes et al., 1990) or thermally converted (reduced) to H_2 for D/H analysis (GC-red-IRMS; Tobias and Brenna, 1997, Burgoyne and Hayes, 1998; Hilkert et al., 1999).

Two basic designs of gas handling inlets have been developed for analysis by GC-ox-IRMS and GC-red-IRMS. Commercially available GC injection loops (typically 0.06 to 1.0 µL, Valco Instruments Co., Inc., Houston, TX, USA) conveniently inject samples in which the sample is dominated by a single gas component. For more dilute components such as atmospheric methane (1.7 ppm) or CO_2 (~380 ppm), analytes are extracted from larger samples (20 - 200 mL) and preconcentrated and cryofocussed prior to injection onto the GC column (Miller et al., 2002; Merritt et al., 1995; Rice et al., 2001). Each type of inlet has been optimized for relatively narrow mixing ratios and

delivers appropriate amounts of analyte to the IRMS source. These inlets are not suitable

for analysis of complex mixtures, such as natural gas, with widely varying concentrations

of components. In natural gas, for example, methane is often >95%, while C_2, C_3, C_4, and

C_5 hydrocarbons are present in much lower concentrations, often <0.1 volume % of the

gas sample. In this paper we describe a new inlet termed GASIS which allows the

isotopic analysis of multiple components of a gas mixture with widely ranging mixing

ratios (Henning, 2002). A GASIS sample is loaded into three loops of varying size (0.06

µL to 500 µL). Sequential injection from each sampling loop allows the analyst to

determine stable isotopic composition of all components, major and minor, with minimal

effort. This inlet can also be used for mixtures of any gases containing carbon and/or

hydrogen, e.g. CO_2, CO, H_2, and H_2S.

2.2. Methods

2.2.1. Inlet system design

The GASIS inlet consists of three two-position sampling valves (Valco). A

schematic of the GASIS inlet is shown in Figure 1. Two of the valves are four-port,

internal-sample injecting valves with fixed sampling volumes of 0.06 µL and 0.5 µL.

The third is a six-port, external-sampling-loop valve with interchangeable loops of 5, 10,

50, 100, and 500 µL. The external loop can be switched to different size within 5

minutes if needed. Four 1/16-inch crosses (Valco) are arranged so that the sampling

volumes of the three valves are connected in parallel. Two stainless-steel (SS) toggle

valves with 1/8-inch Swagelok fittings (Whitey Co., Highland Heights, OH, USA)

control the vacuum from an oilless diaphragm pump (Gast Manufacturing, Inc., Benton

17
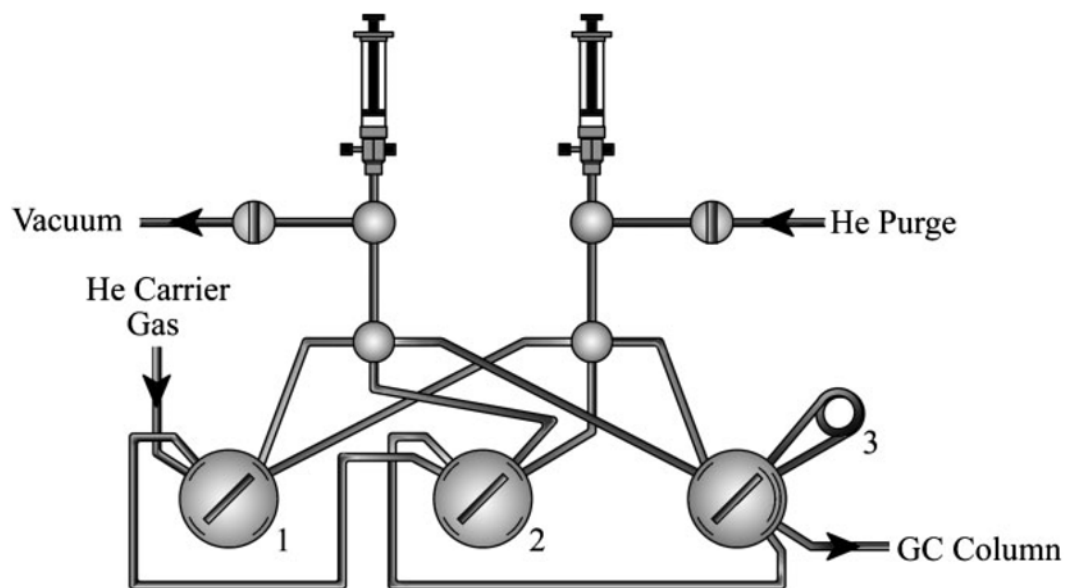
Fig. 1. Schematic of the GASIS inlet. Valve 1 corresponds to the 0.06 µL internal sampling loop, Valve 2 corresponds to the 0.5 µL internal sampling loop, and Valve 3 corresponds to the variable-volume external sampling loop (5 - 500 µL).

Harbor, MI, USA) and the flow of zero-grade helium for rinsing and purging the GASIS inlet. All connections are made via 1/16-inch outside diameter (OD) by 1/50-inch inside diameter (ID) 316-series SS tubing (Valco). The total volume of the GASIS inlet (with the 500 µL external loop attached and with the syringe push-button valves closed) is 1.2 mL.

2.2.2. Introduction of samples to the GASIS inlet

Samples are loaded/introduced to the GASIS inlet via Luer-lock, glass-body syringes. One of the two syringes always remains fixed to the GASIS inlet and is referred to as the mixing syringe. The other syringe is removed for gas sampling and is referred to as the sampling syringe. Two 10 or 5 mL) gas-tight syringes (SGE, Inc., Austin, TX, USA) with removable Luer-lock push-button dispenser valves (SGE) are fitted to 1/16-inch SS Luer-lock needles (Popper and Sons, New Hyde Park, NY, USA). The Luer-lock needles are, in turn, each fitted to a cross on the inlet. The unique arrangement of the two syringes enables them to work together in a tandem push-pull/hydraulic manner, passing a gas sample out of one syringe, through the entire GASIS inlet, including the three Valco sample valves, and into the other syringe. The entire GASIS inlet system is purged with helium and evacuated several times in between samples to avoid contamination by air and cross contamination of samples. Once the sample is loaded, each sample volume can be injected sequentially and/or repeatedly, enabling analysis of major and trace components with a minimum of operator effort.

For gas samples storage we used either 60 mL glass bottles with blue butyl stoppers (Bellco Glass, Inc., Vineland, NJ, USA) or 10 mL sterile blood collection

vacuum tubes (BD Vacutainer™, Franklin Lakes, NJ, USA). Gases were transferred into the storage containers either by water displacement (in case of bottles, water was sterilized using benzalkonium chloride 2 g/L) or with a needle (Vacutainers™). We tested both of these storage methods for gas molecular and isotopic variability and no changes has been observed over the time period of six months.

2.2.3. GC-MS analytical procedures

Gas samples were injected via the GASIS inlet onto a PoraBOND Q gas chromatographic column (30m, Varian, Inc, Palo Alto, CA, USA) for compound separation utilizing zero-grade helium carrier gas with a flow rate of 1.5 mL/minute. The GC oven and column are cooled to

-20 ºC by a spray of liquid nitrogen at the initial stage of the GC temperature program in order to enhance peak separation. The GC program can be easily adjusted for a particular sample type. For example, the GC program for coalbed gases with typically very low C_{2+} concentrations was: 7 minutes at -20 ºC, 4 minutes at 30 ºC, 4 minutes at 80 ºC, 6 minutes at 130 ºC, and 4 minutes at 250 ºC, with ramps of 50 ºC/minute.

To obtain peaks in the measurable size range for coalbed gas samples, runs consisted of two injections separated by 3 minutes: (i) 0.5 μL to obtain a C_1 peak and (ii) 50 or 500 μL to obtain CO_2 and C_{2+} peaks (Fig. 2b). To avoid overloading the high temperature reactor and the mass spectrometer, methane from the second injection was back-flushed. For typical natural-thermogenic or laboratory-pyrolysis gas samples containing more than 1% of each C_{1-4} hydrocarbons, runs with one 5 or 50 μL injection were sufficient (Fig. 2a). For such a run, the GC program was modified to be held at -20 ºC for 5 minutes. Gas species separated on the GC column are subjected to either on-line

oxidation to CO_2 in a 1Pt-1Ni-1Cu (wires) reactor at 950 ºC or on-line reduction to H_2 in an Al_2O_3 ceramic reactor at 1420ºC. The Al_2O_3 ceramic tubes for both reactors were 320 mm long with 0.5 mm inner diameter. Pre-run conditioning of reactors was required. Initial graphitization of the reducing reactor's ceramic tube was achieved via 5 injections of methane using a 500 µL external loop. This process assured (i) complete reactions (by monitoring m/z = 16 on the mass spectrometer) and (ii) a minimization of the memory effect of the reactor. Oxidation of the combustion reactor was achieved overnight prior to analysis by holding the reactor at 550 ºC with a constant O_2 flow at a pressure of 0.5 atm. Water removal was accomplished using a 60 cm long Nafion® tube sealed in 1/8-inch OD copper tubing. To improve efficiency and isotopic accuracy, the dryer assembly of our design was kept at 0ºC in an ice-water bath and flushed with a counter-flow of dry helium (Leckrone and Hayes, 1997).

On-line CO_2 and H_2-reference gas tanks and two distinct methane reference gas lecture bottles were calibrated off-line versus VPDB (Vienna Peedee Belemnite), L-SVEC (lithium carbonate), VSMOW (Vienna Standard Mean Ocean Water), and SLAP (Standard Light Antarctic Precipitation). For carbon isotopic analyses one methane reference gas ($\delta^{13}C$ = -38.25 ± 0.03‰) was used as an internal on-line reference. For hydrogen isotopic analyses, two methane reference gases (δD = -41.3 ± 1.3 and -160.8 ± 2.1‰) were used. The isotopically distinct methanes were obtained by mixing deuterium-labeled methane with non-labeled methane in lecture bottles. For both carbon and hydrogen analyses, methane reference gas(es) were injected in two sets of four injections at the beginning and end of the each day and at 6-hour intervals throughout the day. Our technique for monitoring of two H-isotopically distinct methane reference gases allowed
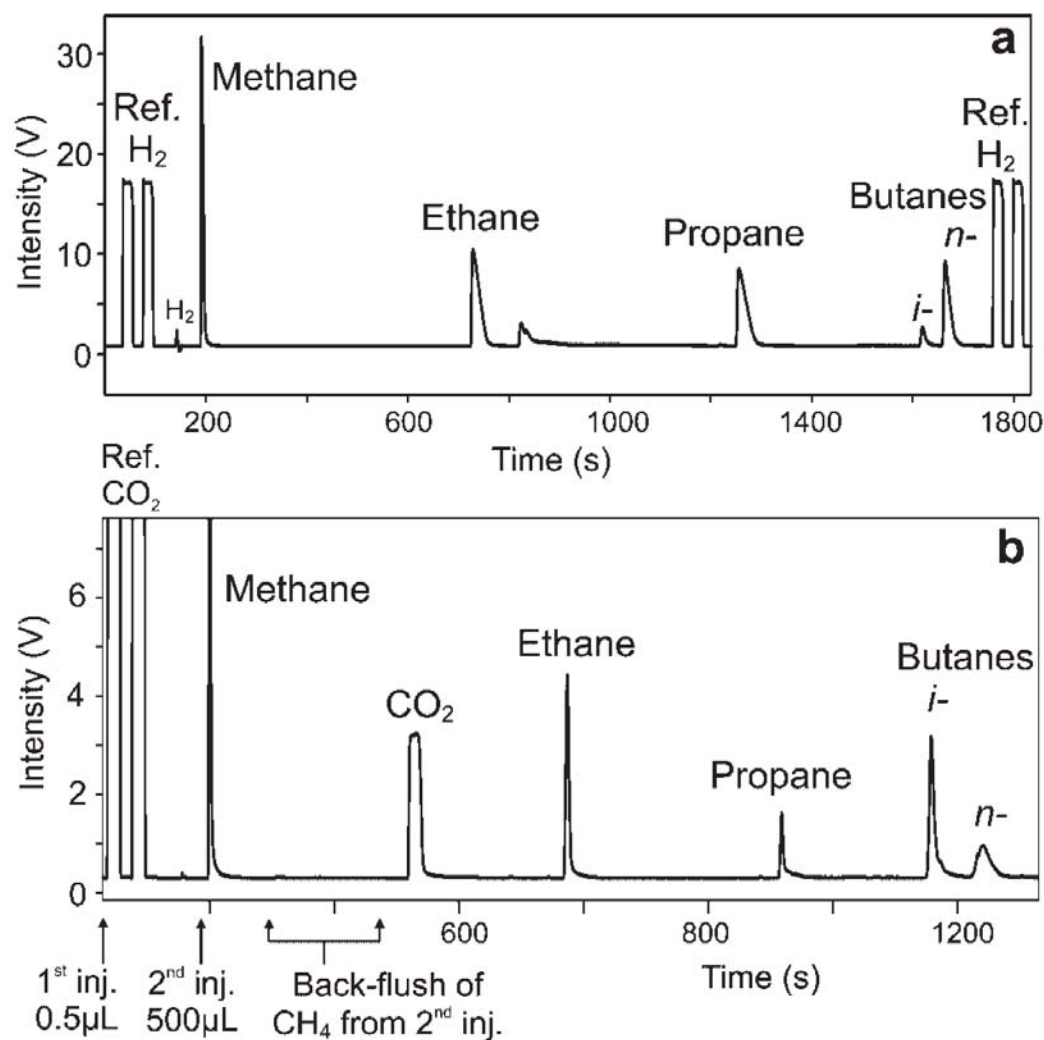
Fig. 2. Chromatograms obtained with GASIS-GC-ox/red-IRMS system: a) hydrogen chromatogram of pyrolysis gas having 0.5, 47.0, 22.1, 14.2, 5.2, and 11.0% of H_2, methane, ethane, propane, i-butane and n-butane, respectively ; b) carbon chromatogram of coal gas having 99.210, 0.740, 0.022, 0.004, 0.012, and 0.006% of methane, CO_2, ethane, propane, i-butane, and n-butane, respectively (note the two injections, first 0.5 μL from which the methane peak came from, second 500 μL for the rest of the gases at very low concentrations; methane from the second injection was back-flushed).

us to (i) monitor and compensate for daily drifts of the H_3-factor (cross-checked by injections of variable reference gas volumes), (ii) achieve off-line to on-line calibration of the mass spectrometer (single point calibration for carbon and regression line calibration for hydrogen), and (iii) quantify the daily variability of the machine slope, defined as the slope of the regression plot of accepted versus measured δD values of our two isotopically distinct reference methanes. This slope ranged from 1.030 to 1.200, with an average of 1.089 (n=14).

Relative gas concentrations were obtained by integrating peak areas. Concentrations of gases, compensated for number of C and/or H atoms per molecule, for which isotopic values were measurable and reliable were on the order of 10 ppm for carbon and 100 ppm for hydrogen. Typical analytical errors (standard deviation, n≥8) for $\delta^{13}C$ were 0.2, 0.9, 0.7, 1.0, and 1.6‰ for C_1, CO_2, C_2, C_3, and C_4 (*iso* and *n*), respectively. For δD, standard deviations were 2.0, 3.5, 4.8, and 10.0‰ for C_1, C_2, C_3, and C_4 (*iso* and *n*), respectively (Fig. 3a). Nonetheless, the uncertainties of isotopic values increase exponentially with decreasing gas concentrations, especially for hydrogen (Fig. 3b). Additional comparisons of off-line and on-line values of seven different methanes generated differences in $\delta^{13}C$ ranging from 0.02 to 0.29‰, with an average of 0.15‰ (n=7; Henning, 2002).
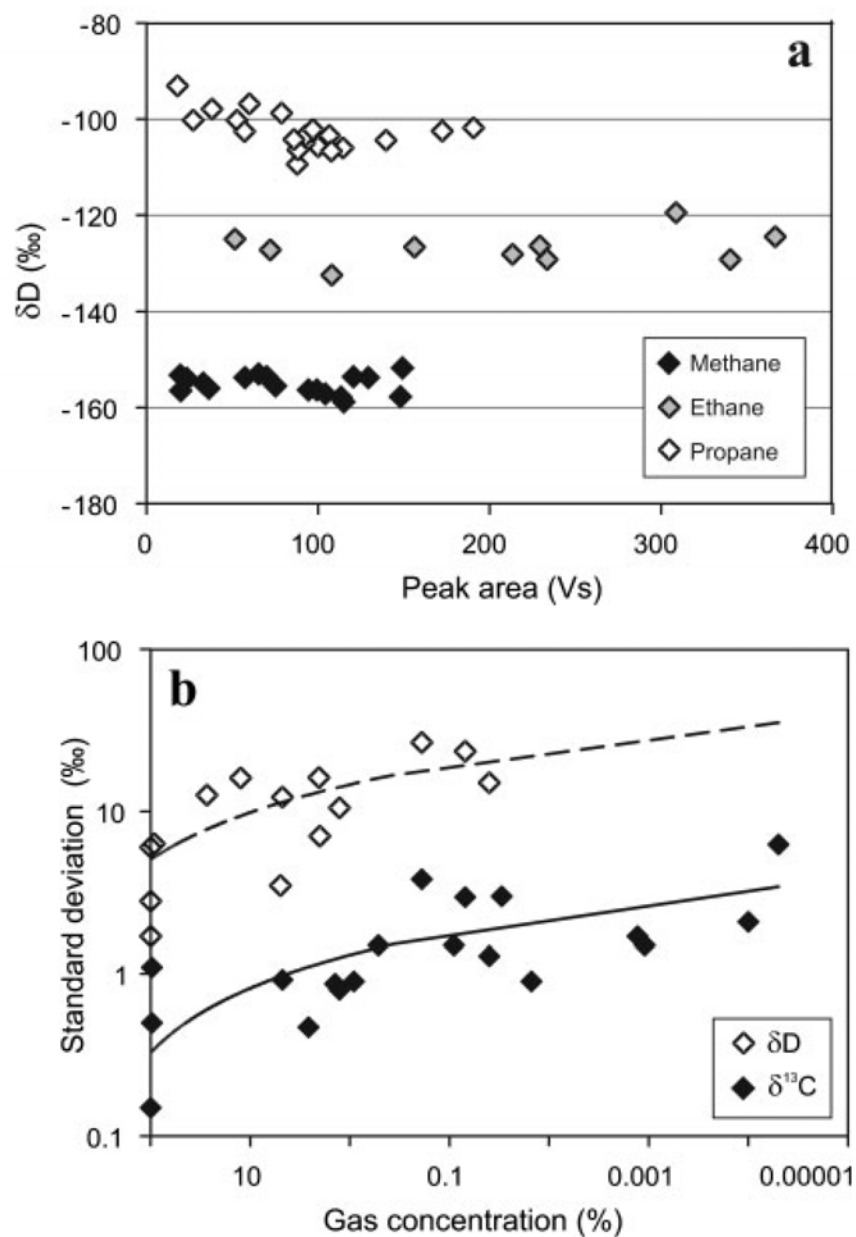
Fig. 3. Repeatability of $\delta^{13}C$ and δD values of GASIS-GC-ox/red-IRMS system as a function of peak areas (a) and concentrations (b); a) Multiple injections of the same gas mixture using varying sample sizes; b) Standard deviations of multiple runs of gas

2.3. Applications and significance

Our versatile GASIS inlet system can be applied to a variety of gas samples, including mixtures of gases containing hydrogen and/or carbon with individual component concentrations mixtures containing C_1-C_4 hydrocarbons of varying concentrations, with each point representing the standard deviation of one gas species that was analyzed at least four times. higher than 10 ppm (e.g. natural gases including coalbed (Strąpoć et al., 2007) and shale gases, pyrolysis gases, atmospheric gases, head space gases from microbial incubations). The GASIS inlet system conveniently allows the user to obtain relative gas concentrations and isotopic data for multiple gas species over a wide range of concentrations in a single GC-ox/red-IRMS run. The user can design individualized parameters for specific sample types by varying (i) sampling loop sizes, (ii) the timing of injections and back-flushes within the run, and (iii) the GC program over a wide temperature range.

References

Burgoyne, T.W., Hayes, J.M., 1998. Quantitative production of H_2 by pyrolysis of gas chromatographic effluents. Analytical Chemistry 70, 5136-5141.

Hayes, J.M., Freeman, K.H., Popp, B.N., Hoham, C.H., 1990. Compound-specific isotopic analyses: A novel tool for reconstruction of ancient biogeochemical processes. Organic Geochemistry 16, 1115-1128.

Henning, M.J., 2002. Development and assessment of inlet system for stable carbon isotopic analysis of individual compounds in gas mixtures. M.Sc. Thesis, Department of Geological Sciences, Indiana University, Bloomington, December 2002, 40p.

Hilkert, A.W., Douthitt, C.B., Schlüter, H.J., Brand, W.A., 1999. Isotope ratio monitoring gas chromatography / mass spectrometry of D/H by high temperature conversion isotope ratio mass spectrometry. Rapid Communications in Mass Spectrometry 13, 1226-1230.

Leckrone, K.J., Hayes, J.M., 1997. Efficiency and temperature dependence of water removal by membrane dryers. Analytical Chemistry 69, 911-918.

Merritt, D.A., Hayes, J.M., Des Marais, D.J., 1995. Carbon isotopic analysis of atmospheric methane by isotope-ratio-monitoring gas chromatography/mass spectrometry. Journal of Geophysical Research 100D, 1317-1326.

Miller, J.B., Mack, K.A., Dissly, R., White, J.W.C., Dlugokencky, E.J., Tans, P.P., 2002. Development of analytical methods and measurement of $^{13}C/^{12}C$ in atmospheric CH_4 from the NOAA Climate Monitoring and Diagnostic Laboratory Global Air Sampling Network. Journal of Geophysical Research 107D, 4178.

Morasch, B., Richnow, H.H., Schink, B., Meckenstock, R.U., 2001. Stable hydrogen and carbon isotopic fractionation during microbial toluene degradation: Mechanistic and environmental aspect. Applied and Environmental Microbiology 67, 4842-4849.

Quay, P., King, S.L., Stutsman, J., Wilbur, D.O., Steele, L.P., Fung, I., Gammon, R.H., Brown, T.A., Farwell, G.W., Grootes, P.M., Schmidt, F.H., 1991. Carbon isotopic composition of atmospheric CH_4: Fossil and biomass burning source strengths. Global Biogeochemical Cycles 5, 25-47.

Quay, P., Stutsman, J., Wilbur, D., Shover, A., Dlugokencky, E., Brown, T., 1999. The isotopic composition of atmospheric methane. Global Biogeochemical Cycles 13, 445.

Rice, A.L., Gotoh, A.A., Ajie, H.O., Tyler, S.C., 2001. High-precision continuous-flow measurement of $\delta^{13}C$ and δD of atmospheric CH_4. Analytical Chemistry 73, 4103-4110.

Schoell, M., 1983. Genetic characterization of natural gases. AAPG Bulletin, 67, 2225-2238.

Strąpoć, D., Mastalerz, M., Eble, C., Schimmelmann, A., 2007. Characterization of the origin of coalbed gases in southeastern Illinois Basin by compound-specific carbon and hydrogen stable isotope ratios. Organic Geochemistry 38, 267-287.

Tobias, H.J., Brenna, J.T., 1997. On-line pyrolysis as a limitless reduction source for high-precision isotopic analysis of organic-derived hydrogen. Analytical Chemistry 69, 3148.

Valentine, D.L., Chidthaisong, A., Rice, A., Reeburgh, W.S., Tyler, S.C., 2004. Carbon and hydrogen isotope fractionation by moderately thermophilic methanogens. Geochimica et Coscmochimica Acta, 68, 1571-1790.

Ward, J.A.M., Ahad, J.M.E., Lacrampe-Couloumbe, G., Slater, G.F., Edwards, E.A., Sherwood Lollar, B., 2000. Hydrogen isotope fractionation during methanogenic degradation of toluene: Potential for direct verification of bioremediation. Environmental Science and Technology, 34, 4577-4581.

CHAPTER 3

Carbon isotopic fractionation of CH_4 and CO_2 during canister desorption of coal*

Dariusz Strąpoć[1], Arndt Schimmelmann[1], and Maria Mastalerz[2]

[1]Department of Geological Sciences, Indiana University,
1001 E. Tenth Street, Bloomington, IN 47405-1405, U.S.A.
[2]Indiana Geological Survey, Indiana University, 611 N. Walnut Grove,
Bloomington, IN 47405-2208, U.S.A.

Abstract

Canister desorption of coal gas from freshly sampled coal is commonly used for exploratory assessment of the coalbed methane (CBM) potential of a basin or prospect, as well as for the sampling of gas for isotopic determination of the gas origin. Compositional and $\delta^{13}C$ isotopic time-series of desorbing CBM and carbon dioxide (CO_2) over 3 to 4 months demonstrate considerable compositional and isotopic shifts over time. Non-stationary chemical and isotopic characteristics are due to differences in diffusivity and adsorbance behavior of gas molecules and must be taken into account when attempting to reproducibly sample coal gases.

Off-line gas processing on a vacuum line and on-line GC/MS analyses were performed on coal gas samples from the Springfield and Seelyville coal members of Pennsylvanian age that were cored in the SE Illinois Basin in SW Indiana, USA. The coals cover a narrow range of maturity from 0.54 to 0.64% vitrinite reflectance. Methane initially desorbed faster than CO_2, resulting in 50% increase of the CO_2 content in bulk desorbing gas on the fiftieth day relative to the first day of desorption. After 50 days of desorption, about 90% of all coal gas was desorbed. Over the same time period, $\delta^{13}C$ values of incrementally sampled coal gas increased by 2‰ and 9‰, for CH_4 and CO_2, respectively, testifying to the greater retention of $^{13}CH_4$ and $^{13}CO_2$ relative to $^{12}CH_4$ and $^{12}CO_2$. An isotopic mass balance of the individual, sequentially desorbed and sampled gas amounts yielded weighted mean $\delta^{13}C_{CH4}$ and $\delta^{13}C_{CO2}$ values for characterizing the cumulatively desorbed gas. The overall mean $\delta^{13}C$ values were equivalent to $\delta^{13}C$ values of gases that desorbed at a time when half of the potentially available gas had been desorbed from coal, corresponding in this study to a time between day 5 and day 12 of

canister desorption at 15 to 18 ºC. The total expected gas volume and the ~50% midpoint can thus be approximated for a desorbing coal gas sample, based on a dynamic prediction after the first five days of canister desorption.

3.1. Introduction

The use of stable isotope ratios in coalbed methane (CBM) exploration requires a practical and reasonably fast method for desorbing and sampling of gas. Coal from freshly drilled cores is typically placed in desorption canisters (Gas Research Institute, 1995) from which desorbed gas is subsequently sampled for isotopic analysis. Desorption from coal proceeds over weeks and months, with gas yields decreasing exponentially over time and desorbed gases expressing isotope fractionation. In this study, we quantify gas speciation and isotopic fractionation along sequential desorption of methane and CO_2 from high-volatile, bituminous coal expressing a narrow range of maturity from 0.54 to 0.64% vitrinite reflectance (R_o). Our method for rapid partial canister desorption and gas sampling arrives at $^{13}C/^{12}C$ ratios (expressed as $\delta^{13}C$ values) that are representative of the total gas desorbed from the coal.

Stable isotope ratios of natural gases are routinely used to distinguish between geochemical sources of coal gases, for example, to discriminate between thermogenic and biogenic (i.e., microbially generated) gases (Schoell, 1983; Scott et al., 1994; Smith and Pallasser, 1996; Katz et al., 2002; Martini et al., 2003). Typical $\delta^{13}C_{CH4}$ values of thermogenic methanes range from -20 to -50‰, whereas biogenic methane from microbial acetate fermentation ranges ~ -45 to -65‰, and methane from microbial CO_2-reduction is even more depleted at ~ -60 to -110‰ (Scott, 1994; Jedrysek, 1995; Whiticar, 1996). Methane generated microbially via CO_2-reduction is typically accompanied by residual ^{13}C-enriched CO_2 with $\delta^{13}C_{CO2}$ ~ zero to 20‰, whereas thermogenic methane is typically associated with CO_2 ranging between -10 and -30‰ (Scott et al., 1994). Because thermogenic and biogenic gas mixtures express distinct

carbon isotopic characteristics in their methane and CO_2 components, the differences $\Delta\delta^{13}C_{(CH4-CO2)}$ range from 60 to 80‰ for biogenic, and from 20 to 40‰ for thermogenic gases (Smith et al., 1992). The diagnostic value of isotopic parameters of desorbed gases from coal can be compromised by isotope fractionation during partial gas desorption. Earlier observations noted increases in $\delta^{13}C$ of gases desorbing from Sydney Basin coal (Gould et al., 1987); (i) methane and CO_2 emanating from 20-liter drums filled with 2- to 10-cm-diameter coal lumps increased their $\delta^{13}C$ values over five months by 5.0 to 10.0‰ and by 2.5‰, respectively; (ii) methane from a pillar borehole became enriched in ^{13}C by 4.0‰, and from a virgin coal borehole by 1‰. It was suggested that carbon isotopic shifts of individual gas species ($\Delta\delta^{13}C$) are diffusion-controlled and decrease with increasing size of the desorbing body of coal. A canister-desorption study of Sydney Basin CBM found 1 to 2‰ ^{13}C-enrichment in CH_4 over two weeks for coals ranging in vitrinite reflectance R_o from 0.7 to 1.5% (Faiz et al., 2002). CBM desorbing over one month from higher-rank (R_o 2.6 – 3.7%), vitrinite-rich coal from the Qinshui Basin expressed an even larger $\Delta\delta^{13}C_{CH4}$ of 3 to 15‰ (Hu et al., personal communication). A recent study by Niemann et al. (2005) reports ^{13}C-enrichment of CBM desorbing form coals across a wide range of maturities.

3.2. Materials and methods

Whole cores were obtained from Springfield and Seelyville coal members in Sullivan and Gibson counties, Indiana, in the southeastern part of the Illinois Basin, from depths between 114 and 170 m (374 – 560 ft) (Table 1). These high-volatile bituminous coals of Pennsylvanian age with R_o from 0.54 to 0.64% are potential CBM targets in

31

Coal seam	County	Depth (m)	R_o (%)	No. of gas samples for $\delta^{13}C$ analyses during desorption	Coal core name
Seelyville	Sullivan	128	0.62	11	V-3/1
Seelyville	Sullivan	170	0.64	3	IV-3/4
Springfield	Sullivan	114	0.59	3	III-5
Seelyville	Gibson	137	0.64	3	II-3/2
Seelyville	Gibson	138	0.54	6	II-3/5
Seelyville	Gibson	139	0.57	4	II-3/7

Tab. 1. Coal samples analyzed for coal gas desorption in this study. Gases from coal sample V-3/1 were analyzed both off-line and on-line for comparison. Desorbed gases from all coals were sampled and excess gases were vented on a daily basis, except for coal sample II-3/5 where desorbed gas volumes were sampled in six steps without any venting between measuring and sampling, each step representing 5 to 30% of the total gas volume. V-3/1, IV-3/4, etc. represent sample designations given in the field.

Indiana (Drobniak et al., 2004; Mastalerz et al., 2004). Immediately after recovery of a whole core in the field, one or more coal core segments with a diameter of ~7.6 cm (3 inch) and a length of ~30 cm (1 ft) were quickly sealed in a nitrogen-purged desorption canister with a 2.7-liter internal volume. Desorption took place at ambient pressure and temperature of ~15 to 18 ºC first in the field and subsequently in the laboratory, similar to reservoir temperatures for Indiana coals.

Desorbed gas was measured using a volume displacement apparatus (Fig. 1), following the standard canister desorption protocol (Gas Research Institute, 1995) until desorption completely ceased and the total desorbed gas volume and coal gas content were obtained. At selected time intervals, mostly on daily basis, the desorbed gas volumes were volumetrically measured and either vented or selected samples were taken for compositional and isotopic analyses. The frequency of volumetric measurement of desorbing gas and venting was highest in the first 24 hours, followed by increasingly longer intervals between measurements to ensure that sufficient gas was available for individual analyses. Most data are thus time-series with unequal spacing. The rapid series of initial gas desorption measurements within minutes to hours after coring allows to back-extrapolate the rate of desorption to the "time zero" of coal coring, and thus, to estimate the volume of gas lost during the time (usually about thirty minutes) between coring and sealing of the fresh coal in desorption cylinders in the field (Diamond and Levine, 1981).

Desorbed gas volumes from coal sample II-3/5 were sampled and vented in only six steps without venting in between steps. Five of the six gas samples represented 5 to
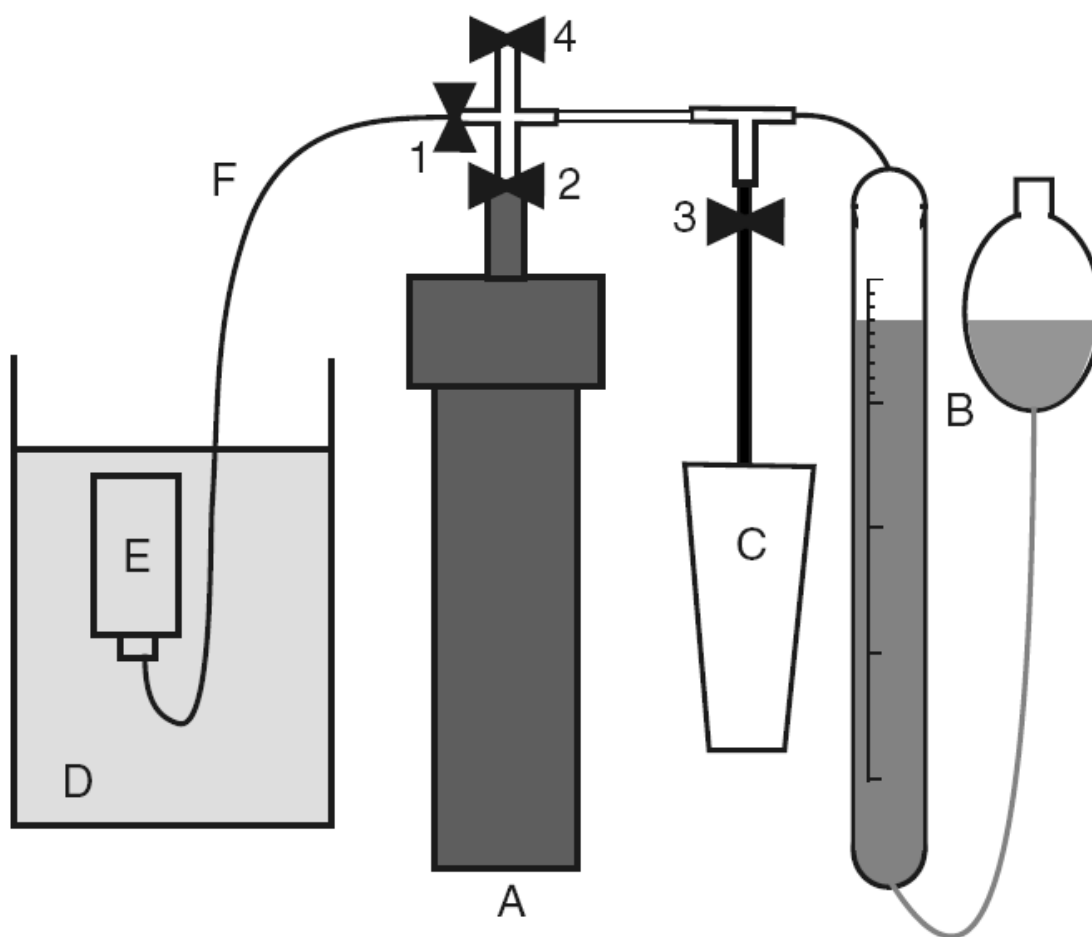
Fig. 1. Apparatus for volumetric measurements and sampling of desorbed coal gas. A - desorption canister, B -volume displacement apparatus, C - pressurized N_2 container, D – deionized water with bezalkonium chloride, E – inverted sample bottle, F – flexible tubing, 1,2,3,4 - valves. Procedure: purging of tubing (2, 4 – closed; 1, 3 opened; tip of F outside of E; then 4 opened to release overpressure of N_2), volume measurement (1, 3, 4 closed, 2 opened), sampling (1 opened), venting (4 opened).

37% of the total gas volume. This approach permitted a complete isotopic mass-balance calculation for sample II-3/5, thus characterizing the entire gas volume compositionally and isotopically. This sample represents the same coal bed (Seelyville) as most of the samples analyzed in this paper.

Gas from desorption canisters flowed through flexible tubing and was bubbled into inverted, water-filled 50 ml glass bottles held under deionized water (Fig. 1). Prior to sampling, a microbicide (benzalkonium chloride, 2 g/l) had been added to the water to prevent microbial loss or generation of gas components during storage, and all dead volumes, including the gas sampling tubing, had been purged with nitrogen. Each partially gas-filled glass sample bottle was closed with a rubber septum, crimp-sealed, and stored in inverted position with an internal water level ~1 cm above the rubber septum, thus limiting the diffusion and loss of hydrophobic hydrocarbon gases during storage. The volume of water in bottles was limited (1-2 ml) to minimize any isotopic fractionation owing to partial dissolution of gases in water. For example, a ~3% vol:vol solubility of methane in water at atmospheric pressure and room temperature could fractionate the gaseous methane relative to the dissolved methane by about -0.3‰ (Fuex, 1980) to -0.6‰ (Bacsik et al., 2002) for carbon. At the same time, an isotope fractionation factor $\alpha^{13}C_{(bicarbonate-CO2)}$ of 1.008 in the $CO_2 - HCO_3^-$ system (Szaran, 1997) can lead to ~1.3‰ ^{13}C-depletion of gaseous CO_2 relative to DIC, assuming a CO_2 partial pressure of 2 kPa (0.02 bar) and 16% CO_2-solubility in water, based on Henry's Law.

For off-line isotopic analyses, methane aliquots were collected on a vacuum line with a Toepler pump and sealed in 9 mm o.d. quartz ampoules together with copper (II)

oxide. Following combustion of methane in the sealed quartz ampoules at 800°C, the oxidation products H_2O and CO_2 were cryogenically separated on a vacuum line and CO_2 samples were sealed in 6 mm o.d. Pyrex® tubes. Values of $\delta^{13}C_{CO2}$ were determined in manual dual-inlet mode using a Finnigan MAT 252 stable isotope mass-spectrometer.

Some coal gases that were analyzed off-line were also analyzed on-line for gas composition and compound-specific $\delta^{13}C$ values using a Finnigan 252 irm-GC/MS system. A customized GASIS injection system (Henning, 2002) with injection loops of 0.06μL for methane and 0.5 μL for CO_2 was used to inject gas aliquots onto a PoraBOND Q gas chromatographic column for compound separation. Following on-line combustion, integrated CO_2 peak areas were used to quantify relative abundances of gas components. All $\delta^{13}C$ values presented in this paper are calibrated against NBS-19 having a $\delta^{13}C$ value of exactly +1.95‰ on the VPDB scale. Analytical errors for $\delta^{13}C$ are: for methane determined off-line ±0.18‰ (standard deviation for five replicate determinations), for methane on-line ±0.22‰ (two sets of three replicates), and for CO_2 on-line ±0.89‰ (two sets of duplicates and one set of three replicates).

3.3. Results

3.3.1. Methane.

The data in $\delta^{13}C_{CH4}$ time-series show similar patterns for off-line and on-line data reflecting 10 desorbing CBM gas samples from coal sample V-3/1 (Fig. 2). The ~2‰ increase in $\delta^{13}C_{CH4}$ over 3 months of desorption appears to be linearly related to the desorbed methane as a fraction of total coal gas desorbed (Fig. 2A). A systematic ~0.3‰ offset between on-line and off-line data is likely due to different preparations and inlet

a

b
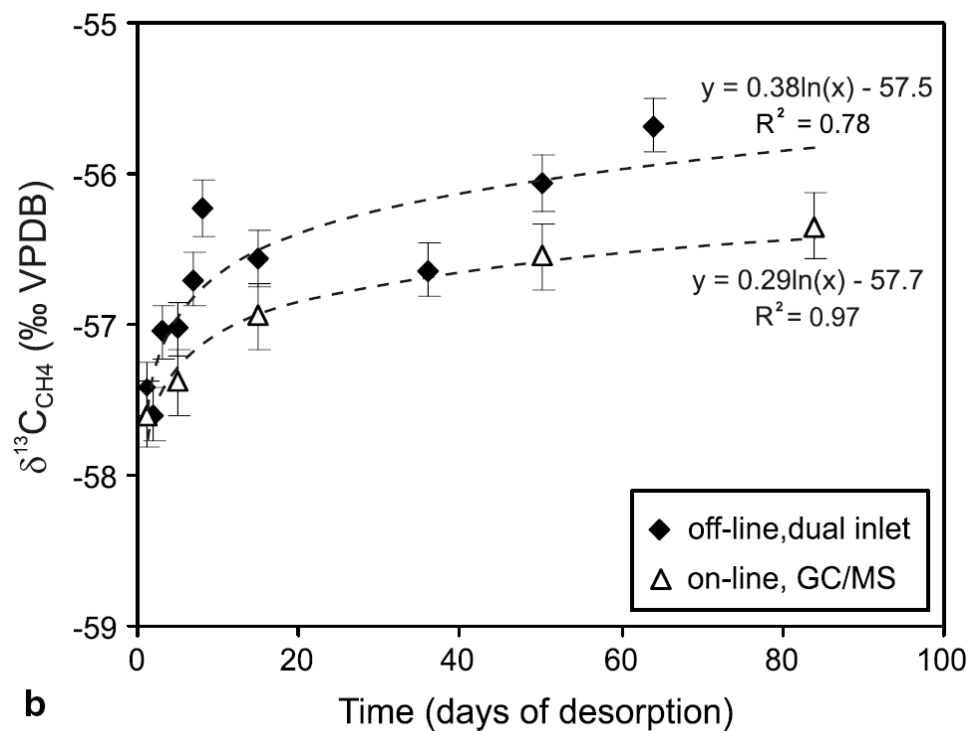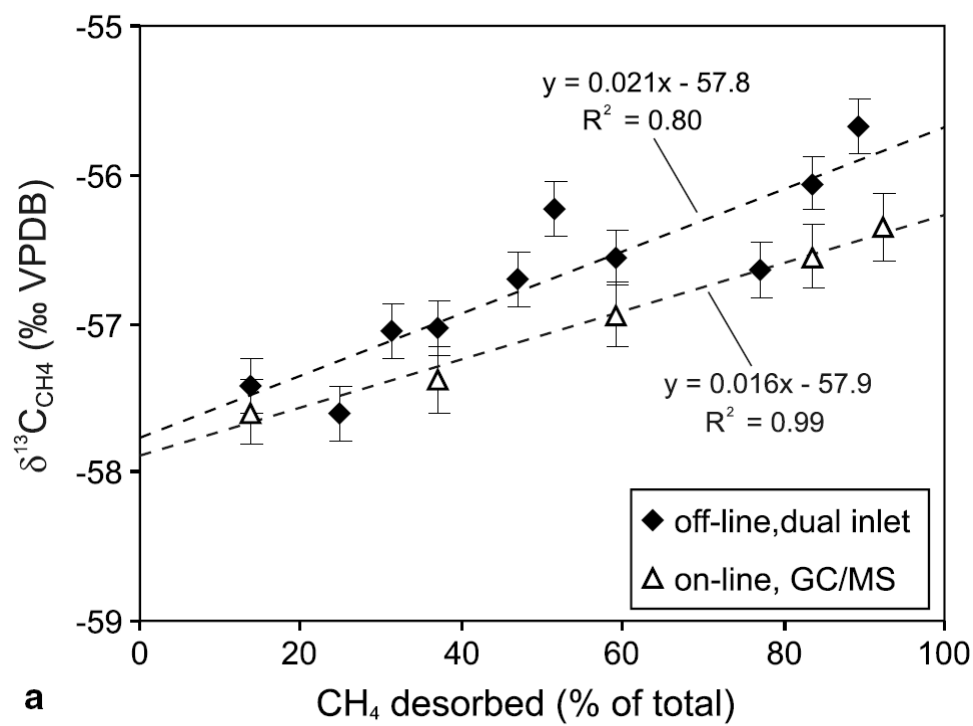
Fig. 2. Carbon isotopic changes of methane during coalbed gas desorption from coal sample V-3/1: a - scaled to percentage of methane desorbed; b - scaled to the duration of desorption.

modes of calibration gases, but is not relevant for the purpose of this study. A logarithmic relationship between $\delta^{13}C_{CH4}$ and the duration of desorption (Fig. 2B) is similar to the relationship between cumulative desorbed gas volume and time (Fig. 3).

Weighted mean values of $\delta^{13}C_{CH4}$ for cumulative CBM from each coal sample were calculated via mass balances derived from volumetric measurements of desorbing gas over time (Tab. 2, Figs. 3 and 4). At a late stage of desorption, when ~95% of gas was already desorbed, sampling of gases was not possible on a daily basis because incremental daily volumes were insufficient. Figure 3 shows $\Delta\delta^{13}C_{CH4}$ deviations of individual gas samples from the weighted $\delta^{13}C_{CH4}$ mean as they relate to the fraction of desorbed CH_4 from six canisters (Tab. 1). The $\Delta\delta^{13}C_{CH4}$ pattern over the fraction of desorbed CBM from five canisters matches the pattern observed for coal sample V-3/1 (Fig. 2A). The overall weighted mean $\delta^{13}C_{CH4}$ 'midpoint' value is best approximated by CBM samples that were taken when 33 to 66% of total CBM had been desorbed (Fig. 4). CBM desorbing from coal sample II-3/5 was vented only six times coincident with six sampling steps that were at least 7 days apart from each other. Interestingly, the six individual $\delta^{13}C_{CH4}$ values for sample II-3/5 did not increase over the duration of desorption and stayed within the confidence interval of the weighted mean $\delta^{13}C_{CH4}$ (Fig. 5).

3.3.2. Carbon dioxide.

Our limited matrix of four $\delta^{13}C$ values for desorbing CO_2 from coal core V-3/1 suggests that the carbon isotope fractionation is about 5 times larger for CO_2 (Fig. 6) than for CBM during desorption (Fig. 2). There is a 9‰ difference between the first sample of desorbed CO_2 (first day of desorption with 10% of CO_2 desorbed) and the last sample

Table 2
Carbon isotopic data collected for desorbed coal gas fractions

Sample	Day of desorption	Fraction of gas desorbed up to date of sampling	δ^{13}C CH$_4$ (‰)	Fraction of total gas represented by δ^{13}C	Weighted average δ^{13}C (‰)	$\Delta\delta^{13}$C (daily sampling minus weighted average) (‰)	CH$_4$ (%)	C$_{2,3,4}$ (%)	CO$_2$ (%)	δ^{13}C CO$_2$ (‰)
V-3/1 (off-line)	1	0.14	−57.42	0.19		−0.69	n.d.	n.d.	n.d.	n.d.
	2	0.25	−57.60	0.09		−0.87	n.d.	n.d.	n.d.	n.d.
	3	0.31	−57.05	0.06		−0.32	n.d.	n.d.	n.d.	n.d.
	5	0.37	−57.03	0.08		−0.30	n.d.	n.d.	n.d.	n.d.
	7	0.47	−56.70	0.07		0.03	n.d.	n.d.	n.d.	n.d.
	8	0.51	−56.23	0.06		0.50	n.d.	n.d.	n.d.	n.d.
	15	0.59	−56.56	0.13		0.17	n.d.	n.d.	n.d.	n.d.
	36	0.77	−56.64	0.12		0.09	n.d.	n.d.	n.d.	n.d.
	50	0.84	−56.06	0.06		0.67	n.d.	n.d.	n.d.	n.d.
	64	0.89	−55.68	0.14	−56.73	1.05	n.d.	n.d.	n.d.	n.d.
V-3/1 (on-line)	1	0.14	−57.60	0.25		−0.56	98.00	0.015	1.99	6.92
	5	0.37	−57.38	0.23		−0.34	97.46	0.022	2.52	12.54
	15	0.59	−56.94	0.20		0.10	97.02	0.015	2.97	15.27
	36	0.77	−56.55	0.12		0.49	97.02	0.019	2.96	15.65
	50	0.84	−56.35	0.20	−57.04	0.69	n.d.	n.d.	n.d.	n.d.
IV-3/4 (off-line)	1	0.15	−60.06	0.20		−0.11	n.d.	n.d.	n.d.	n.d.
	2	0.25	−60.17	0.21		−0.22	n.d.	n.d.	n.d.	n.d.
	13	0.56	−59.84	0.59	−59.95	0.11	n.d.	n.d.	n.d.	n.d.
III-5 (off-line)	1	0.17	−55.47	0.30		−0.09	n.d.	n.d.	n.d.	n.d.
	6	0.43	−55.52	0.22		−0.14	n.d.	n.d.	n.d.	n.d.
	19	0.61	−55.26	0.48	−55.38	0.12	n.d.	n.d.	n.d.	n.d.
II-3/2 (off-line)	5	0.40	−56.86	0.65		−0.33	n.d.	n.d.	n.d.	n.d.
	57	0.89	−56.02	0.29		0.51	n.d.	n.d.	n.d.	n.d.
	95	0.98	−55.55	0.06	−56.53	0.98	n.d.	n.d.	n.d.	n.d.
II-3/7 (off-line)	1	0.14	−61.17	0.54		−0.67	n.d.	n.d.	n.d.	n.d.
	70	0.94	−59.82	0.42		0.68	n.d.	n.d.	n.d.	n.d.
	95	0.98	−58.59	0.04	−60.50	1.91	n.d.	n.d.	n.d.	n.d.

Tab. 2. Carbon isotopic data collected for desorbed coal gas fractions. Weighted average values are calculated via mass balances derived from volumetric measurements of gas desorbed over time.
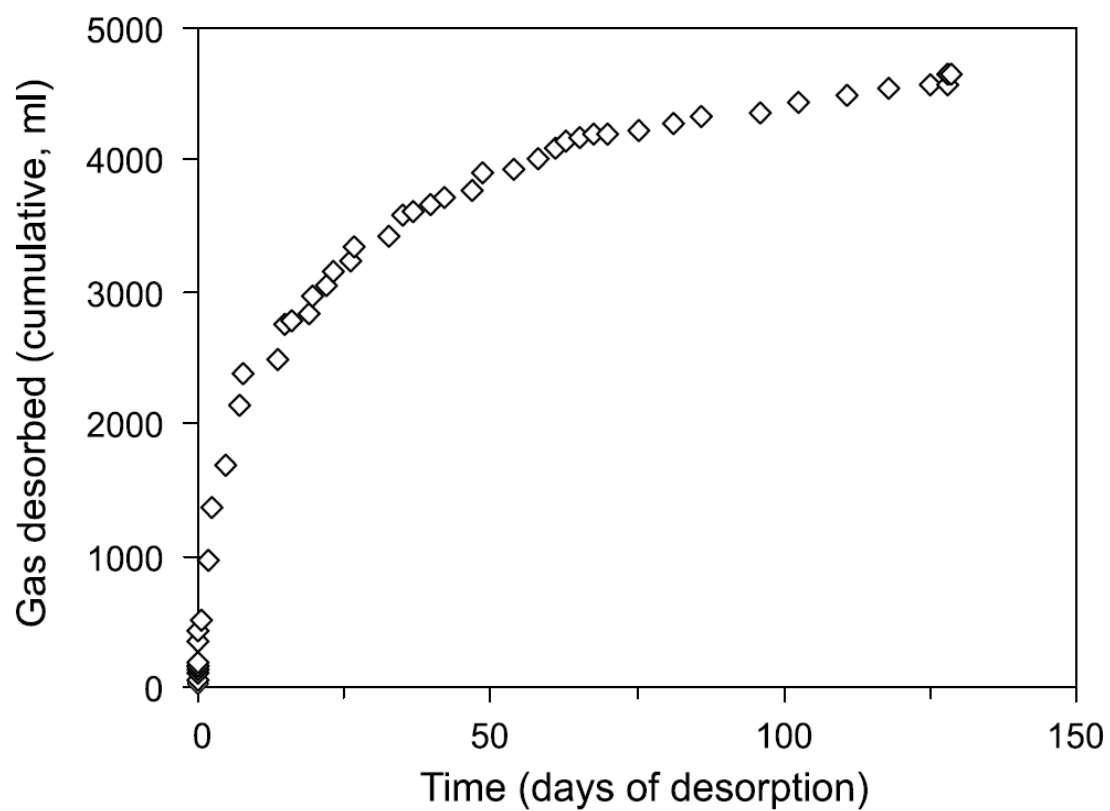
Fig. 3. Cumulative desorption curve of gas from coal sample V-3/1.

Fig. 4. Carbon isotopic differences between individual methane measurements and the weighted mean value for each canister (based on off-line data from six desorption canisters from which gas was vented on daily basis). The weighted mean is represented by the horizontal zero line. Thick horizontal lines represent average values for three desorption intervals. The average δ^{13}C value for the 33 to 66% desorption interval (grey rectangle) most closely approximates the overall weighted mean value (zero line).

Fig. 5. $\delta^{13}C_{CH4}$ values for coal sample II-3/5. Desorbed gas volumes were measured, sampled, and vented only six times, allowing at least seven days of equilibration between consecutive measurements. Dotted line represents weighted mean $\delta^{13}C$ value of the entire methane volume.

Fig. 6. Changes of $\delta^{13}C_{CO2}$ versus changes in CO_2 content (A) and versus $\delta^{13}C_{CH4}$ (B) during coal gas desorption from coal sample V-3/1. Numbers in brackets indicate the percent of total CO_2 desorbed at the time of sampling. Dashed lines guide the eye along paths of desorption.

(fiftieth day, 95% of CO_2 desorbed). This isotopic shift is accompanied by a gradual increase in the CO_2 content of the desorbing gas mixture (Fig. 6A). The percentage of desorbed CO_2 for a particular day was calculated by extrapolating gas chromatographic data (peak areas) onto the volumetric measurements of desorbing total coal gas.

3.4. Discussion

3.4.1. Carbon isotopic changes and representative sampling of coal gas.

Canister desorption is primarily used for coal gas content estimation by volumetric measurements of desorbing coal gases on a daily basis. The daily sampling of gas for geochemical analyses is typically followed by venting of excess gas. Alternatively, accumulation of gas can proceed over many days without intermittent measurements and venting (e.g., coal sample II-3/5 in this study). Although the latter approach seems to offer isotopically representative coal gas samples (see below), it also has disadvantages. First, it does not allow back-extrapolation for estimating the gas that is lost between coal core retrieval and the sealing of coal in desorption canisters. Also, less frequent venting of excess gas causes larger intermittent pressure buildup in the headspace of the canister and distorts the pattern of desorption that would otherwise be observed at consistently low ambient pressures. Given the fact that dynamic canister desorption with daily volume measurement and subsequent venting of gas is the generally preferred technique, a feasible method for collecting isotopically representative gas samples is needed.

Representative and reproducible sampling of desorbing coal gas mandates that the sampling strategy accounts or compensates for carbon isotopic changes of methane and

CO$_2$ during desorption. The timing of sampling is especially important when a gas sample needs to be representative of the theoretical entire gas volume. In Figure 4, the horizontal "zero-line" (representing the mass balance-based average $\delta^{13}C_{CH4}$ value for each of the canisters) is close to the average $\delta^{13}C_{CH4}$ value for CBM samples taken when 33 to 66% of the entire gas volumes had already been desorbed. For coal sample V-3/1, mass-balance calculations based on daily desorption measurements indicate that isotopically representative "average gas" desorbs when 48% (according to off-line data) or 52% (on-line data) of the total gas has already been desorbed and removed. Thus, a ~50% desorption midpoint is suggested for taking representative gas samples for carbon isotopic CBM analysis. This opportune time window for gas sampling occurred in our coals between the fifth and the twelfth day of desorption (Fig. 7A).

The absence of a large isotopic variance over time in coal gas desorbed from coal sample II-3/5 (Fig. 5) may be due to the considerable length of time (>7 days) allowed between each of the six sampling events. Longer re-equilibration between desorbed and sorbed gas may have reduced any kinetic isotope fractionation associated with initial rapid desorption following the venting of earlier desorbed CBM. A slightly lower vapor pressure (or slightly higher boiling point) of isotopically heavier molecules can probably influence the isotopic separation between sorbed and desorbed phases if equilibrium was reached after >7 days, but our data suggest this fractionation effect to be minor. In contrast, the dynamically desorbing samples with daily volumetric measurement and venting of freshly desorbed CBM from other coal samples (i.e., non-equilibrium conditions) fostered the expression of a kinetic isotope effect (Figs. 2, 4, 6), whereby $^{13}CH_4$ and $^{13}CO_2$ molecules diffused slower out of coal than $^{12}CH_4$ (Gould et al., 1987;
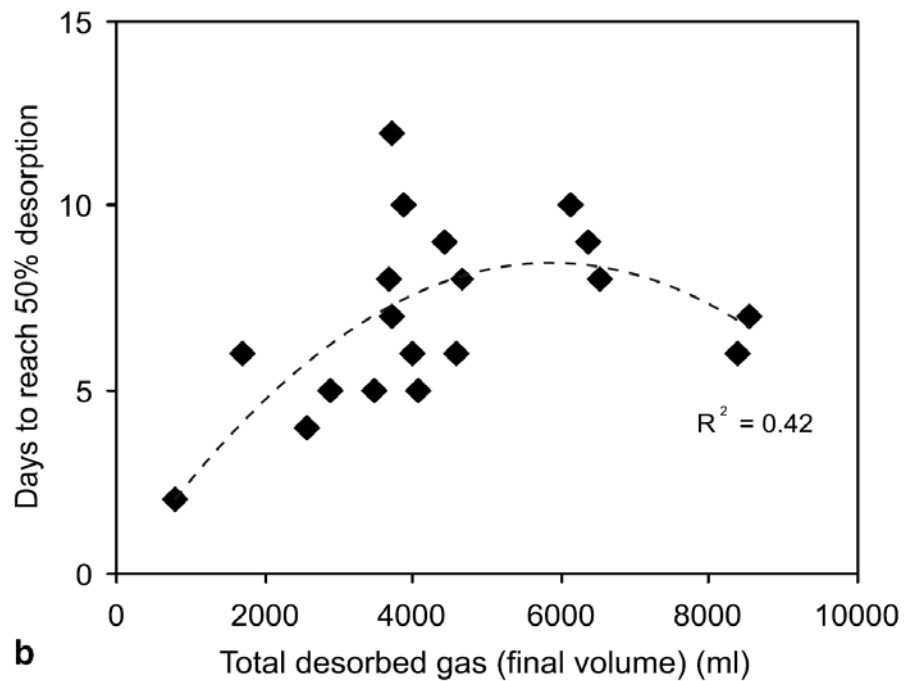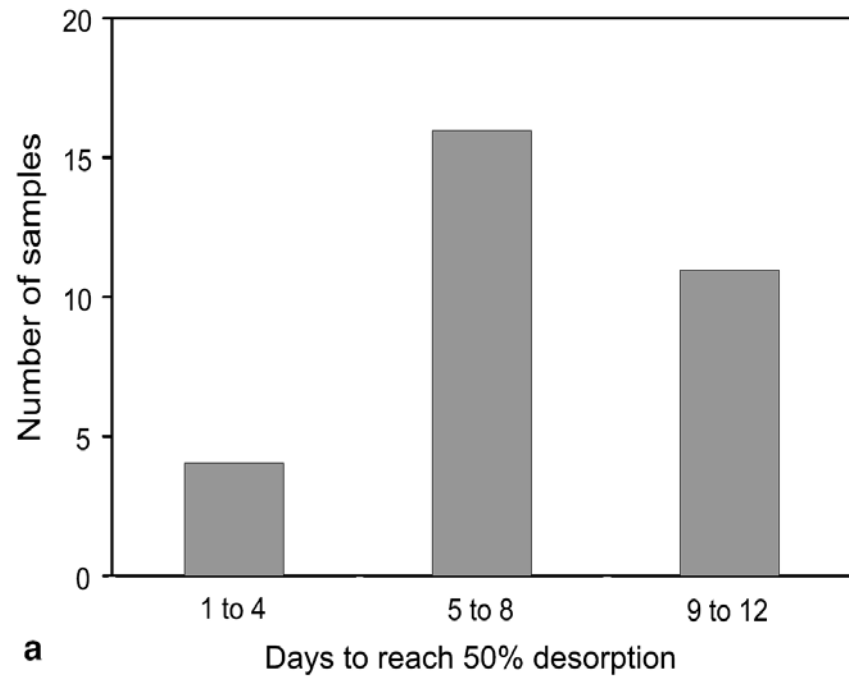
Fig. 7. A - Histogram depicting the timing of midpoint gas desorption from 31 canisters using Illinois Basin Pennsylvanian coals; B – Dependence of timing of desorption midpoint on the total desorbed gas (final volume, obtained when desorption ceases, usually after three months) for 19 canisters using Seelyville coal. The solid line is a 2nd order polynomial regression.

Faiz et al., 2002; Hu et al., personal communication) and $^{12}CO_2$ (Gould et al., 1987) (Fig. 6B).

The timing of the ~50% desorption midpoint can be predicted from closely-spaced early desorption measurements. We compared the timing of midpoints with the total desorbed gas volumes, in order to better constrain the midpoints within their estimated 5- to 12-day window of occurrence. Theoretical total gas volumes could be predicted by extrapolating volumetric data from the first five days of desorption (Fig. 8). An example of the correspondence between total desorbed gas and the timing of midpoint desorption is shown in Fig. 7B for Seelyville coals. The scatter of data may result from the coals' variability in maceral composition, moisture and ash content, and pore-size distribution influencing gas desorption.

3.4.2. Diffusion-controlled carbon isotopic variability of desorbing coal gases

The initial release of molecules from an adsorption site could fractionate gas isotopically according to Langmuir desorption, but the small differences between physical properties (i.e. boiling point) of isotopically lighter and heavier molecular species suggest limited associated fractionation. This is corroborated by our observation that $^{13}CO_2/^{12}CO_2$ is about four times more fractionated than $^{13}CH_4/^{12}CH_4$, although the relative molecular mass difference for $^{13}CH_4$ and $^{12}CH_4$ (1/16) is much larger than for $^{13}CO_2$ and $^{12}CO_2$ (1/44). Furthermore, no isotopic fractionation of CH_4 was observed in sample II-3/5, where much time was allowed for equilibration between adsorbed and free gas.

Although negligible fractionation seems to occur during the initial release of gas molecules from adsorption sites, much stronger isotopic fractionation results from the
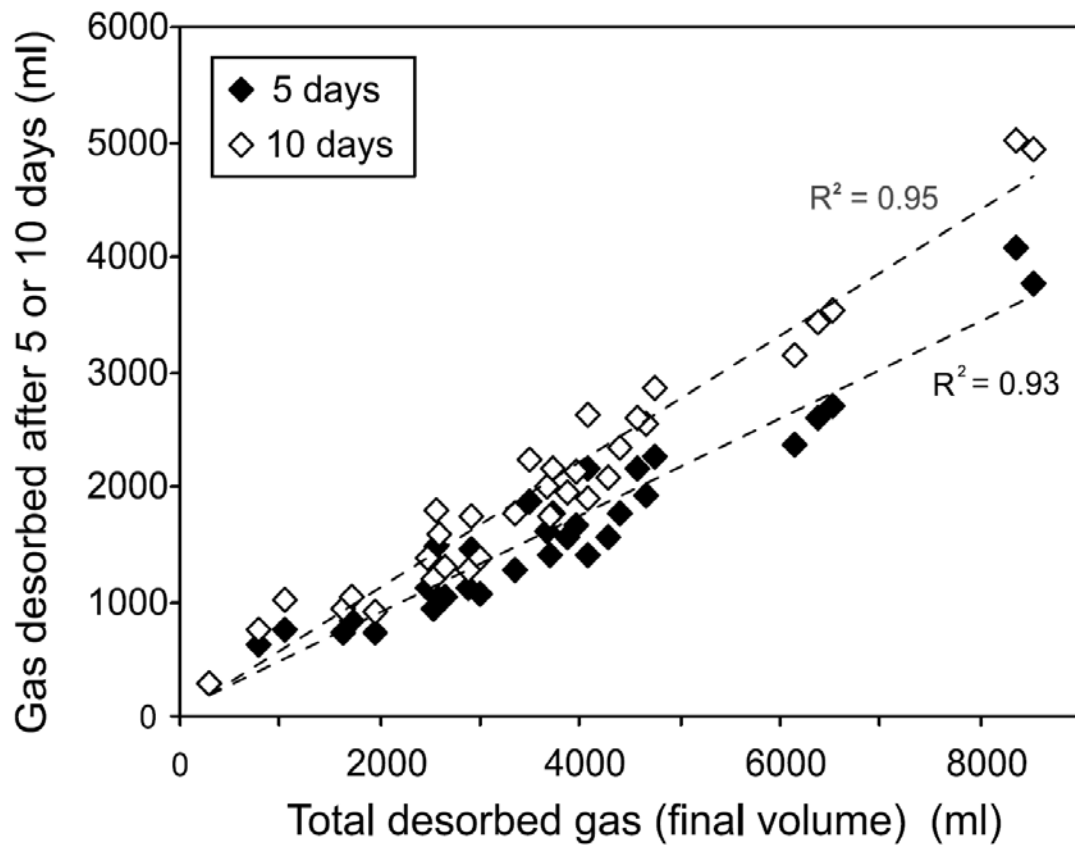
Fig. 8. Relationships between measured cumulative gas volumes after 5 or 10 days of desorption and total desorbed gas. These relationships can be used to predict total gas volume via extrapolation of shorter-term initial desorption measurements. The data are based on over 30 canister samples from Illinois Basin Pennsylvanian coals.

subsequent diffusional transport of gas through microporous coal. Isotopic fractionation via diffusion through micropores intensifies with increasing coal maturity (Fig. 9), because the relative abundance of micropores increases (Clarkson et al., 1993). We hypothesize that under non-equilibrium conditions of frequent venting of gas and dynamic desorption of new gas the differences in diffusivity between [13]C- and ^{12}C-containing methane and CO_2 molecules are likely controlling kinetic isotope effects during coal gas desorption. Kinetic isotope effects imply that ^{12}C-containing molecules diffuse faster in microporous coal than ^{13}C-containing molecules of the same chemical species (Fig. 6B). Similar diffusion-related carbon isotopic fractionation of methane migrating through shale cores was observed in laboratory experiments by Zhang and Krooss (2001). Fractionation of gaseous hydrocarbons via diffusive transport into gas reservoirs was proposed by Prinzhofer and Permaton (1997) for some natural gas accumulations.

Gas transport in coal occurs in different modes depending on pore size. In micropores ($\varnothing$ <2nm; according to Harpalani and Chen, 1997), desorption and diffusion of gases are strongly affected by (i) gas adsorption affinities in slit-shaped pores typical for coals, (ii) by diffusion via molecule-pore wall collisions (Knudsen diffusion), and (iii) by surface diffusion (hopping of adsorbed gas molecules from one adsorption site to another) (Cui et al., 2004; Gudmundsson, 2003). Transport of gases in macropores ($\varnothing$ >50nm) is dominated by viscous flow or continuum diffusion (molecule-molecule collisions) (Cui et al., 2004; Faiz, 2004). In the latter mode of transport, the flow of gas is only slightly restricted and the isotopic effect during diffusion out of macropores and cleats may be limited. In contrast, isotopic fractionation can be expected from the more
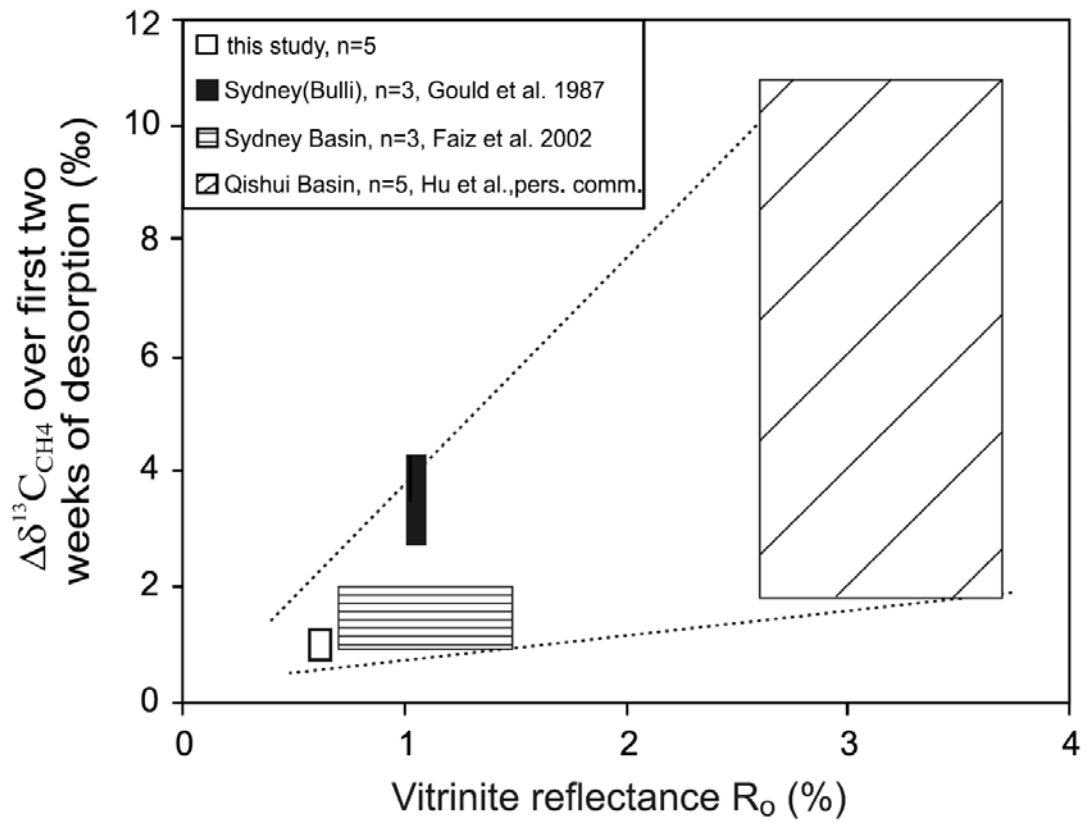
Fig. 9. Changes in $\delta^{13}C$ of CH_4 over the first two weeks of coal gas desorption from coals of various maturities. Rectangular fields represent ranges of data (R_o and $\Delta\delta^{13}C$) provided in the literature.

restricted flow of gas out of a three-dimensional network of micropores (Radovic et al., 1997) when gas molecules are strongly interacting with micropore walls.

Gas flow constriction is enhanced in more mature coals with R_o>1.5% because (i) micropores constitute a larger portion of the overall porosity (Clarkson et al., 1993; Bustin, 2000) and (ii) additional micropore-dominated secondary porosity is generated via cracking of higher hydrocarbons and the loss of volatiles (Rodrigues and Sousa, 2002). Limited data (Fig. 9) support the hypothesis that more mature coal with increasingly important microporosity leads to more efficient "molecular sieving" and larger isotope effects during coal gas desorption. Late desorbed methane can differ isotopically from early desorbed methane by 2 to 16‰.

Additional factors influencing the isotopic fractionation of desorbing coal gases may include maceral composition, the presence of competing fluids such as moisture and higher molecular-weight hydrocarbons, in-situ stress, overpressure, and coal shrinkage or swelling. All these factors contribute to the diffusion coefficient. Large isotopic fractionation during diffusion suggests a small diffusion coefficient, which implies possible high coal gas content (e.g., in the greater Green River Basin; Scott and Ambrose, 1992).

3.4.3. Gas compositional variability

Coal gases are mainly adsorbed on the microporous structure of the organic coal matrix (Bustin and Clarkson, 1996; Faiz et al., 2002) due to physical (not chemical) attraction including van der Waals and electrostatic forces (Yee et al., 1993). Spontaneous desorption of adsorbed gases is initiated by changes in pressure and temperature from reservoir to canister conditions (canister temperatures approximated

reservoir temperatures in our experiments). Some gas species are more strongly kept adsorbed on coal than other gases (i.e., CH_4 will desorb preferentially and faster than CO_2), depending on adsorption affinities and geometries of gas molecules and pores in coal. The linear structure, small molecular size, and electric properties of the CO_2 molecule (O=C=O) translate into a high adsorption affinity for most pore sizes in coal (Cui et al., 2004), whereas the tetrahedral and more voluminous molecular structure of CH_4 limits its adsorption affinity.

Sorption capacity increases with increasing molecular weight of a sorbed gas species following Langmuir's theory. The theory compares adsorption/desorption to evaporation/condensation processes, in which heavier gas tends to have a higher boiling point and therefore is more strongly sorbed to a solid phase. The ratio of sorption capacities of CO_2 and methane in coal is typically 2:1 or higher. Their sorption ratio in Indiana coals averages ~ 4:1 (Mastalerz et al., 2004), including coals used in this study. As a consequence, we observe a relatively small CO_2 concentration in bulk gas at the beginning of desorption, followed by increasing CO_2 concentrations with ongoing depletion of adsorbed gases in coal.

This compositional fractionation of desorbing coal gas could be alternatively explained by decreasing pressure (e.g., during prolonged gas production) causing an increase in relative sorption capacities for CO_2 over CH_4 on coal (Arri et al., 1992). However, all our desorption experiments, except one, took place at ambient pressure with daily venting of desorbed gas. Therefore, we can exclude pressure decrease as a major factor controlling gas compositional variability during our canister desorption experiments.

3.4.4. Implications

3.4.4.1. Coal gas origins

The observed ~2‰ isotopic fractionation in $\delta^{13}C_{CH4}$ during desorption of CBM from low-rank (high-volatile bituminous) coal far exceeds the experimental uncertainty of $\delta^{13}C$ determination. If improper partial sampling of coal gas fails to account for fractionation, an error in $\delta^{13}C_{CH4}$ of up to ~2‰ (or more in higher rank coals), together with a respective error in $\delta^{13}C_{CO2}$ of up to ~9‰, can lead to improper classification of coal gases, or at least to ambiguity much larger than typical analytical error. For example, the distinction between thermogenic, mixed and microbial gas origins can be blurred (Fig. 10), especially for detailed studies where biogenic and thermogenic end-members can be more precisely constrained than the general fields suggest in Fig. 10. End-member gases can be obtained by pyrolysis and culturing experiments for a particular coal.

Imprecise $\delta^{13}C_{CH4}$ results may also lead to improper estimation of biogenic gas participation in bulk coal gas (Chung et al., 1988) where ± 2‰ error can lead to about ± 10% difference. This is important for basins with mixed origin of gases where admixing of secondary biogenic gases might be significant. For example, in regions with low maturity coals (i.e. basin margins), the biogenic contribution can be the deciding factor for the CBM potential, for example in the eastern Illinois Basin, where low maturity coals with low thermogenic gas potential feature 50% or more secondary biogenic methane contribution (Strąpoć et al., 2005). Some basins with high coal rank may be expected to contain purely thermogenic gases, but post-coalification microbial gas may have been added following uplift and introduction of meteoric water and bacteria into permeable coal (e.g., Zongdulak Basin; Hoşgörmez et al., 2002).
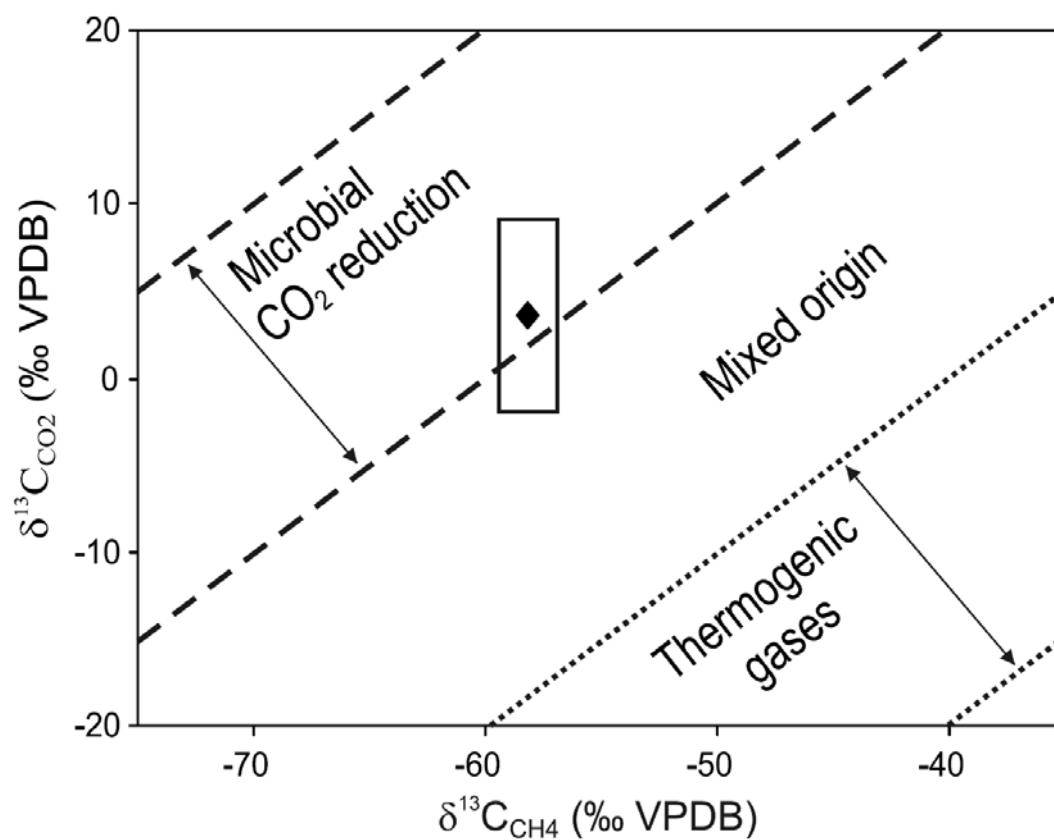
Fig. 10. Genetic classification of coalbed gases with three distinguishable fields, according to Smith and Pallasser (1996). The filled diamond (♦) indicates the average for Seelyville coal gas. Symbol size relates to the typical analytical error. The rectangle around the symbol relates to the expected desorption-related isotopic variance in $\delta^{13}C$ of CH_4 and CO_2.

3.4.4.2. CBM production

In addition to an isotopic bias caused by inappropriate gas sampling from canisters affecting the assessment of coal gas origin, any bias in the molecular composition (e.g., the CH_4/CO_2 ratio, important when CO_2 content >5%) of desorbing coal gases will propagate an error in the evaluation of the methane abundance in a coal sample, a field, or on a basin scale. The overall trend of increasing CO_2 concentrations in bulk desorbing gas over time from canisters may be mirrored on a reservoir scale by the observation of increasing CO_2 concentrations from older CBM production wells as coal gases become depleted (Arri et al., 1992).

On the other hand, decreasing reservoir gas pressure and increasing relative CO_2 content during gas production may cause shrinkage of the coal matrix (Mavor and Vaughn, 1998). If shrinkage modifies pore-size distribution (e.g., increasing relative micropore volume), it might as well, modify the isotopic fractionation of diffusion. Nevertheless, if isotopic fractionation patterns of methane produced in the field and from desorption canisters (Fig. 2B) are similar, then $\delta^{13}C$ values could be used to monitor production of CBM and depletion of a reservoir. Our ongoing research comparing laboratory and production trends will test this hypothesis

3.5. Conclusions

Kinetic isotope effects cause ^{13}C-depletion of free methane and CO_2 relative to adsorbed gas species during desorption of coal gases in canisters. Observed fractionations are likely caused by faster diffusion of ^{12}C-containing gas species relative to $^{13}CH_4$ and $^{13}CO_2$. Amplitudes of $\delta^{13}C$ shifts over the duration of desorption are probably linked to

the pore structure of coal, which is controlled by maceral composition, maturity, in-situ stress, etc.

A linear relationship exists between $\delta^{13}C_{CH4}$ and the volume of desorbed CH_4 as a fraction of total CBM. Thus, isotopically representative sampling of desorbed CBM for carbon-isotopic analysis should be performed for a gas sample that is collected after about half of all gas has been desorbed and vented/removed (i.e., gas from the ~50 vol. % mid-point of gas desorption). Our coals' desorption midpoints occurred between the fifth and twelfth days of desorption. The timing of a midpoint can be predicted by extrapolating narrowly spaced measurements from the first few days of desorption.

The chemical composition of desorbing coal gas changes over the duration of desorption because different coal gas species express different adsorption affinities in microporous coal. CO_2 has a higher adsorption affinity than methane, causing early desorbed gas to be relatively enriched in methane, whereas late desorbed gas is relatively enriched in CO_2.

Awareness and avoidance of pitfalls of compositional and isotopic analyses of coal gases from canister desorption can minimize the analytical bias of geochemical assessment, for example in the evaluation of gas origins.

and also the generosity of the Black Beauty Coal Company (BBCC) for allowing us to

sample freshly drilled coal cores.

References

Arri, L.E., Yee, D., Morgan, W.D., Jeansonne, M.W., 1992. Modeling coalbed methane production with binary gas sorption. SPE 24363, SPE Rocky Mountain Regional Meeting, Casper, Wyoming, May 18-21, 1992.

Bacsik, Z., Canongia Lopes, J.N., Costa Gomes, M.F., Jancsó, G., Mink, J., Pádua, A.A.H., 2002. Solubility isotope effects in aqueous solutions of methane. Journal of Chemical Physics 116, 10816-10824.

Bustin, R.M., Clarkson, C., 1996. Importance of fabric and composition on permeability, gas capacity and gas desorption of coals from the Sydney Basin, Australia. Abstract. GSA, 28th Annual Meeting. Abstracts 28(7), p. 41.

Bustin, R.M., 2000. Variation in pore size distribution with coal rank and composition; potential for substantial resources of free gas in matrix porosity in low rank. AAPG Bulletin 84, 1409.

Chung, H.M., Gormly, J.R., Squires, R.M., 1988. Origin of gaseous hydrocarbons in subsurface environments: theoretical considerations of carbon isotope distribution. Chemical Geology 71, 97-103.

Clarkson, C., Lamberson, M., Bustin, R.M., 1993. Variation in surface area and micropore size distribution with composition of medium volatile bituminous coal of the Gates Formation, northeastern British Columbia; implications for coalbed methane potential. In: Current Research; Part E. Geological Survey of Canada, 97-104, 1993.

Cui, X., Bustin, R.M., Dipple, G., 2004. Selective transport of CO_2, CH_4, and N_2 in coals: insights from modeling of experimental gas adsorption data. Fuel 83, 293–303.

Diamond, W.P., Levine, J.R., 1981. Direct method determination of the gas content of coal: procedures and results. US Bureau of Mines R.I. 8515, 36p.

Drobniak, A., Mastalerz, M., Rupp, J., 2004. Evaluation of coalbed gas potential of the Seelyville Coal Member, Indiana, USA. International Journal of Coal Geology 57, 265-282.

Faiz, M.M., Barclay, S., Saghafi, A., Stalker, L., Wold, M., Esterle, J., Sherwood, N., 2002. Coal bed methane reservoir characterization – KP-1 and WG-1, PEL-2, Southern Sydney Basin, Report Prepared for Sydney Gas Company, CSIRO Petroleum Confidential Report No. 02-055, July 2002, 220, unpublished.

Faiz, M., 2004. Microbial infuences on coal seam gas reservoirs – a review. Abstract. Bac-Min Conference, Bendigo, Victoria, Australia, 8-10 Nov., Program and Abstracts, 133-142.

Fuex, A.N., 1980. Experimental evidence against an appreciable isotopic fractionation of methane during migration. In Advances in Organic Geochemistry, 1979, 725-732.

Gas Research Institute, 1995. A guide to determining coalbed gas content. Gas Research Institute, 1995, GRI-94/0396.

Gould, K.W., Hargraves, A.J., Smith, W.J., 1987. Variation in the composition of seam gases issuing from the coal. Australasian Institute of Mining and Metallurgy Bulletin 292, 69-73.

Gudmundsson, K., 2003. An approach to determining the water transport properties of building materials. Nordic Journal of Building Physics 3, 1-10.

Harpalani, S., Chen, G., 1997. Influence of gas production induced volumetric strain on permability of coal. Geotechnology of Geological Engineering 15, 303-325.

Henning, M.J., 2002. Development and assessment of inlet system for stable carbon isotopic analysis of individual compounds in gas mixtures. M.Sc. Thesis, Department of Geological Sciences, Indiana University, Bloomington, December 2002, 40p.

Hoşgörmez, H., Yalçin, M.N., Cramer, B., Gerling, P., Faber, E., Schaefer, R.G., Mann, U., 2002. Isotopic and molecular composition of gas occurrences in the Thrace basin (Turkey): origin of the gases and characteristics of possible source rocks. Organic Geochemistry 33, 1429-1439.

Jędrysek, M.O., 1995. Carbon isotope evidence for diurnal variations in methanogenesis in freshwater lake sediments. Geochimica et Cosmochimica Acta 59, 557-561.

Katz, B.J., Narimanov, A., Huseinzadeh, R., 2002. Significance of microbial processes in gases of the South Caspian basin. Marine and Petroleum Geology 19, 783-796.

Martini, A.M., Walter, L.M., Ku, T.C.W., Budai, J.M., McIntosh, J.C., Schoell, M., 2003. Microbial production and modification of gases in sedimentary basins: A geochemical case study from a Devonian shale gas play, Michigan basin. AAPG Bulletin 87, 1355-1375.

Mastalerz, M., Gluskoter, H., Rupp, J., 2004. Carbon dioxide and methane adsorption in high volatile bituminous coals from Indiana. International Journal of Coal Geology 60, 43-55.

Mavor, M.J., Vaughn, J.E., 1998. Increasing coal natural fracture permability in the San Juan Basin Fruitland Formation. Abstract. AAPG Annual Convention Abstracts, Salt Lake City, Utah, May 17-28, 1998.

Niemann, M., Whiticar, M.J., Ryan, B.D., 2005. Stable isotope systematic of coalbed methane. Abstract. Goldschmidt Conference, Moscow, Idaho, USA, 20 - 25 May 2005; section 52, A502.

Prinzhofer, A., Pernaton, E., 1997. Isotopically light methane in natural gas: bacterial imprint or diffusive fractionation? Chemical Geology 142, 193-200.

Radovic, L.R., Menon, V.C., Leon, C.A., Kyotani, T., Danner, R.P., Anderson, S., Hatcher, P.G., 1997. On the porous structure of coals: evidence for an interconnected but constricted micropore system and implications for coalbed methane recovery. Adsorption 3, 221-232.

Rodrigues, C.F., Lemos de Sousa, M.J., 2002. The measurement of coal porosity with different gases. International Journal of Coal Geology 48, 245-251.

Schoell, M., 1983. Genetic characterization of natural gases. AAPG Bulletin 67, 2225-2238.

Scott, A.R., Ambrose, W.A., 1992, Thermal maturity and coalbed methane potential of the Greater Green River, Piceance, Powder River and Raton basins. AAPG, 1992 Annual Convention Official Program, p.116.

Scott, A.R., Kaiser, W.R., Ayers, W.D. Jr., 1994. Thermogenic and secondary biogenic gases, San Juan Basin, Colorado and New Mexico - Implications for coalbed gas production. AAPG Bulletin 78, 1186-1209.

Smith, J.W., Pallasser, R.J., 1996. Microbial origin of Australian coalbed methane. AAPG Bulletin 80, 891-897.

Smith, J.W., Pallasser, R., Rigby, D., 1992. Mechanisms for coalbed methane formation. Coalbed methane symposium, Townsville, November 1992, 63-73.

Strąpoć, D., Mastalerz, M., Schimmelmann, A., Eble, C., 2005. Biogenic and thermogenic coalbed gas in the Illinois Basin: insight from compound-specific carbon isotopic ratios. Abstract. The 22nd International Meeting on Organic Geochemistry, Seville, Spain, September 12 -16, 2005, Vol. 1, 113-114.

Szaran, J., 1997. Achievement of carbon isotope equilibrium HCO_3^- (solution)–CO_2 (gas). Chemical Geology 142, 79-86.

Whiticar, M.J., 1996. Stable isotope geochemistry of coals, humic kerogens and related natural gases. International Journal of Coal Geology 32, 191-215.

Yee, D., Seidle, J.P., Hanson, W.B., 1993. Gas sorption on coal and measurement of gas content. In: Law, B.E., Rice, D.D. (Eds.), Hydrocarbons from coal. AAPG Studies in Geology 38, 203-218.

Zhang, T.W., Krooss, B.M., 2001. Experimental investigation of the carbon isotope fractionation of methane during gas migration by diffusion through sedimentary rocks at elevated temperature and pressure. Geochimica et Cosmochimica Acta 65 (16), 2723-2742.

CHAPTER 4

Characterization of the origin of coalbed gases in southeastern Illinois Basin by compound-specific carbon and hydrogen stable isotope ratios*

Dariusz Strąpoć [1], Maria Mastalerz [2], Cortland Eble [3], and Arndt Schimmelmann [4]

[1] Department of Geological Sciences, Indiana University,
1001 E 10th Street, Bloomington, IN 47405-1405, U.S.A.
[2] Indiana Geological Survey, Indiana University, 611 N. Walnut Grove,
Bloomington, IN 47405, U.S.A.
[3] Kentucky Geological Survey, University of Kentucky, Lexington, KY 40506, U.S.A.

Abstract

Coalbed gases and waters from exploratory and production gas wells in the southeastern Illinois Basin were sampled to geochemically assess the origin of coalbed gases, with an emphasis on the Springfield and Seelyville Coal Members that are commercially targeted for coalbed methane production in Indiana. On-line analyses of hydrocarbon gases methane to butanes (C_1, C_2, C_3, n-C_4, i-C_4) and CO_2 yielded concentrations, δD, and $\delta^{13}C$ values. The low thermal maturity of Indiana coals with vitrinite reflectance $R_o \sim 0.6\%$ is in agreement with an overwhelmingly biogenic isotopic signature of coalbed gases containing $\geq 96\%$ methane generated via bacterial CO_2-reduction. In contrast, thermogenic gas was generated in the stratigraphically equivalent coal beds in western Kentucky's Rough Creek Graben zone where higher maturities of up to $R_o \sim 0.8\%$ were reached due to tectonic and hydrothermal activity. No secondary biogenic methane was observed in more mature western Kentucky coal beds where greater burial depth limits the recharge of meteoric water. Biogenic and thermogenic coalbed gases represent two end-members that are compositionally and isotopically distinct. Microbial biodegradation of thermogenic C_{2+} hydrocarbon gases in Indiana coal beds preferentially targets C_3 and introduces isotope fractionation whereby remaining C_3 is enriched in deuterium and ^{13}C.

61

4.1. Introduction

Empirical compositional and isotopic classifications for discerning different origins of natural gases (e.g., Schoell, 1983; Chung et al., 1988; Whiticar, 1999) have been applied to coalbed gases in various basins (e.g., Scott et al., 1994; Smith and Pallasser, 1996; Ahmed and Smith, 2001; Hoşgörmez et al., 2002; Katz et al., 2002; Aravena et al., 2003; Faiz et al., 2003; Thielemann et al., 2004). This study focuses on coalbed gases from the Illinois Basin where a gradient of thermal maturity gives rise to biogenic and/or thermogenic coalbed gases depending on coal properties and geologic setting. Relatively shallow eastern Illinois Basin coals in Indiana with low maturity (vitrinite reflectance $R_o \sim 0.6\%$) contain significant resources of coalbed methane (CBM) (Drobniak et al., 2004; Mastalerz et al., 2004). Important questions about these relatively immature coals center on (i) the amount of secondary biogenic CBM that can be continuously contributed to bulk coalbed gas, and (ii) biogeochemical controls of modern CBM generation. With regard to higher maturity coals in the southern part of the Illinois Basin, we hypothesize that past tectonic and volcanic activities associated with Rough Creek Graben zone (Hower and Gayer, 2002; Rowan et al., 2002) triggered thermogenic gas generation in western Kentucky (where R_o ranges from 0.7 to 0.8%). Our analytical approach towards resolving the diverse origins of coalbed gases in the southeastern Illinois Basin utilizes the molecular and isotopic compositions of coalbed gases, associated reservoir waters, and gases that were generated during artificial maturation of coal via hydrous pyrolysis.
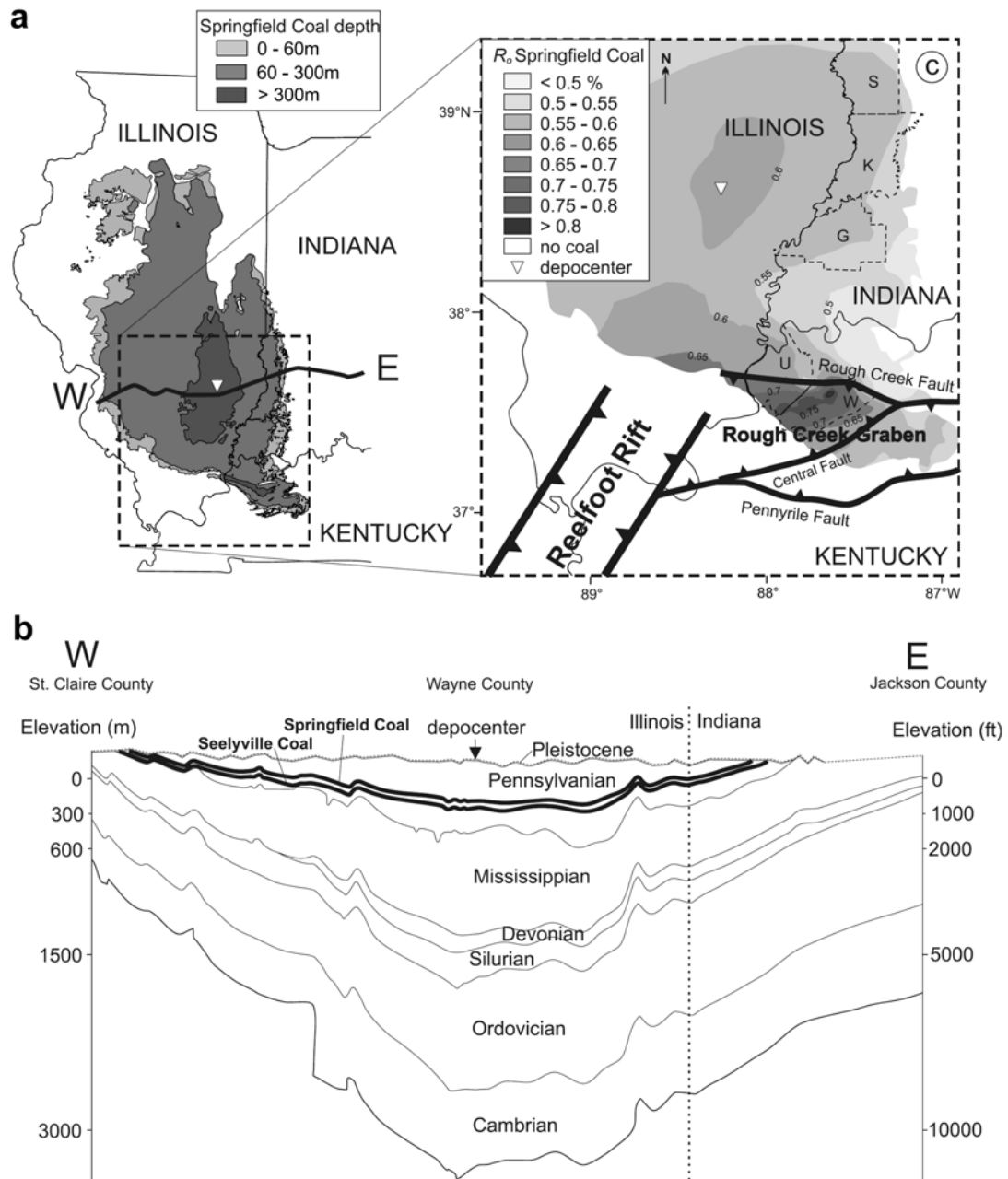
Fig. 1. Study area: (a) map of Springfield Coal Member depth; (b) East-West stratigraphic profile across Illinois Basin (along line indicated in Fig. 1a) with 52x vertical exaggeration; (c) map of vitrinite reflectance R_o of Springfield Coal Member overlain by major tectonic structures in southeastern Illinois Basin (after Greb et al., 1992; Hower et al., 2005). Dashed lines distinguish counties: S – Sullivan, K – Knox, G – Gibson, U – Union, W – Webster.

63

4.2. Study area

The depocenter of the asymmetric, spoon-shaped Illinois Basin is located in the southeast (Fig. 1a). The basin is an intracratonic structural depression that successively accumulated sediments of shallow marine origin (up to 3500 m, 530 to 280 Ma; Fig. 1b) during the Cambrian to Pennsylvanian. The post-Paleozoic history of the basin was dominated by erosion, and more recently included northern glacial loading. Only the very southeastern part of the basin in western Kentucky was subjected to intense tectonic activity along the Rough Creek and Pennyrile Fault systems. Tectonic activity began in the early Paleozoic as an east-west extension of the abandoned Reelfoot Rift zone (Fig. 1c; Macke, 1995) and continued throughout basin-filling. Vertical translocations at the Rough Creek Graben and an increased geothermal gradient locally induced $\sim$ 400 m greater present-day depths and higher coal maturity ($R_o \sim$ 0.7 to 0.8%; Fig. 1a, c).

Pennsylvanian coal-bearing sediments in the Illinois Basin reach 750 m in thickness. Pennsylvanian lithostratigraphy is characterized by relatively thin and laterally extensive units deposited due to multiple transgressions and regressions. The depositional environment has been recently described as mainly nearshore to marginal marine characterized by tidal coastal plains (Kvale et al., 2004), although it was formerly thought to have been coal swamps developing on deltaic platforms (Roseman Wright, 1977). Our study focuses on the Springfield and Seelyville Coal Members in the southeastern Illinois Basin that are commercial CBM targets (Solano-Acosta et al., 2005) (Fig. 2) ranging in thickness from 0.7 to 1.6 m and from 0.4 to 1.6 m, respectively. Average coalbed gas contents, on a raw basis (moisture and mineral matter included), range from 2.0 to 3.0 cm^3g^{-1} in the Springfield Coal Member and from 2.2 to 4.6 cm^3g^{-1} in the Seelyville
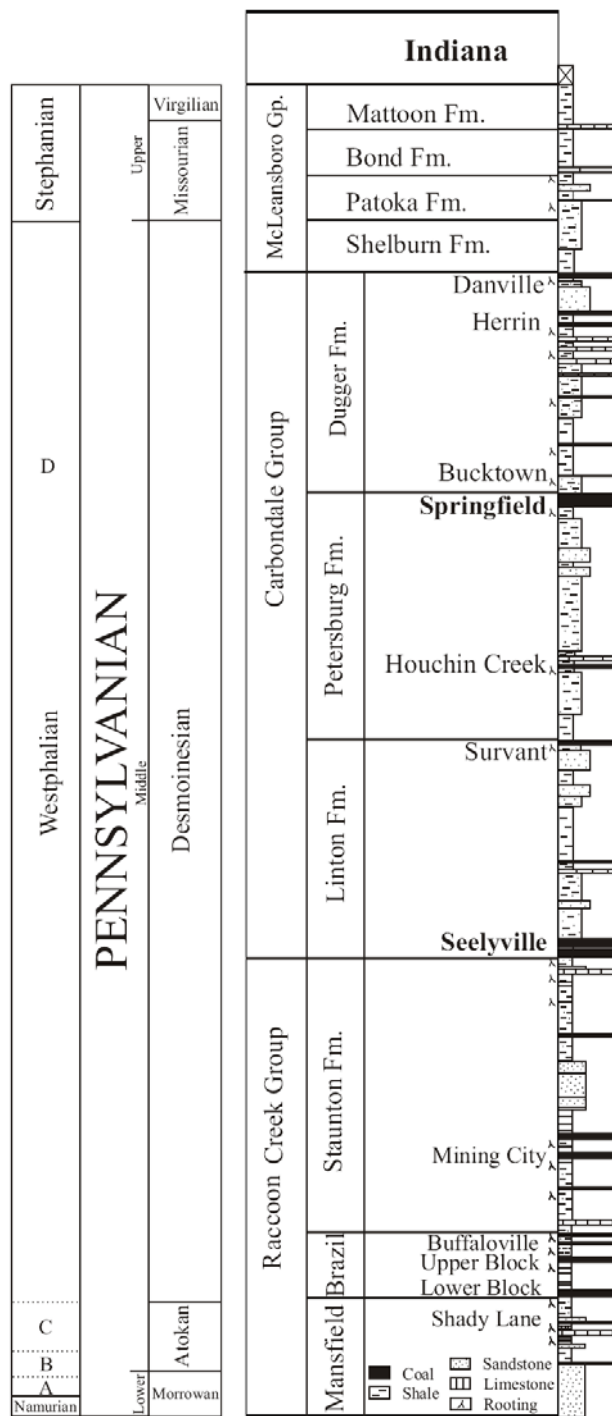
Fig. 2. Litostratigraphic column of Pennsylvanian in the Indiana part of Illinois Basin, with positions of sampled coal beds indicated (modified from Mastalerz and Harper, 1998).

Coal Member (Mastalerz et al., 2004). The Springfield and Seelyville coals in Indiana are located at typical depths of between 60 and 200 m (Mastalerz et al., 2004), and have high volatile bituminous C and B rank throughout the state, with an average $R_o \sim 0.56\%$ for the Springfield Coal (Hower et al., 2005) and 0.60% for the Seelyville Coal (Drobniak et al., 2004). The stratigraphically equivalent coal beds in western Kentucky feature increased R_o from 0.7 to 0.8% and rank as high volatile bituminous A coals.

4.3. Materials and methods

Coal cores were obtained at eleven drill sites in Sullivan, Knox, and Gibson counties of southwestern Indiana (Fig. 1b), and coalbed gases were collected during canister desorption (Gas Research Institute, 1995). Additionally, 10 CBM production wells in Sullivan County were sampled. Most data from Indiana represent Seelyville (n=27) and Springfield (n=13) coal beds. Another set of coalbed gas samples was received from four exploratory wells located in Webster and Union counties in western Kentucky (Fig. 1b). All twelve analyzed coal members are depicted on the lithostratigraphic diagram in Figure 2. Production well INS-3 was sampled during its exploratory coring and production phase. This facilitated a direct comparison between coalbed gas from canister desorption of fresh coal and commercially-produced coalbed gas.

Immediately after recovery of a sediment core in the field, one or more coal core segments with a diameter of ~7.6 cm and a length of ~30 cm were quickly sealed in a nitrogen-purged desorption canister with a 2.7 liter internal volume. Desorbed gas volumes were measured daily following standard canister desorption protocol (Gas

66

Research Institute, 1995) using a volume displacement apparatus until desorption essentially ceased after ~90 days. Gas sampling from canisters for compositional and isotopic analyses was performed at the midpoint of coalbed gas desorption, when newly desorbed gas is representative of the bulk coalbed gas (Strąpoć et al., 2006). Additionally, residual coalbed gas was obtained by crushing previously desorbed coal core segments and quickly refilling the crushed coal into canisters for continued desorption.

Two Springfield and Seelyville coal samples were selected for hydrous pyrolysis experiments in order to obtain isotopic signatures of artificially generated thermogenic end-member gases. Hydrous pyrolysis of coal chips at 320 ºC for 72 hours was performed in waters with initial δD_{H2O} values of -137 and +1196‰ in sealed quartz ampoules that were housed in partially water-filled and sealed stainless steel pipe reactors (Schimmelmann et al., 1999).

Coalbed gas samples were analyzed on-line for gas composition and compound-specific $\delta^{13}C$ and δD values using a Delta Plus XP isotope-ratio mass spectrometer with a specialized GASIS inlet system (Henning, 2002), a gas chromatograph (GC), as well as oxidative and glassy carbon reductive interfaces to generate CO_2 and H_2 analytes. The GASIS inlet system utilized various injection loop sizes (0.5, 50, and 500 μL) to admit gas volumes that were adequate for measuring gas species at diverse concentrations. At the beginning of the GC program, the PoraBOND Q column was cooled to -20 ºC for seven minutes by liquid nitrogen-spraying for improved peak separation. This was followed by successive 50 ºC/min warming to a series of isothermal plateaus of 4 min at 30 ºC, 4 min at 80 ºC, 6 min at 130 ºC, and 4 min at 250 ºC. To obtain resolved peaks of suitable sizes for various gas components, each gas analysis consisted of an initial gas

injection from the 0.5 µL loop for methane (C_1), followed three minutes later by a second injection from the 50 or 500 µL loops targeting carbon dioxide (CO_2) and ethane to butanes (C_{2+}). Excessive amounts of methane from the second injection were GC-separated and eliminated from the analyte flow by back-flushing. On-line combustion of hydrocarbons yielded CO_2 at 950 ºC in a reactor containing partially oxidized Pt/Ni/Cu wires. Alternatively, the pyrolytic decomposition of hydrocarbons at 1420 ºC in an Al_2O_3 reactor lined with glassy carbon formed H_2. The integrated H_2 and CO_2 peak areas of the ions with 2 and 44 amu (atomic mass units) were used to quantify relative abundances of gas components, which are reported as volume %. Analytical errors for relative gas abundances are expressed as [standard deviation/average concentration·100] in volume % and depend on concentration. Highly concentrated gas components such as methane bear an uncertainty of ±1 vol. %. Gas components with concentrations of 0.5 to 10 vol. % were typically quantified within ±10 to ±20 vol. %. Gas components with low concentrations below 0.5 vol. % could be quantified within errors of typically ±20 to ±40 vol. %. The detection limit was 1 vol. ppm.

Isotopic on-line measurements utilized CO_2 and H_2 reference gases from cylinders and methane reference gases from lecture bottles that had been calibrated off-line against VPDB for $\delta^{13}C$ and against VSMOW with normalization to SLAP for δD. Our two methane reference gases with distinct $\delta^{13}C$ and δD values were injected daily between coalbed gases as an internal on-line laboratory reference material and to monitor the H_3 factor. Analytical $\delta^{13}C$ errors (as standard deviations of 8 repeat measurements) for C_1, CO_2, C_2, C_3, i-C_4, n-C_4 were ±0.4, 0.9, 0.7, 1.1, 1.0, and 1.6‰, respectively. Equivalent analytical δD errors for C_1, C_2, C_3, i-C_4, n-C_4 were ±4, 7, 10, 13, and 11‰.

The concentrations of seven major anions in water samples from production wells were determined using a DIONEX ICS-2000 ion chromatograph with a precision of $\pm 10\%$. The isotopic compositions of waters δD_{H2O} and $\delta^{18}O_{H2O}$ were measured with a Delta Plus XP isotope-ratio mass spectrometer using two attached interfaces. δD_{H2O} values were determined on-line using an HDevice by Thermo Finnigan, in which water is reduced to H_2 in contact with chromium at 850 ºC. $\delta^{18}O_{H2O}$ values were measured after equilibrating standard CO_2 gas with waters in a gas bench. Analytical precisions of isotopic analyses of waters were $\pm 0.9‰$ (n=5) for δD_{H2O} and $\pm 0.4‰$ (n=6) for $\delta^{18}O_{H2O}$.

4.4. Results

Compositional and isotopic characteristics of coalbed gases are presented in Table 1 and represent 9 coal beds from 11 exploratory holes in southwestern Indiana, and 7 coal beds from 4 exploratory wells in western Kentucky. In addition, data from coalbed gases and waters from 10 Indiana production wells are listed in Table 2. Table 3 presents average values of chemical and isotopic characteristics of coalbed gases for all investigated coal members in Indiana and Kentucky. In this paper we compare gases from stratigraphically equivalent coal beds that differ in maturity. Results from desorption of crushed coals and from two artificial maturation experiments via hydrous pyrolysis are presented in Table 4.

Table 1
List of exploratory wells cored and sampled for coalbed gases in Indiana and Kentucky; petrographic and R_0 data from Mastalerz et al. (2005a)

INDIANA

Well name	County	Coalbed	Depth (m)	R_0 (%)	$\delta^{13}C_{CH_4}$ (‰)	δD_{CH_4} (‰)	$\delta^{13}C_{CO_2}$ (‰)	$\Delta^{13}C_{CO_2\text{-}CH_4}$ (‰)	$C_1/(C_2+C_3)$	n	Coal petrography (vol.%) V	L	I	M
ING-1	Gibson	Seelyville	138	0.59	−63.7	−187	n.a.	n.a.	1143	1	75.3	5.2	8.1	11.5
INS-1	Sullivan	Springfield	100	0.58	−60.2	−195	−2.3	57.9	7185	1	71.1	5.2	9.3	14.4
		Seelyville	160	0.57	−59.5	−198	−0.1	59.4	2353	5	77.3	6.7	8.9	7.1
INS-2	Sullivan	Houchin Creek	112	0.58	−58.7	−197	8.2	66.9	7460	1	83.6	4.1	7.1	5.2
		Survant	114	n.a.	−58.4	−202	9.9	68.3	8072	3	n.a.	n.a.	n.a.	n.a.
		Seelyville	128	0.58	−56.8	−195	10.3	67.1	5541	3	74.9	5.5	13.5	6.1
ING-2	Gibson	Springfield	97	0.57	−63.3	−191	3.1	66.4	7590	5	80.4	5.8	8.3	5.6
ING-3	Gibson	Springfield	148	0.72	−63.3	−191	−4.7	58.6	17529	2	83.3	5.8	10.5	0.4
		Seelyville	214	0.57	−61.2	n.a.	−2.8	58.4	3880	1	62.8	3.6	9.6	24.0
ING-4	Gibson	Danville	126	0.58	−66.5	−197	−1.8	64.7	2520	1	83.2	8.8	4.8	3.2
		Seelyville	239	0.61	−64.3	−204	2.2	66.5	986	3	72.0	6.7	9.9	12.1
INK-1	Knox	Seelyville	187	0.59	−62.1	n.a.	9.5	71.6	893	2	70.1	4.5	12.7	12.7
INS-3	Sullivan	Seelyville	108	0.57	−60.4	−206	7.4	67.7	1962	4	76.6	6.1	11.5	5.8
INS-4	Sullivan	Danville	78	n.a.	−57.2	n.a.	11.4	68.6	10376	1	n.a.	n.a.	n.a.	n.a.
INS-5	Sullivan	Survant	90	n.a.	−62.7	n.a.	7.4	70.1	7077	2	n.a.	n.a.	n.a.	n.a.
		Seelyville	97	0.56	−60.3	−203	11.3	71.6	4001	2	78.8	3.4	6.2	11.6
		Buffaloville	112	0.55	−59.9	−199	2.5	62.4	3932	1	77.8	5.0	9.8	7.4
		Upper Block	120	0.55	−60.3	−197	3.6	63.8	4727	1	66.4	8.8	18.4	6.4
		Lower Block	127	0.61	−59.1	−196	2.9	62.0	3214	1	61.3	5.7	13.2	19.8
		Shady Lane	134	0.58	−61.1	−196	−1.0	60.2	4976	1	60.0	15.6	12.8	11.6
INS-6	Sullivan	Seelyville	113	n.a.	−61.8	n.a.	9.0	70.8	12467	1	n.a.	n.a.	n.a.	n.a.

WESTERN KENTUCKY

Well name	County	Coalbed	Depth (m)	R_0 (%)	$\delta^{13}C_{CH_4}$ (‰)	δD_{CH_4} (‰)	$\delta^{13}C_{CO_2}$ (‰)	$\Delta^{13}C_{CO_2\text{-}CH_4}$ (‰)	$C_1/(C_2+C_3)$	n
KYW-1	Webster	Danville	310	0.7–0.8*	−50.9	−201	−17.9	32.9	17	1
		Bucktown	324	0.7–0.8	−50.7	n.a.	−21.3	29.4	16	1
		Springfield	347	0.7–0.8	−48.2	−219	−21.6	26.6	11	2
KYU-1	Union	Danville	412	0.7–0.8	−48.4	−217	−27.3	21.1	12	1
		Herrin	421	0.7–0.8	−48.4	−225	−23.2	25.2	14	1
		Bucktown	433	0.7–0.8	−48.3	−205	−21.5	26.7	10	1
		Springfield	454	0.7–0.8	−49.7	−217	−23.4	26.3	14	1
		Survant	484	0.7–0.8	−47.1	−215	−20.3	26.9	21	1
		Seelyville	516	0.7–0.8	−50.1	−219	−22.1	28.0	25	3
		Mining City	606	0.7–0.8	−49.4	−225	−21.7	27.7	43	2
KYU-2	Union	Danville	411	0.7–0.8	−48.1	n.a.	−22.8	25.3	7	1
		Herrin	422	0.7–0.8	−49.5	n.a.	−28.0	21.6	5	1
		Bucktown	433	0.7–0.8	−48.0	n.a.	−21.2	26.8	7	2
		Springfield	454	0.7–0.8	−49.0	n.a.	−28.4	20.6	7	2
		Survant	484	0.7–0.8	−49.1	n.a.	−24.3	24.8	10	1
		Seelyville	528	0.7–0.8	−48.4	n.a.	−25.1	23.3	11	1
		Mining City	606	0.7–0.8	−50.5	n.a.	−25.1	23.4	5	1
KYU-3	Union	Danville	412	0.7–0.8	−49.9	n.a.	−23.4	21.9	8	1
		Herrin	422	0.7–0.8	−49.0	n.a.	−24.6	25.3	7	2
		Springfield	455	0.7–0.8	−48.8	n.a.	−29.2	19.9	8	2
		Survant	474	0.7–0.8	−48.8	n.a.	−26.8	21.9	7	1
		Seelyville	511	0.7–0.8	−50.1	n.a.	−23.2	26.9	14	2
		Mining City	605	0.7–0.8	−49.4	n.a.	−24.5	24.9	12	1

n – number of core sections, each 0.3 m long, sampled for desorbed gases from a single coal bed at one coring location; – based on Ro maps (Greb, 1992; Hower and Gayer, 2005), precise measurements not available; n.a. – not available; V – vitrinite, L – liptinite, I – inertinite, M – mineral matter.

Table 2
List of production wells that were sampled for coalbed gas and water in Sullivan County, Indiana

Well name	Coal bed	Depth (m)	$\delta^{18}O_{H_2O}$ (‰)	δD_{H_2O} (‰)	Total anions[a] (mg/l)	Cl^- (mg/l)	$\delta^{13}C_{CH_4}$ (‰)	δD_{CH_4} (‰)	$\delta^{13}C_{CO_2}$ (‰)	$\Delta^{13}C_{CO_2-CH_4}$ (‰)	$\Delta D_{H_2O-CH_4}$ (‰)	$C_1/(C_2+C_3)$
INS-P1	Springfield	86	−6.28	−41.4	3768	3754	−60.3	−213	0.6	60.9	171	7866
INS-P2	Springfield	94	−5.74	−41.6	4746	4731	−57.9	−212	5.5	63.4	170	14329
INS-P3	Springfield	99	−5.68	−41.5	4008	3995	−57.3	−210	5.7	63.0	168	21860
INS-P4	Springfield	90	−6.79	−40.8	5477	5447	−56.9	−212	5.0	61.9	171	22384
INS-P5	Springfield	75	n.a.	n.a.	n.a.	n.a.	−57.5	−212	2.5	60.0	n.a.	18417
Average		89	−6.12	−41.3	4500	4482	−58.0	−212	3.9	61.8	170	16971
INS-3	Seelyville	107	−5.73	−43.8	3437	3416	−59.9	−210	2.3	62.2	166	9385
INS-P6	Seelyville	140	−5.89	−39.8	4403	4389	−58.5	−202	4.7	63.2	162	1553
INS-P7	Seelyville	120	−6.18	−44.8	2895	2881	−60.0	−211	−0.2	59.8	166	8701
INS-P8	Seelyville	99	−7.28	−46.0	212	185	−65.9	−211	n.a.	n.a.	165	19627
INS-P9	Seelyville	109	−6.38	−45.8	304	153	−66.6	−208	n.a.	n.a.	162	24927
Average		115	−6.29	−44.0	2250	2205	−62.2	−208	2.3	61.7	164	12838

n.a. – not available.
[a] not including bicarbonate.

71

Table 3
Compound-specific C and H isotopic average data for each coal bed sampled in the SE Illinois Basin

Coal bed	n	Methane Content (vol.%)	Methane δ13C (‰)	Methane δD (‰)	CO2 content (vol.%)	CO2 δ13C (‰)	Ethane Content (vol.%)	Ethane δ13C (‰)	Ethane δD (‰)	Propane Content (vol.%)	Propane δ13C (‰)	Propane δD (‰)	i-Butane Content (vol.%)	i-Butane δ13C (‰)	i-Butane δD (‰)	n-Butane Content (vol.%)	n-Butane δ13C (‰)	n-Butane δD (‰)
INDIANA																		
Danville	2	97.7	−61.9	−197	2.3	4.8	0.023	−38.7	−102	0.001	−26.9	−1	0.0006	−27.9	−73	0.0006	−30.1	n.a.
Springfield	8 + 5	98.6	−60.5	−202	1.3	2.0	0.008	−38.5	−108	0.001	−26.8	−19	0.0011	−31.2	−39	0.0004	−31.2	−25
Springfield – standard deviation		1.7	2.8	11	1.7	3.9	0.004	2.1	56	0.002	6.8	49	0.0033	3.6	18	0.0006	2.3	19
Houchin Creek	2	97.0	−58.7	−197	3.0	8.2	0.010	−37.8	−81	0.003	−30.1	8	0.0010	−43.3	−31	0.0018	−29.3	n.a.
Survant	4	97.0	−61.3	−202	2.9	8.2	0.013	−40.0	−97	0.001	−28.7	−47	0.0002	−28.4	−72	0.0005	−31.1	n.a.
Seelyville	21 + 5	98.4	−60.8	−203	1.5	4.9	0.034	−37.2	−87	0.005	−22.0	−50	0.0017	−31.6	−74	0.0013	−27.5	−74
Seelyville – standard deviation		1.5	2.8	8	1.5	5.5	0.041	2.6	38	0.009	6.6	66	0.0043	4.1	53	0.0027	8.1	77
Buffaloville	1	97.9	−59.9	−199	2.0	2.5	0.024	−42.6	n.a.	0.001	−23.1	n.a.	0.0001	n.a.	n.a.	0.0005	−29.5	n.a.
Upper Block	1	97.5	−60.3	−197	2.5	3.6	0.020	−39.5	n.a.	0.001	−9.0	n.a.	0.0001	n.a.	n.a.	0.0003	−26.7	n.a.
Lower Block	1	98.4	−59.1	−196	1.5	2.9	0.029	−40.4	n.a.	0.001	−8.7	n.a.	0.0001	−43.8	n.a.	0.0003	−28.5	n.a.
Shady Lane	1	98.3	−61.1	−196	1.7	−1.0	0.018	−39.2	−68	0.002	−28.5	n.a.	0.0005	−26.2	n.a.	0.0016	−28.3	n.a.
Weighted average		98.2	−60.7	−202	1.7	4.3	0.024	−38.1	−93	0.003	−23.9	−37	0.0012	−31.7	−57	0.0010	−28.9	−63
WESTERN KENTUCKY																		
Danville	4	89.3	−49.5	−213	1.7	−22.3	5.5	−36.2	−218	2.4	−30.6	−137	0.12	−30.5	−26	0.19	−30.0	−68
Herrin	4	92.6	−49.7	−219	1.0	−23.4	4.9	−35.4	−216	1.4	−30.9	−103	0.04	−29.4	−66	0.06	−29.6	−44
Bucktown	3	90.4	−48.4	−215	2.2	−23.0	5.5	−36.0	−227	1.8	−31.1	−109	0.06	−28.7	−52	0.13	−28.8	−64
Springfield	7	87.8	−48.8	−219	1.1	−25.3	7.5	−37.1	−225	2.7	−30.7	−128	0.12	−29.7	−60	0.17	−29.5	−83
Springfield – st.dev.		3.7	1.0	5	0.5	4.2	2.1	1.5	12	1.8	0.7	6	0.12	0.8	36	0.15	1.2	34
Survant	3	87.7	−48.4	−205	1.2	−23.9	7.8	−37.2	−227	3.0	−30.8	−130	0.11	−29.3	−22	0.15	−25.9	−124
Seelyville	6	88.3	−49.1	−225	1.6	−24.5	7.2	−36.6	−222	2.6	−30.1	−123	0.11	−28.5	−35	0.18	−28.4	−61
Seelyville – standard deviation		4.3	2.1	2	0.5	3.5	2.3	1.3	1	1.6	0.8	1	0.13	1.1	12	0.14	1.0	15
Buffaloville	4	88.0	−48.9	−217	2.7	−26.5	7.6	−34.7	−191	1.6	−28.5	−101	0.05	−26.8	−32	0.04	−23.0	−72
Weighted average		89.0	−49.0	−217	1.6	−24.3	6.7	−36.3	−218	2.3	−30.4	−120	0.09	−29.0	−44	0.14	−28.1	−72

n – number of separate cores from exploratory wells analyzed (0.3 m each) plus number of sampled producing wells from the same coal bed; n.a. – not available.

72

Table 4
Comparison of desorbed coalbed gas samples from Indiana coal cores with corresponding residual gases from Indiana crushed coal and with gases from hydrous pyrolysis of Indiana coal

INDIANA coal bed/Well	Gas type	Methane			CO₂		Ethane			Propane			i-Butane			n-Butane		
		content (vol.%)	$\delta^{13}C$ (‰)	δD (‰)	content (vol.%)	$\delta^{13}C$ (‰)	content (vol.%)	$\delta^{13}C$ (‰)	δD (‰)	content (vol.%)	$\delta^{13}C$ (‰)	δD (‰)	content (vol.%)	$\delta^{13}C$ (‰)	δD (‰)	content (vol.%)	$\delta^{13}C$ (‰)	δD (‰)
Springfield																			
INS-1	Desorbed	98.2	−63.3	−191	1.7	3.1	0.012	−37.2	−78	0.0009	−32.2	44	0.010	−30.8	−52	0.0012	−30.7	n.a.
	Residual	99.1	−60.4	−212	0.83	−0.1	0.016	−36.9	3	0.0007	−25.6	n.a.	0.0019	−30.2	n.a.	0.0010	−35.8	n.a.
	Pyrolysis[a,b]	56.5	−34.3	−327	21.6	−21.1	23.9	−27.8	−309	13.9	−27.3	−257	2.0	−27.5	−238	3.6	−26.0	−249
ING-3	Desorbed	99.7	−63.3	−191	0.32	−4.7	0.005	−41.2	−93	0.0004	−23.1	−32	n.a.	n.a.	−26	0.0002	−33.0	n.a.
	Residual	99.4	−61.3	−194	0.56	6.7	0.023	−41.5	−98	0.0012	−17.1	n.a.	0.0002	−36.0	n.a.	0.0002	−29.8	n.a.
Survant																			
INS-5	Desorbed	97.1	−62.7	−202	2.9	7.4	0.013	−41.6	n.a.	0.0004	−28.3	n.a.	0.0002	−28.4	n.a.	0.0002	−30.6	n.a.
	Residual	99.5	−62.0	−210	0.51	8.7	0.022	−40.5	−50	0.0005	−24.1	n.a.	0.0001	−25.7	n.a.	0.0002	−23.1	n.a.
Seelyville																			
INS-2	Pyrolysis[a,c]	61.3	−39.1	363	2.1	−19.9	21.0	−29.1	463	12.5	−27.9	540	1.9	−28.0	589	3.3	−27.8	555
ING-4	Desorbed	99.2	−64.3	−204	0.75	2.2	0.10	−35.6	−104	0.0005	−18.8	10	0.0022	−28.2	−59	0.0003	−27.0	−144
	Residual	98.3	−63.8	−115	1.5	4.4	0.23	−35.9	−114	0.0008	1.8	n.a.	0.0018	−23.2	n.a.	0.0002	−19.4	n.a.
INK-1	Desorbed	98.1	−62.1	n.a.	1.8	9.5	0.097	−35.8	n.a.	0.013	−18.4	n.a.	0.0075	−29.5	n.a.	0.0067	n.a.	−18
	Residual	97.7	−59.7	−215	1.8	14.2	0.32	−35.6	−80	0.069	−17.1	66	0.059	−29.1	−16	0.0031	−15.5	n.a.
INS-3	Desorbed	99.1	−60.4	−206	0.80	7.4	0.042	−36.5	−77	0.0081	−21.6	−33	0.0061	−29.9	−43	0.0014	−33.8	n.a.
	Residual	98.9	−59.3	−224	1.0	15.2	0.030	−38.1	−100	0.0007	−18.4	n.a.	0.0004	−32.1	n.a.	0.0002	−25.9	n.a.
Buffaloville																			
INS-5	Desorbed	97.9	−59.9	−199	2.0	2.5	0.024	−42.6	n.a.	0.0012	−23.1	n.a.	0.0001	n.a.	n.a.	0.0005	−29.5	n.a.
	Residual	98.6	−56.7	n.a	1.3	10.9	0.056	−41.6	n.a.	0.0013	−3.2	n.a.	0.0001	−41.8	n.a.	0.0001	−36.1	n.a.
Upper Block																			
INS-5	Desorbed	97.5	−60.3	−197	2.5	3.6	0.020	−39.5	n.a.	0.0011	−9.0	n.a.	0.0001	n.a.	n.a.	0.0003	−26.7	n.a.
	Residual	98.8	−56.6	n.a	1.2	8.5	0.039	−39.4	n.a.	0.0013	9.5	n.a.	0.0001	−27.5	n.a.	0.0002	−26.8	n.a.
Lower Block																			
INS-5	Desorbed	98.4	−59.1	−196	1.5	2.9	0.029	−40.4	n.a.	0.0013	−8.7	n.a.	0.0001	−43.8	n.a.	0.0003	−28.5	n.a.
	Residual	98.6	−57.7	n.a.	1.4	11.4	0.041	−40.0	n.a.	0.0014	−2.3	n.a.	0.00004	n.a.	n.a.	0.0003	−26.3	n.a.
Shady Lane																			
INS-5	Residual	98.3	−61.1	−196	1.7	−1.0	0.018	−39.2	−68	0.0016	−28.5	n.a.	0.0005	−26.2	n.a.	0.0016	−28.3	n.a.
	Desorbed	98.4	−58.4	−177	1.6	9.6	0.037	−39.5	−55	0.0008	−14.6	n.a.	0.0001	−32.2	n.a.	0.0002	−28.6	n.a.

[a] Hydrous pyrolysis; type of water applied.
[b] $\delta D\ H_2O = -137‰$.
[c] $\delta D\ H_2O = 1196‰$; n.a. – not available.

4.4.1. Chemical composition of coalbed gases

Methane is the predominant component of all Indiana coalbed gases accounting for >99.9% of all hydrocarbons and >97% of bulk coalbed gas. Another main component is CO_2, with typical concentrations of 1 to 3 vol. % (1.3 vol. % in Springfield coalbed gas and 1.5 vol. % in Seelyville coalbed gas) (Fig. 3a). Nitrogen N_2 concentrations were not quantified in this study because we used N_2-purging of desorption canisters. Indiana coalbed gases are 'dry' with an average of only 0.03 vol. % C_{2+} hydrocarbons that translate into an average gas wetness ratio $C_1/(C_2+C_3)$ of 5200 (10600 in Springfield coalbed gas, 2500 in Seelyville coalbed gas). In contrast, coalbed gases from the stratigraphically equivalent but thermally more mature coal beds in western Kentucky have much higher average thermogenic C_{2+} concentrations of ~9.5 vol. % with a typical gas wetness ratio of ~10 (Fig. 3b). CO_2 concentrations in coalbed gases are fairly uniform across the study area with an average of 1.3 vol. %. The chemical compositions of gases derived from primary desorption of coal cores are essentially equivalent to the compositions of secondary, residual desorbed gases from coals after crushing (Table 4). Gases from artificial maturation of coals via hydrous pyrolysis experiments contain ~36 vol. % C_{2+} hydrocarbons (Table 4).

4.4.2. Carbon stable isotope ratios in gases

Compound-specific $\delta^{13}C$ values of individual gas species from Indiana coal beds vary distinctly. CO_2 with an average $\delta^{13}C_{CO2}$ value of 4.3‰ (n=20) is ^{13}C-enriched by several tens of permil relative to organic carbon in hydrocarbons (Table 1). Methane $\delta^{13}C_{CH4}$ values range from -66.6 to -56.8‰ and average -60.7‰ ± 1.7‰, n=31 (Tables 1, 2). Average $\delta^{13}C$ values of $C_{2,3,i-4,n-4}$ hydrocarbons are -38.1, -23.9, -31.1 and -28.4‰,
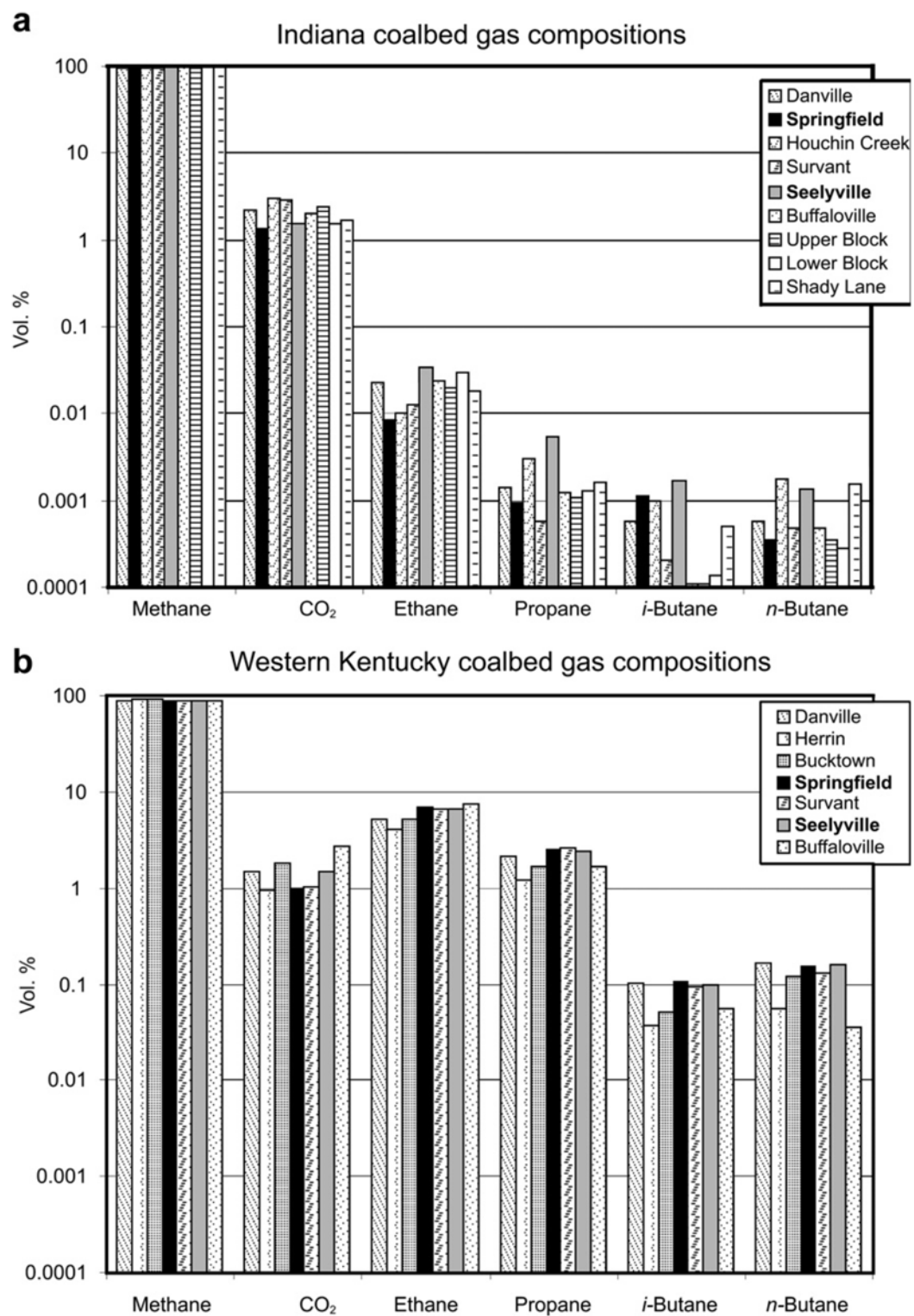
74

Fig. 3. Major gas components of coalbed gases in SE Illinois Basin; coals are listed in stratigraphic sequence according to Fig. 2.
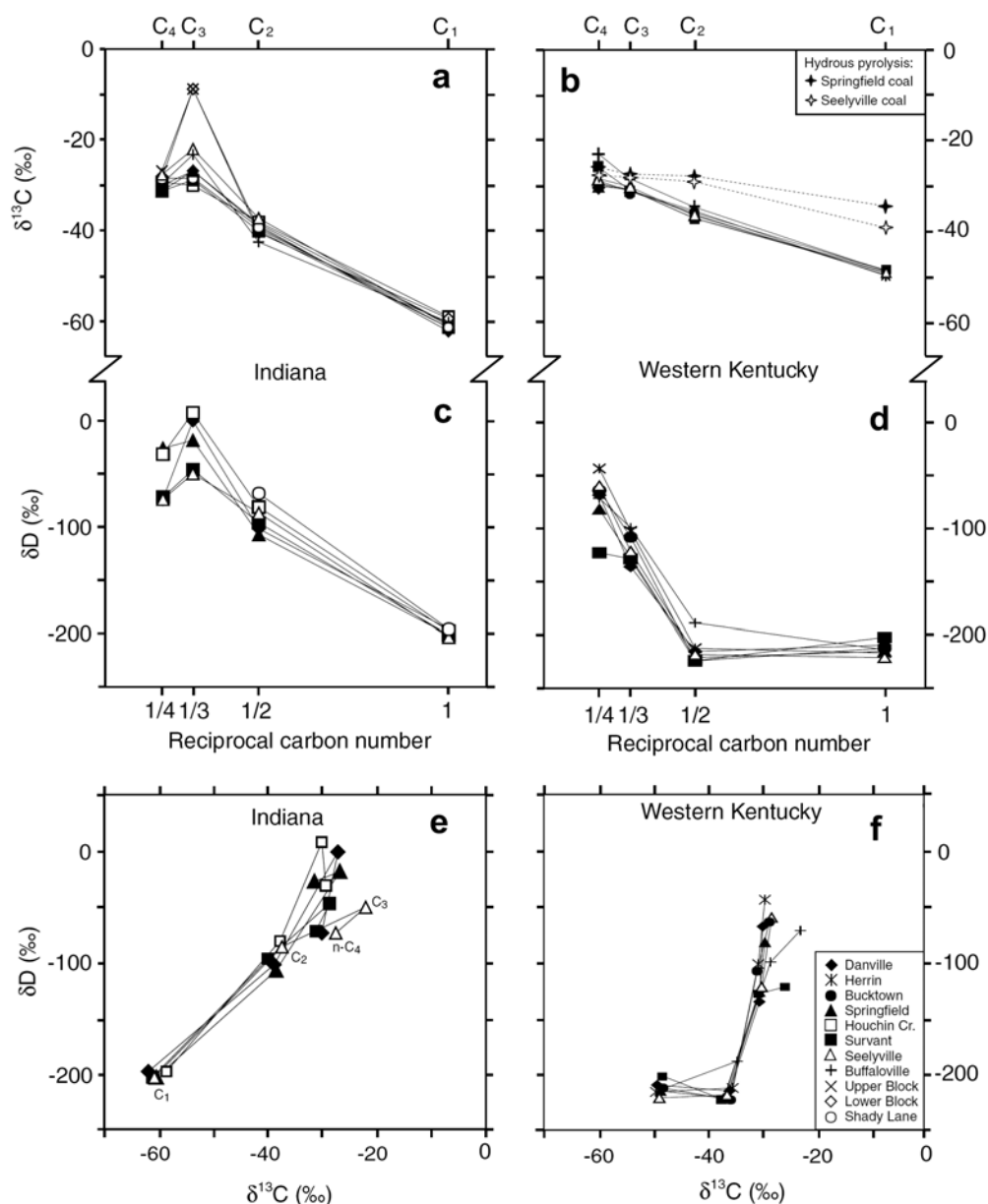
Fig. 4. Compound specific isotopic data for Indiana and Kentucky coalbed gases. (a) and (b) show $\delta^{13}C$ values, and (c) and (d) show δD values of hydrocarbons plotted against the reciprocal carbon numbers of methane to butane according to Chung et al. (1988). The same $\delta^{13}C$ and δD data are cross-plotted for Indiana (e) and western Kentucky (f). The inserted legend in (f) is valid for symbols in all parts of Fig. 4. Section (b) also plots data from hydrous pyrolysis artificial maturation experiments that generated thermogenic end-member gases from Indiana coals. Therefore we compare artificial and natural thermogenic gases generated from the same coals. δD_{i-C4} values were plotted for coals where δD_{n-C4} values were unavailable due to microbial degradation of n-butane (see Table 3).

respectively, with few outliers and standard deviations of 1.5 to 3‰ (Table 3). Propane C_3 is significantly ^{13}C-enriched relative to all other hydrocarbons (Tables 3, 4; Fig. 4a, c, e). In contrast to Indiana, the western Kentucky coalbed gases from the Springfield and Seelyville Coal Members are characterized by less negative $\delta^{13}C_{CH4}$ values of ~ -49.0‰ ±1.3‰ (n=31) and more negative $\delta^{13}C_{CO2}$ values of -24.3‰ ± 3.4‰, n=31 (Table 3). Consequently, the isotopic offset $\Delta^{13}C_{CO2-CH4}$ between $\delta^{13}C_{CO2}$ and $\delta^{13}C_{CH4}$ in Indiana coalbed gases is typically 65‰, and the much smaller $\Delta^{13}C_{CO2-CH4}$ of only ~ 25‰ in western Kentucky coalbed gases strongly suggests that Indiana and western Kentucky gases are of different origins (Table 1). When plotting $\delta^{13}C$ values over the reciprocal carbon number $1/C_n$ according to Chung et al. (1988) (Fig. 4b), the western Kentucky coal hydrocarbon gases show a pattern similar to thermogenic gases obtained from artificial maturation via hydrous pyrolysis. Residual CH_4 and CO_2 gases from pre-desorbed and subsequently crushed coals show a consistent ^{13}C-enrichment when compared to gases that had been desorbed prior to coal-crushing. This observation agrees with the larger diffusion coefficients of $^{12}CH_4$ and $^{12}CO_2$ facilitating the preferential loss of isotopically light moieties during primary desorption from coal cores (Strąpoć et al., 2006) (Table 4, Fig. 5).

4.4.3. Hydrogen stable isotope ratios in gases

Coalbed methane δD_{CH4} values from SW Indiana range from -195 to -208‰ and average -202 ± 5‰, n=33 (Table 3). The low abundances of C_{2+} hydrocarbons in Indiana coalbed gases increased the uncertainty of δD_{C2+} values relative to those from western Kentucky C_{2+} hydrocarbons. Nonetheless, the sequences of δD_{C2+} from Indiana and western Kentucky coalbed gases show distinct patterns (Fig. 4). There is a clear trend for
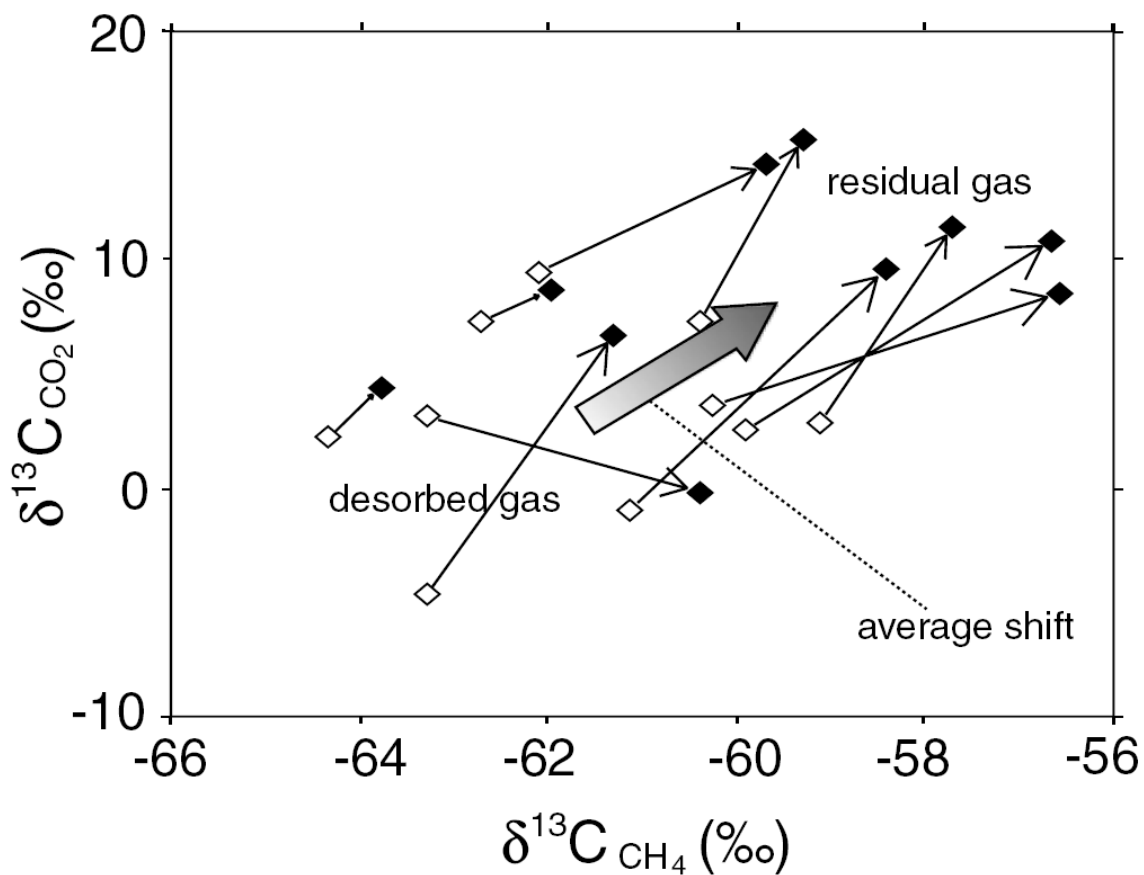
Fig. 5. Carbon isotopic shifts of residual methane and CO_2 from crushed coals in comparison with gases that were desorbed from coal core segments. Residual gases tend to be enriched in ^{13}C.

D-enrichment in Indiana propane relative to ethane and butanes (Fig. 4c), which parallels the ^{13}C-enrichment in C_3 mentioned above. Interestingly, western Kentucky ethane δD_{C2} values of ~ -219 ± 12‰ (n=13) are far more negative than Indiana δD_{C2} values (~ -92 ± 20‰, n=15) but are similar to those of western Kentucky methanes (δD_{CH4} ~ -217 ± 6‰,n=13) (Table 3, Fig. 4c, d). Two hydrous pyrolysis experiments of coals in contact with isotopically heavy (δD_{H2O} = 1196‰) or light waters (δD_{H2O} = -137‰) generated two series of hydrocarbon δD_{C1-C4} values featuring uniformly increasing D-enrichment by several hundred permil in the sequence C_1, C_2, C_3, n-C_4, i-C_4 (Table 4), testifying to the important isotopic influence of water hydrogen during the generation of thermogenic hydrocarbons via cracking (Table 4). We caution that the magnitude of isotopic fractionation and the kinetics of cracking reactions are likely different between natural maturation and artificial maturation via hydrous pyrolysis.

4.4.4. Chemical and isotopic compositions of waters

Waters associated with the Springfield and Seelyville coals were sampled from coalbed gas production wells in Sullivan County, Indiana. Chloride Cl⁻ concentrations indicate moderate chlorinities averaging 4.5 gL⁻¹ in the Springfield Coal and 2.2 gL⁻¹ in the Seelyville Coal (Table 2) that are 10 to 20 times lower than reported chlorinities in undiluted deep Illinois Basin brines (McIntosh et al., 2002). Other anions in waters associated with Indiana coals are usually at least two orders of magnitude less abundant than Cl⁻. δD_{H2O} values of waters from coal beds average -41.3‰ ± 0.3‰ (n=5) for the Springfield Coal and -44.0 ± 2.5‰ (n=5) for the Seelyville Coal (Table 2). The corresponding values for $\delta^{18}O_{H2O}$ are -6.1 ± 0.5‰ (n=5) for the Springfield Coal and -6.3 ± 0.6‰ (n=5) for Seelyville Coal (Table 2). These values closely resemble the average

isotopic composition of modern regional meteoric water $\delta D_{H2O} \sim -40‰$ and $\delta^{18}O_{H2O} \sim -6.3‰$ (Stueber and Walter, 1994).

4.5. Discussion

Illinois Basin coals in Indiana have a CBM potential of up to ~ 2 cm^3g^{-1} on average (Mastalerz et al., 2004), although they are of relatively low maturity with average vitrinite reflectance $R_o \sim 0.6\%$. The fact that Indiana coal beds contain more gas than can be expected according to the theoretical maximum thermogenic gas potential of a low-maturity coal (Meissner, 1984) (Fig. 6) suggests an alternative, non-thermogenic source of the gas. The 'dry' nature of Illinois coalbed gases with high ratios $C_1/(C_2+C_3)$ is indicative of large contributions of biogenic methane. The following sections will utilize compositional and isotopic information from gas components and waters to identify gas origins and to evaluate the importance of contrasting gas generation pathways in Illinois Basin coals at lower maturity in Indiana and at higher maturity in western Kentucky. Our data also constrain the extent and timing of secondary microbial methanogenesis in coals, as well as selective microbial alteration of C_{2+} hydrocarbons in coal beds.

4.5.1. Coalbed gas origin in Indiana

Disproportionately large quantities of methane in the presence of small amounts of C_{2+} in shallow, high volatile, bituminous C/B, Indiana coal beds (Figs. 3a, 6) argue for mixing of a substantial amount of microbially generated C_1 with minor thermogenic C_{2+} contributions. Indiana's average $\delta^{13}C_{CH4}$ value for coalbed methane of -60.7‰ is just below the threshold of -60‰ that classifies methanes of microbial origin (Schoell, 1980; Whiticar, 1996).
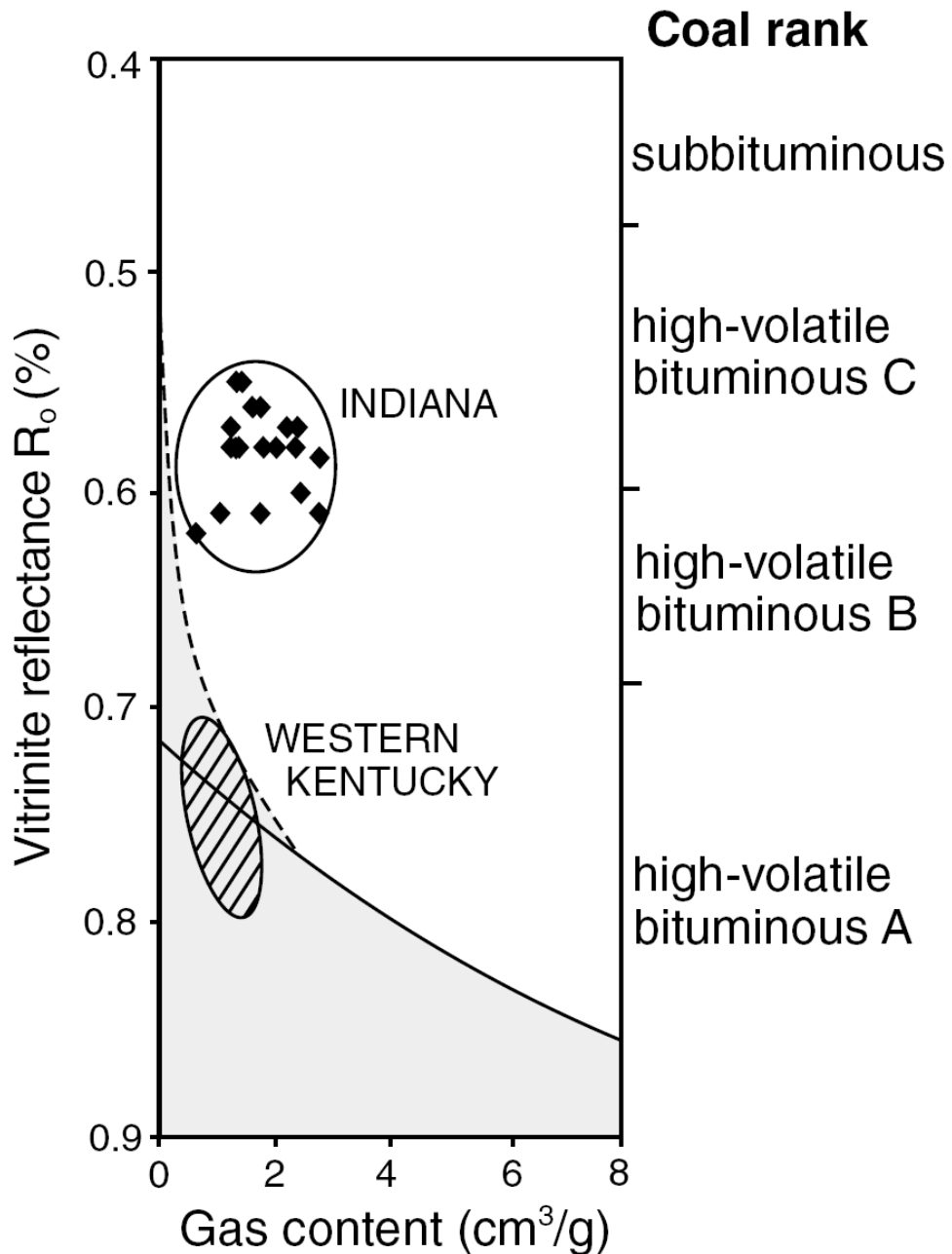
Fig. 6. The solid line demarcates the maximum expected thermogenic gas potential in relation to coal maturity (after Meissner, 1984). The dashed line suggests additional early thermogenic gas generation (Schimmelmann et al., 2006). The ellipse with hachure indicates the observed thermogenic gas content in coals from the studied area of western Kentucky. The upper oval outlines the observed coalbed gas content of less mature Indiana coals.

A model of Berner and Faber (1988) builds on the empirical relationship between thermal maturity in terms of vitrinite reflectance R_o and the expected relative abundances of thermogenic gas components methane, ethane, and propane.

$$C_1 \text{ (vol. \%)} = 9.1 \ln R_o + 93.1$$

$$C_2 \text{ (vol. \%)} = -6.3 \ln R_o + 4.8 \qquad (1)$$

$$C_3 \text{ (vol. \%)} = -2.9 \ln R_o + 1.9$$

Based on these equations, our measured C_1 and C_2 concentrations in Indiana coalbed gases provide estimates of thermogenic methane contributions of 0.1 vol. % and 0.4 vol. % in bulk coalbed methanes from the Springfield and Seelyville coals, respectively. The overwhelming remainder of methane must be of biogenic origin. The calculations assume the absence of significant oxidation/alteration of both C_1 and C_2 (isotopic evidence presented below).

Our isotopic results provide three arguments for microbial methanogenesis via CO_2-reduction in Indiana coal beds. (i) A cross-plot of δD_{CH4} over $\delta^{13}C_{CH4}$ (Fig. 7b) characterizes Indiana CBM mostly as a result of methanogenesis via microbial CO_2-reduction, possibly with minor additions of thermogenic methane (Schoell, 1980; Whiticar, 1996). (ii) The observed 65‰ mean carbon isotopic difference $\Delta^{13}C_{CO2-CH4}$ between CO_2 and CH_4 falls into the typical $\Delta^{13}C_{CO2-CH4}$ range of 60 to 80‰ for microbial CO_2-reduction to methane (Smith and Pallasser, 1996; Fig. 7a). This carbon isotopic difference arises from preferential microbial utilization of $^{12}CO_2$. As a result, residual CO_2 becomes ^{13}C-enriched (average $\delta^{13}C_{CO2} \sim 4.3‰$) and thus contrasts sharply against CO_2 in thermogenic gases with $\delta^{13}C$ values of $\sim -20‰$ (Smith and Pallasser, 1996). The observed $\Delta^{13}C_{CO2-CH4}$ values in Indiana coalbed gases translate into fractionation factors
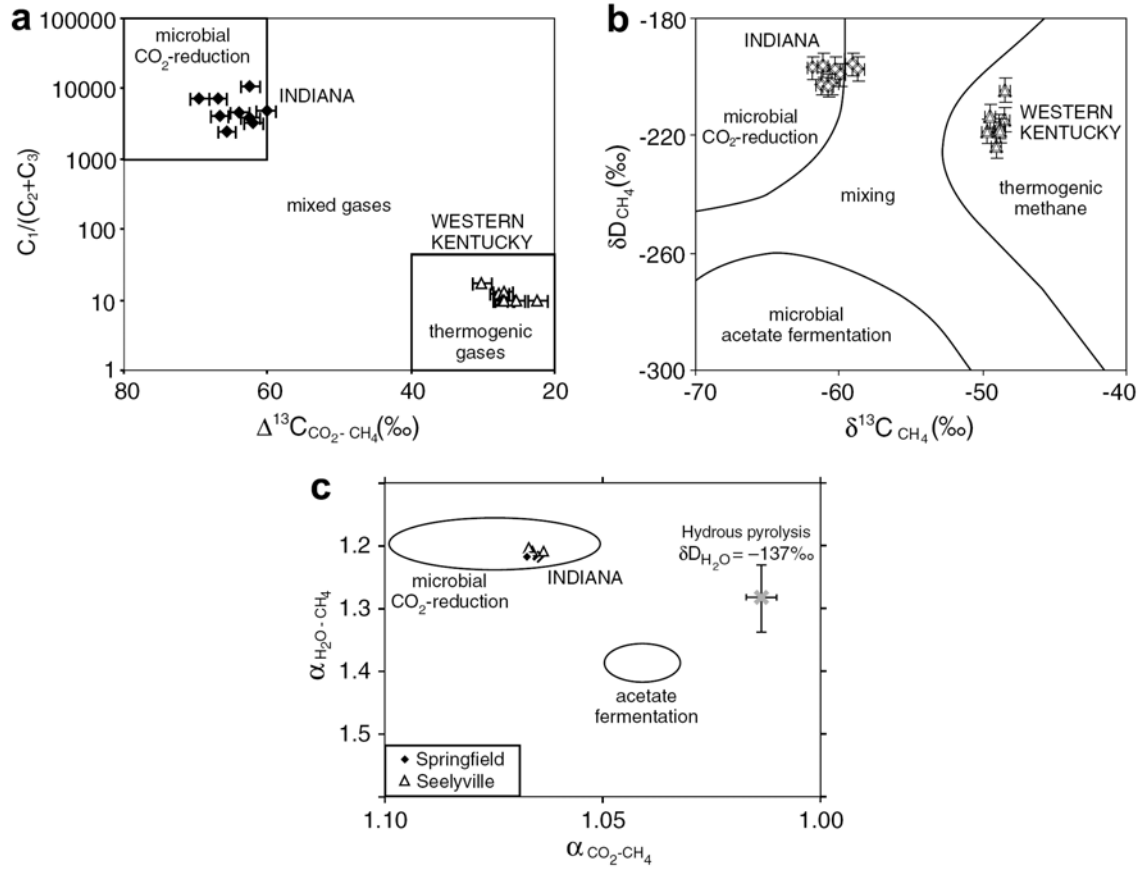
Fig. 7. Graphic stable isotopic gas classifications of Indiana and Kentucky coalbed gases and gases from hydrous pyrolysis experiments: (a) natural gases from this study; (b) natural gases from this study cross-plotted isotopically according to Whiticar (1996); (c) Indiana coalbed gases from this study cross-plotted isotopically according to Whiticar et al. (1986) where ellipses enclose typical ranges of values for microbially generated gases. Additionally one data point from hydrous pyrolysis is plotted to highlight significant difference between $\alpha_{CO2-CH4}$ values of microbial (via CO_2-reduction) and thermogenic generation of methane.

$\alpha_{CO2\text{-}CH4}$ of 1.066 for the Springfield Coal and 1.070 for the Seelyville Coal (Fig. 7c), which are typical α values for CO_2-reducing methanogens (Whiticar et al., 1986) where $\alpha_{CO2\text{-}CH4} = (\delta^{13}C_{CO2} + 10^3)/(\delta^{13}C_{CH4} + 10^3)$. (iii) The measured mean hydrogen isotopic differences between waters and methanes $\Delta D_{H2O\text{-}CH4}$ of 170‰ for the Springfield Coal and 164‰ for the Seelyville coal correspond to hydrogen isotopic fractionations $\alpha_{H2O\text{-}CH4}$ of 1.216 and 1.207, respectively. These values are in agreement with typical fractionation during methanogenesis via CO_2-reduction, within the specified uncertainty of Schoell's (1980) equation:

$$\delta D_{CH4} = \delta D_{H2O} - 160 \pm 10‰ \qquad (2)$$

This semi-quantitative empirical relationship has been confirmed for the Elk Valley coalfield in Canada (Aravena et al., 2003) and describes the overall hydrogen isotopic fractionation along the transfer of water-derived hydrogen through intermediary reactions into biogenic methane that is produced by methanogenic Archaea.

A plausible scenario for decomposition of coal organic matter by microbial consortia leading to methanogenesis via CO_2-reduction can be expressed as follows. Methanogens require elemental hydrogen H_2 and CO_2 that may be produced by other microbes. H_2 and CO_2 are probably provided by cooperating species that decompose organic matter, such as CO_2-generating fermentative anaerobes, H_2-producing acetogens (Scott, 1999), proton reducers, and others. In shallow coals with enhanced connectivity to meteoric water the successive oxidation and decarboxylation of organic molecules cannot be excluded (Ahmed and Smith, 2001). However, the relevance of oxidative reactions must be limited by the low oxygen tolerance of methanogens (redox potential below -330 mV, or partial pressure of oxygen below 2 ppm vol.; Kiener and Leisinger, 1983).

About 74 vol. % of the analyzed Indiana coals consists of vitrinite (Mastalerz et al., 2005a) (Table 1), a maceral that is chemically characterized by abundant aromatic moieties with aliphatic side chains. Vitrinite, as compared to other macerals in Indiana coals, is rich in oxygen (~ 15 wt. %) (Walker and Mastalerz, 2004). Most vitrinite oxygen resides in $C=O$ groups such as ketones and carboxylic groups of aliphatic side chains (Robin et al., 1975). Another 6 vol. % of Indiana coals is contributed by liptinite, a predominantly aliphatic maceral that is rich in organic hydrogen. Scott et al. (1994) and Zengler et al. (1999) demonstrated that long-chain aliphatic molecules, which are typical for liptinite, are readily biodegraded by anaerobes that are presumably similar to coal microbial consortia proposed above. The remaining 20 vol. % are equally split between the maceral inertinite and mineral matter (Mastalerz et al., 2005a). The carbon in inertinite is almost exclusively aromatic and thus not readily accessible for microbial decomposition. Nonetheless, both vitrinite and liptinite contain sufficient O-H and $C=O$ groups for acetogenic and fermentative microbes for the production of CO_2 and H_2. Lower bond energies may favor utilization of vitrinite because C_α-C_β bonds in aliphatic side chains of aromatic moieties are easier to cleave than C-C bonds of longer aliphatic carbon chains (Hartgers et al., 1994). Therefore, it follows that both predominant macerals of Indiana coals, and especially vitrinite, are suitable substrates to support microbial generation of H_2 and CO_2 by fermenters and acetogens, thus providing the raw materials for methanogenesis as a terminal step of organic matter decomposition in coal.

CO$_2$ can also be generated abiotically at the early coalification stage due to maturation of kerogen type III, for example in western Kentucky coalbed gases containing ~1 vol. % thermogenic CO_2 (Fig. 3). This process does not provide H_2 gas,

therefore the onset of biogenic methanogenesis is inhibited until coal becomes colonized by complex microbial consortia that decompose organic matter. Therefore, the presence of H_2 can be considered one of the growth-limiting factors for subsurface methanogenesis, in addition to the presence of relatively abundant CO_2. On the other hand, alternative supplies of H_2 could result from thermal maturation of underlying marine organic matter-rich shales, or may be generated by deep metamorphic processes (e.g., in aquifers within igneous rocks of the Fennoscandian Shield; Pedersen, 2001). If that is the case, then methanogenic Archaea could generate methane in the subsurface independently from bacterial consortia decomposing organic molecules to CO_2 and H_2.

4.5.2. Origin of western Kentucky coalbed gas

Several lines of evidence argue for a thermogenic origin of coalbed gases in western Kentucky. (i) The amount of gas in western Kentucky coals corresponds to the expected amount of generated thermogenic gas in relation to these coals' higher thermal maturity (Fig. 6), as a likely response to regional tectonic activity with burial along vertical displacements and migration of hot hydrothermal fluids (Greb et al., 1992). (ii) The relative abundances of C_1, C_2 and C_3 and the average gas wetness ratio $C_1/(C_2+C_3) \sim$ 10 are typical for thermogenic gas (Fig. 7a). The average contents of $C_2 = 7.5$ vol. % and of $C_3 = 2.7$ vol. % for the Springfield Coal (n=7) is similar to the respective data for the Seelyville Coal ($C_2 = 7.2$ vol. %; $C_3 = 2.6$ vol. %; n=6; Table 3). These C_2 and C_3 abundances are similar to those predicted by equations (1), namely $C_2 = 6.6$ vol. % and $C_3 = 2.7$ vol. %. (iii) The graphic classification of methanes in terms of plotting δD_{CH4} versus $\delta^{13}C_{CH4}$ (Fig. 7b) unambiguously characterizes western Kentucky CBM as thermogenic, with average values $\delta D_{CH4} \sim -217‰$ and $\delta^{13}C_{CH4} \sim -49‰$. (iv) The

observed carbon isotopic fractionation between CO_2 and methane averages $\alpha_{CO2-CH4} \sim$ 1.026 with corresponding isotopic offsets $\Delta^{13}C_{CO2-CH4} \sim 20$ to 33‰ (Fig. 7a). These values are consistent with carbon isotopic fractionation during thermal cracking of organic matter (Smith and Pallasser, 1996). Values of $\alpha_{CO2-CH4}$ from natural coalbed gases in western Kentucky are similar to $\alpha_{CO2-CH4} \sim 1.020$‰ obtained from artificial maturation via hydrous pyrolysis experiments of coals that produced thermogenic gas during heating. (v) Plotting $\delta^{13}C$ values of the $C_{1, 2, 3, n-4}$ hydrocarbons over their reciprocal carbon numbers yields quasi-linear trends for Springfield and Seelyville coalbed gases (Fig. 4b). Linearity is expected for essentially pure thermogenic gases (Chung et al., 1988) and at the same time confirms the absence of secondary diagenetic effects, e.g. via microbial alteration. Artificially generated thermogenic gases from hydrous pyrolysis experiments of the Seelyville and Springfield coals also express quasi-linearity but are systematically ^{13}C-enriched relative to their naturally generated counterparts (Fig. 4b). We interpret this difference in terms of the time/temperature (72 hours at 320 ºC) conditions of hydrous pyrolysis. In particular the higher temperature of artificial gas generation reduces carbon isotopic fractionation during cracking reactions and yields hydrocarbon gases that are isotopically more similar to their parent organic matter.

Although all of the western Kentucky samples (all from Rough Creek Graben) analyzed in this study show thermogenic signatures, a biogenic or mixed origin of coalbed gases can be expected in Kentucky in less mature coals at more shallow depths and in areas with a less tectonically influenced history. Thermogenic coal gases in

tectonically fractured Rough Creek Graben zone can be partially migrated from underlying shale formations, e.g. New Albany Shale (comment by Joe Hatch, USGS).

4.5.3. Constraints on the timing of microbial methane generation in Indiana

Our geochemical data suggest a plausible scenario to constrain the age of microbially-derived coalbed methane. Dynamic hydrologic connectivity between coals and meteoric water is suggested by the low chlorinity of Indiana coalbed waters indicating a 10 to 20-fold dilution of basinal brines (McIntosh et al., 2002) (Table 2). Regional meteoric waters during glacial periods were undoubtedly depleted in D and ^{18}O, below -78 and 11‰, respectively, relative to modern meteoric water (McIntosh and Walter, 2005). The close isotopic similarity of Indiana coalbed waters and modern regional meteoric precipitation (Fig. 8) proves that penetration of Holocene surface waters deep into coal beds has been fast enough to flush out D and ^{18}O-depleted waters of glacial age since the beginning of the Holocene ~10 ka ago. Nonetheless, the deeper Seelyville coalbed water is slightly depleted in heavy isotopes relative to the more shallow Springfield coalbed waters, owing to incomplete flushing of Pleistocene waters from the deeper coal bed. This suggests a mean residence time of coalbed waters on the order of several thousand years. The low hydrocarbon solubilities in water (27, 36, 26, 15 and 19ppm mol for C_1, C_2, C_3, i-C_4, and n-C_4, respectively; Yaws et al., 1990) and the high adsorption affinity of hydrocarbons in the microporous coal matrix (Clarkson and Bustin, 2000) would have limited the loss of hydrocarbon gases from coal beds during water washing, whereas the loss of readily soluble carbon dioxide is less constrained.
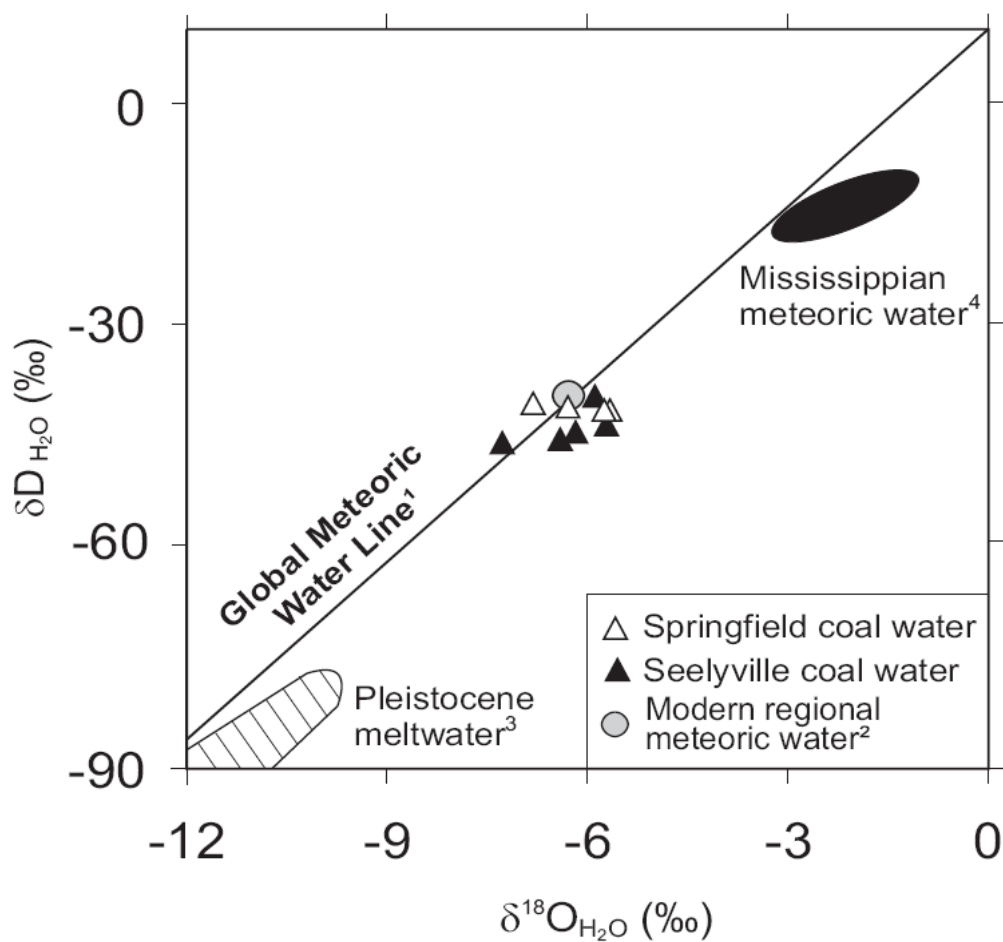
Fig. 8. Indiana coal bed-associated waters are isotopically similar to modern regional meteoric water but are distinctly different from Mississippian and Pleistocene environmental waters. Data sources: [1] Craig (1961), Rozanski et al. (2003); [2] Stueber and Walter (1994); [3] McIntosh and Walter (2005); [4] McIntosh et al. (2002).

The δD_{CH4} value of biogenic methane from CO_2-reduction is related to the δD_{H2O} of water in coal beds according to equation (2) (Schoell, 1980). Thus δD_{CH4} could serve as an isotopic proxy for constraining δD_{H2O} of paleowaters and the time of bacterial methane generation in Indiana coal beds across glacial and interglacial time periods with their isotopically diverse meteoric waters. However, equation (2) bears significant uncertainty that currently limits its usefulness for relative dating of methanogenesis. Studies of various environments and methanogen culturing experiments revealed that enzymatic isotopic fractionation in acetate fermentation (CH_4-H_2O) and CO_2-reduction (CH_4-CO_2) systems is dependent on temperature (Games et al., 1978; Botz et al., 1996; Valentine et al., 2004). For example, according to Gutsalo (2003), equation (2) for $\alpha_{CH4\text{-}H2O}$ is valid at ~ 40 °C, whereas current Indiana coalbed temperatures are ~16 to 18 °C. Gutsalo's (2003) relationship in combination with our δD_{CH4} field data predicts an unreasonable δD_{H2O} of -25‰. Similarly, experimental data gathered for $\alpha_{CH4\text{-}CO2}$ are dependent on temperature (Conrad, 2005) and also possibly on microbial species, nutrient availability, and environmental stress limiting microbial productivity.

Some microbial communities in coal beds might have colonized the organic substrate during shallow burial at the peat stage and survived/evolved through time since the Pennsylvanian (Parkes et al., 2000; Head et al., 2003). If coalbed gas loss over time was negligible, biogenic methane in coal beds would have been generated at an extremely low rate (the average time for cell division in subsurface environments can reach 10^5 years; Parkes et al., 2000). The isotopic composition of CBM would represent an integrated response to subsurface conditions over the entire history of methanogenesis. Such a scenario is unlikely, however, due to (i) a maximum coalification temperature of ~

80 °C, which was probably lethal for most non-extremophilic microbes and essentially destabilized or annihilated the initial microbial consortia of peat/coal; and (ii) turnover of formation water by infiltrating meteoric waters that may have entailed the loss of some dissolved gases. Also, erosional and postglacial uplift may have caused fracturing, opening of gas migration pathways, and gas loss via upward seepage. On the other hand, infiltration of freshwater may have enhanced microbial methane generation by introducing microbes into coal beds and by diluting basinal brines (as observed in New Albany Shale, Devonian-Mississippian strata in the Illinois Basin; McIntosh et al., 2002). Our hypothesis of active and ongoing microbial coalbed methane generation in Indiana coals cannot be proven with simple geochemical data, but can be addressed in the future by noble gas abundances, radiocarbon measurements in dissolved inorganic carbon in the hydrological cycle, other radioisotope dating (i.e. ^{4}He; Zhou and Ballentine, 2006), microbial culturing, and DNA-sequencing of microbial communities in coals. Our preliminary experiments proved the presence of viable methanogens in coalbed waters by anaerobically trapping microbes on 0.22 μm filters, growing them in methanogen-specific media with CO_2/H_2 headspace, and detecting newly generated methane.

4.5.4. Microbial alteration of hydrocarbon gases in Indiana coal beds

Thermogenic C_{2+} hydrocarbon gases are generated in predictable proportions (Fig. 3b) and with distinct isotopic patterns relating to carbon chain length (Berner and Faber, 1988; Chung et al., 1988; Fig. 4b, d). Higher temperature coalification conditions of western Kentucky coals might have caused their sterilization. We find no geochemical evidence for microbial alteration of western Kentucky thermogenic hydrocarbon gases and therefore conclude that deep western Kentucky coal beds remained hydrologically

91

isolated and were not re-inoculated with hydrocarbon-biodegrading microbes. Less mature Indiana coals from stratigraphically equivalent coal beds also contain some C_{2+} gases of thermogenic origin, albeit in much smaller concentrations (Fig. 3a). However, in Indiana coalbed gases the C_3 abundance is selectively lowered (Fig. 3a) and C_3 is disproportionately enriched in D and ^{13}C relative to ethane and butanes (Fig. 4a, c). Other than maturity, the main difference between Indiana and western Kentucky coal beds is the presence of a thriving and presumably diverse microbial community in Indiana coals.

We need to consider two separate chemical and isotopic biases affecting C_3 during microbial degradation of C_{2+} hydrocarbons. First, the susceptibility of hydrocarbons toward biodegradation depends on the carbon molecular skeleton. C_3 is a preferred substrate for biodegradation relative to C_2 (Larter and di Primio, 2005), n-C_4, and i-C_4, although the microbiological reasons are not understood. We hypothesize that a methyl group is more readily cleaved enzymatically from C_3 than from C_2. Alternatively, microbes may be equipped to metabolyze entire propane molecules, because molecular units with three carbon atoms are common in metabolic pathways within cells (e.g., pyruvate) and in the cell structure (e.g., glycerol backbone of membrane phospholipids). Molecular size and carbon chain configuration are important, as witnessed by the fact that straight-chain n-C_4 is more readily biodegraded than i-C_4 (Katz et al., 2002; Larter and di Primio, 2005), which is evident from butane concentrations in Indiana coalbed gases (Table 3, Fig. 3a).

Second, microbial degradation preferentially targets $^{12}C_3{}^{1}H_8$ relative to C_3 molecules containing ^{13}C and D atoms. The resulting ^{13}C and D-enrichment relative to other C_{2+} hydrocarbons in Indiana coalbed gases (Figs. 4a, c), which we informally call

Fig. 9. Gas alteration diagrams. (a) Ratio of vol. % of C_2 over C_3 versus isotopic difference between C_2 and C_3 depicting the biodegradation of C_3 and the increase in $\Delta^{13}C_{C3-C2}$. We assume that C_2 is not subject to significant alteration. The asterisks * identify values for thermogenic gases that were calculated according to Berner and Faber (1988). (b) Increasing $\delta^{13}C_{C3}$ values with decreasing remaining fraction of C_3 suggest preferential microbial alteration of $^{12}C_3$. Samples with the highest C_2 and C_3 concentrations presumably reflect the initial concentrations prior to alteration; α values represent preference for biodegradation, for example $^{12}C_3H_8$ over $^{13}C^{12}C_2H_8$. (c) A comparison of average data for Springfield and Seelyville coalbed gases from Indiana and western Kentucky suggests preferential microbial C_3-alteration in Indiana.

the "propane hiccup", suggests a kinetic carbon isotopic fractionation factor of microbial alteration of C_3 with $\alpha \sim 0.9982$ (Fig. 9b). This translates to a relatively insignificant $\alpha \sim 1.002$ preference for biodegradation of $^{12}C_3^1H_8$ over $^{13}C^{12}C_2^1H_8$, as compared, for example, with a typical $\alpha_{CO2\text{-}CH4} \sim 1.068$. Yet, extensive biodegradation can lead to significant ^{13}C-enrichment in residual fractions of C_3 as small as 10^{-2} volume percent. Moreover, the potential cleavage of terminal methyl groups preferentially eliminates ^{12}C-methyl carbon from C_3 and as a byproduct forms relatively ^{13}C-enriched C_2. This newly produced C_2 isotopically shifts the entire C_2 pool toward less negative $\delta^{13}C_{C2}$ values (Fig. 9b). Accordingly, partially biodegraded Indiana propane is also ^{13}C-enriched relative to non-biodegraded western Kentucky propane (Fig. 9a, c). Furthermore, C_2/C_3 abundance ratios and carbon isotopic differences $\Delta^{13}C_{C3\text{-}C2}$ between propanes and ethanes in thermogenic western Kentucky coalbed gases cluster tightly and compare favorably with theoretical values for thermogenic gases (Berner and Faber, 1988) whereas microbially altered C_{2+} hydrocarbons from Indiana coal beds plot diversely and are distinct from unaltered thermogenic gases (Fig. 9a). In general, increasing C_3 biodegradation exacerbates ^{13}C-enrichment of residual C_3 (Fig. 9a, b). As the size of the carbon molecular skeleton increases the isotope fractionation during partial biodegradation decreases, making it impossible to discern significant isotopic trends between Indiana and western Kentucky n-C_4 and i-C_4 (Figs. 4, 9c).

4.5.5. Comparison between coal core-desorbed and well-produced coalbed gases

Desorbed gases were available from freshly cored Indiana exploratory well INS-3. Soon after drilling and coring, the well started producing gas from Seelyville Coal. Coalbed gas from the producing INS-3 well was sampled 9 months after drilling. Isotopic

differences between canister-desorbed and commercially produced gases were insignificant, whereas the $C_1/(C_2+C_3)$ ratio increased five-fold in commercially-produced gas (Tables 1, 2). This suggests that CH_4 is transported faster than C_{2+} hydrocarbons from surrounding coal towards the production well. The observed chemical compositional shift from initial gas in coal to produced coalbed gas does not significantly affect the geochemical classification of gases because C_{2+} hydrocarbon abundances are low.

4.5.6. Implications for CBM exploration and production in the Illinois Basin

The largest coalbed gas potential in Indiana is related to biogenic methane in the shallow zone of the Illinois Basin between depths of 100 m and 300 m. At even shallower depths, we may expect hydrocarbon loss and oxidation (Kotelnikova, 2002; Riedinger et al., 2005). The depth of 50 m has been assigned as a cutoff for coalbed gas preservation in Indiana (Mastalerz and Kvale, 1998). The gas content in coals does not systematically correlate with depth (Mastalerz and Kvale, 2000), but instead depends on many other complex factors such as moisture and ash contents, maceral composition, and the micropore structure of coal (Clarkson, 1994; Mastalerz et al., 2006). Thus, the loading of Indiana coal beds with biogenic methane varies laterally and vertically from undersaturated to saturated (Mastalerz et al., 2005b). Coal chemical composition and pore connectivity (permability) are important factors limiting the populations of methanogenic microbes. Typical apertures of densely spaced (average spacing ~100 μm) microfractures in Indiana coals of 0.5-4 μm (Solano-Acosta, pers. comm.) are similar in size with microbes (typically around 1 μm). The moisture-coated interconnected microfracture network of coals is thus a plausible niche habitat for microbes.

In the Rough Creek Graben zone of western Kentucky, where coalbed gases are exclusively of thermogenic origin (generated in-situ from coal OM or potentially migrated from underlying fractured shale formations, e.g. New Albany Shale; comment by Joe Hatch, USGS), the amount of coalbed gases in general is similar or smaller than in the stratigraphically equivalent but less mature coal beds in Indiana. Optimal gas plays in Kentucky are local zones of high maturity and accelerated thermogenic gas generation, for example fault and breccia zones or regions of high hydrothermal mineralization (Hower and Gayer, 2002; Rowan et al., 2002).

4.6. Conclusions

Stratigraphically equivalent and geographically widespread coal beds (e.g., Springfield and Seelyville Coal Members) in Indiana and western Kentucky can regionally generate and store coalbed gases of contrasting and distinct origins. Biogenic methane from CO_2-reduction is prevalent in less mature Indiana coals, whereas more mature coals in the Rough Creek Graben of western Kentucky produced predominantly thermogenic hydrocarbons via cracking of coal organic matter. The two differently sourced biogenic and thermogenic types of coalbed gases are compositionally and isotopically distinct.

Due to differences in the origin of coalbed gases in the Illinois Basin, gas generation pathways are controlled by many factors. (i) Geologic regional history (e.g., tectonic and hydrothermal activity, burial depth, geothermal gradient, intensity of maturation/coalification, erosional or post-glacial uplift and fracture opening); (ii) hydrogeology (e.g., infiltration of meteoric water, residence time of formation water);

(iii) microbiology (e.g., presence of microbial communities that are able to thrive on decomposing coal, probably primarily utilizing vitrinite; habitability of coals in terms of temperature, pore structure, moisture content, salinity of pore waters).

The rate of microbial methane generation in Indiana coals is difficult to discern based on hydrocarbon-based evidence alone. However, the modern (Holocene) isotopic characteristics of waters associated with Indiana coal beds suggest that the residence time of water is less than 10,000 years. Such fast fluid exchange with oxygenated surface waters makes it unlikely that hydrocarbon gases have been accumulating since the deposition of Pennsylvanian coal swamps. Instead, fast fluid turnover in the presence of abundant coalbed methane and the presence of viable methanogens in coal waters suggest that biogenic methane in Indiana coal beds are continuously forming today as a quasi-renewable form of fossil energy, although the rate of in-situ methane generation remains unknown.

Microbial biodegradation of thermogenic C_{2+} hydrocarbon gases in coal beds preferentially targets propane and introduces isotope fractionation whereby remaining propane is enriched in heavy isotopes D and ^{13}C.

Acknowledgments

97

References

Ahmed, M., Smith, J.W., 2001. Biogenic methane generation in the degradation of eastern Australian Permian coals. Organic Geochemistry 32, 809-816.

Aravena, R., Harrison, S.M., Barker, J.F., Abercrombie, H., Rudolph, D., 2003. Origin of methane in the Elk Valley coalfield, southeastern British Columbia, Canada. Chemical Geology 195, 219-227.

Berner, U., Faber, E., 1988. Maturity related mixing model for methane, ethane and propane, based on carbon isotopes. Advances in Organic Geochemistry 13, 67-72.

Botz, R., Pokojski, H.-D., Schmitt, M., Thomm, M., 1996. Carbon isotope fractionation during bacterial methanogenesis by CO_2 reduction. Organic Geochemistry 25, 255-262.

Chung, H.M., Gormly, J.R., Squires, R.M., 1988. Origin of gaseous hydrocarbons in subsurface environments: Theoretical considerations of carbon isotope distribution. Chemical Geology 71, 97-104.

Clarkson, C.R., 1994. The effect of coal composition upon gas sorption and transmissibility of bituminous coal. M.Sc. thesis, Department of Geological Sciences, The University of British Columbia, Vancouver, August 1994, p.182.

Clarkson, C.R., Bustin, R.M., 2000. Binary gas adsorption/desorption isotherms: effect of moisture and coal composition upon carbon dioxide selectivity over methane. International Journal of Coal Geology 42, 241-271.

Conrad, R., 2005. Quantification of methanogenic pathways using stable carbon isotopic signatures: a review and a proposal. Organic Geochemistry 36, 739–752.

Craig, H., 1961. Isotopic variations in meteoric waters. Science 133, 1702-1703.

Drobniak, A., Mastalerz, M., Rupp, J., Eaton, N., 2004. Evaluation of coalbed gas potential of the Seelyville Coal Member, Indiana, USA. International Journal of Coal Geology 57, 265–282.

Faiz, M., Stalker, L., Sherwood, N., Saghafi, A., Wold, M., Barclay, S., Choundhury, J., Barker, W., Wang, I, 2003. Bio-enhancement of coal bed methane resources in the southern Sydney Basin. Australian Petroleum Production and Exploration Association Journal 43, 595-610.

Games, L.M., Hayes, J.M., Gunsalus, R.P., 1978. Methane-producing bacteria: natural fractionations of the stable carbon isotopes. Geochimica et Cosmochimica Acta 42, 1295-1297.

Gas Research Institute, 1995. A Guide to Determining Coalbed Gas Content. Gas Research Institute, GRI-94/0396.

Greb, S.F., Williams, D.A., Williamson, A.D., 1992. Geology and stratigraphy of the western Kentucky coal field. Kentucky Geological Survey, Bulletin 2, Series XI, 1992.

Gutsalo, L.K., 2003. Hydrogen isotope partitioning in the natural CH_4-H_2O system during microbial methane genesis. Doklady Earth Sciences 392, 1018-1021.

Hartgers, W.A., Sinninghe Damsté, J.S., de Leeuw, J.W., 1994. Geochemical significance of alkylbenzene distributions in flash pyrolysates of kerogens, coals, and asphaltenes. Geochimica et Cosmochimica Acta 58, 1759-1775.

Head, I.M., Jones, D.M., Larter, S.R., 2003. Biological activity in the deep subsurface and the origin of heavy oil. Nature 426, 344-352.

Henning, M.J., 2002. Development and assessment of inlet system for stable carbon isotopic analysis of individual compounds in gas mixtures. M.Sc. thesis, Department of Geological Sciences, Indiana University, Bloomington, December 2002, 40p.

Hoşgörmez, H., Yalçin, M.N., Cramer, B., Gerling, P., Faber, E., Schaefer, R.G., Mann, U., 2002. Isotopic and molecular composition of coal-bed gas in the Amasra region (Zonguldak basin – western Black Sea). Organic Geochemistry 33, 1429-1439.

Hower, J.C., Gayer, R.A., 2002. Mechanisms of coal metamorphism: case studies from Paleozoic coalfields. International Journal of Coal Geology 50, 215-245.

Hower, J.C., Mastalerz, M., Drobniak, A., Quick, J.C., Eble, C.F., Zimmerer, M.J., 2005. Mercury content of the Springfield coal, Indiana and Kentucky. International Journal of Coal Geology 63, 205-227.

Katz, B.J., Narimanov, A., Huseinzadeh, R., 2002. Significance of microbial processes in gases of the South Caspian basin. Marine and Petroleum Geology 19, 783-796.

Kiener, A., Leisinger, T., 1983. Oxygen sensitivity of methanogenic bacteria. Systematic and Applied Microbiology 4, 305-312.

Kotelnikova, S., 2002. Microbial production and oxidation of methane in deep subsurface. Earth-Science Reviews 58, 367-395.

Kvale, E.P., Mastalerz, M., Furer, L., Engelhardt, D.W., Rexroad, C.B., Eble, C., 2004. Atokan and early Desmoinesian coal-bearing parasequences in Indiana, U.S.A. In: Paschin, J.C., Gastaldo, R.A. (Eds.), Sequence stratigraphy, paleoclimate, and tectonics of coal-bearing strata. American Association of Petroleum Geologists, Studies in Geology 51, 71-88.

Larter, S., di Primio, R., 2005. Effects of biodegradation on oil and gas field PVT properties and the origin of oil rimmed gas accumulations. Organic Geochemistry 36, 299-310.

Macke, D.L., 1995. Illinois Basin Province. In: Gautier, D.L., Dolton, G.L., Takahashi, K.I., and Varnes, K.L. (Eds.), National assessment of United States oil and gas resources - Results, methodology, and supporting data: U.S. Geological Survey Digital Data Series 30 (064).

Mastalerz, M., Harper, D., 1998. Coal in Indiana: A Geologic Overview. Indiana Geological Survey Special Report 60.

Mastalerz, M., Kvale, E.P., 1998. Coal-bed gas potential in Daviess County, Indiana. Indiana Geological Survey Open File Report 98-7.

Mastalerz, M., Kvale, E.P., 2000. Coal quality variation and coalbed gas content in boreholes SDH-383 and SDH-384 in Posey County, Indiana. Indiana Geological Survey Open File Study 00-5.

Mastalerz, M., Drobniak, A., Rupp, J., Shaffer, N., 2004. Characterization of Indiana's coal resource: availability of the reserves, physical and chemical properties of the coal, and present potential uses. Indiana Geological Survey Open-File Study 04-02, July 2004.

Mastalerz, M., Drobniak, P. Irwin, 2005a. Indiana Coal Quality Database. Indiana Geological Survey Open-File Study 05-02.

Mastalerz, M., Strąpoć, D., Schimmelmann, A., 2005b. Isotopic signatures of coalbed gases from high volatile bituminous coals and roof rocks in Indiana, Illinois Basin. 2005 Gussow Geoscience Conference on Coalbed Methane, March 2005, Calgary, Canada.

Mastalerz, M., Drobniak, A., Strąpoć, D., Solano-Acosta, W., Rupp, J., 2006. Variations in coal properties in high volatile bituminous coals; Implications for coalbed gas content. Program and Abstracts, 23rd Annual Meeting of The Society for Organic Petrology, Beijing, China, September 2006.

McIntosh, J.C., Walter, L.M., Martini, A.M., 2002. Pleistocene recharge to midcontinent basins: Effects on salinity structure and microbial gas generation. Geochimica et Cosmochimica Acta 66, 1681-1700.

McIntosh, J.C., Walter, L.M., 2005. Volumetrically significant recharge of Pleistocene glacial meltwaters into epicratonic basins: Constrains imposed by solute mass balances. Chemical Geology 222, 292-309.

Meissner, F.F., 1984. Cretaceous and lower Tertiary coals as sources for gas accumulations in the Rocky Mountain area. In: Woodward, J., Meissner, F.F., Clayton, J.L. (Eds.), Hydrocarbon source rocks of the Greater Rocky Mountain region. Rocky Mountain Association of Geologists, Denver, Colorado, 401-430.

Parkes, J.R., Cragg, B.A., Wellsbury, P., 2000. Recent studies on bacterial populations and processes in subseafloor sediments: A review. Hydrogeology Journal 8, 11-28.

Pedersen, K., 2001. Diversity and activity of microorgsanisms in deep igneous rock aquifers of the Fennoscandian Shield. In: Fredrickson, J.K. and Fletcher, M. (Eds.), Subsurface Microbiology and Biogeochemistry. Wiley-Liss, Inc.

Riedinger, N., Pfeifer, K., Kasten, S., Garming, J.F.L., Vogt, C., Hensen, C., 2005. Diagenetic alteration of magnetic signals by anaerobic oxidation of methane related to a change in sedimentation rate. Geochimica et Cosmochimica Acta 69, 4117-4126.

Robin, P., Rouxhet, P.G., Durand, B., 1975. Charactérisation des kérogenes et de leur evolution par spectroscopie infrarouge. In: Campos, R., Goni, J. (Eds.), Advances in Organic Geochemistry. Madrid, 1977, 693-716.

Roseman Wright, C., 1977. Depositional history of the Pennsylvanian System in the Illinois Basin – A summary of work by Dr. Harold R. Wanless and associates. In: Palmer, J.E., Dutcher, R.R. (Eds.), Depositional and structural history of the Pennsylvanian System of the Illinois Basin. Part 2: Invited papers, 21-26. Ninth International Congress of Carboniferous Stratigraphy and Geology, May 26 to June 1, 1979.

Rowan, E.L., Goldhaber, M.B., Hatch, J.R., 2002. Regional fluid flow as a factor in the thermal history of the Illinois basin: Constraints from fluid inclusions and the maturity of Pennsylvanian coals. American Association of Petroleum Geologists Bulletin 86, 257-277.

Rozanski, K., Araguás-Araguás, L., Gonfiantini, R., 1993. Isotopic patterns in modern global precipitation. AGU Geophysical Monograph 78, 1-37.

Schimmelmann, A., Lewan, M.D., Wintsch, R.P., 1999. D/H isotope ratios of kerogen, bitumen, oil, and water in hydrous pyrolysis of source rocks containing kerogen types I, II, IIS, and III. Geochimica et Cosmochimica Acta 63, 3751-3766.

Schimmelmann, A., Sessions, A.L., Mastalerz, M., 2006. Hydrogen isotopic (D/H) composition of organic matter during diagenesis and thermal maturation. Annual Review of Earth and Planetary Science 34, 501-533.

Schoell, M., 1980. The hydrogen and carbon isotopic composition of methane from natural gases of various origins. Geochimica et Cosmochimica Acta 44, 649-661.

Schoell, M., 1983. Genetic characterization of natural gases. American Association of Petroleum Geologists Bulletin 67, 2225–2238.

Scott, A.R., Kaiser, W.R., Ayers, W.B., Jr., 1994. Thermogenic and secondary biogenic gases, San Juan Basin, Colorado and New Mexico - Implications for coalbed gas producibility. American Association of Petroleum Geologists Bulletin 78, 1186-1209.

Scott, A.R., 1999. Improving coal gas recovery with microbially enhanced coalbed methane. In: Mastalerz, M., Glikson, M., Golding, S.D. (Eds.), Coalbed Methane: Scientific, Environmental and Economic Evaluation, 89-110. Kluver Academic Publishers.

Smith, J.W., Pallasser, R.J., 1996. Microbial origin of Australian coalbed methane. American Association of Petroleum Geologists Bulletin 80, 891–897.

Solano-Acosta, W., Mastalerz, M., Rupp, J.A., Strapoc, D., Schimmelmann, A., 2005. Coal-bed gas potential in Pennsylvanian coal beds of Indiana. Proceedings of the 2005 International Coalbed Methane Symposium, Tuscaloosa, Alabama, May 2005, Paper No. 0526, CD edition.

Strąpoć, D., Schimmelmann, A., Mastalerz, M., 2006. Carbon isotopic fractionation of CH_4 and CO_2 during canister desorption of coal. Organic Geochemistry 37, 152-164.

Stueber, A.M., Walter, L.M., 1994. Glacial recharge and paleohydrologic flow systems in the Illinois basin: Evidence from chemistry of Ordovician carbonate (Galena) formation waters. Geological Society of America Bulletin 106, 1430-1439.

Thielemann, T., Cramer, B., Schippers, A., 2004. Coalbed methane in the Ruhr Basin, Germany: a renewable energy source? Organic Geochemistry 35, 1537-1549.

Valentine, D.L., Chidthaisong, A., Rice, A., Reeburgh, W.S., Tyler, S.C., 2004. Carbon and hydrogen isotope fractionation by moderately thermophilic methanogens. Geochimica et Cosmochimica Acta 68, 1571-1590.

Walker, R., Mastalerz, M., 2004. Functional groups and individual maceral chemistry of high volatile bituminous coals from southern Indiana: controls on coking. International Journal of Coal Geology 58, 181-191.

Whiticar, M.J., 1999. Carbon and hydrogen isotope systematics of bacterial formation and oxidation of methane. Chemical Geology 161, 291-314.

Whiticar, M.J., Faber, E., Schoell, M., 1986. Biogenic methane formation in marine and freshwater environments: CO_2 reduction vs. acetate fermentation - sotope evidence. Geochimica et Cosmochimica Acta 50, 693-709.

Yaws, C.L., Yang, H.-C., Hopper, J.R., Hansen, K.C., 1990. 232 hydrocarbons: water solubility data. Chemical Engineering, April 1990, 177-181.

Zengler, K., Richnow, H.H., Rosselló-Mora, R., Michaelis, W., Widdel, F., 1999. Methane formation from long-chain alkanes by anaerobic microorganisms. Nature 401, 266-269.

Zhou, Z., Ballentine, C.J., 2006. [4]He dating of groundwater associated with hydrocarbon reservoirs. Chemical Geology 226, 309-327.

CHAPTER 5

Variability of geochemical properties in a microbially-dominated coalbed gas system from the eastern margin of the Illinois Basin*

Dariusz Strąpoć [1], Maria Mastalerz [2], Arndt Schimmelmann [1], Agnieszka Drobniak [2], Sheila Hedges [3]

[1]Department of Geological Sciences, Indiana University, Bloomington, IN 47405, U.S.A.
[2] Indiana Geological Survey, Indiana University, Bloomington, IN 47405, U.S.A.
[3]National Energy Technology Laboratory, Pittsburgh, PA 15236, U.S.A.

103

Abstract

This study outlines gas characteristics along the southeastern margins of the Illinois Basin and scrutinizes regional versus local gas variations in Seelyville and Springfield coal beds. Our findings suggest that high permeability and shallow (100-250 m) depths of these Indiana coals allowed inoculation with methanogenic microbial consortia, thus leading to abundant microbial methane generation along eastern marginal part of the Illinois Basin. These relatively low maturity coals with a vitrinite reflectance $R_o \sim 0.6\%$ contain significant amounts of coal gas (~ 3 cm^3/g, 96 scf/t) with ≥ 97 volume % microbial methane. Amounts of coal gas can vary significantly vertically within a coal seam and laterally from location to location. Therefore sampling of entire core section is required to make accurate estimates of coal gas reserves. Some gas and co-produced water parameters drift over the time of production, e.g. $C_1/(C_2+C_3)$ increases, $\delta^{13}C_{CH4}$ and TDS decrease.

5.1. Introduction

Coals worldwide contain biogenic methane representing easily accessible, and often large, microbial coalbed gas deposits. Economically important reservoirs occur in coals of low rank (e.g., in the Powder River Basin; Ayers, 2002) and also higher rank coals where brine dilution initiated methanogenesis, for example in the Black Warrior Basin (Pitman et al., 2003), San Juan Basin (Scott et al., 1994), Alberta Basin (Bachu and Michael, 2003), and Sydney Basin (Faiz and Hendry, 2006). Distributions and compositions of gases in biogenic systems are governed by numerous factors including salinity (McIntosh et al., 2002), microbe-accessible porosity, and coal permeability. In contrast, thermogenic gas systems are primarily controlled by coal rank and depth (Scott et al., 1994; Scott, 1998; Schimmelmann et al., 2006). Determination of gas origin is therefore critical for a successful exploration strategy.

Compositional and isotopic gas characteristics discriminate between gases of biogenic and thermogenic origins (Lillis, 2007; Vandré et al., 2007; Faiz and Hendry, 2006; Gurgey et al., 2005; Smith and Pallasser, 1996). Frequently used diagnostic parameters are (i) the ratio of methane to the sum of ethane and propane $C_1/(C_2+C_3)$ (i.e., gas wetness; Bernard et al., 1978), (ii) carbon $\delta^{13}C_{CH4}$ and hydrogen δD_{CH4} isotopic compositions of methane (Schoell, 1980; Whiticar et al., 1986), and (iii) the carbon isotopic difference between CO_2 and methane $\Delta^{13}C_{CO2\text{-}CH4}$ (Smith and Pallasser, 1996; Strąpoć et al., 2007a). Typical diagnostic values for thermogenic versus microbial gases are, respectively, (i) <15 versus >1000 for $C_1/(C_2+C_3)$, (ii) >-50‰ versus <55‰ for $\delta^{13}C_{CH4}$ (i.e., more ^{13}C-enriched versus more ^{13}C-depleted), and (iii) <40‰ versus >55‰ for $\Delta^{13}C_{CO2\text{-}CH4}$. In addition, plotting of compound-specific $\delta^{13}C$ values of methane C_1 to

butane C_4 hydrocarbon gas components against the reciprocal carbon number (Chung et al., 1988) is useful for discriminating thermogenic from biogenic gases, whereby only thermogenic C_1 to C_4 plot along a straight line. Addition of microbial methane and microbial alteration of particular gas species can alter the straight line signature of exclusively thermogenic gases on the Chung diagram. The $\delta^{13}C_{CH4}$ value of mixtures of microbial and thermogenic methanes shifts towards more negative values with the addition of microbial methane. Selective biodegradation of hydrocarbon gas components can cause enrichment in ^{13}C in residual C_3 and n-C_4 (Katz et al., 2002).

The Illinois Basin contains relatively low-rank coals that host biogenic methane in amounts of 2 to 3 cm^3/g. In Indiana, these coals dominantly are of high volatile C and B bituminous rank (vitrinite reflectance R_o 0.5 - 0.65%; Mastalerz et al., 2004) which imply that they have not yet reached the window of significant thermogenic gas generation. More than 99% of the hydrocarbon component of coalbed gases from the eastern part of the Illinois Basin is microbially generated methane (Strąpoć et al., 2007a). In the Indiana portion of the Seelyville Coal Member alone, the estimates of microbial methane reserves are about 30 x 10^9 m^3 (1.06 Tcf; Drobniak et al., 2004). Inoculation of coal beds with methane-generating microbial consortia and initiation of coal biodegradation and methanogenesis probably occurred by recharge with post-glacial melt waters that diluted basinal brines and made coal environments microbially habitable (McIntosh et al., 2002; Strąpoć et al., 2007a). Since the glacial time, shallow and highly permeable coals likely have served as a densely populated habitat for methanogenic microbial community across the entire coal-bearing marginal area of the Illinois Basin.
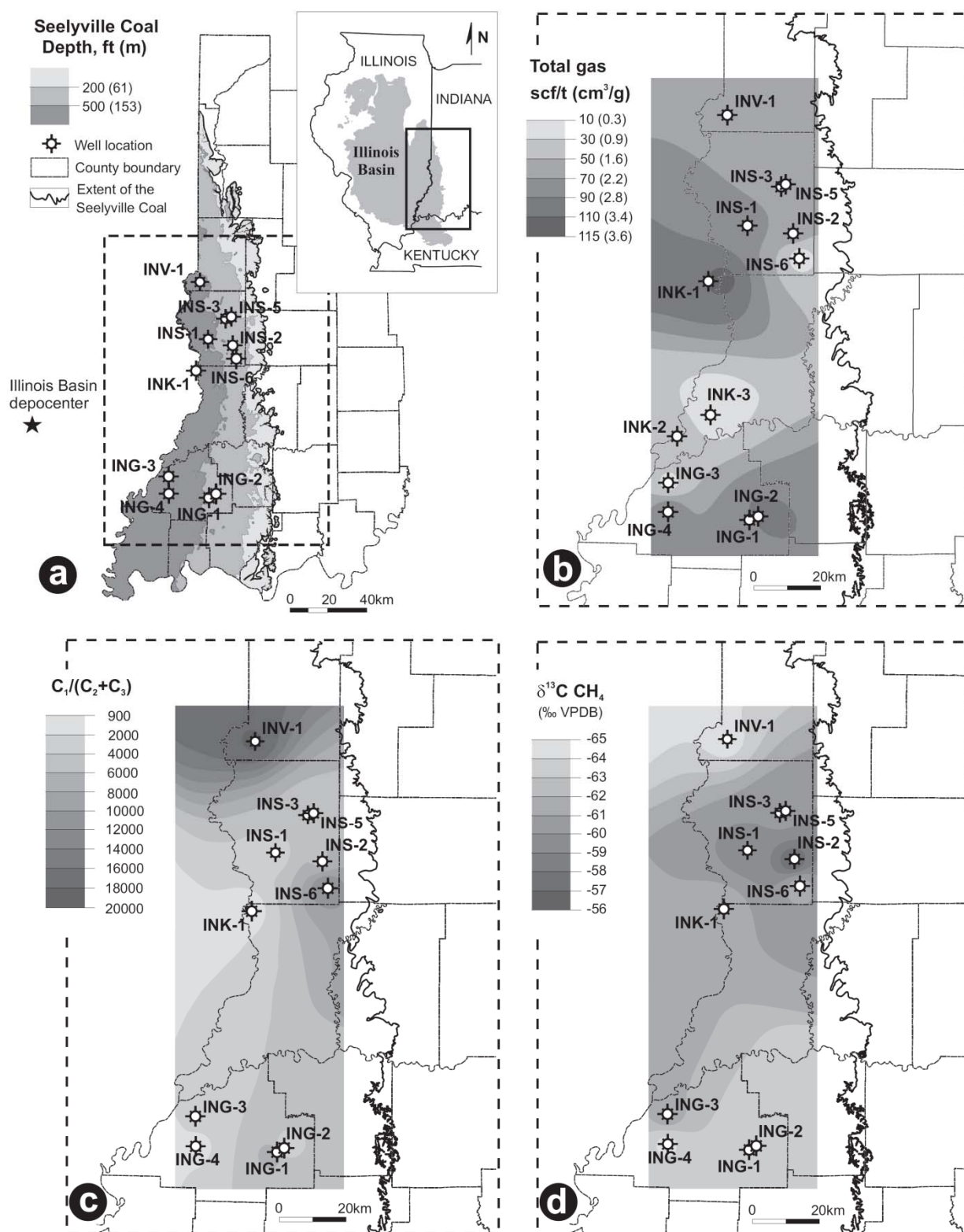
Fig. 1. Study area and gas properties: (a) eastern margin of the Illinois Basin showing the depth of the Seelyville Coal and the locations studied; (b) variation in gas content in the Seelyville Coal; (c) slight decrease towards basin's depocenter of $C_1/(C_2+C_3)$ ratio; (d) low variability of $\delta^{13}C_{CH4}$.

This study documents variations in gas composition and isotopic signatures in two Pennsylvanian coal beds in Indiana, the Springfield Coal Member of the Petersburg Formation and the Seelyville Coal Member of the Dugger Formation. We sampled coals and gases from these two coal beds from multiple locations at various coal depths. In each case, the entire thickness of a coal seam was sampled using multiple desorption canisters. This resulted in extensive data coverage. The resulting overall data set allows us to contrast the regional range of variations in gas characteristics against the variability that can occur among multiple samples through a coal seam in a single location. Furthermore, our coalbed methane (CBM) production time-series data provide insights into the compositional and isotopic variability during ongoing gas production.

5.2. Methods

Exploration boreholes (Fig. 1) drilled in four counties of southeastern Indiana provided ten access locations for the Seelyville Coal and four access locations for the Springfield Coal. Freshly retrieved coal cores through entire seams were sequentially split into ~30 cm long segments, immediately sealed in desorption canisters, and subsequently analyzed for total gas content (i.e., lost gas + gas from canister desorption + residual gas from crushed coal; Gas Research Institute, 1995), moisture, ash, heating value, maceral composition, and vitrinite reflectance. Desorbed gases from coal segments in canisters were volumetrically quantified and analyzed compositionally and isotopically (Strąpoć et al., 2006, Henning et al., 2007). Analyses were also performed on gases and co-produced waters from 14 coalbed methane production wells (Fig. 2).
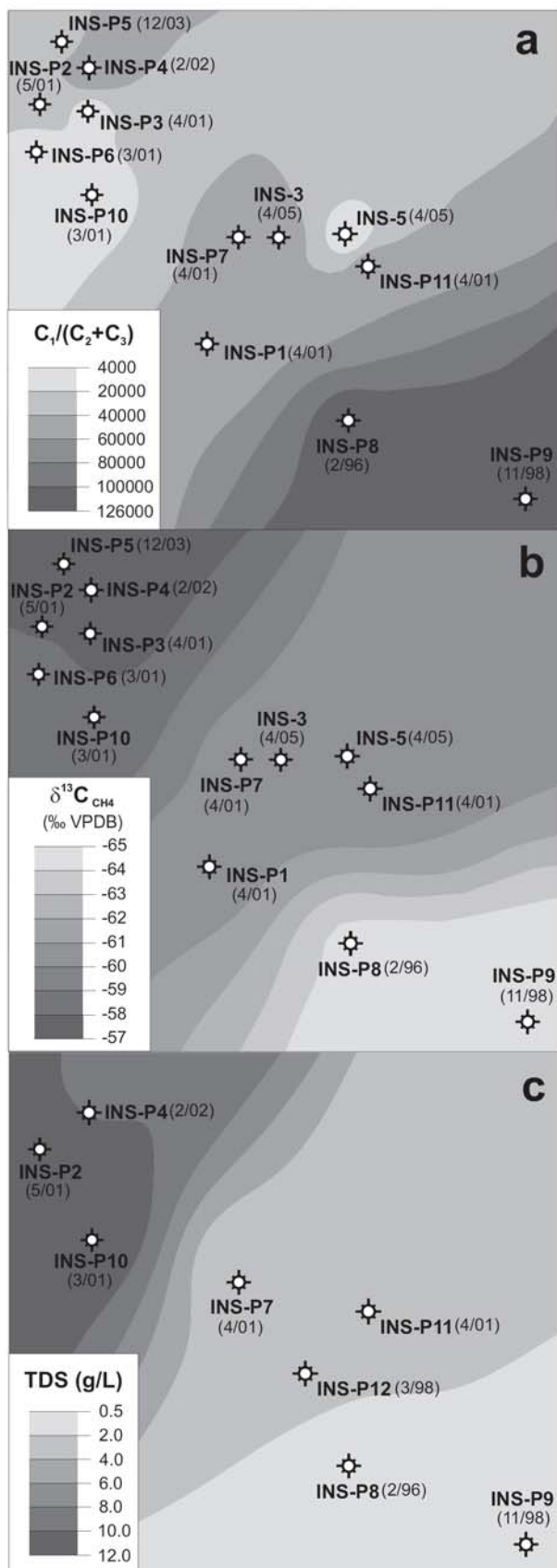
Fig. 2. Coalbed methane production field within the study area and gas (a, b) and water (c) properties. All parameters show shifts depending on the age of the production well. Travel distance of diffusing/migrating coal gas from adsorption sites increases with ongoing production, and longer distances exacerbate gas fractionation. Prolonged production of gas and co-produced water increases the influx of fresh water (c); the production start dates are presented in brackets in the month/year format.

Gas desorption and GC/MS analytical procedures are described in detail in Strąpoć et al. (2006, 2007a) and Henning et al. (2007). In brief, gas samples were analyzed using gas chromatography-oxidation/reduction-mass spectrometry (GC-ox/red-MS) using a Thermo GC connected on-line to oxidative and reductive reactors and a DeltaPLUS XP stable isotope mass spectrometer. Gases were injected by a glass syringe into a customized GASIS injection system consisting of three alternative loops of variable sample volume sizes (0.06 to 500μL). This loop system allowed measuring compound-specific concentrations and isotopic compositions in gas mixtures at highly variable compound concentrations of 10ppm to 100 vol. % in a single run (Henning et al., 2007). A PoraBOND Q capillary column in the GC separated the gas components. Concentrations were calculated from integrated peak areas. Relative concentrations of gas species did not take into account nitrogen because N_2 was used to flush the headspace of desorption canisters before the sealing of coal core segments.

Temperature, specific conductivity, pH, Eh, and alkalinity of co-produced waters from gas production wells were analyzed on-site using a multi-functional probe YSI 600XL (Yellow Springs Instruments, Inc., Yellow Springs, Ohio). Metal cation concentrations were determined using inductively coupled plasma-atomic emission spectroscopy (ICP-AES) on a Perkin Elmer Optima 3000 ICP spectrometer at the National Energy Technology Laboratory (NETL), Pittsburgh, PA. Water samples were analyzed as received except for sodium-rich waters that required 15-fold dilution with distilled water prior to analysis. Sodium analyses were performed separately with 1400-fold dilution. The reproducibility of metal cation analytical ICP data was approximately ±3%. Anion analyses were performed using a Dionex DX-600 ion chromatograph

equipped with an IonPac AG11-HC guard column, a Dionex 4 mm IonPac AS11-HC analytical column, and an electrochemical detector. Multi-step gradient analyses of anions were performed at 30ºC using an eluent flow rate of 1.5 mL/min. Sample dilutions necessary to determine chloride varied from 1/100 to 1/1000, and were 1/2.5 for fluoride, bromide, phosphate, and sulfate. Lower quantitation limits ranged from 0.07 ppm to 0.3 ppm in undiluted samples and were raised according to the necessary dilutions.

5.3. Results

Results from 11 exploratory boreholes and 8 production wells are presented in Tables 1 through 4. Table 1 lists moisture content, ash yield, sulfur content, heating value, petrographic composition, vitrinite reflectance and total gas content for ~30 cm long coal core sections from ten locations of the Seelyville Coal and four locations of the Springfield Coal. Seelyville coal samples derived from 96 to 240 m (316 to 786 feet) depth, represent high volatile C and B bituminous rank, and express vitrinite reflectance R_o values of 0.54 to 0.58%. Average moisture content ranges from 11.2 wt. % in the shallowest location INS-5 to 5.4 wt. % in location INS-2. Ash yield ranges from 8.3 wt. % in location INS-5 to 43.6 wt. % in location ING-3. Large variations in ash content occur vertically across coal seams within a location. Intra-seam variations in moisture content are small. Petrographically determined maceral contents on a mineral matter free basis are for vitrinite 68.5 to 84.6 vol. %, for liptinite 4.7 to 10.0 vol. %, and for inertinite 10.0 to 21.5 vol. %. Gas contents range from 0.6 to 3.6 cm^3/g (20 to 115 scf/t, Table 1,

111

SEELYVILLE COAL

Borehole	Month drilled	Depth (m)	Depth (feet)	R_o (%)	Total gas (air-dry) (cm³/g)	Total gas (air-dry) (scf/t)	V (vol.%, mmf)	L (vol.%, mmf)	I (vol.%, mmf)	Moisture (as rec.) (%)	Ash (dry) (%)	S-total (dry) (%)	Heating value (dry) (MJ/kg)
INS-5	Jun-05	96	316	0.56	2.6	82	68.2	9.4	22.4	12.2	5.6	2.9	32.3
		98	323	0.54	2.4	77	68.8	10.6	20.6	10.3	11.1	6.1	30.0
average		97	319	0.55	2.5	80	68.5	10.0	21.5	11.2	8.3	4.5	31.2
INS-3	Dec-04	108	353	0.56	1.5	47	71.8	2.4	25.7	8.1	37.6	5.1	19.7
		108	354	0.56	0.6	19	86.1	6.1	7.8	9.6	16.2	6.1	28.0
		108	355	0.57	0.9	29	78.8	7.8	13.5	8.7	8.2	4.6	31.3
		109	356	0.59	2.6	82	82.9	4.6	12.5	11.7	10.2	5.7	30.4
average		108	355	0.57	1.4	44	79.9	5.2	14.9	9.5	18.1	5.4	27.4
INS-6	Jan-06	113	372	n.d.	0.6	20	n.d.	n.d.	n.d.	n.d.	n.d.	n.d.	n.d.
INS-2	May-04	128	420	0.57	2.3	74	72.7	10.4	16.9	4.3	29.8	10.2	23.4
		128	421	0.57	2.9	92	76.4	4.7	18.9	6.5	13.0	6.9	29.4
		129	422	0.59	0.6	20	90.0	2.7	7.3	5.3	11.6	5.1	29.7
average		128	421	0.58	1.9	62	79.7	5.9	14.4	5.4	18.2	7.4	27.5
ING-1	Jul-03	138	453	0.54	3.2	104	75.1	5.1	19.8	7.2	19.7	7.7	26.9
INV-1	Apr-06	158	517	n.d.	2.0	66	n.d.	n.d.	n.d.	n.d.	n.d.	n.d.	n.d.
		158	518	n.d.	2.3	72	n.d.	n.d.	n.d.	n.d.	n.d.	n.d.	n.d.
		158	519	n.d.	n.a.	n.a.	n.d.	n.d.	n.d.	n.d.	n.d.	n.d.	n.d.
average		158	518	n.d.	2.2	69	n.d.	n.d.	n.d.	n.d.	n.d.	n.d.	n.d.
INS-1	Feb-04	159	522	0.56	3.5	111	90.0	4.3	5.7	7.6	17.9	5.8	26.6
		160	523	0.57	2.6	84	80.3	9.0	10.7	8.2	9.2	3.3	30.9
		160	524	0.60	1.1	35	83.3	5.3	11.4	6.6	34.0	5.5	21.2
		160	525	0.60	3.6	116	82.3	7.5	10.2	7.7	20.3	6.2	26.4
		160	526	0.58	2.4	78	78.9	3.5	17.6	10.3	30.7	17.8	21.3
average		160	524	0.58	2.6	85	83.0	5.9	11.1	8.1	22.4	7.7	25.3
INK-1	Oct-04	186	611	0.59	3.2	102	82.6	4.7	12.6	8.4	29.9	4.8	22.4
		187	612	0.57	4.0	127	86.5	6.2	7.3	11.6	10.6	6.0	30.4
average		187	612	0.58	3.6	115	84.6	5.5	10.0	10.0	20.3	5.4	26.4
ING-3	Sep-04	214	700	0.57	0.7	23	82.6	4.7	12.6	6.5	43.6	3.9	18.2
ING-4	Oct-04	238	781	0.60	3.6	115	84.3	6.9	8.8	8.9	12.7	4.0	29.1
		239	784	0.59	1.7	54	80.2	11.1	8.6	7.7	9.7	5.5	30.8
		240	786	0.61	3.0	96	77.9	5.7	16.4	6.5	29.3	4.8	23.4
average		239	783	0.60	2.8	88	80.8	7.9	11.3	7.7	17.2	4.8	27.8
coal average		152	500	0.55	2.2	71	80.0	6.3	13.7	7.8	18.7	5.9	25.6
st. dev.		45	147	0.02	1.1	34	6.2	2.6	5.6	2.1	11.1	3.1	4.3

SPRINGFIELD COAL

Borehole	Month drilled	Depth (m)	Depth (feet)	R_o (%)	Total gas (air-dry) (cm³/g)	Total gas (air-dry) (scf/t)	V (vol.%, mmf)	L (vol.%, mmf)	I (vol.%, mmf)	Moisture (as rec.) (%)	Ash (dry) (%)	S-total (dry) (%)	Heating value (dry) (MJ/kg)
ING-2	Aug-04	97	317	0.58	3.6	116	78.6	5.9	15.5	9.4	28.3	2.5	23.6
		97	318	0.58	1.8	57	86.5	6.6	7.0	9.6	13.6	5.3	28.7
		97	319	n.d.	1.9	61	n.d.	n.d.	n.d.	n.d.	n.d.	n.d.	n.d.
		98	321	0.57	2.3	72	89.0	4.2	6.9	9.5	19.2	4.4	27.1
average		97	319	0.58	2.4	76	84.7	5.5	9.8	9.5	20.4	4.0	26.5
INV-1	Apr-06	99	325	n.d.	n.a.	n.a.	n.d.	n.d.	n.d.	n.d.	n.d.	n.d.	n.d.
		99	326	n.d.	1.0	32	n.d.	n.d.	n.d.	n.d.	n.d.	n.d.	n.d.
average		99	326	n.d.	1.0	32	n.d.	n.d.	n.d.	n.d.	n.d.	n.d.	n.d.
INS-1	Feb-04	100	329	0.61	1.3	43	74.1	10.7	15.2	5.7	19.0	12.1	26.6
ING-3	Sep-04	148	486	0.69	3.3	106	76.9	7.2	15.9	11.9	5.0	0.8	32.4
		149	487	0.74	3.4	109	90.4	4.4	5.2	12.5	4.8	0.7	32.1
average		148	486	0.72	3.4	107	83.6	5.8	10.5	12.2	4.9	0.8	32.3
coal average		109	359	0.63	2.3	74	82.6	6.5	10.9	9.8	15.0	4.3	28.4
st. dev.		22	73	0.07	1.0	32	6.9	2.4	5.1	2.4	9.1	4.2	3.4

Table 1. Properties of Seelyville and Springfield coal core sections from boreholes in eastern Indiana; V – vitrinite, L – liptinite, I – inertinite, mmf – mineral matter free, as rec. – as received, scf/t – standard cubic feet per ton, st. dev. – standard deviation, n.d. – not determined.

112

SEELYVILLE COAL Borehole	Depth (m)	Depth (feet)	C$_1$ (vol. %)	CO$_2$ (vol. %)	C$_2$ (vol. %)	C$_3$ (vol. %)	i-C$_4$ (vol. %)	n-C$_4$ (vol. %)	C$_1$/(C$_2$+C$_3$)	δ^{13}C C$_1$ (‰)	δD C$_1$ (‰)	δ^{13}C CO$_2$ (‰)	δ^{13}C C$_2$ (‰)	δ^{13}C C$_3$ (‰)	δ^{13}C i-C$_4$ (‰)	δ^{13}C n-C$_4$ (‰)	Δ^{13}C CO$_2$-CH$_4$ (‰)
INS-5	96	316	97.38	2.59	2.2E-02	2.7E-04	1.6E-04	5.0E-05	4284	-61.9	n.d.	8.4	-37.5	-17.5	-26.1	-5.6	70.2
	98	323	97.17	2.80	2.1E-02	4.7E-03	0.0E+00	2.0E-03	3752	-58.7	-203	14.3	-34.8	-26.9	n.d.	-28.9	73.0
average	**97**	**319**	**97.28**	**2.70**	**2.2E-02**	**2.5E-03**	**8.0E-05**	**1.0E-03**	**4018**	**-60.3**	**-203**	**11.3**	**-36.2**	**-22.2**	**-26.1**	**-17.2**	**71.6**
INS-3	108	353	99.33	0.66	1.4E-02	3.3E-04	2.7E-04	2.3E-05	7096	-61.0	n.d.	14.3	-38.0	-18.8	-32.5	n.d.	75.3
	108	354	98.84	0.99	1.3E-01	2.5E-02	1.9E-02	3.8E-04	638	-62.7	n.d.	5.1	-36.0	-17.2	-29.2	n.d.	67.8
	108	355	99.16	0.82	1.7E-02	5.6E-04	5.4E-04	9.5E-05	5533	-57.7	n.d.	3.7	-37.1	-20.6	-27.0	n.d.	61.5
	109	356	99.25	0.73	9.1E-03	6.1E-03	4.7E-03	5.2E-03	6538	-60.0	-206	6.4	-34.9	-29.9	-30.8	-33.8	66.4
average	**108**	**355**	**99.14**	**0.80**	**4.2E-02**	**8.1E-03**	**6.1E-03**	**1.4E-03**	**4951**	**-60.4**	**-206**	**7.4**	**-36.5**	**-21.6**	**-29.9**	**-33.8**	**67.7**
INS-6	113	372	98.35	1.64	7.6E-03	3.2E-04	2.0E-03	3.5E-03	12467	-61.8	n.d.	9.0	-43.1	-22.4	-35.4	-28.7	70.8
INS-2	128	420	97.37	2.61	1.5E-02	1.3E-03	0.0E+00	1.1E-03	5901	-57.1	-204	12.6	-33.8	-28.1	n.d.	-30.3	69.7
	128	421	96.61	3.38	1.3E-02	2.0E-03	0.0E+00	5.0E-04	6441	-56.7	-199	12.6	-35.0	-28.0	n.d.	-28.9	69.3
	129	422	96.91	3.07	1.5E-02	6.0E-03	5.0E-04	1.8E-03	4615	-56.6	-191	5.8	-34.2	-32.0	-15.6	-26.8	62.3
average	**128**	**421**	**96.96**	**3.02**	**1.4E-02**	**3.1E-03**	**1.7E-04**	**1.1E-03**	**5652**	**-56.8**	**-198**	**10.3**	**-34.3**	**-29.3**	**-28.7**	**-28.7**	**67.1**
ING-1	138	453	92.57	7.23	4.3E-02	n.d.	1.7E-04	0.1298	1143	-63.7	n.d.	n.d.	-38.5	-31.2	n.d.	-29.1	42.5
INV-1	158	517	99.83	0.16	4.5E-03	3.6E-04	0.0E+00	0.0E+00	20721	-65.1	n.d.	-7.0	-37.8	-28.0	n.d.	n.d.	58.1
	158	518	99.80	0.20	4.2E-03	3.9E-04	0.0E+00	0.0E+00	21846	-65.1	n.d.	-13.7	-37.6	-28.3	n.d.	n.d.	51.4
	158	519	99.80	0.19	6.8E-03	1.4E-03	5.5E-04	0.0E+00	12311	-62.8	n.d.	-0.1	-37.1	-35.6	-34.5	n.d.	62.8
average	**158**	**518**	**99.82**	**0.18**	**4.3E-03**	**3.8E-04**	**0.0E+00**	**0.0E+00**	**21284**	**-65.1**	**n.d.**	**-10.3**	**-37.7**	**-28.2**	**-34.5**	**n.d.**	**57.4**
INS-1	159	522	97.69	2.28	3.0E-02	1.0E-03	0.0E+00	1.0E-03	3151	-60.9	-207	3.1	-33.5	-27.1	n.d.	-37.2	64.0
	160	523	98.15	1.73	9.6E-02	1.5E-02	1.0E-03	2.0E-03	884	-59.1	-200	-0.4	-33.9	-29.8	-32.6	-31.8	58.7
	160	524	97.23	2.74	2.0E-02	6.0E-03	3.0E-04	4.0E-04	3740	-58.1	-187	-5.6	-34.2	-30.9	-23.6	-26.8	52.5
	160	525	98.12	1.86	1.7E-02	3.0E-03	0.0E+00	7.0E-04	4906	-60.2	-195	2.6	-36.2	-30.6	n.d.	-32.3	62.8
	160	526	98.23	1.75	1.7E-02	3.0E-03	3.0E-04	2.0E-04	4912	-59.0	-203	-0.1	-36.7	-30.6	-34.5	-46.9	59.0
average	**160**	**524**	**97.9**	**2.07**	**3.6E-02**	**5.6E-03**	**5.0E-04**	**8.6E-04**	**2353**	**-59.5**	**-198**	**-0.1**	**-34.9**	**-29.8**	**-30.2**	**-35.0**	**59.4**
INK-1	186	611	98.88	0.98	1.2E-01	1.3E-02	7.2E-03	2.4E-04	730	-62.9	n.d.	14.3	-35.9	-14.5	-30.0	-18.8	77.2
	187	612	97.33	2.56	7.1E-02	1.3E-02	7.8E-03	1.3E-02	1155	-61.3	n.d.	4.7	-35.8	-22.2	-28.9	-29.2	66.0
average	**187**	**612**	**98.11**	**1.77**	**9.7E-02**	**1.3E-02**	**7.5E-03**	**6.7E-03**	**942**	**-62.1**	**n.d.**	**9.5**	**-35.8**	**-18.4**	**-29.5**	**-24.0**	**71.6**
ING-3	214	700	98.63	1.34	2.1E-02	4.1E-03	1.1E-03	2.4E-03	3880	-61.2	n.d.	-2.8	-34.5	-29.9	-50.6	-30.8	58.4
ING-4	238	781	99.06	0.85	8.1E-02	4.9E-04	2.8E-03	2.6E-04	1209	-64.5	-204	1.3	-36.2	-20.2	-27.5	-29.4	65.8
	239	784	98.97	0.92	1.1E-01	2.7E-04	1.3E-03	1.6E-04	860	-63.9	n.d.	2.4	-34.3	n.d.	-29.3	-25.3	66.2
	240	786	99.43	0.46	1.0E-01	6.3E-04	2.3E-03	4.9E-04	949	-64.7	n.d.	3.0	-36.3	-17.4	-27.9	-26.2	67.6
average	**239**	**783**	**99.15**	**0.75**	**1.0E-01**	**4.7E-04**	**2.2E-03**	**3.0E-04**	**1006**	**-64.3**	**-204**	**2.2**	**-35.6**	**-18.8**	**-28.2**	**-27.0**	**66.5**
coal aver.	**152**	**500**	**98.05**	**1.89**	**4.1E-02**	**4.6E-03**	**2.1E-03**	**1.5E-03**	**5320**	**-60.8**	**-200**	**4.3**	**-36.0**	**-25.5**	**-30.1**	**-28.8**	**64.1**
st. dev.	45	147	1.51	1.49	4.2E-02	6.3E-03	4.3E-03	2.8E-03	5652	2.7	6	7.2	2.1	5.6	7.2	7.9	8.0

Table 2 (to be continued).

SPRINGFIELD COAL Borehole	Depth (m)	(feet)	C_1 (vol. %)	CO_2 (vol. %)	C_2 (vol. %)	C_3 (vol. %)	$i\text{-}C_4$ (vol. %)	$n\text{-}C_4$ (vol. %)	$C_1/(C_2+C_3)$	$\delta^{13}C$ C_1 (‰)	δD C_1 (‰)	$\delta^{13}C$ CO_2 (‰)	$\delta^{13}C$ C_2 (‰)	$\delta^{13}C$ C_3 (‰)	$\delta^{13}C$ $i\text{-}C_4$ (‰)	$\delta^{13}C$ $n\text{-}C_4$ (‰)	$\Delta^{13}C$ $CO_2\text{-}CH_4$ (‰)
ING-2	97	317	98.54	1.45	1.0E-02	8.0E-04	0.0E+00	6.0E-04	9124	-63.8	-197	4.7	-38.0	-31.4	n.d.	-32.1	68.5
	97	318	98.71	1.28	1.1E-02	1.2E-04	1.7E-04	1.0E-04	9004	-62.6	n.d	5.2	-38.5	-13.3	-34.6	-31.2	67.8
	97	319	98.19	1.80	9.0E-03	1.0E-03	0.0E+00	1.5E-03	9819	-63.7	-190	4.2	-36.9	-34.4	n.d.	-30.9	67.9
	98	321	98.23	1.75	1.2E-02	1.0E-03	0.0E+00	1.5E-03	7556	-63.4	n.d.	2.2	-37.2	-31.9	n.d.	-31.0	65.5
average	97	319	98.42	1.57	1.0E-02	7.3E-04	4.4E-05	9.3E-04	8876	-63.4	-193	4.1	-37.7	-27.7	-34.6	-31.3	67.4
INV-1	99	325	99.74	0.25	3.4E-03	3.3E-04	3.0E-03	0.0E+00	27093	-56.3	n.d.	-1.0	-37.5	-35.5	-35.5	n.d.	55.3
	99	326	99.72	0.27	7.3E-03	2.7E-03	1.3E-04	4.3E-04	9978	-62.0	n.d.	-1.5	-42.6	-36.4	-37.2	-31.1	60.5
average	99	326	99.73	0.26	5.3E-03	1.5E-03	1.6E-03	2.2E-04	18536	-59.1	n.d.	-1.2	-40.1	-36.0	-36.3	-31.1	57.9
INS-1	100	329	93.40	6.59	7.0E-03	6.0E-03	3.0E-04	2.0E-04	7185	-60.2	-195	-2.3	-41.4	-31.8	-9.8	-12.7	57.9
ING-3	148	486	99.67	0.33	2.2E-03	5.0E-04	0.0E+00	2.7E-04	37034	-62.6	n.d.	-7.7	-38.6	-27.9	n.d.	-29.8	55.0
	149	489	99.69	0.30	8.4E-03	2.4E-04	2.2E-04	8.6E-05	11483	-63.9	-191	-1.7	-43.8	-18.3	-37.8	-36.1	62.2
average	149	487	99.68	0.32	5.3E-03	3.7E-04	1.1E-04	1.8E-04	24258	-63.3	-191	-4.7	-41.2	-23.1	-37.8	-33.0	58.6
coal aver.	109	359	98.43	1.56	7.8E-03	1.4E-03	4.3E-04	5.2E-04	14253	-62.1	-193	0.2	-39.4	-29.0	-31.0	-29.4	62.3
st. dev.	22	73	2.00	2.00	3.3E-03	1.9E-03	9.7E-04	5.8E-04	10477	2.4	3	4.2	2.5	8.0	11.9	7.0	5.4

Table 2 (continued). Concentration and isotopic parameters of coal gases desorbed from fresh cores, eastern Indiana. N_2 not determined; C_1 – methane, C_2 – ethane, C_3 – propane, $i\text{-}C_4$ – iso-butane, $n\text{-}C_4$ – n-butane, n.d. – not determined.

114

GASES FROM PRODUCTION WELLS

Sep. 2005	production started	from coal	C_1 (vol. %)	CO_2 (vol. %)	C_2 (vol. %)	C_3 (vol. %)	$i\text{-}C_4$ (vol. %)	$n\text{-}C_4$ (vol. %)	$C_1/(C_2+C_3)$	$\delta^{13}C$ C_1 (‰)	δD C_1 (‰)	$\delta^{13}C$ CO_2 (‰)	$\delta^{13}C$ C_2 (‰)	$\delta^{13}C$ C_3 (‰)	$\delta^{13}C$ $i\text{-}C_4$ (‰)	$\delta^{13}C$ $n\text{-}C_4$ (‰)	$\Delta^{13}C$ $CO_2\text{-}CH_4$ (‰)
INS-3	4/05	III	99.90	0.09	1.0E-02	1.5E-04	2.6E-05	0.0E+00	9385	-59.9	-210	2.3	-37.5	-14.4	-39.4	n.d.	62.2
INS-P1	4/01	III	99.93	0.06	1.3E-02	1.7E-04	5.8E-05	0.0E+00	7866	-60.3	-203	0.6	-35.4	-15.8	-30.1	n.d.	60.9
INS-P2	5/01	III+V	99.57	0.43	6.1E-03	8.0E-04	6.6E-05	0.0E+00	14329	-57.9	-202	5.5	-39.2	-30.2	-28.4	n.d.	63.4
INS-P3	4/01	III+V	99.44	0.56	4.3E-03	2.4E-04	3.4E-05	0.0E+00	21860	-57.3	-199	5.7	-38.5	-30.1	-28.3	n.d.	63.0
INS-P4	2/02	III+V	99.36	0.64	4.4E-03	8.4E-05	2.1E-05	0.0E+00	22384	-56.9	-202	5.0	-38.5	-25.5	n.d.	n.d.	61.9
INS-P5	12/03	III+V	99.60	0.40	5.3E-03	1.2E-04	4.7E-05	1.7E-05	18417	-57.5	-202	2.5	-37.7	-26.3	-28.5	-29.3	60.0
INS-P6	3/01	III	99.74	0.20	6.4E-02	3.6E-04	9.2E-05	3.0E-05	1553	-58.5	-193	4.7	-33.8	-14.7	-27.1	-16.8	63.2
INS-P7	8/01	III	99.93	0.06	1.1E-02	1.1E-04	0.0E+00	0.0E+00	8701	-60.0	-201	-0.2	-38.9	-11.6	n.d.	n.d.	59.8
INS-P8	2/96	III	99.99	0.004	5.0E-03	4.7E-05	6.3E-05	0.0E+00	19627	-65.9	-200	-32.9	-37.4	-16.6	-27.8	n.d.	33.0
INS-P9	11/98	III	99.99	0.01	4.0E-03	4.4E-05	5.5E-05	0.0E+00	24927	-66.6	-198	-33.9	-44.3	-27.5	-36.8	n.d.	32.7
average			**99.74**	**0.24**	**1.3E-02**	**2.1E-04**	**4.6E-05**	**4.8E-06**	**14905**	**-60.1**	**-201**	**-4.1**	**-38.1**	**-21.3**	**-30.8**	**-23.1**	**56.0**
Jul. 2006																	
INS-3	4/05	III	99.96	0.04	1.3E-03	1.8E-05	1.1E-05	0.0E+00	77626	-59.7	-216	8.9	-38.1	-20.6	n.d.	n.d.	68.6
INS-P2	5/01	III+V	99.62	0.36	1.5E-02	2.1E-04	2.6E-05	3.1E-05	6736	-60.3	-201	10.5	-36.2	-36.4	n.d.	n.d.	70.8
INS-P3	4/01	III+V	99.97	0.03	4.6E-03	1.7E-05	1.0E-05	1.6E-05	21609	-62.6	-201	10.7	-35.7	-21.9	-32.6	-4.3	73.3
INS-P4	2/02	III+V	99.89	0.11	4.0E-03	2.5E-05	7.0E-06	1.1E-05	24792	-57.9	-206	10.0	-39.1	n.d.	n.d.	n.d.	67.9
INS-P7	8/01	III	99.96	0.04	1.5E-03	1.4E-05	0.0E+00	0.0E+00	65420	-58.2	-201	2.6	-35.3	-31.0	-28.1	-29.0	60.9
INS-P8	2/96	III	99.97	0.03	1.6E-03	1.3E-05	1.2E-05	0.0E+00	62220	-61.4	-211	4.8	-37.2	-15.9	n.d.	n.d.	66.2
INS-P9	11/98	III	99.99	0.01	3.6E-04	2.5E-04	1.5E-04	4.8E-05	163361	-62.4	-216	-14.1	-41.2	n.d.	n.d.	n.d.	48.3
INS-P10	3/01	V	99.96	0.03	5.0E-03	4.2E-03	1.6E-03	9.4E-04	10955	-57.9	-206	10.0	-39.1	n.d.	n.d.	n.d.	67.9
INS-P11	4/05	III	99.96	0.04	1.5E-03	1.9E-03	0.0E+00	0.0E+00	67063	-60.5	-207	5.4	-36.5	n.d.	n.d.	n.d.	66.0
average			**99.92**	**0.08**	**3.8E-03**	**5.3E-04**	**2.0E-04**	**1.2E-04**	**55531**	**-60.1**	**-207**	**5.4**	**-37.6**	**-25.2**	**-30.4**	**-16.7**	**65.5**
Mar. 2007																	
INS-3	4/05	III	99.90	0.10	2.0E-03	7.8E-05	1.0E-03	0.0E+00	48932	-60.2	n.d.	-5.8	-38.7	-32.7	-45.8	n.d.	54.4
INS-P1	4/01	III	99.91	0.09	2.3E-03	5.7E-05	7.7E-04	0.0E+00	42720	-60.6	n.d.	-2.1	-37.0	n.d.	-39.5	n.d.	60.9
INS-P2	5/01	III+V	99.89	0.10	3.5E-03	7.1E-05	4.8E-04	0.0E+00	28026	-57.9	n.d.	4.0	-37.0	-27.5	-43.4	n.d.	63.4
INS-P3	4/01	III+V	99.96	0.02	1.1E-02	6.9E-05	2.3E-04	0.0E+00	8704	-57.3	n.d.	-5.0	-36.3	-39.4	-45.2	n.d.	63.0
INS-P4	2/02	III+V	99.82	0.18	1.3E-02	3.8E-05	6.0E-04	0.0E+00	74777	-57.7	n.d.	4.1	-39.9	-27.7	-44.8	n.d.	61.9
INS-P5	12/03	III+V	99.80	0.19	3.2E-03	5.2E-05	5.1E-04	0.0E+00	31133	-57.4	n.d.	5.3	-36.4	-29.4	-45.0	n.d.	60.0
INS-P6	3/01	III	99.89	0.10	1.0E-02	8.9E-05	6.3E-04	0.0E+00	9768	-58.8	n.d.	-2.3	-34.3	-22.6	-46.4	n.d.	56.4
INS-P7	8/01	III	99.95	0.05	1.9E-03	4.8E-05	5.0E-04	0.0E+00	51855	-60.3	n.d.	-4.2	-39.0	-33.0	-47.0	n.d.	56.1
INS-P8	2/96	III	99.98	0.02	8.8E-04	3.2E-05	5.2E-04	0.0E+00	109611	-64.1	n.d.	-33.6	-39.5	-16.2	-43.9	n.d.	30.6
INS-P9	11/98	III	99.97	0.03	7.6E-04	3.9E-05	7.7E-04	0.0E+00	125142	-64.7	n.d.	-35.1	-43.3	n.d.	-42.2	n.d.	29.6
INS-P11	4/05	III	99.92	0.08	2.0E-03	3.6E-05	3.7E-04	0.0E+00	49088	-60.2	n.d.	3.6	-35.2	n.d.	-46.9	n.d.	63.7
average			**99.91**	**0.09**	**3.6E-03**	**5.5E-05**	**5.8E-04**	**0.0E+00**	**52705**	**-59.9**	**n.d.**	**-6.5**	**-37.9**	**-28.6**	**-44.6**	**n.d.**	**54.5**

Table 3. Concentration and isotopic parameters of produced coal gases, eastern Indiana; III – production from the Seelyville Coal, V – from the Springfield Coal, III+V – single well penetrates and produces gas from both coal seams. N_2 not determined, start of production given in month/year format, n.d. – not determined.

115

PRODUCTION WELLS

July 2006

| production well | | INS-P2 | INS-P4 | INS-P7 | INS-P8 | INS-P9 | INS-P10 | INS-P11 | INS-P12 | |
production from coal		III+V	III+V	III	III	III	V	III	III	average
Temp.	°C	16.7	16.6	17.0	16.8	16.7	16.0	17.5	17.4	**16.8**
Sp.Cond.	µS/cm	19446	17345	6205	1923	2210	16939	4134	7765	**9496**
pH		7.66	7.80	8.01	8.72	8.79	7.47	8.09	8.28	**8.10**
Eh	mV	-373	-398	-403	-411	-409	-388	-426	-316	**-390**
Alk (CaCO$_3$)	mg/L	1171	1378	1260	788	964	1189	1761	1420	**1241**
δD_{VSMOW}	‰	-45.5	-40.3	-40.6	-45.5	-43.0	-41.1	-42.7	-44.6	**-42.9**
TDS	g/L	11.28	9.53	2.43	0.59	0.76	12.08	3.11	3.39	**5.40**
Fl	mg/L	0.56	0.21	2.40	7.65	7.36	0.27	0.56	2.46	**2.68**
Cl	mg/L	6767	5670	1455	125	55	4741	1812	1790	**2802**
SO$_4$	mg/L	123.1	5.5	b.d.l.	3.2	212.4	3493.5	16.7	2.6	**551.0**
PO$_4$	mg/L	b.d.l.	0.52	0.62	1.36	0.33	b.d.l.	b.d.l.	0.34	**0.63**
B	mg/L	0.83	0.95	0.67	0.85	0.99	0.77	0.73	0.75	**0.82**
Ba	mg/L	0.37	6.49	0.87	0.11	0.08	0.09	1.56	0.84	**1.30**
Ca	mg/L	32.29	26.39	6.71	1.00	1.07	31.19	10.19	6.12	**14.37**
Co	mg/L	0.00	0.01	0.00	b.d.l.	b.d.l.	0.00	0.01	b.d.l.	**0.01**
Cu	mg/L	0.02	0.04	0.15	b.d.l.	b.d.l.	0.01	0.03	b.d.l.	**0.05**
Fe	mg/L	3.52	41.12	3.15	0.17	1.36	1.78	5.10	1.19	**7.17**
K	mg/L	15.97	13.20	4.53	1.19	1.27	11.96	6.08	5.15	**7.42**
Mg	mg/L	26.84	22.31	2.98	0.31	0.43	30.67	5.17	3.63	**11.54**
Mn	mg/L	0.06	0.47	0.05	0.01	0.02	0.05	0.07	0.02	**0.09**
Mo	mg/L	0.01	0.02	0.01	0.00	0.01	0.01	0.02	0.01	**0.01**
Na	mg/L	4310	3740	954	449	479	3765	1255	1580	**2066**
P	mg/L	0.02	0.02	0.04	0.08	0.07	0.03	0.04	0.03	**0.04**
Pb	mg/L	b.d.l.	b.d.l.	0.02	b.d.l.	b.d.l.	b.d.l.	0.01	b.d.l.	**0.01**
S	mg/L	31.3	0.3	b.d.l.	10.9	372.0	599.8	2.1	b.d.l.	**169.4**
Si	mg/L	0.49	0.52	0.48	0.52	0.50	0.49	0.52	0.48	**0.50**
Sr	mg/L	3.01	2.98	0.34	0.12	0.13	2.36	0.56	0.45	**1.24**
V	mg/L	0.00	0.01	0.01	b.d.l.	b.d.l.	0.01	0.01	b.d.l.	**0.01**
Zn	mg/L	0.02	0.04	0.17	0.01	0.01	0.01	0.03	0.01	**0.04**

September 2005

| production well | | INS-P2 | INS-P3 | INS-3 | INS-P6 | INS-P7 | INS-P10 | INS-P8 | INS-P9 | |
production from coal		III+V	III+V	III	III	III	V	III	III	average
δD_{VSMOW}	‰	-41.6	-41.5	-43.8	-39.8	-44.8	-41.4	-46.0	-45.8	**-43.1**
$\delta^{18}O_{VSMOW}$	‰	-5.7	-5.7	-5.7	-5.9	-6.2	-6.3	-7.3	-6.4	**-6.1**
Cl	mg/L	5657	4337	2438	5058	2042	5276	143	97	**3131**

Table 4. Physicochemical and isotopic parameters of co-produced coalbed waters, eastern Indiana; b.d.l. – below detection limit, III – production from the Seelyville Coal, V – from the Springfield Coal, III+V – single well penetrates and produces gas from both coal seams.

Fig. 1b) and express much variability across individual coal seams, as determined by data from consecutively desorbed ~30cm long coal core intervals.

The Springfield Coal samples represent high volatile C-A bituminous rank with R_o values of 0.58 to 0.72% and derive from depths between 97 and 149 m (317 to 487 feet) (Table 1). Moisture content ranges from 5.7 to 12.2 wt. %. Ash contents span from 4.9 wt. % in location ING-3 to 20.4 wt. % in location ING-2. Petrographically determined maceral contents on a mineral matter free basis are for vitrinite 74.1 to 84.7 vol. %, for liptinite 5.5 to 10.7 vol. %, and for inertinite 9.8 to 15.2 vol. %. Gas contents range from of 1.0 to 3.4 cm^3/g (32 to 107 scf/t) in a similar fashion as for the Seelyville Coal.

Table 2 displays gas compositional (C_1, C_2, C_3, i-C_4, n-C_4, CO_2) and compound-specific $\delta^{13}C$ and δD values from exploratory boreholes. Table 3 displays similar data in a time-series from coalbed methane production wells. Methane often accounts for > 97 vol. % of the total gas volume from exploratory boreholes (not including N_2) and for > 99 vol. % in gas from production wells. The second major component of investigated coal gases was CO_2, averaging 1.7 vol. % in exploratory boreholes and 0.15 vol. % in production wells. The sum of C_{2+} hydrocarbons (i.e., ethane, propane, and butanes) amounted to < 0.25 vol. % in exploratory boreholes and < 0.1 vol. % in gas from production wells. Low concentrations of C_{2+} hydrocarbons result in dry gas with very high C_1/(C_2+C_3) ratios on the order of 10^3 to 10^5. The C_1/(C_2+C_3) ratio tends to decrease westward in the direction towards the depocenter of the Illinois Basin (Fig. 1c).

Stable hydrogen and carbon isotopic data for C_1 to C_4 hydrocarbons and CO_2 express small variations across the study area (Tables 2 and 3, Figs. 1d and 2b). Ranges

are for δD_{CH4} from -216 to -187‰, for $\delta^{13}C_{CH4}$ within -66.6 to -56.3‰ (average -60.7‰, n=64), for $\delta^{13}C_{C2}$ within -44.3 to -33.5‰ (average -37.4‰, n=64), and for $\delta^{13}C_{CO2}$ within -14.1 to 14.3‰ (average +3.2‰, n=58). Exceptions are noted in the oldest production wells INS-P8 and INS-P9 where (i) $\delta^{13}C_{CO2}$ is very negative down to -35.1, and (ii) $\delta^{13}C_{C3}$ values are usually higher than -30‰, which is typically expected for thermogenic propane (Berner and Faber, 1988). The above cited averages of $\delta^{13}C_{CH4}$ and $\delta^{13}C_{CO2}$ do not include the exceptional data from wells INS-P8 and INS-P9. The resulting average $\Delta^{13}C_{CO2-CH4}$ of more than 60‰ is strongly indicative of a microbial origin of methanes generated via CO_2-reduction (Fig. 3).

Data from consecutive coal core sections from the bottom towards the top of entire coal seams express slight trends of increasing ^{13}C-depletion in methane and higher $\Delta^{13}C_{CO2-CH4}$ isotopic offsets (Table 2). However, this small isotopic variance within each location remains well within the range that is characteristic of microbial methane generated via CO_2 reduction (Fig. 3). Throughout the coal beds the gases are compositionally quite uniform, as reflected by very high $C_1/(C_2+C_3)$ ratios (Table 2). Top and bottom sections of coal beds usually contain more gas than middle sections (Table 1).

Time-series of gas compositional and isotopic data from production wells do not show any significant changes or obvious trends over 27 months of monitoring (i.e., the cumulative time between three sampling events). However, with increasing ages of production wells from one to 11 years, we observe (i) decreasing relative abundances of C_{2+} hydrocarbons (i.e., increasing $C_1/(C_2+C_3)$ ratios), (ii) decreasing $\delta^{13}C_{CH4}$ values, and
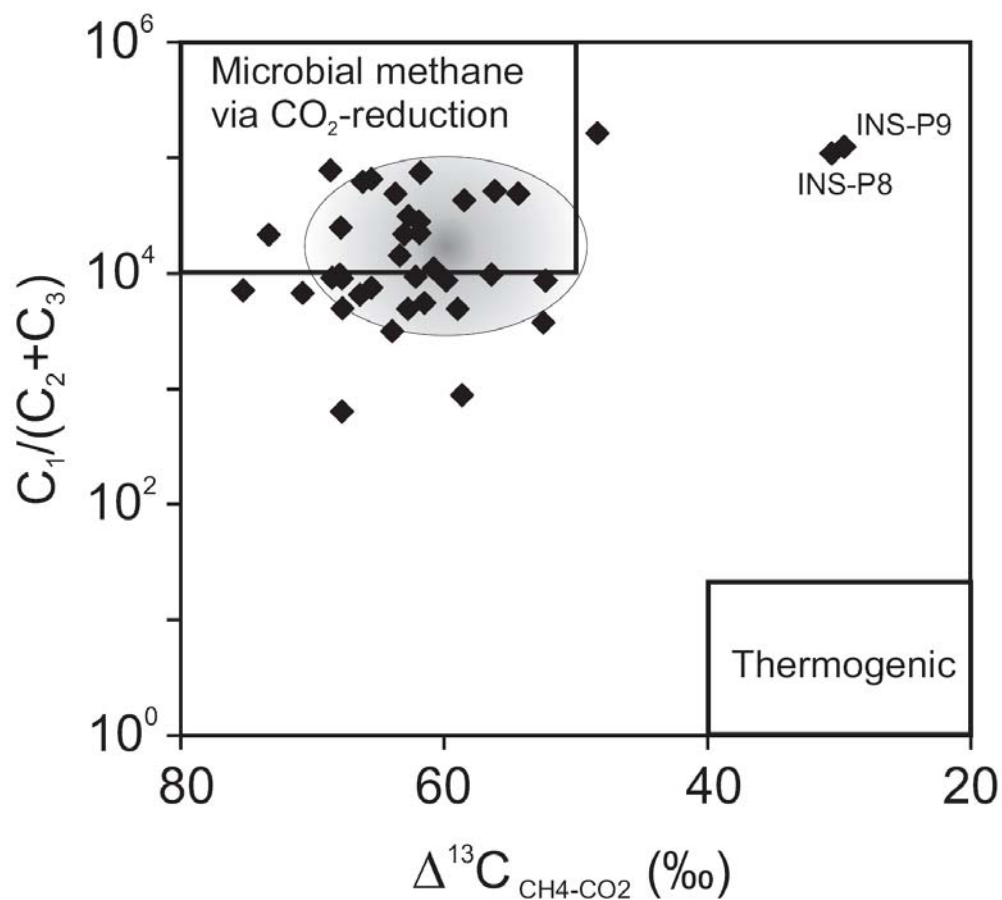
Fig. 3. Geochemical classification of Indiana's coal gas origin (Strąpoć et al., 2007a). This graph plots all samples from the entire study area. Plotted data from production wells are limited to the most recent March 2007 measurements. Gases are dominated by methane of microbial origin via CO_2-reduction. Gases from wells INS-P8 and INS-P9 are characterized by exceptionally low $\delta^{13}C_{CO2}$ values, probably due to microbial methane oxidation.

(iii) increasing total dissolved solids in co-produced waters (TDS; see below) (Fig. 2). For example, the oldest production wells INS-P8 and INS-P9 wells with ages of 11 and 9 years, respectively, show the lowest values for $C_1/(C_2+C_3)$ and $\delta^{13}C_{CH4}$, and the highest values for TDS (Table 4). A wide range of analytical characteristics of co-produced waters from production wells, such as pH, Eh, temperature, alkalinity, concentrations of major ions, and isotopic compositions are listed in Table 4. The wells are characterized by pH ~8, Eh ~ -400mV, temperature ~17ºC, and relatively high alkalinity (~1200 mg/L as $CaCO_3$). TDS values range from 0.6 to 12g/L, with Cl^- and SO_4^{2-} representing the major anions (wells INS-P9 and INS-P10) and Na^+ being the dominant cation.

5.4. Discussion

5.4.1. Regional distribution and properties of coalbed gas

The three geochemical indicators of coal gas origin $C_1/(C_2+C_3)$, $\delta^{13}C_{CH4}$, and δD_{CH4} display fairly uniform signals across the study area (Fig. 1c, d) and identify microbial CO_2-reduction as the main source of coalbed methane (Fig. 3). Interestingly, $C_1/(C_2+C_3)$ ratios slightly decrease towards the depocenter of the Illinois Basin (Fig. 1a, c), suggesting that some early thermogenic C_{2+} hydrocarbons have been generated from these coals during coalification. Nonetheless, the total gas content in Seelyville and Springfield coals is mainly controlled by microbial methanogenesis because methane is more abundant than the sum of ethane and propane by at least three orders of magnitude. Widespread methanogenesis in eastern Illinois Basin coal beds can be attributed to the access of interglacial Pleistocene, early Holocene melt water and modern meteoric water

to highly fractured and shallow coals which outcrop 20 to 60 km east of the study area (Fig. 1). Relatively recent inoculation of formerly sterilized coals by microbial methanogenic consortia has also been suggested by carbon isotopic signatures of coal cleat-filling calcites with an average $\delta^{13}C_{calcite}$ -4.3‰ indicative of the absence of microbial CO_2 utilization (Solano-Acosta et al., in press). These calcites show no isotopic influence from expected carbon isotope fractionation via microbial CO_2-reduction and, thus, seem to have crystallized in sterile coal during the Mesozoic. Interglacial dilution of brines and initiation of methanogenesis were previously suggested for the Antrim Shale in the Michigan Basin and for the New Albany Shale in the Illinois Basin by McIntosh et al. (2002).

Permeability of coal is important for fluid transport processes and for access of microbial consortia into the coal matrix. A high permeability of ~ 40 md was estimated from the aperture distribution of fractures (Solano-Acosta et al., 2007a) and is supported by direct permeability measurements downhole (confidential data). Repeated interglacial uplifts presumably enhanced the permeability of Indiana coals along their cleat and fracture systems and facilitated the recharge of meteoric water. Dilution of the brine and inoculation with a coal-biodegrading and methanogenic microbial communities along the eastern, and probably also northern and western margins of the Illinois Basin triggered the generation of biogenic methane. Interglacial inoculation of coals is supported by (i) low salinity of formation waters (average TDS 5.4 g/L; Table 4), (ii) modern meteoric isotopic signatures of co-produced coal waters (average δD_{water} -42.9‰ and $\delta^{18}O_{water}$ -6.1‰ VSMOW; Table 4), and (iii) the presence of viable methanogens in co-produced coalbed waters (Strąpoć et al., 2007b).
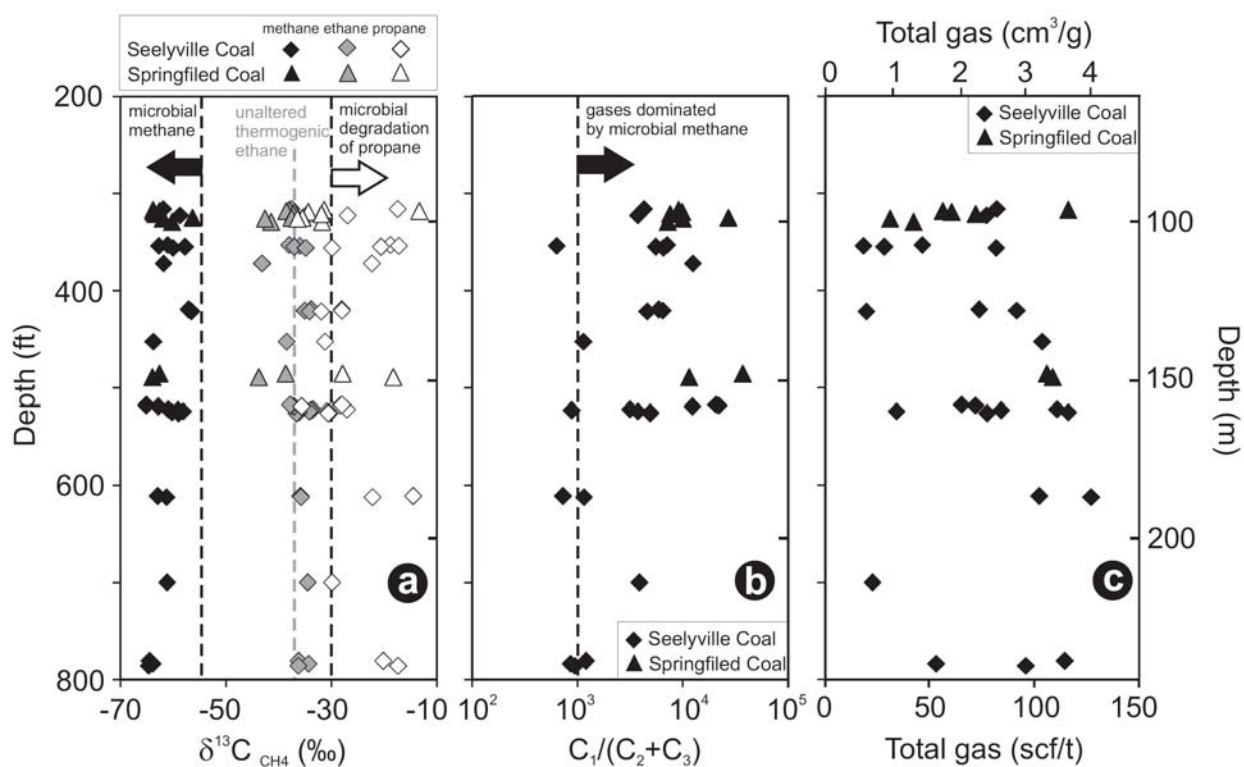
Fig. 4. Coalbed gas properties and coal depth: data points from the entire study area. (a) Carbon stable isotopic signatures pointing to microbial methanogenesis. (b) The ratios of methane over the sum of ethane and propane indicate that propane biodegradation occurs over the entire depth range of coal occurrence. (c) The concentration of total gas in coal does not depend on depth.

Although CBM in Indiana is uniformly of microbial origin, regardless of coal depth (Fig. 4a), we observe significant geographic and depth-variations in the concentration of CBM (Fig. 1b, 4c). This suggests that the amount of locally produced and stored methane is dependent on the accessibility of coal by the microbial community and on the extent of methanogenesis. The accessibility of coal varies spatially because transport routes for microbes through coal are primarily provided by anisotropic, paleo-stress-related cleat/microfracture networks coated with moisture. The average cleat intensity in Indiana coals is 340 cleats per meter. Apart from less common, but easily microbe-accessible larger cleats, microcleats with apertures < 4μm are most abundant (250 per meter; average aperture 0.8μm; Solano-Acosta et al., 2007a). These data combined with the typical diameter of a microbial cell of 1 μm (Prescott et al., 2002) and even smaller 0.4 μm cells of our identified dominant methanogenic genus *Methanocorpusculum* (Strąpoć et al., 2007b) confirm that Indiana coals can be an accessible niche for microbial life. However, there are likely some factors that limit methanogenesis and CBM content in this post-Pleistocene microbial gas play, for example nutrient limitations and/or the lack of certain microbes that are necessary within proper methanogenic microbial consortia. Methanogens require CO_2 and H_2, which are end-products of coal biodegradation performed by various groups of microorganisms. For example, H_2 is required for methanogenesis via CO_2 reduction and is usually available at very low concentrations.

5.4.2. Vertical variations of coal gas properties

It has been our practice in Indiana to sample and desorb the whole coal thickness for gas volumes determinations. However, some of the desorption canisters leaked, and
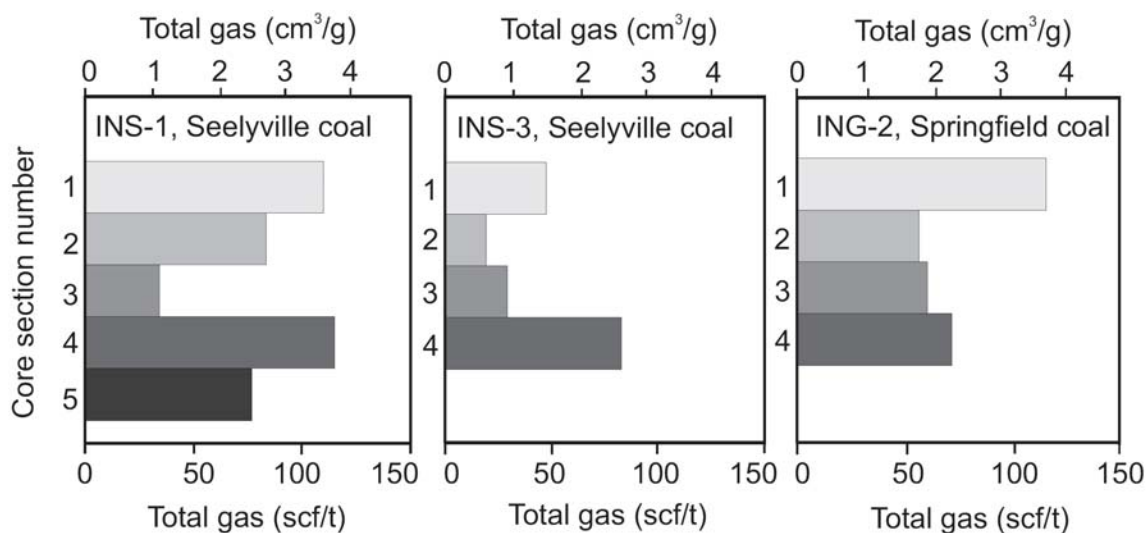
123

Fig. 5. Total gas contents across three coal cores from which consecutive 30 cm core sections generated contiguous gas desorption data. Y-axis numbers represent successive 30 cm core sections counting from the top of each coal bed. Top and bottom sections of cores tend to contain more gas than middle sections.

124

therefore we selected three locations where all 30 cm sections generated reliable desorption data across entire coal beds (Fig. 5). In addition, total gas data for 30cm core sections from all locations, including partial data sets, are plotted according to their positions within coal beds in Figure 6. We observed significant variations in gas content across individual coal beds. In general, the total gas content is larger in top and bottom sections of coal cores compared with their middle sections (Figs. 5, 6). This puzzling pattern of variability requires further study. We hypothesize that higher gas contents in top and bottom parts of a coal seam are related to higher permeability and increased nutrient availability causing higher intensity of microbial activity in coal/bed rock and coal/roof rock contact zones. Variability in gas contents among different 30 cm core sections across a coal bed can also be caused by inhomogeneous distributions of microfracture apertures (important for microbial access), pore sizes, and adsorption surface areas limiting adsorption sites for CBM. Additionally, higher accumulations of buoyant gas in the presence of denser water can be expected beneath poorly permeable, usually shaly, roof rock.

The pattern of predominantly higher gas contents in top and bottom sections of coal seams is accompanied by decreased $\delta^{13}C_{CH4}$ and increased values of $C_1/(C_2+C_3)$ and $\Delta^{13}C_{CO2-CH4}$ relative to the middle sections of coal seams in two (INS-1 and INS-3) out of three cores with complete coverage of data (Fig. 7). These slightly more biogenic geochemical signatures of gases and increased total gas contents (Fig. 5) in top and bottom sections of cores support our hypothesis of higher microbial gas-generation potential. The third core (ING-2) is characterized by low variances of the three
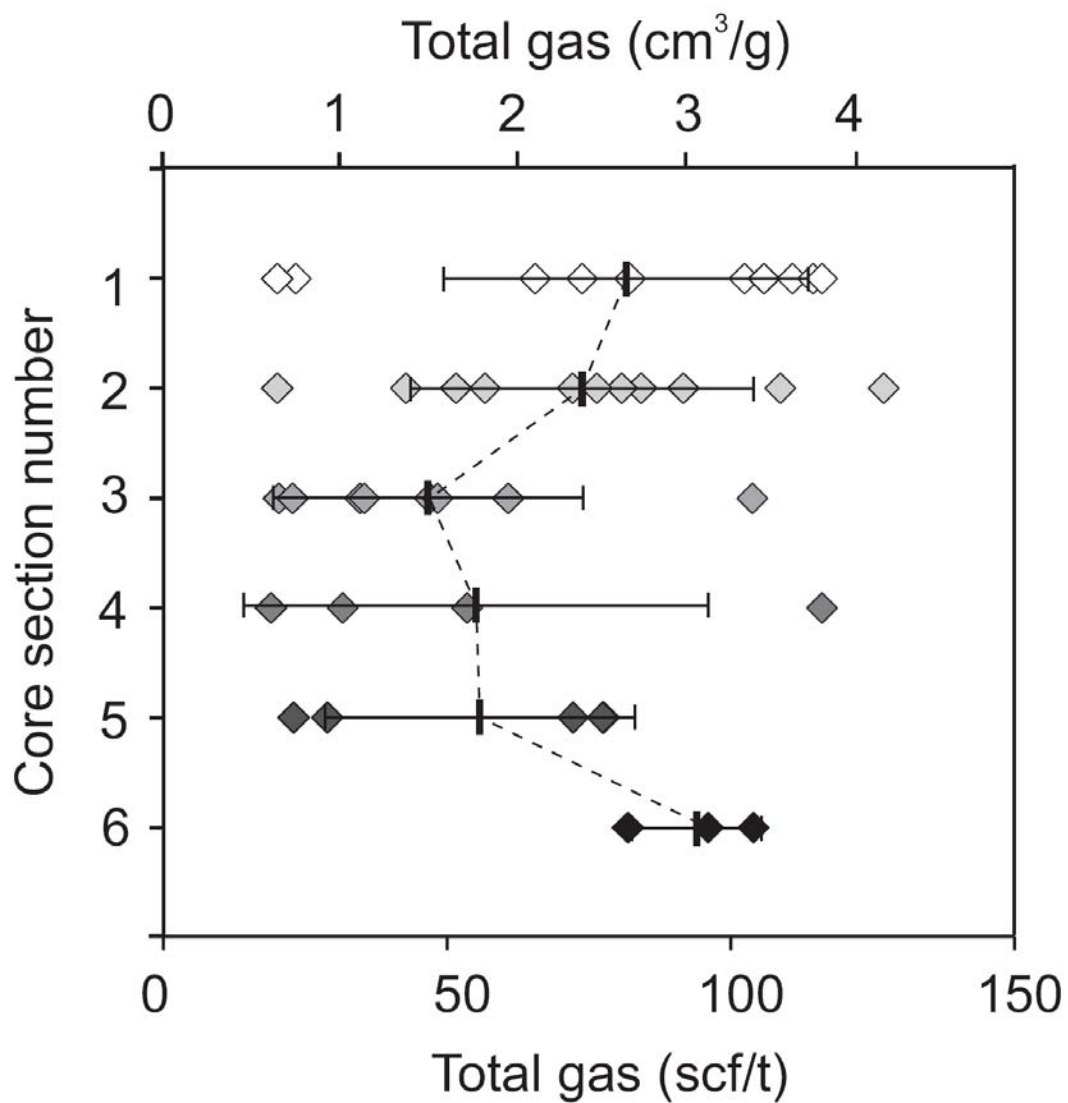
125

Fig. 6. Total gas contents in all 30 cm coal core sections plotted according to their relative positions within coal beds counting from the top in each location. Middle sections of coal cores tend to contain less gas than top and bottom sections.
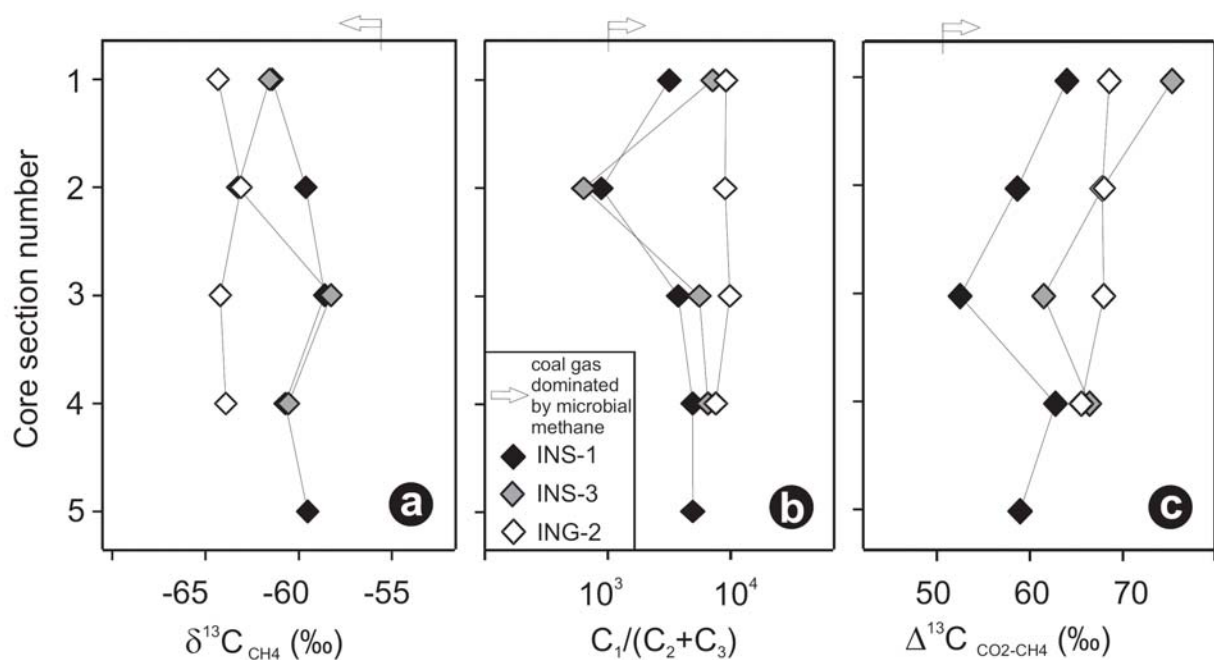
Fig. 7. Gas geochemical parameters of continuously sampled and desorbed coal cores of Seelyville Coal (INS-1 and INS-3) and Springfield Coal (ING-2). Y-axis numbers represent successive 30 cm core sections counting from the top of each coal bed. Desorbed gases from cores INS-1 and INS-3 express more distinctly microbial isotopic signatures in their top and bottom sections (in direction of the arrows). Top and bottom sections also contained larger gas concentrations (see Figure 5) suggesting slightly higher microbial methanogenic activity in top and bottom coal sections.

parameters mentioned above. In general, variations of the geochemical signatures of gases from 30 cm coal sections in all analyzed cores are not significantly impacting the >99% microbial classification of these coalbed gases (Fig. 3).

Local variations in gas content across coal seams have important implications for CBM exploration. Representative measurements of adsorbed gas in coal cores across coal seams are necessary to arrive at reliable estimates of gas reserves. Limited desorption data from selected portions of a coal bed may result in overestimates or underestimates of gas resources. The entire coalbed thickness needs to be sampled (usually in several canisters) and desorbed, followed by weighted averaging of the data.

Figure 8 compares the maximum methane adsorption capacity (obtained using a volumetric adsorption apparatus, as described by Mavor et al., 1990) to the total gas content (determined by canister desorption of consecutive 30 cm core sections and averaging of data for each core) of the Seelyville Coal in four locations, where the coal occurred at different depths from 97 to 187 m and, consequently, at different *in situ* pressures. In these locations, the measured gas content (MGC) oscillates near maximum adsorption capacities (AC) and therefore suggests coal saturation with coal gas (Fig. 8).

Maceral composition is one of the factors influencing methane sorption capacity (e.g, Mastalerz et al., 2004; Chalmers and Bustin, 2007). However, although Indiana coals expressed high variation in maceral composition in this study, maceral composition appears to have little influence on the amount of the gas present in the coals studied (Fig. 9). The lack of correlation between maceral composition and gas content may imply that the methanogenic microbial community as a whole has no significant maceral preference for biodegradation in coal. In addition to coal macerals, microbial biodegradation may
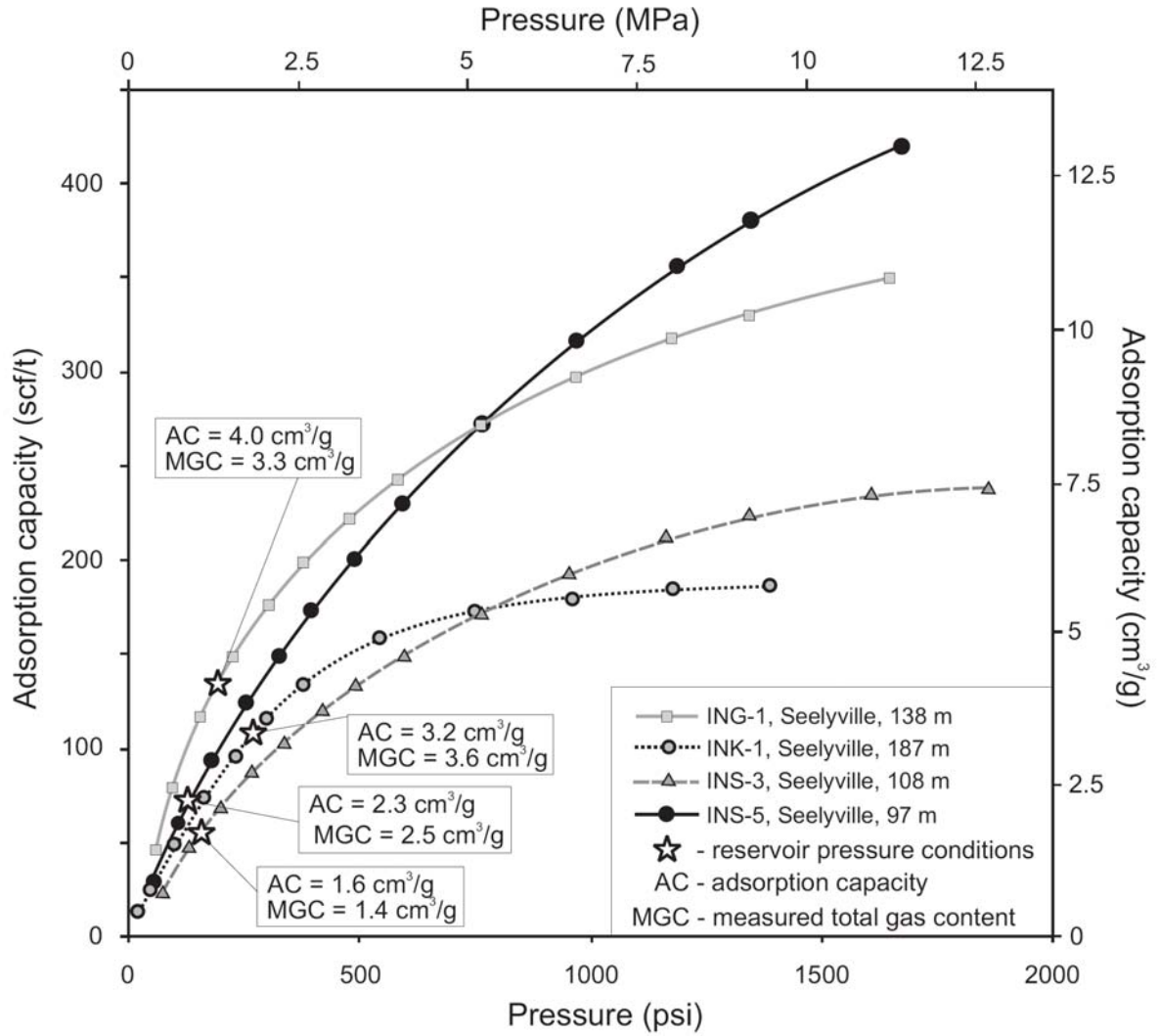
128

Fig. 8. Methane adsorption isotherms of the Seelyville Coal in Indiana from four locations determined via volumetric adsorption. Star symbols represent maximum values of gas adsorption capacity (AC) of a particular coal at its reservoir pressure. Matching values of AC and measured total gas contents (MGC, obtained using desorption canisters) for each location suggest coal saturation with coal gases.
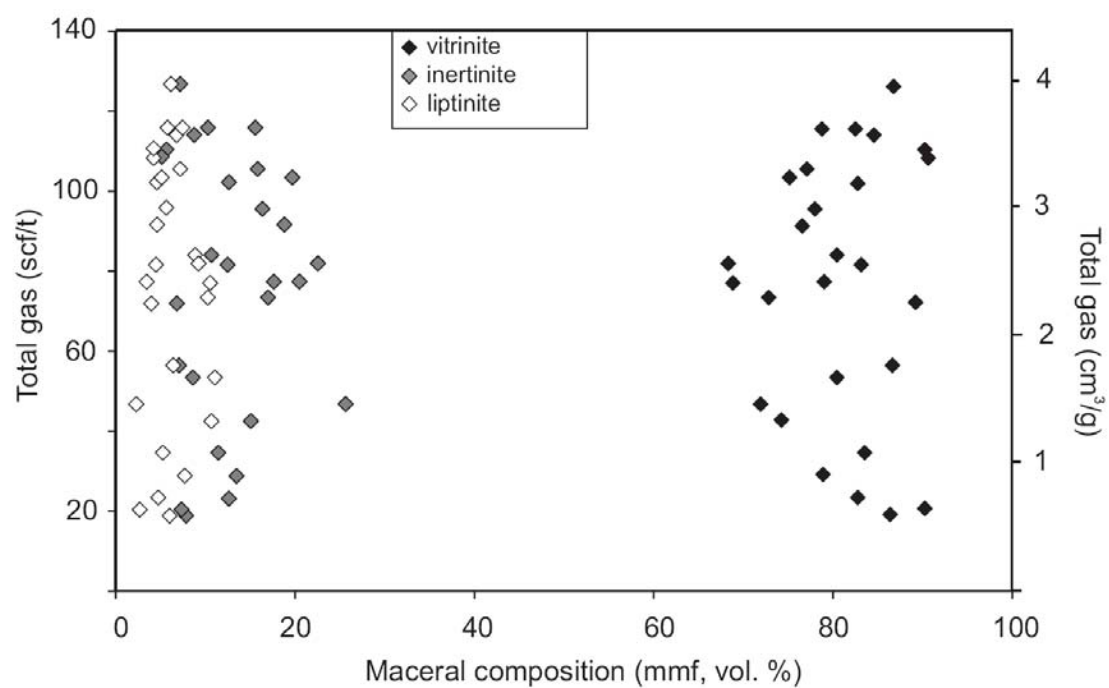
Fig. 9. Maceral composition (volume %, mmf – mineral matter free basis) of coals from all core sections versus total gas content desorbed from coals. No correlation is evident between maceral composition and total gas content.

also target disseminated micrometer-size droplets of liquid bitumen ('oil') that have been generated during coalification. The calculated oil yield from our coals using typical values of the atomic ratios of hydrogen to carbon (H/C ~0.7) and oxygen to carbon (O/C ~0.1) is ~8 weight %, using equation by Saxby (1980):

oil yield wt. %= 66.7 H/C - 57.0 O/C - 33.3

Our microbiological phylogenetic study of Indiana coals indicates the presence of a complex microbial community capable of biodegrading aliphatic and aromatic moieties in organic macromolecules (Strąpoć et al., 2007b). For example, in our studies of gaseous *n*-alkanes in Indiana coal beds, we observed microbial consumption of propane and *n*-butane. Microbial alteration of propane in Indiana coal gases leads to (i) C_2/C_3 ratios of 20 to 100 that are far higher than the theoretical value of 2.4 expected for early thermogenic gas generated at R_o 0.6% (Berner and Faber, 1988), and (ii) ^{13}C-enrichment of residual propane due to preferential microbial utilization of $^{12}C_3H_7$ relative to $^{13}C^{12}C_2H_7$ (Strąpoć et al., 2007a). Similarly, preferential microbial depletion of *n*-butane relative to *i*-butane generates *n*-C_4/*i*-C_4 ratios < 1. The absence of *n*-butane in some coalbed gases containing *i*-butane suggests efficient removal of *n*-butane (Tables 2 and 3). Extensive microbial consumption of C_{3+} *n*-alkanes, observed also for *n*-alkanes in biodegraded oils (e.g., Holba et al., 2004), might suggest a microbial preference for biodegradation of aliphatic moieties in coal, e.g. disseminated oil or liptinite with abundant aliphatic side chains, as opposed to largely aromatic inertinite. However, our data set does not confirm any pronounced maceral preference for microbial biodegradation (Fig. 9).

5.4.3. Changes in coalbed gas properties from gas wells during prolonged production

The observed small variations in $C_1/(C_2+C_3)$ ratios and $\delta^{13}C_{CH4}$ values in gases from monitored CBM production wells in Indiana could not influence the geochemical assessment of coal gas origin (Fig. 3). However, gradual changes are evident with ongoing gas production in characteristics of gas and co-produced water, e.g. $\delta^{13}C_{CH4}$, $C_1/(C_2+C_3)$, and TDS. Specifically, gases produced in 2007 from the oldest wells (INS-P8 and INS-P9) with continuous gas production since 1996 and 1998, respectively, were characterized by very high $C_1/(C_2+C_3)$ ratios and very low $\delta^{13}C_{CH4}$ values (Fig. 2a, b). This 'aging' trend in gases from CBM production wells may derive from molecular and isotopic fractionation of gases during transport through the network of microfractures and cleats in coal. Methane and especially $^{12}CH_4$ diffuses/flows relatively faster than heavier gas molecules from increasingly distant coal desorption sites to the well, as suggested in models of CO_2/CH_4 coalbed gas production by Cui and Bustin (2006). The transport distance from adsorption sites in coal to the well becomes longer with increasing duration of gas production. Furthermore, older CBM wells develop depression cones in the overlying water table and thus promote increased recharge of freshwater into coal seams and dilution of TDS in co-produced waters. Enhanced influx of oxygenated freshwater and contact with surficial aerobic microbial communities can lead to microbial methane oxidation in later stages of CBM production, and can negatively affect methanogenesis because methanogenic Archaea are strict anaerobes. Microbial methane oxidation is plausibly occurring in the two oldest wells, which are characterized by very negative $\delta^{13}C_{CO2}$ values of about -34‰ (Table 3).
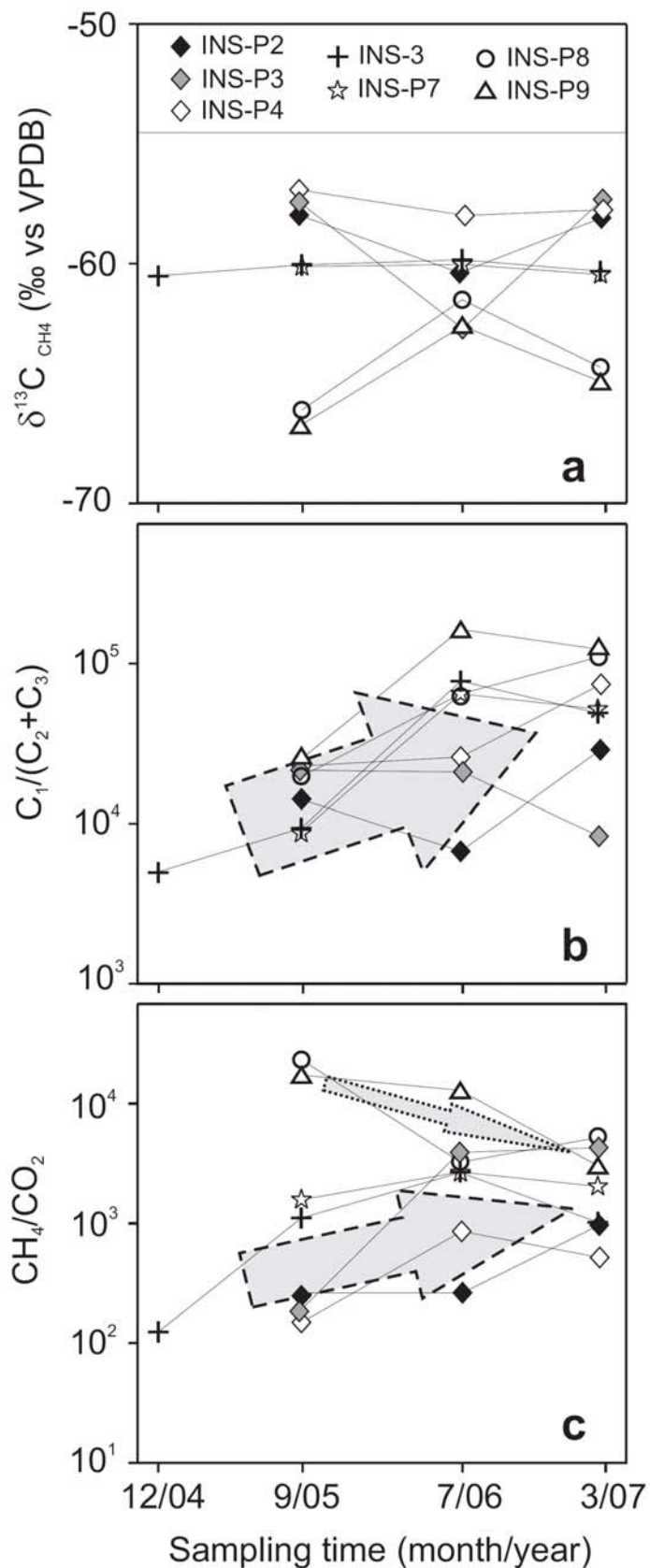
Fig. 10. Geochemical coalbed gas data from seven Indiana CBM production wells that have been sampled every nine months. Well INS-3 was also sampled during the original drilling. Most wells exhibit slight increases in $C_1/(C_2+C_3)$ and CH_4/CO_2 over time (dashed arrows). Decreasing values of CH_4/CO_2 in the oldest wells INS-P8 and INS-P9 (dotted arrow) suggest production-induced microbial oxidation of methane.

133

We observed a trend of gradually increasing $C_1/(C_2+C_3)$ ratios over 27-month of monitoring the same production field at 9-month intervals (Table 3; Fig. 10b). CH_4/CO_2 ratios express a slow increase over time except in gases from the oldest wells INS-P8 and INS-P9 (Fig. 10c), supporting our hypothesis of production-induced long-term accelerated influx of fresh waters promoting methane oxidation. No systematic shift in $\delta^{13}C_{CH4}$ values was observed, possibly because 27 months of monitoring of CBM production was insufficient time to reveal in significant carbon isotopic fractionation of produced methanes (Fig. 10a).

5.5. Conclusions

Geographic lateral and vertical variations of coal gas parameters such as $\delta^{13}C_{CH4}$, $C_1/(C_2+C_3)$, and $\Delta^{13}C_{CO2-CH4}$ in Springfield and Seelyville coals in Indiana are typically small. All data are consistent with a predominantly biogenic gas system where methane is produced microbially via CO_2-reduction pathway. High permeability of shallow coals likely allowed inoculation of coals with a methanogenic microbial community. The resulting widespread methanogenesis caused similar geochemical fingerprints of coalbed gases along the entire marginal zone of the Illinois Basin in Indiana.

Assuming regionally uniform pre-CBM-production coalbed gas compositions, prolonged CBM production from monitored wells caused molecular and isotopic trends in production gases of (i) increasing $C_1/(C_2+C_3)$ ratios, (ii) decreasing $\delta^{13}C_{CH4}$ values, and (iii) decreasing TDS values. Furthermore, prolonged CBM production may enhance access of fresh oxygenated meteoric waters into relatively shallow coal seams resulting in microbial methane oxidation.

The total coalbed gas content is controlled by the amount of generated, adsorbed and preserved microbial methane, and therefore can be locally variable depending on (i) microbial accessibility (via cleats and microfractures of proper size), (ii) adsorption potential for methane molecules (micropore distribution) of a particular coal section, and (iii) availability of target organic moieties for potential biodegradation and methanogenesis.

To accurately assess the CBM potential and gas saturation level of a coal bed requires investigation across the entire thickness of a coal seam, because total gas contents can vary significantly vertically across seams.

References

Ayers, W.B. Jr, 2002. Coalbed gas systems, resources, and production and a review of contrasting cases from the San Juan and Powder River basins. American Association of Petroleum Geologists Bulletin 86, 1853-1890.

Bachu, S., Michael, K., 2003. Possible controls of hydrogeological and stress regimes on the producibility of coalbed methane in Upper Cretaceous-Tertiary strata of the Alberta basin, Canada. American Association of Petroleum Geologists Bulletin 87, 1729-1754.

Bernard, B.B., Brooks, J.M., Sackett, W.M., 1978. Light hydrocarbons in recent Texas continental shelf and slope sediments. Journal of Geophysical Research 83, 4053–4061.

Berner, U., Faber, E., 1988. Maturity related mixing model for methane, ethane and propane, based on carbon isotopes. Organic Geochemistry 13, 67–72.

Chalmers, G.R.L., Bustin, R.M., 2007. On the effects of petrographic composition on coalbed methane sorption. International Journal of Coal Geology 69, 288-304.

Chung, H.M., Gormly, J.R., Squires, R.M., 1988. Origin of gaseous hydrocarbons in subsurface environments: Theoretical considerations of carbon isotope distribution. Chemical Geology 71, 97–104.

Cui, X., Bustin, M., 2006. Controls of coal fabric on coalbed gas production and compositional shift in both field production and canister desorption tests. Society of Petroleum Engineers Journal 11, 111-119.

Drobniak, A., Mastalerz, M., Rupp, J., Eaton, N., 2004. Evaluation of coalbed gas potential of the Seelyville Coal Member, Indiana, USA. International Journal of Coal Geology 57, 265–282.

Faiz, M., Hendry, P., 2006. Significance of microbial activity in Australian coal bed methane reservoirs – a review. Bulletin of Canadian Petroleum Geology 54, 261-272.

Gas Research Institute, 1995. A Guide to Determining Coalbed Gas Content. Gas Research Institute, GRI-94/0396.

Gurgey, K., Philp, R.P., Clayton, C., Emiroglu, H., Siyako, M., 2005. Geochemical and isotopic approach to maturity/source/mixing estimations for natural gas and associated condensates in the Thrace Basin, NW Turkey. Applied Geochemistry 20, 2017-2037.

Henning, M.J., Strąpoć, D., Lis, G.,Sauer, P., Fong, J., Schimmelmann, A., Pratt, L.D., 2007. Versatile inlet system for on-line compound-specific δD and $\delta^{13}C$ GC-c/pyr-IRMS analysis of gaseous mixtures. Rapid Communications in Mass Spectrometry, in press.

Holba, A.G., Wright, L., Levinson, R., Huizinga, B., Scheihing, M. 2004. Effects and impact of early-stage anaerobic biodegradation on Kuparuk River Field, Alaska. In: Cubitt, J.M., England, W.A., Larter, S. (eds), 2004. Understanding Petroleum Reservoirs: towards an Integrated Reservoir Engineering and Geochemical Approach. Geochemical Society, London, Special Publicationsn 237, 53-88.

Katz, B.J., Narimanov, A., Huseinzadeh, R., 2002. Significance of microbial processes in gases of the South Caspian basin. Marine and Petroleum Geology 19, 783–796.

Lillis, P.G., 2007. Upper Cretaceous microbial petroleum systems in Nort-Central Montana. The Mountain Geologist 44, 11-35.

Mastalerz, M., Drobniak, A., Rupp, J., Shaffer, N., 2004. Characterization of Indiana's coal resource: availability of the reserves, physical and chemical properties of the coal, and present potential uses. Indiana Geological Survey Open-File Study 04-02, July 2004.

Mavor, M.J., Owem, L.B., Pratt, T.J., 1990. Measurement and evaluation of coal sorption isotherm data. 65th Annual Technical Conference and Exhibition of the Society of Petroleum Engineers, New Orleans, LA, September 23-26, 1990, 157-170.

McIntosh, J.C., Walter, L.M., Martini, A.M., 2002. Pleistocene recharge to midcontinent basins: effects on salinity structure and microbial gas generation. Geochimica et Cosmochimica Acta 66, 1681–1700.

Pitman, J.K., Pashin, J.C., Hatch, J.R., Goldhaber, M.B., 2003. Origin of minerals in joint and cleat systems of the Pottsville Formation, Black Warrior basin, Alabama: Implications for coalbed methane generation and production. AAPG Bulletin 87, 713-731.

Prescott, L.M., Harley, J.P., Klein, D.A., 2002. Microbiology, fifth edition, McGraw-Hill, New York.

Saxby, J.D., 1980. Atomic H/C ratios and the generation of oil from coals and kerogens. Fuel 59, 305-307.

Schimmelmann, A., Sessions, A.L., Mastalerz, M., 2006. Hydrogen isotopic (D/H) composition of organic matter during diagenesis and thermal maturation. Annual Review of Earth and Planetary Sciences 34, 501–533.

Schoell, M., 1980. The hydrogen and carbon isotopic composition of methane from natural gases of various origins. Geochimica et Cosmochimica Acta 44, 649–661.

Scott, A.R., Kaiser, W.R., Ayers Jr., W.B., 1994. Thermogenic and secondary biogenic gases, San Juan Basin, Colorado and New Mexico - Implications for coalbed gas producibility. AAPG Bulletin 78, 1186–1209.

Scott, A.R., 1998. Application of burial history to coalbed methane producibility. In: Geologic and Hydrologic and Hydrologic Controls Critical to Coalbed Methane Production and Resource Assessment. Coalbed methane short course presented by Scott, A.R. and Tyler, R. at the International Conference on Coal-Seam Gas and Oil, Brisbane, Australia, March 22-23, 1998.

Smith, J.W., Pallasser, R.J., 1996. Microbial origin of Australian coalbed methane. American Association of Petroleum Geologists Bulletin 80, 891–897.

Solano-Acosta, W., Mastalerz, M., Schimmelmann, A., 2007a. Cleats and their relation to geologic lineaments and coalbed methane potential in Pennsylvanian coals in Indiana. International Journal of Coal Geology, in press.

Solano-Acosta, W., Schimmelmann, A., Mastalerz, M., Arango, I., 2007b. Diagenetic mineralization in Pennsylvanian coals from Indiana, USA: $^{13}C/^{12}C$ and $^{18}O/^{16}O$ implications for cleat origin and coalbed methane generation. International Journal of Coal Geology, in press.

Strąpoć, D., Schimmelmann, A., Mastalerz, M., 2006. Carbon isotopic fractionation of CH_4 and CO_2 during canister desorption of coal. Organic Geochemistry 37, 152–164.

Strąpoć, D., Mastalerz, M., Eble, C., Schimmelmann, A., 2007a. Characterization of the origin of coalbed gases in southeastern Illinois Basin by compound-specific carbon and hydrogen stable isotope ratios. Organic Geochemistry 38, 267-287.

Strąpoć, D., Picardal, F., Schaperdoth, I., Macalady, J., Turich, C., Mastalerz. M., Schimmelmann, A., 2007b. Coalbed methane-producing microbial community in the Illinois Basin. The annual ASM (American Society for Microbiology) Conference, Toronto, Canada, May 2007, Poster Abstract N-251.

Vandré, C., Cramer, B., Gerling, P., Winsemann, J., 2007. Natural gas formation in the western Nile delta (Eastern Mediterranean): Thermogenic versus microbial. Organic Geochemistry 38, 523-539.

Whiticar, M.J., Faber, E., Schoell, M., 1986. Biogenic methane formation in marine and freshwater environments: CO_2 reduction vs. acetate fermentation – isotope evidence. Geochimica et Cosmochimica Acta 50, 693–709.

CHAPTER 6

**An analysis of the methane-producing microbial community
in a coal bed of the Illinois Basin ***

Dariusz Strąpoć[1*], Flynn Picardal[2], Courtney Turich[3†], Irene Schaperdoth[3], Jennifer Macalady[3], Julius Lipp[4], Yu-Shih Lin[4], Tobias Ertefai[4], Florence Schubotz[4], Kai-Uwe Hinrichs[4], Maria Mastalerz[5], Arndt Schimmelmann[1]

[1] Indiana University, Dept. of Geological Sciences, Bloomington, IN 47405, USA
[2] Indiana University, School of Public and Environmental Affairs, Bloomington, IN 47405, USA
[3] Penn State University, Dept. of Geosciences, University Park, PA 16802, USA
[4] Research Center Ocean Margins, Dept. of Geosciences, University of Bremen, 28334 Bremen, Germany
[5] Indiana University, Indiana Geological Survey, Bloomington, IN 47405, USA
[†] currently at Skidaway Institute of Oceanography, Savannah, GA 31411

Abstract

The phylogeny of the microbial community responsible for generation of large coalbed methane (CBM) reserves in the Indiana portion of the Illinois Basin was analyzed. The molecular and geochemical studies implied that coal organic matter is biodegraded to simple molecules, such as H_2 and CO_2, which fuel methanogenesis. Small subunit rRNA analysis of both the *in-situ* microbial community and methanogenic enrichments indicated that *Methanocorpusculum* is the dominant genus. Additionally, we characterized this methanogenic microorganism using scanning electron microscopy (SEM) and distribution of intact polar cell membrane lipids (IPLs). A clone library was developed from nucleic acid extracts of the coal water sample; some clones were phylogenetically related to species capable of anaerobic degradation of a variety of molecules, including polyaromatic, aromatic, and aliphatic hydrocarbons. Based on enrichment results, phylogenetic analyses, and calculated free energies at *in-situ* subsurface conditions for important metabolisms (CO_2-reduction and acetoclastic methanogenesis, homoacetogenesis, and syntrophic acetate oxidation), CO_2-reduction methanogenesis appears to be the dominant terminal process of biodegradation of coal organic matter at this location.

6.1. Introduction

Isotopic signatures of methane accumulations in coals (Thielemann et al., 2004), shales (McIntosh et al., 2002), biodegraded oils (Bekins et al., 2005; Milkov and Dzou, 2007), and ocean floor sediments (Newberry et al., 2004) demonstrate that much of the subsurface methane results from microbial activity. Coal is extremely rich in complex organic matter (OM), and therefore could be considered very attractive carbon source for microbial biodegradation. However, coal is a solid rock, often dominated by recalcitrant, partially aromatic and largely lignin-derived macromolecules which tend to be relatively resistant to degradation. The rate-limiting step of coal biodegradation is the initial fragmentation of geomacromolecular polycyclic lignin-derived aromatic network of coal. Lignin degradation can be achieved by extracellular enzymes used by fungi and some microbes (Deobald and Crawford, 1987; Fakoussa and Hofrichter, 1999) and it has been also shown that up to 40 wt.% of some coals can be dissolved using extracted microbial enzymes (Scott et al., 1994). Furthermore, there are known microbial species capable of anaerobic degradation of methylated and ethylated aromatic compounds (Chakraborty et al., 2005; Coates et al., 2001; Jothimani et al., 2003; Townsend et al., 2004) or even polycyclic aromatic hydrocarbons (PAHs; Chang et al., 2002; Christensen et al., 2004; Coates et al., 1997; Meckenstock et al., 2004).

Methane generation from coal by microbial consortia has been documented previously. For example, microflora present in water leached from coal mines can generate methane (Thielemann et al., 2004). Furthermore, a methane-generating consortium extracted from coal was observed to grow on low volatile bituminous coal as a sole carbon source (Shumkov et al., 1999). A microbial community may also target the

dissipated oil droplets that can be generated from coal by anaerobically degrading long-chain *n*-alkanes, the main constituents of non-biodegraded oil (Anderson and Lovley, 2000; Hostettler, 2004; Sei et al., 2003; Zengler et al., 1999).

Several lines of evidence point to a biogenic rather than thermogenic origin of coalbed methane (CBM) along the eastern margin of the Illinois Basin (Strąpoć et al., 2007). The goals of the current study were to confirm the presence of methanogens in Illinois Basin coals, and using culture-dependent and culture-independent methods, to explore the complexity of the microbial communities required for methanogenic, complex OM biodegradation.

6.2. Materials and methods

6.2.1. Sampling site

Coal water samples were collected from CBM-producing wells of a small production field in western Indiana, along the eastern margin of the Illinois Basin (Fig. 1). Our sampling target was the Seelyville Coal Member at a depth of 95 to 110 m. This coal contains significant reserves of biogenic methane, approximately 3 cm^3/g which corresponds to a total of 30 x 10^9 m^3 in the Indiana part of the Illinois Basin (Mastalerz et al., 2004; Strąpoć et al., 2007). The CBM wells co-produce significant quantities of water. Average *in-situ* conditions at the depth studied are as follows: moisture content from 4 to 12 wt. %, pH from 7.5 to 8.8, E_h -330 to -410 mV, temperature 16.0 to 17.5° C, salinity 1 to 12 g/L, and oxygen content below detection limit (1 mg/L). The sampled coal is highly fractured and therefore has a high permeability of ~ 40 millidarcy (mD), and an average fracture density (including cleats) of 340 fractures/m (Solano-Acosta et

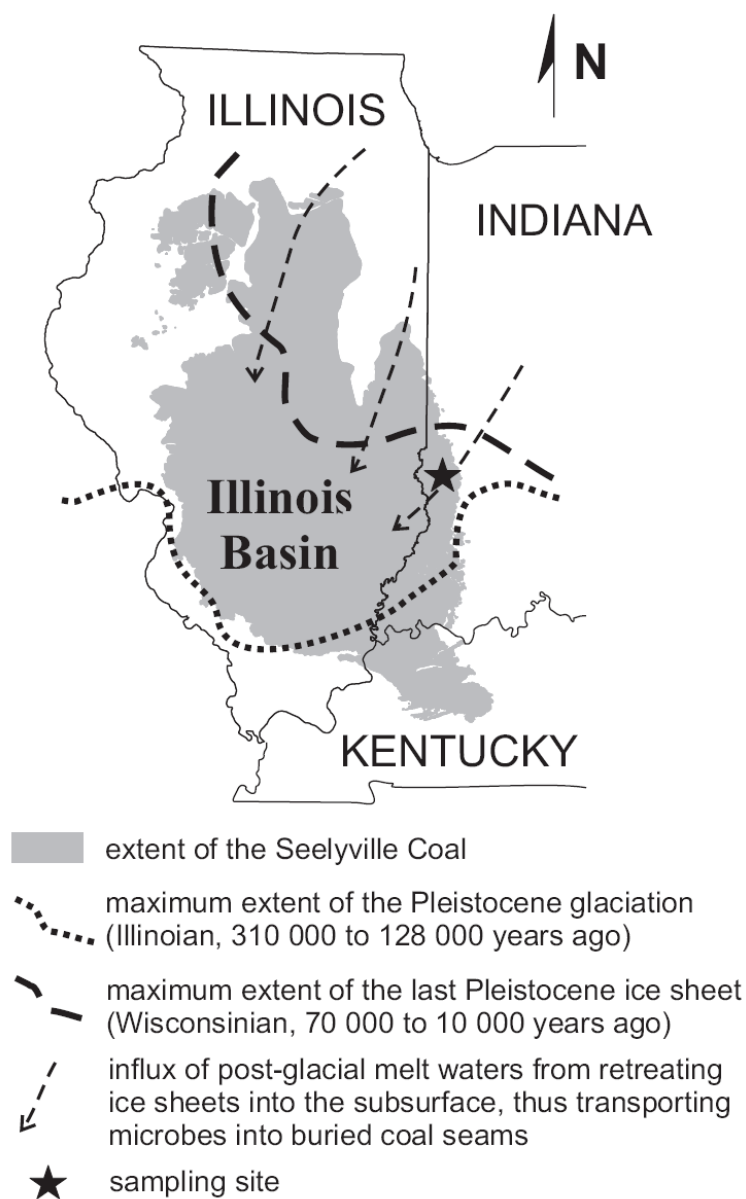Fig. 1. Map showing the extent of the Seelyville Coal in the Illinois Basin. The sampling site is located in the eastern marginal zone of the basin. It is a coal gas producing well from a depth of 105 m. The dotted and dashed lines represent the southernmost extents of the most recent Pleistocene glaciations. The arrows indicate the inferred direction of melt water influxes during inter- and post-glacial periods.

al., 2007). In addition to large scale fractures and cleats (apertures 4 to 250 μm) present in the coal, the main population (74%) are microfractures with apertures <4 μm (0.8 μm on average).

6.2.2. Sample collection for enrichment experiments

Water for enrichment experiments was sampled from the CBM producing well INS-P11 in Sullivan County, western Indiana. The INS-P11 produces coal gas from the Seelyville Coal from approximately 105 m depth. Water for microbial enrichments (2 L) was collected during measurements of physicochemical properties of coal waters using multi-functional probe YSI 600XL (Yellow 102 Springs Instruments, Inc., Yellow Springs, Ohio) equipped with a flow through chamber. Prior to water sampling, bottles were autoclaved and 1 mL of 1% resazurin, a redox indicator, was added. Subsequently, 40 mL of 1.25% cysteine/1.25% Na_2S, a reducing agent, was added inside an anaerobic chamber. Finally, the bottles were purged with argon to remove oxygen. Each bottle had two inlets consisting of short (~10 cm x 6 mm) Pyrex tubes connected with hose clamps to the longer Tygon tubing. After ~10 min of purging and stabilization of physico-chemical parameters of water (i.e. specific conductivity, pH, Eh) and after reaching oxygen levels below the detection limit, the outlet of the flow-through chamber was attached to one of the two inlets of the 1 L glass bottles equipped with double port rubber stoppers. At the same time, argon pressure from a 50 L tank was applied via Tygon tubing with an attached cotton-filled syringe to prevent microbial contamination. After several seconds, the outlet of the sampling bottle was opened by loosening the hose clamp to release overpressure created by inflowing water and argon. Net gas outflow controlled by the 1 atm overpressure of argon prevented access of oxygen. Additionally,

sulfide added prior to sampling quickly removed any oxygen contamination. Resazurin additions indicated successful anoxic sampling.

6.2.3. Enrichments

Aliquots of sample water (2 L) were passed through sterile 0.22 μm filters in the anaerobic chamber. For enrichment of H_2-utilizing methanogens, the filters were placed in 120-mL serum bottles containing 50 mL of pre-reduced anaerobic medium and crimp-sealed with butyl rubber stoppers (Bellco Glass, Inc., Vineland NJ, USA). One L of medium consisted of 230 mL of DI water, 500 mL of general salts solution, 10 mL of trace metals and vitamin solutions, 200 mL of 50 mmol HEPES buffer, 1 mL of 1% resazurin, 1 mL of 0.2% $Fe(NH_4)_2(SO_4)_2$, 40 mL of 1.25% cysteine/1.25% Na_2S, and 10 mL of 100 g/L yeast extract solution. The general salts solution contained (g/L): 0.67 KCl, 5.5 $MgCl_2·2H_2O$, 6.9 $MgSO_4·7H_2O$, 0.5 NH_4Cl, 0.28 $CaCl_2·2H_2O$, 0.28 K_2HPO_4, and 22.0 NaCl. The targeted salinity of the media was half that of the sea water (35 g/L). The trace minerals solution contained (mg/L): 1500 $FeCl_2·4H_2O$, 70 $ZnCl_2$, 100 $MnCl_2·4H_2O$, 2 $CuCl_2$, 190 $CoCl_2·6H_2O$, 10 $AlK(SO_4)_2$, 24 $NiCl_2·6H_2O$, 36 $NaMoO_4$, 6 H_3BO_3, and 10 mL of 25% HCl. The vitamin solution contained (mg/L): 2 biotin, 2 folic acid, 10 pyroxidine HCl, 5 thiamine HCl, 5 riboflavin, 5 nicotinic acid, 5 lipoic acid, 5 lipobenzoic acid, and 0.1 vitamin B12. The pH of the media was 7.5. The headspaces of the enrichment bottles contained oxygen-free, H_2:CO_2 (4:1 v/v) at 1 bar overpressure. Headspace gases were replaced weekly and 10 vol. % of the enrichments were transferred to fresh media every 2-3 weeks. Beginning with the third transfer, the medium was amended with alternating pairs of antibiotics (either penicillin G and kanamycin or streptomycin and vancomycin) to inhibit growth of Eubacteria. Concentrations of

penicillin G, kanamycin, streptomycin and vancomycin were 80, 80, 60, and 100 µg/mL, respectively. After 8 transfers, we reduced the volume of enrichments to 5 mL and used Balch tubes instead of serum bottles.

6.2.4. Testing of methanogenic enrichments

Enrichments were tested for methane generation biweekly using gas chromatography with flame ionization detector (GC/FID). Periodically, methanogenic enrichments were additionally tested for presence of the F420 cofactor (unique for methanogens) of hydrogenase enzyme using epifluorescence microscopy (van Bruggen et al., 1983). The most fluorescent and most methane generating test tube (2nd transfer in a test tube) was selected for the SEM imaging. The sample was prepared by vacuum-filtering of 0.5 mL of media on a 0.22 µm glass fiber membrane in a phosphate filtration buffer used to distribute cells evenly on the membrane. Subsequently the membrane was transferred onto slide stored inside covered petri dish and transported immediately to the SEM lab and analyzed within 30 minutes. Selected enrichments were tested for the rate of substrate consumption using gas chromatography/mass spectrometry (GC/MS) to observe changes in the CH_4/CO_2 ratio in the headspace over time of enrichment's growth.

6.2.5. DNA Extraction

Twenty mL of methanogen enrichment culture (from the 5th transfer of the enrichment bottles from the T30 well) was centrifuged for 10 min spinning at 7 krpm at 7˚C using a Beckman-Coulter centrifuge. For *in-situ* microbial community of the coals, 8 L of coal water was filtered using autoclaved and acid-washed stainless steel filtering stand and two stacked 0.7 µm glass fiber filter (Whatman). The filters were kept at -20˚ C until extraction. The DNA extraction procedure was the same for both the cell pellet and

filter. For the filter extraction, ¼ of the filter was used. Re-suspension of the cells in 2 mL vials was achieved by adding solution of buffer P1 (50 mM Tris·Cl, 10mM EDTA, 100 μg/mL RNase A; QIAGEN) and chloroform (1:1, v/v) and was followed by centrifuging at 12 krpm, 4˚C for 8 min. Cell lysis was achieved with addition of 20 μL of 10% pyrophosphate and 3 μL of lysozyme and incubation for 40 min at 37˚ C. Afterwards, 60 μL of Proteinase K and 10 μL of 20% sodium dodecyl sulfate SDS were added. The vials were stored at 50˚C for 30 min. To wash and concentrate DNA, phenol-chloroform-isoamyl alcohol (P-C-I) and 0.3 g of acid-washed silica beads were added. The mixture was vortexed at 6 krpm for 2 min for the complete cell lysis and getting DNA into solution, then centrifuged for 3 min at 12 krpm. The top aqueous phase, containing dissolved DNA was extracted once more with P-C-I and centrifuged for 2 min. The extracted aqueous phase was then subjected to DNA overnight precipitation at -20˚C with 1:1 vol. isopropanol and 0.1 vol. Na-acetate. Samples were then centrifuged for 20 min at 12 krpm and 4˚C. Supernatant was removed and 1 mL of ethanol was added to the precipitated DNA and centrifuged for 5 min. The DNA was purified after gel electrophoresis (20 μL per well) using the QIAEX Agarose Gel Extraction Protocol (QIAEX II Handbok, QIAGEN) which (i) solubilizes the agarose gel at 50 ˚C, (ii) sorbs DNA to QIAEX II particles, then (iii) removes supernatant, (iv) washes the pellet with QX1 and PE buffers, and (v) elutes the DNA from the particles with 20 μL of 10 mM Tris·Cl.

6.2.6. 16S rRNA analysis

Purified DNA was amplified by Polymerase Chain Reaction (PCR) using universal primers. Each 50 μL solution for PCR reaction contained 2, 3, 4, 6, or 9 μL of

DNA template (3 μL were the most successful), 5 μL of 10x buffer, 1 μL of 10 mM of dNTPs, 1 μL of 10 μM 1492r universal primer (5'-GGTTACCTTGTTACGACTT-3'), 1 μL of 10 μM 533f universal primer (5'-GTGCCAGCCGCCGCGGTAA-3'), and 0.25 μL of 5 U/μL ExTaq polymerase (TaKaRa Bio Inc., Shiga, Japan). The PCR reaction began with initial melting 94°C for 5 min, followed by 30 cycles of melting at 94°C for 45 sec, annealing of primers at 50°C for 45 sec, and elongation of products at 72°C for 2 min. The final elongation was carried out at 72°C for 20 min followed by cooling to 4°C. The resultant PCR products were checked for DNA fragment sizes of about 1 kbp (1000 base pairs) using gel electrophoresis and standard 1 kb ladder.

Subsequently, the PCR products were cloned into the pCR4-TOPO plasmids, which were transferred into competent OneShot Mach1 *Eserichia coli* cells as specified by the manufacturer (TOPO TA cloning kit; Invitrogen): (i) the 6 μL TOPO mixtures contained of 1 μL of PCR product, 1 μL of kit-provided salt solution, and 1 μL of TOPO vector and were incubated at room temperature for 30 min, (ii) 2 μL of the TOPO mixtures were added to *E. coli* thawed and on ice, and the mixture stirred gently was kept on ice for 30 min, (iii) heat-shock the *E. coli* cells at 40 °C for 30 sec (one plasmid is inserted into one cell) and put back on ice for 2 min, and finally (iv) 250 μL of SOC Medium was added. The 10, 30, 60, and 100 μL of medium was plated on LB agar with 50 μg/mL of Kanamycin and stored at 37 °C overnight. Isolated colonies from the plates were picked and (i) enriched in LB plus Kanamycin liquid media for 3 hours at 37 °C for deep freezing mixed with 1:1 vol. of 50% glycerol; and (ii) were added to PCR vials containing master mix A for colony PCR. Number of colonies picked from plates for colony PCR was: 48 colonies containing plasmids with the DNA representing the

methanogenic enrichments, and 96 colonies containing plasmids with the DNA extracted from the coal water.

The 25 μL of master mix A in the PCR vials contained 5 μL of 10x buffer. Initial cells lysis began at 99˚C for 15 min with a 5 min cool down to 80˚C. Nucleotides and enzymes (25 μL of master mix B contained 1 μL of 10 mM of dNTPs, 10 μM 1492r, and 10 μM 533f, and also 0.25 μL of 5 U/μL ExTaq) were then added. The procedural sequence for colony PCR was as follows: initial heating to 80˚C for 2 min, melting at 95˚C for 7 min, followed by series of annealing steps at different temperatures (2 steps at 60˚C, 2 at 58˚C, 2 at 56˚C, 2 at 54˚C, 2 at 52˚C, and 25 at 50˚C). All annealing steps were preceded by a melting step at 95˚C for 30 sec and followed by an elongation step at 72˚C for 1.5 min. The final elongation was at 72˚C for 20 min, followed by cooling down to 4˚C. Colony PCR amplified DNA products were purified using QIAquick PCR purification Kit 250 (QIAGEN) following manufacturer's manual.

6.2.7. Sequencing and phylogenetic analysis

Plasmids were sequenced at the Penn State University Biotechnology Center, using T3 and T7 primers. Partial sequences were assembled and bases manually checked using CAP application of the BioEdit software (Hall, 1999). The chimera check was performed using the Bellephoron software (Huber et al. 2004). Sequences were then submitted to the NCBI BLAST internet library to compare similarity levels to known phylotypes. All sequences were aligned using ClustalW application in the BioEdit software (Hall, 1999). Additionally, *Methanosarcina* sp., and species related to clones, i.e. species from *Methanocorpusculaceae* family, and several bacterial species were selected for tree anchoring. Phylogenetic trees were constructed in the MEGA 3.1

software (Kumar et al. 2004) using neighbor-joining method (substitution method: p-distance, bootstrap: 3000 replicate trees). The 16S rRNA gene sequences determined in this study have been assigned to GenBank accession numbers from EU168192 to EU168199 for the representative clones from the methanogenic enrichment and from EU168200 to EU168262 for all 63 clones from the filtered coal water sample.

6.2.8. Intact Polar Lipids (IPLs)

Intact polar lipids of the microbial cell membranes were extracted using a modified Bligh-Dyer extraction protocol (White and Ringelberg, 1998). The cell pellets obtained from 20 mL of the methanogenic enrichment were sonication-extracted three times with 1:2:0.8 dichloromethane (DCM):methanol:phosphate buffer (8.7 g/L KH_2PO_4, pH = 7.4) and three times with 1:2:0.8 DCM:methanol:trichloroacetic acid buffer (50 mM). Supernatants were combined to a separatory funnel where separation of organic and aqueous phases was achieved with addition of DCM and 5% NaCl in hexane pre-extracted water. The organic phase was collected and the aqueous phase was washed three times with DCM which was added to organic fraction. The pooled organic phase was dried over Na_2SO_4, and the solvent lipid extract was dried under a stream of nitrogen gas, stored at -80 °C and shipped frozen to Bremen, Germany for analysis.

The lipid components in the total lipid extract were separated according to head group polarity using high-performance liquid chromatography (HPLC) techniques described previously (Biddle et al., 2006; Sturt et al., 2004). Briefly, lipid material was dissolved in dichloromethane/methanol (1:1, v/v) and injected to a LiChrospher Diol-100 column (150 x 2.1 mm, 5 μm; Alltech GmbH, Germany) equipped with a guard column of the same packing material using a ThermoFinnigan Surveyor HPLC system

(ThermoFinnigan, Bremen, Germany). HPLC-MS experiments were performed using a ThermoFinnigan LCQ Deca XP Plus ion-trap mass spectrometer (ThermoFinnigan, Bremen, Germany) with an electrospray ionization (ESI) interface in data-dependent ion-tree mode with automatic fragmentation up to MS^3. Compound classes were identified based on characteristic molecular ions and daughter ion fragments identified previously (Koga et al., 1993; Koga et al., 1998; Sturt et al., 2004).

6.2.9. Analysis of H_2 and acetate concentrations

H_2 concentration was analyzed using a Peak Performer 1 (PP1) Gas Analyzer (Peak Laboratories, LLC, California) equipped with a Reducing Compound Photometer (RCP). Gas samples were taken from serum bottles using a gas tight syringe and diluted to a concentration less than 10 ppm for injection. Measurements on replicate samples generally have a precision of about ± 1 ppm. Measured gas-phase partial pressure values were converted to porewater concentration using solubility constants corrected for temperature and salinity (Crozier and Yamamoto, 1974).

Coal water samples for acetate concentration analysis were stored frozen until measurement. Acetate concentrations were obtained during isotopic analysis of acetate (values not reported due to very low acetate concentrations) according to published protocol (Heuer et al., 2006) using a ThermoFinnigan Surveyor HPLC coupled to a ThermoFinnigan Delta Plus XP isotope ratio mass spectrometer (irMS) via the Finnigan LC IsoLink interface. Separation of acetate was achieved on a Nucleogel Sugar 810 H column (Macherey-Nagel, Germany, 200 x 1.8 mm) equipped with a guard column CC30/4 Nucleogel Sugar 810 H (Macherey-Nagel, Germany, 30 x 4 mm). Degassed aqueous phosphate buffer (5 mM) was used as a mobile phase with a flow rate of 300

μL/min. The oxidation reagent, converting acetate to CO_2, was a solution of sodium peroxidisulfate in phosphoric acid (3 g $Na_2S_2O_8$, 10 mL H_3PO_4, 300 mL MilliQ) pumped at a flow rate of 60 to 80 μL/min. Absolute values of acetate concentration were determined relative to external calibration using peak areas of acetate-derived CO_2 signal recorded by irMS. Enrichment cultures were not tested for acetate concentrations.

6.2.10. Free energy calculations for coal bed conditions

The standard free energies $\Delta G^{\circ}_{P,T}$ of four microbial reactions potentially occurring in coals were calculated using SUPCRT92 (Johnson et al., 1992), which uses published thermodynamic data (Shock and Helgeson, 1990), for the average *in-situ* non-standard state conditions in the studied area (pressure 10.5 atm, temperature 17 ˚C; Table 1). The free energies available for microbial reactions for *in-situ* concentrations of substrates and products were calculated based on

$$\Delta G = \Delta G^o_{P,T} - RT \ln Q \text{ (1)},$$

where R - universal gas constant 8.31 $J \cdot K^{-1} \cdot mol^{-1}$, T - temperature in K, Q – reaction quotient. For the *ΔG* calculations, average *in-situ* conditions were used, i.e. salinity 3.11 g/L, pH = 8, acetate $4.3*10^{-6}$ M. Ionic strength was 0.054 M, and resulting activity coefficient γ of single charged species (Davies equation) was 0.773. The activity coefficients of gaseous species were assumed to be 1, thus their activities were equivalent to their molalities. In order to generate free energies plot presenting -15 kJ isolines, formula (1) was used, e.g. for reaction #1 (Table 1) the calculation was as follows:

$$-15kJ = -230kJ - RT \ln \frac{aCH_{4,aq}}{aHCO_3^- \cdot aH^+ \cdot aH_{2,aq}^4} \quad (2)$$

Subsequently, above equation (2) was recast for $aHCO_3^-$ as a function of $aH_{2,aq}$:

#	Microbial process	Chemical reaction	$\Delta G^\circ_{P,T}$ (kJ) 10.5 atm, 17°C	ΔG (kJ) in situ[&]
1	CO_2-reduction methanogenesis	$HCO_3^- + 4H_{2,aq} + H^+ \rightarrow CH_4 + 3H_2O$	-230.2	-19.8
2	Acetoclastic methanogenesis	$CH_3COO^- + H_2O \rightarrow CH_{4,aq} + HCO_3^-$	-14.7	-4.8
3	Homoacetogenesis	$2HCO_3^- + 4H_{2,aq} + H^+ \rightarrow CH_3COO^- + 4H_2O$	-215.6	-15.1
4	Syntrophic acetate oxidation	$CH_3COO^- + 4H_2O \rightarrow 2HCO_3^- + 4H_{2,aq} + H^+$	+215.6	+15.1

Table 1. Microbial reactions taken into consideration as potentially occurring in Indiana coal beds; chemical formulas, standard free energies, and *in-situ* free energies; [&] - calculated for average concentrations obtained for the area: H^+ 10^{-8} M, $H_{2,aq}$ $3.76 \cdot 10^{-8}$ M, CH_3COO^- $4.3 \cdot 10^{-6}$ M, $CH_{4,aq}$ $1.5 \cdot 10^{-2}$ M, and HCO_3^- $1.7 \cdot 10^{-2}$ M; the $\Delta G^\circ_{P,T}$ and ΔG represent the values for the reactions as written.

$$aHCO_3^- = \frac{aCH_{4,aq}}{e^{\frac{15-230kJ}{RT}} \cdot aH^+ \cdot H_{2,aq}^4} \quad (3)$$

The same procedure was used for calculations for reactions #2 and #4 from Table 2. The ΔG value was assigned to be -15 kJ as the minimum amount of energy that a microbial cell requires to generate ATP (Schink and Stams, 2006). For calculation of the isoline ΔG = -15 kJ for reaction #3, acetate concentration, similarly to the example above, was expressed as a function of HCO_3^- activity. The molalities of $H_{2,aq}$ and $CH_{4,aq}$ were calculated using measured pH_2 and pCH_4 in coal gas and the Bunsen solubility coefficient, dependent on temperature and salinity (Crozier and Yamamoto, 1974). The HCO_3^- activities were calculated based on water physico-chemical properties measured in the wells, and CO_2 concentration data from fresh coal core-desorption, as representative of *in-situ* values, using PHREEQC software (Parkhurst and Appelo, 1999). For calculations of the free energies for the three sampled CBM wells, the *in-situ* measured pH_2, pCO_2, pH, temperature, and salinity were used.

6.3. Results

6.3.1. Enrichments

Biweekly testing of methanogenic enrichments using GC/FID showed the presence of methane. Typically, within 24 to 72 h after inoculation of fresh media with 10 vol.% of transferred enriched culture, we observed a significant drop in pressure and increase of the CH_4 to CO_2 ratio in the headspace caused by consumption of the initial headspace gases $H_2:CO_2$ (4:1 v/v) by methanogens. CO_2-reduction methanogenesis consumes 5 moles of substrate gases (4 H_2 and 1 CO_2) to generate 1 mol of product

methane (reaction #1, Table 1). Under the microscope, ~80% cells from fourth and subsequent transfers had F420 coenzyme-fluorescence. Furthermore, morphologic homogeneity of cells observed under SEM confirmed that the culture was highly enriched and primarily one morphotype, i.e., spherical cells with a diameter of approximately 0.4 μm (Fig. 2).

6.3.2. Phylogeny of microbial community from coal and methanogenic enrichments

In the methanogenic enrichment, all clones were exclusively members of the genus *Methanocorpusculum*, with 99 to 100% similarity to *Methanocorpusculum parvum*, and slightly lower similarity to *Methanocorpusculum lubreanum* (Fig. 3). SEM imaging confirmed submicron size of cells characteristic of the *Methanocorpusculum* genus (Fig. 2). There was no clone similar to any known acetoclastic methanogens, e.g. *Methanosarcina,* suggesting the dominance of the CO_2/H_2-utilizing methanogens in these coals.

Of the 62 clones analyzed from the coal water sample, 13% were related to various bacterial groups: α-Proteobacteria, Firmicutes, Bacterioidetes, and Spirochetes (Fig. 3). The rest of the clones were Archaea, represented exclusively by close relatives (98 to 100% similarity) of *Methanocorpusculum* genus (Fig. 3). The relative abundance of archaeal and bacterial clones in our clone library does not necessarily represent the distributions of species in the environmental populations, due to well known bias of the PCR-based phylogenetic studies.

6.3.3. Distribution of intact polar lipids of the methanogenic enrichment

The IPL distribution in the methanogenic enrichment culture consist of 74% dialkyl glycerol diethers (DGDs) and 36% glycerol dialkyl glycerol tetraethers (GDGTs).
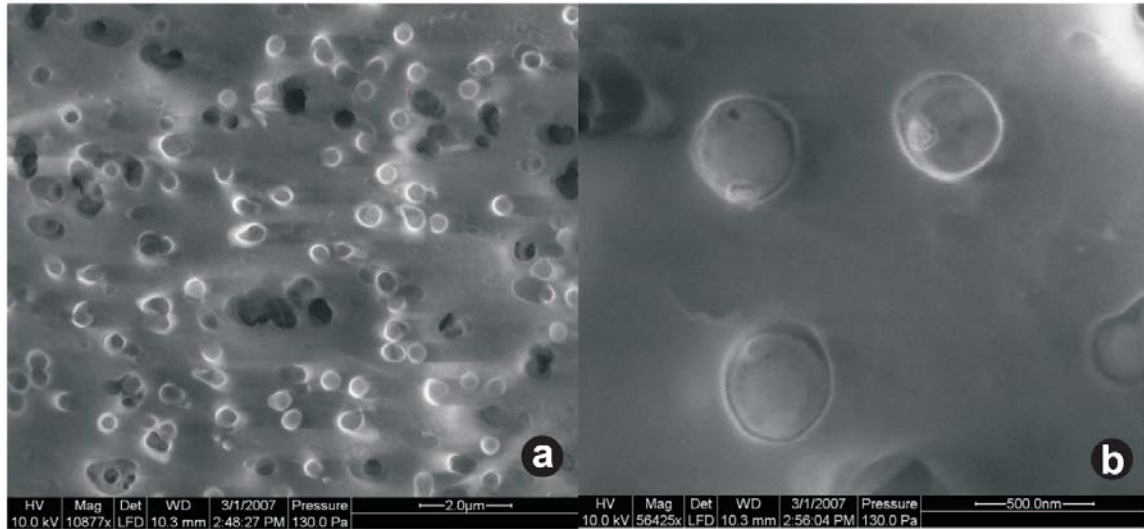
Fig. 2. SEM pictures of methanogenic enrichment filtered on a 0.22 μm membrane; a) predominantly spherical cells with diameters of ≤0.5 μm; b) close up of three typical 0.4 μm spherical cells, most likely *Methanocorpusculum parvum*.

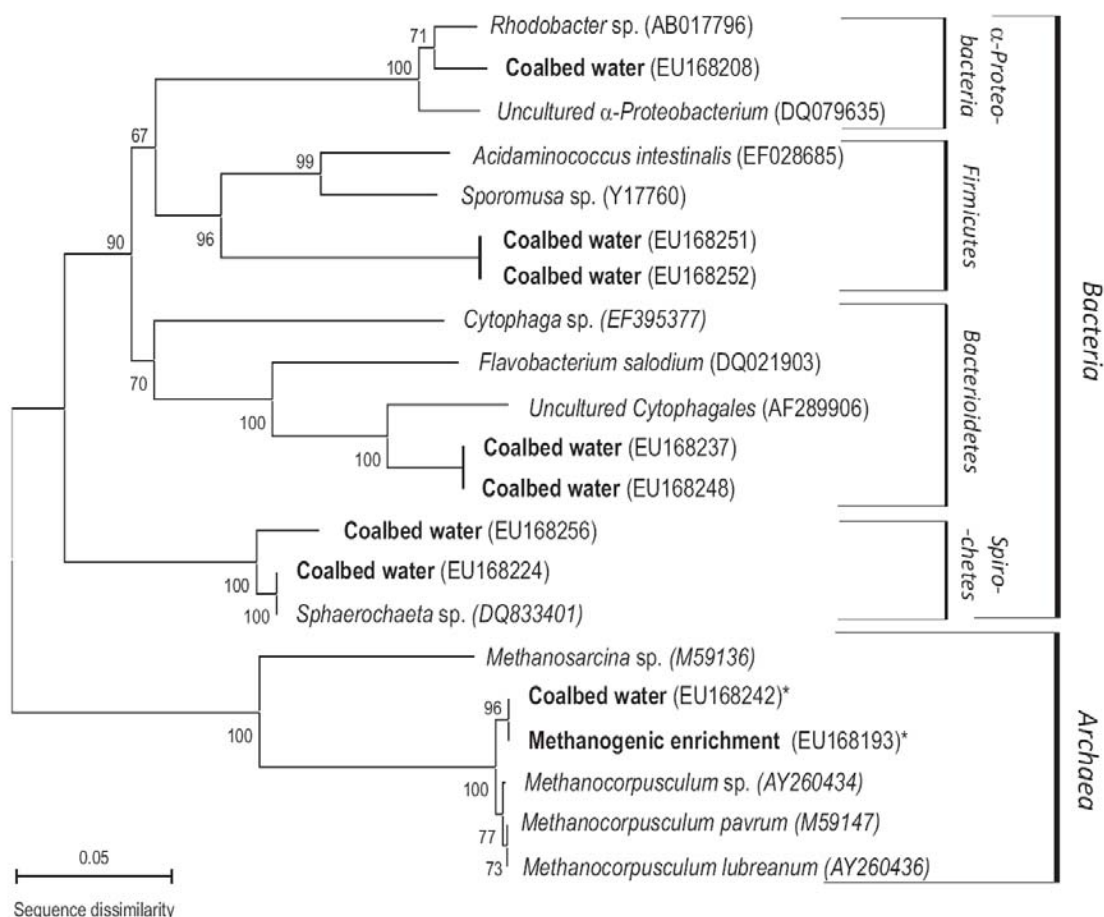Fig. 3. Microbial diversity in the coalbed waters from coal gas-producing well INS-P11, the Seelyville Coal, depth 105 m. The tree was created using neighbor joining method, substitution method: p-distance, bootstrap 3000 replicates generated using MEGA 3.1 software (32); * - among the archaeal clones, 54 coalbed water clones and all enrichment clones were almost identical, therefore each group is represented by one clone.

The main compounds forming the cell membrane of our enriched methanogen were (i) glycerol dialkyl glycerol tetraethers (GDGTs): diglycosyl-GDGT-phosphatidylglycerol* (2G-GDGT-PG*, two glycosyl head groups are attached on one side of GDGT moiety and phosphate group on the other; * - explained in the caption of Figure 4), and (ii) dialkyl glycerol diethers (DGDs): diglycosyl-hydroxyarchaeol (2G-OH-A), phosphatidylglycerol-archaeol (PG-A), and (iii) (N,N,N-trimethyl)-aminopentanetetrol (TMAPT-A*, Fig. 4). The bacterial lipids contributed to less than 1% of total intact lipids, which confirms a high purity of the enrichment.

6.4. Discussion

6.4.1. Methanogens of the Illinois Basin

The presence of methane generated by microbial CO_2-reduction in Indiana coals was implied by stable isotopic composition of CH_4 and CO_2 (Strąpoć et al., 2007). In this study, enrichments from coal waters showed high rates of methane generation and F420 epifluorescence confirmed the presence of abundant methanogens. The sub-micron (0.4 μm) cell size of methanogens, typical for *Methanocorpusculum*, was documented by SEM imaging of the enrichment culture (Fig. 2b). Clone libraries of the enrichments and environmental sample of coal water (Fig. 3) indicated dominance of one archaeal species – *Methanocorpusculum parvum*. The genetic indication of *Methanocorpusculum parvum* as the dominant methanogen is supported by the lipid composition of the cell membranes. The IPLs from the enrichment culture include all the main phospho- and glycol-lipid characteristic of *Methanocorpusculum parvum* (Koga et al., 1998), except for 2G-OH-A (Fig. 4). This combination of geochemical and biological evidence unambiguously
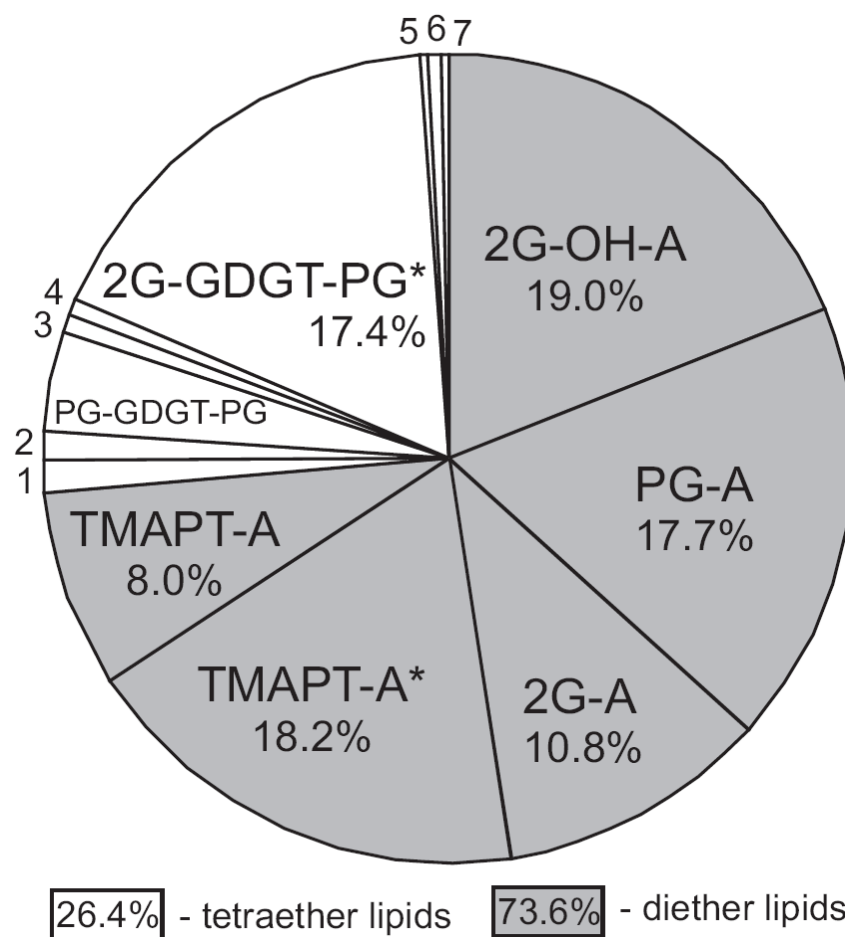
158

Fig. 4. Distribution of archaeal intact polar membrane lipids (IPLs) in the methanogenic enrichment sample dominated by close relatives of *Methanocorpusculum parvum*. GDGT – glycerol dialkyl glycerol tetraether; PG – phosphatidylglycerol; DMAPT - (N,N-dimethyl)-aminopentanetetrol; TMAPT – (N,N,N-trimethyl)-aminopentanetetrol; 1G, 2G, 3G – glycosyl (mono, di, tri); A – archaeol; * - tentatively identified derivative of the original compound (e.g. TMAPT-A) with similar fragmentation pattern and 14 *da* higher mass. [1] PG-GDGT, [2] 1G-GDGT-PG, [3] 2G-GDGT-PG, [4] 3G-GDGT-PG, [5] 2G-GDGT-DMAPT*, [6] 2G-GDGT-DMAPT, [7] PG-GDGT-DMAPT.

implicates the presence and activity of close relatives of *Methanocorpusculum parvum* in the Illinois Basin coals.

The presence of viable methanogens in coal beds has previously been indirectly observed in incubation experiments from several basins, including low volatile bituminous coal from Russia (Shumkov et al., 1999), the Rhein River brown coal from Germany (Catcheside and Ralph, 1999), and the Ruhr Basin coals in Germany (Thielemann et al., 2004). Phylogenetic studies of one sample in the latter location confirmed the presence of relatives of *Methanocalculus pumilus* (Thielemann, 2006) belonging to the *Methanomicrobiaceae* family which is closely related to the *Methanocorpusculaceae* family.

Historically, *Methanocorpusculum* was first reported as *M. aggregans* in 1985 (Ollivier et al., 1985). In 1987 *Methanocorpusculum parvum* was isolated (Zellner et al., 1987). The *Methanocorpusculuceae Family* containing five species (including *parvum),* was introduced in 1989 (Zellner et al., 1989). Subsequently, the 16S rRNA sequence of *Methanocorpusculum parvum* was submitted to the NCBI (National Center for Biotechnology Information) genomic database in 1992 (Rouviere et al., 1992), NCBI record M59147.1. Recently the complete genome of the very closely related *Methanocorpusculum lubreanum* has been sequenced and submitted to NCBI (Copeland et al., 2007). According to the current phylogenetic classification of methanogenic Archaea (Garcia et al., 2000) *Methanocorpusculum parvum* is classified as follows: *Archaea; Euryarchaeota; Methanomicrobia; Methanomicrobiales; Methanocorpusculaceae; Methanocorpusculum.* Since the initial discovery in 1987 (Zellner et al., 1987), *Methanocorpusculum parvum* has been found in an large variety of

anoxic environments, including shales in the Michigan Basin (Waldron et al., 2007), hydrothermally active sediments in the Guaymas Basin (Dhillon et al., 2005), river estuary sediments in the United Kingdom (Purdy et al., 2002), a cold polluted pond in Russia (Simankova et al., 2003), waste waters and landfills (Huang et al., 2002), animal waste storage pits (Whitehead and Cotta, 1999), and as endosymbionts of ciliates (Embley and Finlay, 1993).

Anoxia, low salinity, and temperature are common characteristics of all described *Methanocorpusculum* niches. The major limiting factors are: O_2 >2 ppm (Kiener and Leisinger, 1983), salinity expressed as chlorinity >2M (71 g/L), and SO_4^{2-} >1.0 mM (~100 mg/L). For example, in organic matter-rich shales in the Michigan Basin where there is a gradual shift towards more halophilic methanogens along a salinity gradient, *Methanocorpusculaceae* were found in large quantities only in formation waters and enrichments with lower than marine (~19 g/L) chlorinities of 0.7 to 8.1 g/L, and in smaller quantities in enrichments with chlorinities of 17.8 and 26.6 (Waldron et al., 2007). Similarly, in the estuary of the Colne River, UK, *Methanocorpusculum* was observed in fresh water and brackish sediments (<1 g/L salinity), where intense methanogenesis was also observed (Purdy et al., 2002). However, in transitions from estuarine to marine conditions, methanogenesis decreased dramatically, limited by increasing sulfate concentration and the dominance of the sulfate reduction driven oxidation of OM. Therefore, presence of methanogenesis in marine environment is typically limited to sediments below the sulfate reduction zone (SRZ) (Froelich et al., 1979). In contrast, the fresh, anoxic waters percolating in OM-rich sedimentary rocks usually lack sulfate, or any other electron acceptors, except CO_2 (Waldron et al., 2007).
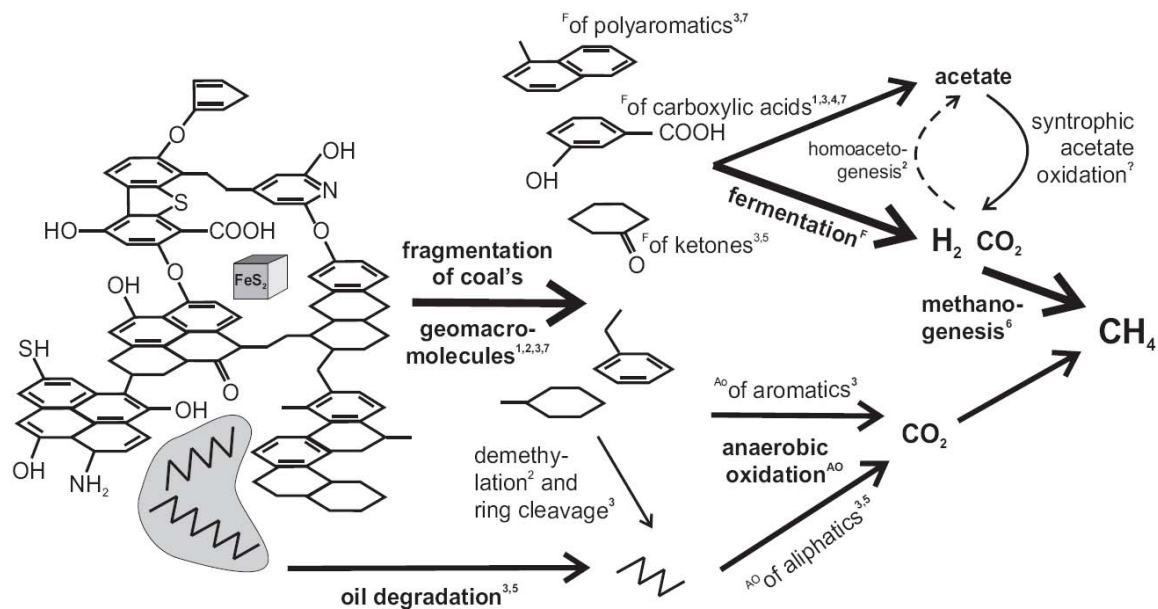
Therefore methanogenesis is not inhibited in these formations, despite chlorinities reaching up to marine concentrations. In terms of temperature, *Methanocorpusculum parvum* has been described in environments as cold as 1 to 5˚ C in a pond in the Polar Ural area, suggesting psychrotolerance although reported optimal temperature is between 25 to 35 ˚C (Simankova et al., 2003).

High temperatures (~90 ˚C) of coalification stage in ~310 million years ago most likely sterilized the Illinois Basin coals and removed the pre-burial microbial community associated with the peat bog-stage. The erosional uplift of coal beds followed by post- and interglacial dilution of the original basinal brines, typically ~70 g/L (McIntosh et al., 2002), to present day chlorinities 0.1 to 6.8 g/L and low SO_4^{2-} concentrations (typically < 20 mg/L) allowed shallow coals to be inoculated with methanogenic consortia (Fig. 1). The chemical conditions of coal water combined with *in-situ* temperatures of ~17 ˚C created a habitable niche for *Methanocorpusculum*.

6.4.2. Biodegradation of coal organic matter and production of methanogenic substrates by complex microbial consortia

If methanogenesis is the terminal step of organic matter degradation in the coal bed habitat, the penultimate step must be the production of methanogenic substrates: H_2, CO_2 and/or acetate. The diversity in the clone library suggests many possible pathways for on-going biodegradation of coal and/or oil generated from coal (Table 2), which can produce both precursor molecules (e.g. simple organic acids) as well as the actual substrates of methanogenesis (Chin and Conrad, 1995).

The main challenge in coal solubilization is first the fragmentation of the macromolecular coal structure (Fig. 5, Table 2). In the coals waters, there are clones

162

Fig. 5. Proposed mechanisms of stepwise biodegradation of organic matter in coal, annotated with microbes found in clone library and capable of performing indicated processes: (i) defragmentation of coal geomacromolecular structure predominately by fermentation targeted at oxygen-linked moieties and oxygen containing functional groups; this process detaches some of the oxygen-linked aromatic rings, generates some short organic acids; (ii) anaerobic oxidation of available aromatic and aliphatic moieties, derived from coal defragmentation or from dispersed oil present in coal in small quantities; major product of this process is CO_2; (iii) fermentation of products available from of step 1 to H_2, CO_2, and acetate; (iv) methanogenesis utilizing H_2 and CO_2 wins the competition with homoacetogenesis and generates the terminal product of OM degradation – CH_4; additionally excess of acetate may get recycled to H_2 and CO_2 by syntrophic oxidation and further fuel up methanogenesis. The brown area represents a droplet of oil. The molecular model of coal after (47). For more detailed environmental functions of listed microbes see Table 2.

163

	Species depicted on the phylogenetic tree	Environmental biodegradation targets	Potential *in-situ* degradation targets of related clones
α-Proteo-bacteria	*Rhodobacter*	petroleum related compounds, aromatics e.g. benzyl alcohol, benzoate	aromatic structure of coal, especially the oxygen bound polyaromatics
Firmi-cutes	*Sporomusa*	anaerobic homoacetogen, de-methylation of aromatic rings	competes with methanogens for H_2 and CO_2, de-methylation facilitates ring cleavage
Firmi-cutes	*Acidaminococcus*	fermentation of amino acids, generates H_2	recycling of dead cells' amino acids
Bacterio-idetes	*Flavobacterium*	petroleum related compounds	oil globules dissipated in coal
Bacterio-idetes	*Cytophaga*	fermentation of polyaromatics; petroleum	depolymerization of coal, oil globules
Spiro-chetes	*Sphaerochaeta*	plant material-derived polymers	depolymerization of coal geomacromolecules
Archaea	*Methanocorpusculum*	methanogen, utilizes H_2 and CO_2	methanogenesis, margins of the Illinois Basin

Table 2. Species related to clones from clone library of the coal water-environmental sample, their environmentally known biodegradation targets, and potential *in-situ* functions of related clones in the coal bed environment.

related to species which produce extracellular enzymes and are capable of degrading PAHs, suggesting these organisms may perform the initial steps of coal biodegradation. For example, *Bacterioidetes* including *Cytophaga* (Fig. 3) are capable of anaerobic degradation of polyaromatic and petroleum-related compounds (Haack and Breznak, 1993). Another group of microbes that could potentially thrive on solid organic matter are clones related to *Rhodobacter (α-Proteobacteria)* capable of degrading benzyl alcohol and benzoate (Shoreit and Shabeb, 1994), compounds which can be part of the oxygen-interlinked geomacromolecular structure of coal (Fig. 5). Potential fragmentation of geomacromolecules of coal could also be performed by the clones associated with *Sphaerochaeta*. Its relatives from the *Spirochetes* phylum are known as plant-polymer fermenters in bovine rumen fluids (Paster and Canale-Parola, 1982), and can also degrade higher plant-derived polymers such as xylan, pectin, and arabinogalactan. Additionally, one homoacetogen, *Sporomusa* which belongs to *Firmicutes* (found also in termites), can demethylate aromatic compounds, which is the key reaction preceding cleavage of a ring structure (Mechichi et al., 1999).

The aromatic structures of coal derived from cellulose and lignin are often interlinked by oxygen bridges and contain numerous oxygen-containing moieties (e.g. carboxyl, hydroxyl, or ketone functional groups, Fig. 5). Although Indiana high-volatile bituminous B and C coals are considered moderately mature (vitrinite reflectance R_o = 0.6%), they still contain ~8 wt. % of oxygen in the coal OM. These oxygen linkages and functional groups can be targeted by fermentation, providing essential by-products, such as succinate, propionate, acetate, CO_2, and H_2. Many clones documented in this study are closely related to known fermenters (Fig. 5, Table 2). For example, the clones related to

Cytophaga and *Flavobacterium* are known for anaerobic degradation of cellulose, proteins, and polysaccharides in methanogenic enrichments of fresh water sediments (Haack and Breznak, 1993). The relatives of *Rhodobacter* and *Sphaerochaeta* are also known for their fermentative abilities. Clones related to *Acidoaminococcus* (Fig. 3) ferment simple amino acids as a sole energy source (Rogosa, 1969). This organism can participate in the recycling of microbial biomass in the coal ecosystem.

Another target for the primary steps of biodegradation can be oil dispersed in the coal (Fig. 5, Table 2). The oil yield of Indiana coals during coalification estimated at 8 wt. %, using the relationship of Saxby, 1980 (Saxby, 1980), can be a substantial biodegradation target. Micrometer-sized oil globules have been observed in the coal under the microscope and could be accessed by microbes by well developed network of microfractures present in Indiana coals (Solano-Acosta et al., 2007). We found clones related to bacteria capable of biodegrading oil compounds, especially hydrocarbons (Fig. 3, Table 2). Additionally some of the aliphatic side chains of the aromatic coal matrix can be potentially targeted by the *n*-alkane degraders by anaerobic oxidation. The main product of anaerobic oxidation of hydrocarbons is CO_2 which may contribute to the pool of substrates for CO_2-reduction methanogenesis.

Well known participants in oil biodegradation are microbes from the *Cytophaga* and *Flavobacterium* group (Rahman et al., 2002) found to grow on *n*-hexane (Fig. 5, Table 2; 1). A detailed molecular model of anaerobic *n*-alkane and ethyl-benzene degradation has been published (Harayama et al., 2004). Another group of species found to get enriched when exposed to oil and hydrocarbons are *α-Proteobacteria* such as *Rhodobacter* (Shoreit and Shabeb, 1994).

6.4.3. Free energy balance of the terminal biodegradation processes

From the degraded coal organic matter and oil, additional fermentation reactions producing CO_2 and acetate, also deliver H_2. In the subsurface, H_2 is typically found in concentrations so low ($H_{2,aq} \sim 10^{-8}$ mol/L) that it can be considered the limiting nutrient. Fermentation is therefore an important link in the sequential biodegradation of coal. Syntrophic relationships between fermenting microorganisms and H_2-utilizing CO_2-reducing methanogens have been previously documented; the low pH_2 maintained by methanogenesis creates exergonic fermentation conditions (Schink, 1997). Syntrophic acetate oxidation to CO_2 and H_2 has also been documented in some methanogenic environments (Nüsslein et al., 2001; Schnürer et al., 1999), although our clone library contains no known acetate oxidizers.

In order to test the possible scenarios leading to terminal coal-OM biodegradation, we examined the free energy balance of several possible microbial reactions. In addition to CO_2-reduction methanogenesis, we also explored the potential role of homoacetogenesis in tandem with acetoclastic methanogenesis as the terminal OM degradation process. Since homoacetogenesis utilizes the same substrates as CO_2/H_2-utilizing methanogenesis, these two microbial reactions may compete, and the environment should promote the more energy-profitable reaction. The free energies ΔG of microbial reactions in the terminal stage of organic matter biodegradation were calculated for *in-situ* conditions of the sampled coal bed waters. The free energy calculations (Fig. 6) indicate that acetoclastic methanogenesis is energetically restricted in our coal beds. Supporting arguments are: (i) fresh water-preference of acetoclastic methanogens (Whiticar et al., 1986), and (ii) saturation of coals with methane having
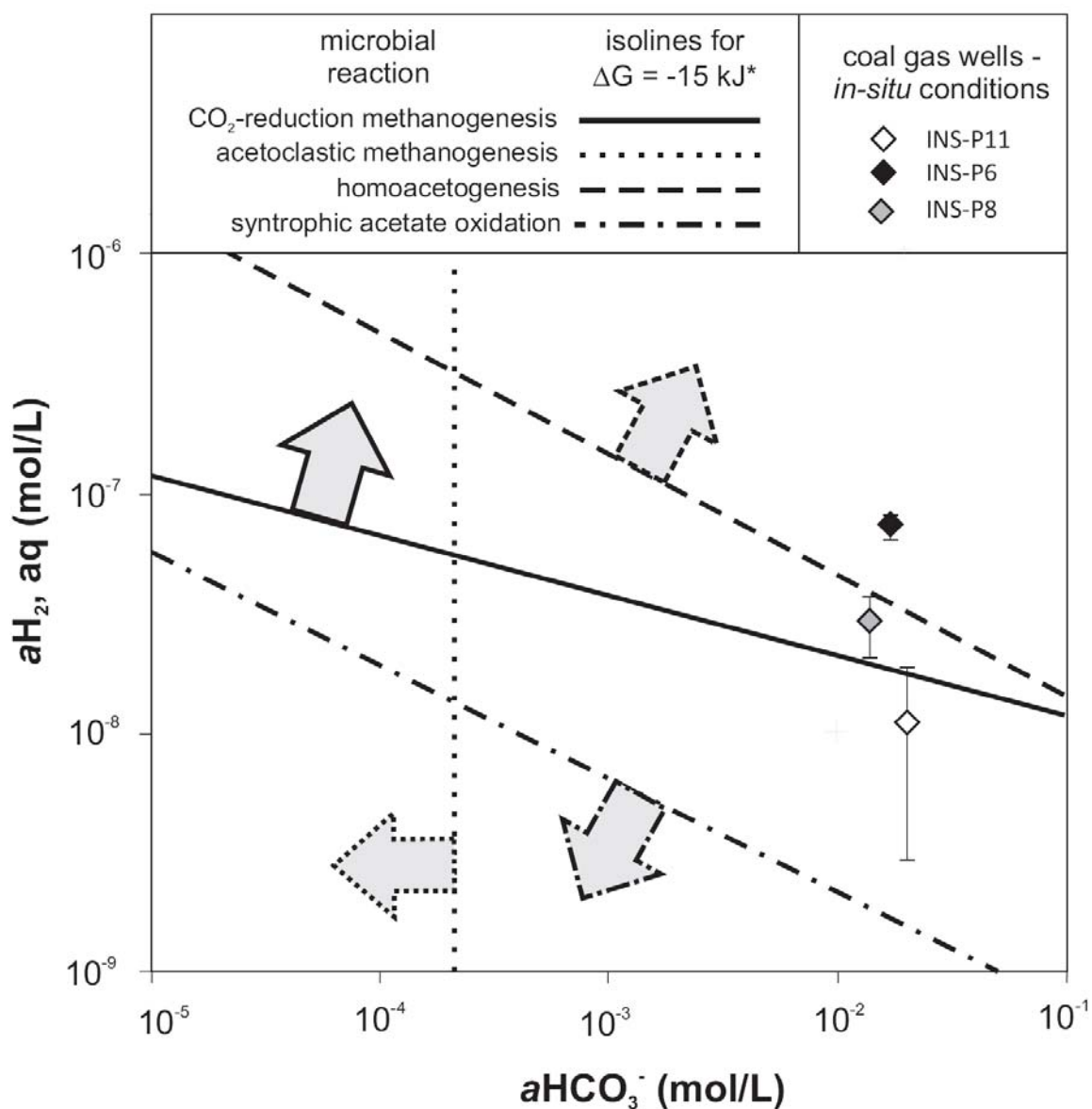
Fig. 6. Free energy dependence on the substrate and product availability of microbial reactions in average measured Indiana coals *in-situ* conditions (salinity 3.11 g/L, temperature 17˚C, pressure 10.5 atm, H^+ 10^{-8} M, $H_{2,aq}$ $3.8 \cdot 10^{-8}$ M, CH_3COO^- $4.3 \cdot 10^{-6}$ M, $CH_{4,aq}$ $1.5 \cdot 10^{-2}$ M, and HCO_3^- $1.7 \cdot 10^{-2}$ M). The data points represent *in-situ* conditions in three coal gas-producing wells within 5 km from each other. Lines represent -15 kJ of available free energy, a minimum required to generate 1 mol of ATP (50), for each microbial reaction. The arrows indicate conditions, under which given reaction will be more exergonic than the required minimum. * - based on the reactions as written (see Table 1).

isotopic fingerprints of CO_2-reduction pathway (Strąpoć et al., 2007). Conversely, the reactions of CO_2-reduction methanogenesis and homoacetogenesis are more exergonic under *in situ* conditions with energy yields more negative than -15 kJ/mol. Therefore, these two pathways may compete for the common substrates. However, free energy conditions in the coal beds promote CO_2-reducing methanogens according to the better energetic sustainability at lower CO_2 and H_2 concentrations (Fig. 6).

Processes which provide substrates for methanogenesis, H_2 and CO_2, are fermentation and anaerobic oxidation of larger organic molecules (Fig. 5). Fermentation also provides acetate (Chin and Conrad, 1995) which can be potentially microbially converted to H_2 and CO_2 via anaerobic syntrophic acetate oxidation (Table 1, reaction #4), a process found to coexist with CO_2-reduction methanogenesis in various environments, e.g. biogas reactor (Schnürer et al., 1999) and sediments of a subtropical lake in Israel (Nüsslein et al., 2001). In order for syntrophic acetate oxidation to provide the minimum of -15 kJ energy, the concentrations of H_2 and CO_2 would have to be ~ one order of magnitude lower (Fig. 6) than *in situ* conditions. Depletion of H_2 and CO_2 during intense methanogenesis and in microniches, accompanied by buildup of acetate from OM fermentation could potentially enable acetate oxidation to recycle acetate into methanogenic substrates (Figs. 5 and 6).

6.5. Summary

The Illinois Basin coals are inhabited by a complex microbial community including species capable of anaerobic degradation of a wide variety of organic molecules that can occur in coal, coal-generated oil, or coal waters, such as polymers

169

(PAHs, humic substances, plant-derived polymers), alkylated aromatic compounds, alkanes, and organic acids. The fermentative fragmentation/degradation of oxygen-containing geomacromolecules of coal, followed by fermentation and anaerobic oxidation of smaller molecules ultimately generates H_2, CO_2, and acetate. Among hypothetical acetate sinks, there is potential syntrophic acetate oxidation, providing additional H_2 and CO_2 for methanogens. Based on the microbiological enrichments, 16S rRNA clone libraries of coal water and methanogenic enrichments, and free energy calculations for in-situ coal conditions, the CO_2-reduction methanogenesis appears to be the dominant terminal step of organic matter degradation. The main methanogen in coal waters of Indiana coals, phylogenetically documented and confirmed by the intact polar lipid study, is *Methanocorpusculum parvum*. Typical characteristics of *Methanocorpusculum* were rapid growth in the H_2 and CO_2 environment, small 0.4 μm spherical cells, and 2:1 diethers to tetraethers ratio in the cell membrane. Past and ongoing biodegradation of coal and coal-derived oil followed by methanogenesis contribute to significant coalbed methane reserves along the north and eastern margins of the Illinois Basin.

References

Amouric, A., Verhé, F., Auria, R., Casalot, L., 2006. Study of a hexane-degrading consortium in a biofilter and in liquid culture: biodiversity, kinetics and characterization of degrading strains. FEMS Microbiology and Ecology 55, 239–247.

Anderson, R.T., Lovely, D.R., 2000. Anaerobic bioremediation of benzene under sulfate-reducing conditions in a petroleum-contaminated aquifer. Environmental Science and Technology 34, 2261–2266.

Bekins, B.A., Hostettler, F.D., Herkelrath, W.N., Delin, G.N., Warren, E., Essaid, H.I., 2005. Progression of methanogenic degradation of crude oil in the subsurface. Environmental Geosciences 12, 139–152.

Biddle, J.F., Lipp, J.S., Lever, M.A., Lloyd, K.G., Sørensen, K.B., Anderson, R., Fredricks, H.F., Elvert, M., Kelly, T.J., Schrag, D.P., Sogin, M.L., Brenchley, J.E., Teske, A., House, C.H., Hinrichs, K.-U., 2006. Heterotrophic Archaea dominate sedimentary subsurface ecosystems off Peru. Proceedings of the National Academy of Sciences of the USA 103, 3846-3851.

Catcheside, D.E.A., Ralph, J.P., 1999. Biological processing of coal. Applied Microbiology and Biotechnology 52, 16-24.

Chakraborty, R., O'Connor, S.M., Chan, E., Coates, J.D., 2005. Anaerobic Degradation of Benzene, Toluene, Ethylbenzene, and Xylene Compounds by *Dechloromonas* Strain RCB. Applied and Environmental Microbiology 71, 8649–8655.

Chang, B.V., Shiung, L.C., Yuan, S.Y., 2002. Anaerobic biodegradation of polycyclic aromatic hydrocarbon in soil. Chemosphere 48, 717-24.

Chapelle, F.H., O'Neill, K., Bradley, P.M., Methé, B.A., Ciufo, S.A., Knobel, L.L., and Lovley, D.R., 2002. A hydrogen-based subsurface microbial community dominated by methanogens. Nature 415, 312-315.

Chin, K.-J., Conrad, R., 1995. Intermediary metabolism in methanogenic paddy soil and the influence of temperature. FEMS Microbiology Ecology 18, 85-102.

Christensen, N., Batstone, D.J., He, Z., Angelidaki, I., Schmidt, J.E., 2004. Removal of polycyclic aromatic hydrocarbons (PAHs) from sewage sludge by anaerobic degradation. Water Science and Technology 50, 237-44.

Coates, J.D., Woodward, J., Allen, J., Philp, P., Lovley, D.R., 1997. Anaerobic Degradation of Polycyclic Aromatic Hydrocarbons and Alkanes in Petroleum-Contaminated Marine Harbor Sediments. Applied and Environmental Microbiology 63, 3589–3593.

Coates, J.D., Chakraborty, R., Lack, J.G., O'Connor, S.M., Cole, K.A., Bender, K.S., and Achenbach, L.A., 2001. Anaerobic benzene oxidation coupled to nitrate reduction in pure culture by two novel organism. Nature 411, 1039-1043.

Copeland, A., Lucas, S., Lapidus, A., Barry, K., Glavina del Rio, T., Dalin, E., Tice, H., Pitluck, S., Goltsman, E., Schmutz, J., Larimer, F., Land, M., Hauser, L., Kyrpides, N., Anderson, I., Whitman, B., Olsen, G., Woese, C., Richardson,P., 2007. Complete sequence of Methanocorpusculum labreanum Z. Submitted (26-JAN-2007) US DOE Joint Genome Institute, 2800 Mitchell Drive B100, Walnut Creek, CA 94598-1698, USA. NCBI record CP000559.

Crozier, T. E., Yamamoto, S., 1974. Solubility of hydrogen in water, seawater, and NaCl solutions. Journal of Chemical and Enggineering Data 19, 242-244.

Dhillon, A., Lever, M., Lloyd, K.G., Albert, D.B., Sogin, M.L., Teske, A., 2005. Methanogen diversity evidenced by molecular characterization of methyl coenzyme M reductase A (*mcrA*) genes in hydrothermal sediments of the Guaymas Basin. Applied and Environmental Microbiology 71, 4592–4601.

Embley, T.M., Finlay, B.J., 1993. Systematic and morphological diversity of endosymbiotic methanogens in anaerobic ciliates. Antonie van Leeuwenhoek 64, 261-271.

Fakoussa, R.M., Hofrichter, M., 1999. Biotechnology and microbiology of coal degradation. Applied Microbiology and Biotechnology 52, 25-40.

Froelich, P.N., Klinkhammer, G.P., Bender, M.L., Luedtke, N.A., Heath, G.R., Cullen, D., Dauphin, P., Hammond, D., Hartman, B., and Maynard, V., 1979. Early oxidation of organic matter in pelagic sediments of the eastern equatorial Atlantic: suboxic diagenesis. Geochimica et Cosmochimica Acta 43, 1075-1090.

Garcia, J.-L., Patel, B.K.C., Ollivier, B., 2000. Taxonomic, phylogenetic, and ecological diversity of methanogenic Archaea. Anaerobe 6, 205-226.

Haack, S.K., Breznak, J.A., 1993. *Cytophaga xylanolytica* sp. nov., a xylan-degrading, anaerobic gliding bacterium. Archives of Microbiology 159 , 6-15.

Hall, T.A., 1999. BioEdit: a user-friendly biological sequence alignment editor and analysis program for Windows 95/98/NT. Nucleic Acids Symposium Series 41, 95-98.

Harayama, S., Kasai, Y., Hara, A., 2004. Microbial communities in oil-contaminated seawater. Current Opinion in Biotechnology 15, 205–214.

Heuer, H., Elvert, M., Tille, S., Krummen, M., Prieto Mollar, X., Hmelo, L.R., Hinrichs, K.-U. 2006. Online δ^{13}C analysis of volatile fatty acids in sediment/porewarer systems by liquid chromatography-isotope ratio mass spectrometry. Limnology and Oceanography: Methods 4, 346-357.

Hostettler, F.D., 2004. Methanogenic biodegradation of n-alkanes and n-alkylated cyclohexanes and benzenes I the oil spill long-term study site at Bemidji, MN. GSA 2004 Denver Annual Meeting (November 7–10, 2004), Paper No. 248-6.

Huang, L.-N., Zhou, H., Chen, Y-.Q., Luo, S., Lan, C.-Y., Qu, L.-H., 2002. Diversity and structure of the archaeal community in the leachate of a full-scale recirculating landfill as examined by direct 16S rRNA gene sequence retrieval. FEMS Microbiology Letters 214, 235-240.

Huber, T., Faulkner, G., Hugenholtz, P., 2004. Bellerophon; a program to detect chimeric sequence alignments. Bioinformatics 20, 2317-2319.

Johnson, J.W., Oelkers, E.H., Helgeson, H.C., 1992. SUPCRT92: A software package for calculating the standard molal properties of minerals gases, aqueous species and reactions among them from 1 to 5000 bars and 0 to 1000°C. Computers & Geosciences 18, 899–947.

Jothimani, P., Kalaichelvan, G., Bhaskaran, A., Selvaseelan, D.A., Ramasamy, K., 2003. Anaerobic biodegradation of aromatic compounds. Indian Journal of Experimental Biology 41, 1046-1067.

Kiener, A., Leisinger, T., 1983. Oxygen sensitivity of methanogenic bacteria. Systematic and Applied Microbiology 4, 305-312.

Koga, Y., Nishihara, M., Morii, H., Akagawa-Matsushita, M., 1993. Ether polar lipids of methanogenic bacteria: structures, comparative aspects, and biosyntheses. Microbiological Reviews 57, 164-182.

Koga, Y., Morii, M., Akagawa-Matsushita, M., Ohga, M., 1998. Correlation of Polar Lipid Composition with 16S rRNA Phylogeny in Methanogens. Further Analysis of Lipid Component Parts. Bioscience, Biotechnology, Biochemistry 62(2), 230-236.

Kumar, S., Tamura, K., Nei, M., 2004. MEGA3: Integrated software for Molecular Evolutionary Genetics Analysis and sequence alignment. Briefings in Bioinformatics 5,150-163.

Mastalerz, M., Drobniak, A., Rupp, J., Shaffer, N., 2004. Characterization of Indiana's coal resource: availability of the reserves, physical and chemical properties of the coal, and present potential uses. Indiana Geological Survey Open-File Study 04-02, July 2004.

McIntosh, J.C., Walter, L.M., Martini, A.M., 2002. Pleistocene recharge to midcontinent basins: effects on salinity structure and microbial gas generation. Geochimica et Cosmochimica Acta 66, 1681–1700.

Mechichi, T., Labat, M., Patel, B.K.C., Woo, T.H.S., Thomas, P., Garcia, J.-L., 1999. Clostridium methoxybenzovorans sp. nov., a new aromatic o-demethylating homoacetogen from an olive mill wastewater treatment digester. International Journal of Systematic Bacteriology 49, 1201–1209.

Meckenstock, R. U., Griebler, C., Safinowski, M., 2004. Anaerobic degradation of polycyclic aromatic hydrocarbons. FEMS Microbiology Ecology 49, 27-36.

Milkov, A.V., Dzou, L., 2007. Geochemical evidence of secondary microbial methane from very slight biodegradation of undersaturated oils in a deep hot reservoir. Geology 35, 455-458.

Newberry, C.J., Webster, G., Cragg, B.A., Parkes, R.J., Weightman, A.J., 2004. Fry Diversity of prokaryotes and methanogenesis in deep subsurface sediments from the Nankai Trough, Ocean Drilling Program Leg 190. Environmental Microbiology 6, 274-287.

Nüsslein, B., Chin, K.-J., Eckert, W., Conrad, R., 2001. Evidence for anaerobic syntrophic acetate oxidation during methane production in the profundal sediment of subtropical Lake Kinneret (Israel). Environmental Microbiology 3, 460-470.

Ollivier, B. M., Mah, R. A.. Garcia, J. L., Robinson, R., 1985. Isolation and characterization of Methanogenium aggregans sp. nov. International Journal of Systematic Bacteriology 35, 127-130.

Parkhurst, D.L., Appelo, C.A.J., 1999. User's guide to PHREEQC (Version2)—A computer program forspeciation, batch-reaction, one-dimensional transport, and inversegeochemical calculations. U.S. Geological Survey, Water-Resources Investigations Report 99-4259, 310 p.

Paster, B.J., Canale-Parola, E., 1982. Physiological diversity of rumen spirochetes. Applied and Environmental Microbiology 43, 686-693.

Purdy, K.J., Munson, M.A., Nedwell, D.B., Embley, T.M., 2002. Comparison of the molecular diversity of the methanogenic community at the brackish and marine ends of a UK estuary. FEMS Microbiology Ecology 39, 17-21.

Rahman, K.S.M., Thahira-Rahman, J., Lakshmanaperumalsamy, P., Banat, I.M., 2002. Towards efficient crude oil degradation by a mixed bacterial consortium. Bioresource Technology 85, 257-261.

Rogosa, M., 1969. *Acidaminococcus* gen. n., *Acidaminococcus fermentans* sp. n., anaerobic gram-negative diplococci using amino acids as the sole energy source for growth. Journal of Bacteriology 98, 756-766.

Rouviere,P., Mandelco,L., Winker,S., Woese,C.R., 1992. A detailed phylogeny for the Methanomicrobiales. Systematic and Applied Microbiology 15, 363-371.

Saroj, K.K., Gupta, A., Srivastava, S.C., 2001. Bacterial gasification as an alternative to methane drainage and subsequent extraction of coal. Proceedings of the 6th US Mine Ventilation Symposium, May 17-22, 1997, Pittsburgh, Pennsylvania, USA.

Saxby, J.D., 1980. Atomic H/C ratios and the generation of oil from coals and kerogens. Fuel 59, 305-307.

Schink, B., 1997. Energetics of syntrophic cooperation in methanogenic degradation. Microbiology and Molecular Biology Reviews 61, 262–280.

Schink, B., Stams, A.J.M., 2006. Syntrophy among prokaryotes. In: Balows, A., Trüper, H.G., Dworkin, M., Schleifer, K.H. (Eds), The Prokaryotes, 3rd edn., Springer, New York.

Schnürer, A., Zellner, G., Svensson, B.H., 1999. Mesophilic syntrophic acetate oxidation during methane formation in biogas reactors. FEMS Microbiology Ecology 29, 249-261.

Sei, K., Sugimoto, Y., Mori, K., Maki, H., Kohno, T., 2003. Monitoring of alkane-degrading bacteria in a sea-water microcosm during crude oil degradation by polymerase chain reaction based on alkane-catabolic genes. Environmental Microbiology 5, 517–522.

Scott, C.D., Woodward, C.A., Scott, T.C., 1994. Use of chemically modified enzymes in organic solvents for conversion of coal to liquids. Catalysis Today 19, 381-394.

Shock, E.L., Helgeson, H.C., 1990. Calculation of the thermodynamic and transport properties of aqueous species at high pressures and temperatures: Standard partial molal properties of organic species. Geochimica et Cosmochimica Acta 54, 915-945.

Shoreit, A.M. and Shabeb, M.S.A., 1994. Utilizationof aromatic compounds by phototrophic purple nonsulfyr bacteria. Earth and Environmental Science 5, 71-76.

Shumkov, S., Terekhova, S., Laurinavichius, K., 1999. Effect of enclosing rocks and aeration on methanogenesis from coals. Applied Microbiology and Biotechnology 52, 99-103.

Simankova, M.V., Kotsyurbenko, O.R., Lueders, T., Nozhevnikova, A.N., Wagner, B., Conrad, R., Friedrich, M.W., 2003. Isolation and characterization of new strains of methanogens from cold terrestrial habitats. Systematic and Applied Microbiology 26, 312–318.

Solano-Acosta, W., Mastalerz, M., Schimmelmann, A., 2007. Cleats and their relation to geologic lineaments and coalbed methane potential in Pennsylvanian coals in Indiana. International Journal of Coal Geology, in press.

Strąpoć, D., Mastalerz, M., Eble, C., Schimmelmann, A., 2007. Characterization of the origin of coalbed gases in southeastern Illinois Basin by compound-specific carbon and hydrogen stable isotope ratios. Organic Geochemistry 38, 267-287.

Sturt, H.F., Summons, R.E., Smith, K.J., Elvert, M., Hinrichs, K.-U., 2004. Intact polar membrane lipids in prokaryotes and sediments deciphered by high-performance liquid chromatography/electrospray ionization multistage mass spectrometry - new biomarkers for biogeochemistry and microbial ecology. Rapid Communications in Mass Spectrometry 18, 617-628.

Thielemann, T., Cramer, B., Schippers, A., 2004. Coalbed methane in the Ruhr Basin, Germany: a renewable energy source? Organic Geochemistry 35, 1537–1549.

Thielemann, T., 2006. Microbial methane in German coal associated gas (CAG). United Nations Economc Commisions for Europe (UNECE) Ad Hoc Group of Experts on Coal Mine Methane (CMM) Geneva, 01.02.2006.

Townsend, G.T., Prince, R.C., Suflita, J.M., 2004. Anaerobic biodegradation of alicyclic constituents of gasoline and natural gas condensate by bacteria from an anoxic aquifer. FEMS Microbiology Ecology 49, 129–135.

van Bruggen, J.J.A., Stumm, C.K., Vogels, G.D., 1983. Symbiosis methanogenic bacteria and sapropelic protozoa. Archives of Microbiology 136, 89-95.

Waldron, P.J., Petsch, S.T., Martini, A.M., Nüsslein, K., 2007. Salinity constraints on subsurface archaeal diversity and methanogenesis in sedimentary rock rich in organic matter. Applied and Environmental Microbiology 73, 4171–4179.

White, D. C., Ringelberg, D.B., 1998. Signature Lipid Biomarker Analysis. In Techniques in Microbial Ecology (R. S. Burlage, R. Atlas, D. Stahl, G. Geesey, G. Sayler, Eds.), Oxford University Press, New York, NY, 255-272.

Whitehead, T.R., Cotta, M.A., 1999. Phylogenetic diversity of methanogenic archaea in swine waste storage pits. FEMS Microbiology Letters 179, 223-226.

Whiticar, M., Faber, E., Schoell, M., 1986. Biogenic methane formation in marine and freshwater environments: CO_2 reduction vs. acetate fermentation - isotope evidence. Chemical Geology 50, 693-709.

Zellner, G., Alten, C., Stackebrandt, E., Conway de Macario, E., Winter, J., 1987. Isolation and characterization of *Methanocorpusculum parvum*, gen. nov., spec. nov., a new tungsten requiring, coccoid methanogen. Archives of Microbiology 147, 13-20.

Zellner, G., Stackebrandt, E., Messner, P., Tindall, B.J., Conway de Macario, E., Kneifel, H., Sleytr, U.B., Winter, J., 1989. *Methanocorpusculaceae* fam. nov., represented by *Methanocorpusculum parvum*, *Methanocorpusculum sinense* spec. nov. and *Methanocorpusculum bavaricum* spec. nov. Archives of Microbiology 151, 381-90.

Zengler, K., Richnow, H.H., Â-Mora, R.R., Michaelis, W., Widdel, F., 1999. Methane formation from long-chain alkanes by anaerobic microorganisms. Nature 401, 266-269.

CHAPTER 7

Summary

7.1. Variability of total gas and its geochemical properties

Accurate assessment of the coalbed methane (CBM) potential and gas saturation level of a coal bed requires investigation across the entire thickness of a coal seam, because total gas content can vary significantly vertically through seams. The total coalbed gas content in the Indiana part of the Illinois Basin is controlled by the amount of generated, adsorbed and preserved microbial methane, and therefore can be locally variable depending on (i) microbial accessibility (via cleats and microfractures), (ii) adsorption potential for methane molecules (micropore distribution) of a particular coal section, and (iii) availability of target organic moieties for potential biodegradation and methanogenesis.

The chemical composition of desorbing coal gas changes over the duration of desorption because different coal gas species express different adsorption affinities in the micropores of coal. CO_2 has a higher adsorption affinity than methane, causing early desorbed gas to be relatively enriched in methane, whereas late desorbed gas is relatively enriched in CO_2.

Kinetic isotope effects cause ^{13}C-depletion of free methane and CO_2 relative to adsorbed gas species during desorption of coal gases in canisters. Observed fractionations are likely caused by faster diffusion of ^{12}C-containing gas species relative to $^{13}CH_4$ and $^{13}CO_2$. Amplitudes of $\delta^{13}C$ shifts over the duration of desorption are probably linked to the pore structure of coal, which is controlled by maceral composition, maturity, in-situ stress, etc. A linear relationship exists between $\delta^{13}C_{CH4}$ and the volume of desorbed CH_4 as a fraction of total CBM. Thus, isotopically representative sampling of desorbed CBM for carbon-isotopic analysis should be performed for a gas sample that is collected after

about half of all gas has been desorbed and vented/removed (i.e., gas from the ~50 vol. % midpoint of gas desorption).

Assuming regionally uniform pre-CBM-production coalbed gas compositions, prolonged CBM production from monitored wells caused molecular and isotopic trends in production gases of (i) increasing $C_1/(C_2+C_3)$ ratios, (ii) decreasing $\delta^{13}C_{CH4}$ values, and (iii) decreasing total dissolved solids (TDS) values. Furthermore, prolonged CBM production may enhance access of fresh oxygenated meteoric waters into relatively shallow coal seams resulting in microbial methane oxidation. Changes in mentioned above parameters (i, ii, and iii) during production from a CBM well should not affect the production of coal gas significantly. From a scientific point of view, increasing oxidative conditions of the well in a depression cone of the ground water table may inhibit further anaerobic biodegradation of coal and methanogenesis.

7.2. Coal gas origin

Stratigraphically equivalent and geographically widespread coal beds (e.g., the Springfield and Seelyville Coal Members) in Indiana and western Kentucky can regionally generate and store coalbed gases of contrasting and distinct origins. Biogenic methane from CO_2-reduction is prevalent in less mature Indiana coals, whereas more mature coals in the Rough Creek Graben of western Kentucky produced predominantly thermogenic hydrocarbons via cracking of coal organic matter. The two differently sourced biogenic and thermogenic types of coalbed gases are compositionally and isotopically distinct.

179

The two sources of coalbed gases in the Illinois Basin, thermogenic and biogenic, are controlled by a variety of factors: (i) the geologic regional history (e.g., tectonic and hydrothermal activity, burial depth, geothermal gradient, intensity of maturation/coalification, erosional or post-glacial uplift and fracture opening); (ii) hydrogeology (e.g., infiltration of meteoric water, residence time of formation water); (iii) microbiology (e.g., presence of a microbial community able to thrive on decomposing coal, probably primarily vitrinite; habitability of coals in terms of temperature, pore structure, moisture content, salinity of pore waters).

7.3. Microbial biodegradation of organic matter in coal

Significant influxes of fresh water during inter- and post-glacial periods caused decreasing salinity of the original basinal brines and allowed inoculation of coal with a complex microbial community. Microbial biodegradation of coal organic matter and associated methanogenesis resulted in the accumulation of significant coalbed methane reserves along the margin of the Illinois Basin. The microbial community was transported by ice sheet melt waters most likely from shallow anoxic subsurface sediments, e.g. swamps, pond and lake sediments.

The Illinois Basin coals are inhabited by a complex microbial community including species capable of anaerobic degradation of a wide variety of organic molecules that can occur in coal, coal-generated oil, or coal waters, such as biopolymers (e.g., plant-derived cellulose and lignin), geomacromolecules (e.g., humic substances), polyaromatic hydrocarbons (PAHs), alkylated aromatic compounds, alkanes, and organic acids. The fermentative fragmentation/degradation of oxygen-containing macromolecules

of coal, followed by fermentation and anaerobic oxidation of smaller molecules ultimately generates H_2, CO_2, and acetate. Among hypothetical acetate sinks, there is potential of syntrophic acetate oxidation, providing additional H_2 and CO_2 for methanogens. Based on the microbiological enrichments, 16S rRNA clone libraries of coal water and methanogenic enrichments, and free energy calculations for in-situ coal conditions, the CO_2-reduction methanogenesis appears to be the dominant terminal step of organic matter degradation. Microbial biodegradation also affects thermogenic C_{2+} hydrocarbon gases in coal beds, preferentially targets C_3, and introduces isotope fractionation whereby remaining C_3 is enriched in heavy isotopes D and ^{13}C.

The main methanogen phylogenetically documented in coal waters and enrichments was *Methanocorpusculum parvum* utilizing H_2 and CO_2. Typical characteristics of *Methanocorpusculum* were rapid growth in the H_2 and CO_2 environment, small 0.4 μm spherical cells, and 2:1 diethers to tetraethers ratio in the cell membrane.

The inhibiting parameters for microbial biodegradation of coal and methanogenesis includes (i) excess of other than CO_2 electron acceptors (i.e. sulfate, nitrate) which may turn on the microbial anaerobic OM oxidation and inhibit methanogenesis, (ii) dissolved oxygen, (iii) lack of basic nutrients required to sustain any microbial life (i.e. phosphorus and nitrogen).

7.4. Timing of microbial methane generation

Two main alternative scenarios of microbial methane generation in the Illinois Basin coals can be considered. First, that swamp peat-derived coal and microbiota
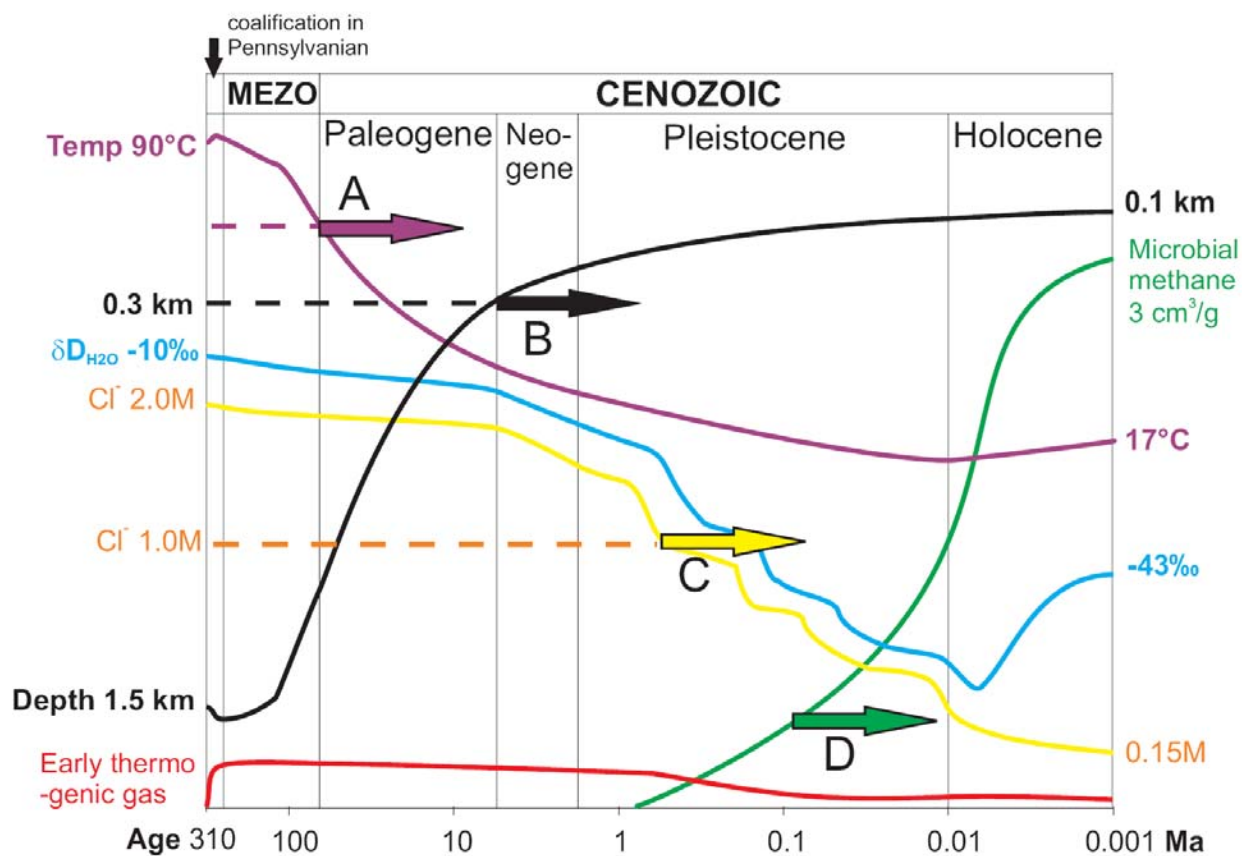
Fig. 1. Model of the geological history of coal beds in the Indiana part of the Illinois Basin in terms of environmental parameters that are important for subsurface micro biota. Initial sterilization of coal occurred at 90 ˚C when small amounts of thermogenic gas were generated (red line); at the same time, about 8 wt.% oil were generated that remained dispersed in coal. A – a temperature below 60 ˚C was a necessary but insufficient requirement for microbial life. B – a relatively shallow depth of 0.3 km allowed slow access of meteoric water. C – inter/post glacial fresh water influx diluted coalbed brines to chlorinities that were tolerable for microbes. D – onset of biodegradation of early thermogenic C_{2+} hydrocarbons, coal-derived oil, and coal organic matter; biodegradation was associated with microbial methanogenesis.

coexisted since Pennsylvanian time in the subsurface allowing extremely slow rates of methanogenesis by microbes and long-term gas accumulation. The second scenario suggests post-glacial uplift and inoculation of coals via meteoric waters that infiltrated coal beds and diluted brines during inter- and post-glacial intervals. Coalification temperatures of southeastern Illinois Basin coals reached about 90 ˚C and were too high for the preservation of the original peat-swamp microbiota. Furthermore, highly saline waters (~2M Cl⁻) in Pennsylvanian coal formations probably exceeded the halotolerance of many of the representatives of the complex organic matter-degrading methanogenic consortium, e.g. *Methanocorpusculum* does not tolerate chlorinities higher than 1M. The modern (Holocene) isotopic characteristics of waters associated with Indiana coal beds also suggest that the residence time of water is less than 10,000 years (Fig. 1).

The following is the more plausible and preferred scenario: the dilution of original basinal brines with meteoric waters during post-uplift and inter/post-glacial Pleistocene time (1.8 million years ago until present) caused inoculation of coals with methanogenic consortia and triggered the generation of significant amounts of coalbed methane. In can be concluded that shallow and highly permeable formations, like coals or fractured shales with diluted brines, can host complex microbial consortia capable of efficient biodegradation and gas generation, whereas deeper strata are more likely to exclude microbes. Even if access to microbes was granted for deeper environments, they often express inhospitable conditions for microbiota in terms of salinity and temperature.

7.5. Significance and applications of this study

This study provides data and discusses concepts important for exploration and production of CBM, with special relevance for basins with contributions of microbial methane. In exploration for thermogenic CBM, the main factor is adequate maturity of coal ($R_o > 0.8\%$). For microbial biodegradation and methanogenesis, maturity of coal is not a limiting factor. However, immature coals can be more biodegradable because of higher functional groups and oxygen content. Yet, regardless of the maturity, coals that are uplifted enough to lower the temperature and to receive fresh water influxes can become a habitable niche for complex microbial community which would most likely generate methane as a terminal product. From an exploration point of view, an optimal CBM basin would most likely contain coals which: (i) reached the thermal maturity within the gas window (0.7 to 1.4%) so that it generated significant amount of thermogenic gas and still are relatively highly biodegradable; and (ii) subsequently were subjected to contact with fresh waters (e.g. by erosional or tectonic uplift, or topography and/or stratigraphy-driven flow regime) which diluted brine and delivered microbial consortia, inducing the additional generation of microbial methane. An example of such coal is the Fruitland Formation in the San Juan Basin (maturity range R_o 0.6 to 1.3%), where topography-driven hydrodynamic pressure diluted brines and inoculated coals at depths of up to 1 km, and charged an already thermogenic coal gas-rich formation with microbial methane. A similar scenario is likely in some Alberta Basin coals.

In the eastern part of the Illinois Basin, current subsurface conditions, temperature < 60°C, salinity < 35 g/L, contact with ground waters, which can dilute the original formation brines and transport the microbial consortia into coals, etc., are

suitable for biodegradation of coal by complex microbial community accompanied by methanogenesis. Present day methanogenic microbial activity in studied coal beds can classify microbial CBM as a renewable energy supply. Simple calculation shows that only 0.2 wt.% of studied coal has been converted into methane so far. Despite unknown *in-situ* rates of coal biodegradation steps and of the methanogenesis itself, potential enhancement of microbial CBM generation could increase the *in-situ* rate of conversion of coal into methane and allow prolonged CBM production over long periods of time.

7.6. Future paths of inquiry

Future research on coal gases in the Illinois Basin should focus on deciphering sequential biodegradation of coal and coal-derived oil by complex microbial communities. For example, one could target a series of incubations and enrichments with various substrates, followed by isolations of specific strains of microbes. Incorporation of fluorescent in-situ hybridization techniques should clarify the functionality of specific groups of microorganisms. In terms of better understanding of geological framework and timing of initiation of microbial gas generation, radioisotope techniques could be applied for dating of the age of coal waters, e.g. by iridium dating. Further studies of the distribution of thermogenic and microbial gas in Illinois Basin coals on a basinwide scale should target different areas: (i) locations closer to the depocenter in Illinois where it is likely that the thermogenic gas component is more prominent and microbes may have had limited opportunity to access coal and generate biogenic CBM; (ii) areas in southern Indiana and northern Kentucky, where relatively shallow depths and proximity to the Rough Creek Graben zone could have resulted in significant generation of both microbial

methane and thermogenic gas, thus making this area a strong candidate for CBM exploration. Continued monitoring of the studied CBM-production field in Indiana should yield insightful data for understanding the isotopic fingerprints of reservoir depletion and continuing production. In addition, further studies on isotopic and molecular effects of gas diffusion, migration, and substitution (e.g. CO_2 replacement by CH_4 at adsorption sites in coal) should yield important constraints for CO_2 sequestration projects (e.g. monitoring wells).

Dariusz Strąpoć

Curriculum Vitae

Department of Geological Sciences
Indiana University
1001E 10th Street
Bloomington, IN 47405

Tel: (812) 856-4560
Fax: (812) 855-7899
dstrapoc@indiana.edu

EDUCATION

Jan 2003-present	**Indiana University, Bloomington**
	Geology major (coalbed gases, shale gas, geochemistry, GC/MS, stable isotopes), Microbiology minor (microbial community in coal beds, culturing, phylogeny); GPA 3.808 Ph.D. October 2007
Oct 2000-Jun 2002	**Wroclaw University, Poland**
	M.Sc. Geology (Stable isotope geochemistry of plant material and ground water related to SO_2 pollution)
Oct 1998-Sep 2000	**Wroclaw University, Poland**
	B.Sc. Geology (Methods in mantle rocks petrology)
Oct 1996-Feb 1998	**Wroclaw University, Poland**
	Three semesters of Astronomy completed

RESEARCH EXPERIENCE

Jan 2003-present	**Coalbed gases** and **shale gases** in Illinois basin, compositional/isotopic analyses (GC/MS), combined with study of associated waters and phylogenetic study of **microbial community**, coal petrography, adsorption properties, fractures, gas origin assessment, timing of microbial gas generation
Jun 2003-Jan 2005	**Iron oxidizing microbial community** in Fe^{2+}-rich creek, Bloomington, IN, isotopic study
Oct 2000-Jun 2002	**Spruce needles** and ground waters in Polish mountains in context of SO_2 pollution, isotopic study

PUBLICATIONS

Strąpoć, D., Picardal, F., Schaperdoth, I., Macalady, J., Turich, C., Mastalerz, M., Arndt Schimmelmann[1], 2007. An analysis of the methane-producing microbial community in a coal of the Illinois Basin. *Applied and Environmental Microbiology,* in press.

Strąpoć, D., Mastalerz, M., Drobniak, A., Schimmelmann, A., 2007. Variability of geochemical properties in a microbially-dominated coalbed gas system from the eastern margin of the Illinois Basin. *International Journal of Coal Geology*, in press.

Henning, M.J., **Strąpoć, D.**, Lis, G., Sauer, P., Fong, J., Schimmelmann, A., Pratt, L.D., 2007. Versatile inlet system for on-line compound-specific δD and δ^{13}C GC-c/pyr-IRMS analysis of gaseous mixtures. *Rapid Communications in Mass Spectrometry*, 21, 2269-2272.

Strąpoć, D., Mastalerz, M., Eble, C., Schimmelmann, A., 2007. Characterization of the origin of coalbed gases in southeastern Illinois Basin by compound-specific carbon and hydrogen stable isotope ratios. *Organic Geochemistry* 38, 267-287.

Strąpoć, D., Schimmelmann, A., Mastalerz, M., 2006. Carbon isotopic fractionation of CH_4 and CO_2 during canister desorption of coal. *Organic Geochemistry* 37, 152-164.

Solano-Acosta, W., Mastalerz, M., Rupp, J.A., **Strąpoć, D.**, Schimmelmann, A., 2005. Coal-bed gas potential in Pennsylvanian coal beds of Indiana. Proceedings of the *2005 International Coalbed Methane Symposium*, Tuscaloosa, Alabama, May 2005, Paper No. 0526. CD Edition.

Kaluzny, A., Jedrysek, M.O., **Strąpoć, D.**, 2003. Stable isotope geochemistry of organic and inorganic sulphur in spruce needles (SW Poland, Karkonosze MTS.). *Mineralogical Society of Poland* – Special Papers, vol. 22.

PUBLICATIONS IN PREPARATION

Górka, M., Jędrysek, M.O., **Strąpoć, D.**, 2007. Isotopic composition of precipitation sulphates as an indicator of pollutant origin in Wrocław (SW Poland) precipitations. Intended for the *Isotopes in Environmental and Health Studies.*

Strąpoć, D., Mastalerz, M., Drobniak, A., Schimmelmann, A., 2007. Characterization of shale gas potential of New Albany and Maquoketa shales, Illinois Basin. Intended for the *International Journal of Coal Geology.*

INVITED TALKS

Strąpoć, D., Mastalerz, M., Schimmelmann, A., Eble, C., Rupp, J., 2007. Compound-specific carbon and hydrogen stable isotope ratios of coalbed gases in southeastern part of the Illinois Basin. Eastern Section AAPG, September 2007, Lexington, Kentucky.

Coalbed gas, shale gas, and CO_2-sequestration in the eastern part of the Illinois Basin. **ConocoPhillips, Houston**, April 2007.

Coalbed gas in Illinois Basin: Geochemical, hydrogeological, and microbiological study. DFG-Research Center Ocean Margins, **University of Bremen, Germany**, October 2006.

Coalbed gas, shale gas, and CO_2-sequestration in Illinois Basin: Geochemical, hydrogeological, and microbiological study. **Shell, Rijkswijk, Netherlands**, October 2006.

Compositional and isotopic characterization of coalbed gases and associated waters in the Illinois Basin, Indiana. **GRC (Gordon Research Conference), New Hampshire, USA**, August 2006.

CONFERENCE PRESENTATIONS

Henning, M., **Strąpoć, D**., Sauer, P., Fong, J., Schimmelmann, A., Mastalerz, M., 2007. Flexible inlet system for on-line compound-specific δD and $\delta^{13}C$ analyses of natural gases. IX **ESIR** Meeting, Cluj, Romania, June 2007.

Strąpoć, D., Schimmelmann, A., Mastalerz, M., 2005. Microbially-derived methane in coalbed gases: compound-specific carbon-isotopic study of coalbed gases from the Illinois Basin, USA. VIII **ESIR** Meeting, Leipzig, June 2005.

Strąpoć, D., Mastalerz, M., Schimmelmann, A., Eble, C., 2005. Biogenic and thermogenic coalbed gas in the Illinois Basin: insight from compound-specific carbon isotopic ratios. **IMOG** (International Meeting on Organic Geochemistry), Seville, Spain, September 2005. **<selected for talk as one of 80 out of 500 submitted abstracts>**

Strąpoć, D., Mastalerz, M., Schimmelmann, A., 2004. Carbon and hydrogen isotopic signatures of coalbed gases from Indiana: methodological and genetic implications. **GSA** (Geological Society of America) Annual Meeting, Denver, November, 2004.

CONFERENCE PRESENTATIONS, CO-AUTHORED

Ochmanski, T., Strąpoć, D., Moore, C., Sarkar, A., 2007. Isotopic signatures of Llandoverian open marine beded cherts from Bardo Syncline, Holy Cross Mountains, Central Poland, Preliminary results. IX **ESIR** Meeting, Cluj, Romania, June 2007.

Gorka, M., Jedrysek, M.-O., Strąpoć, D., 2007. Isotopic composition of precipitation sulphates as an indicator of pollutant origin in Wroclaw (SW Poland) precipitations. IX **ESIR** Meeting, Cluj, Romania, June 2007.

Mastalerz, M., Drobniak, A., Strąpoć, D., Solano-Acosta. W., Rupp, J., 2006. Variations in coal properties in high volatile bituminous coals; Implications for coalbed gas content. **TSOP** (Society for Organic Petrology) meeting, Beijing, China, September, 2006.

Mastalerz, M., Drobniak, A., Rupp, J., Strąpoć, D., 2005. Influence of petrographic composition of coal on desorption and adsorption capacity of carbon dioxide and methane; Examples from Indiana, USA. **ICCP** (International Committee for Coal and Organic Petrology) meeting, Patras, Greece, September 2005.

Mastalerz, M., Strąpoć, D., Schimmelmann, A., 2005. Isotopic signatures of coalbed gases from high volatile bituminous coals and associated roof lithologies in Indiana, Illinois Basin. Coalbed methane: Back to Basics of Coal Geology, 2005 **Gussow Geoscience Conference**, Canmore, Alberta, March 2005.

CONFERENCE POSTERS

Strąpoć, D., Picardal, F., Lin, Y.-S., Hinrichs, K.-U., Schaperdoth, I., Macalady, J., Turich, C., Freeman, K., Mastalerz, M., Schimmelmann, A., 2007. Microbial coalbed methane in the Illinois Basin: substrate competition of the genetic pathways. **IMOG**, Torque, England, September 2007. **<ranked 105th out of 550 submitted abstracts>**

Strąpoć, D., Picardal, F., Schaperdoth, I., Macalady, J., Turich, C., Mastalerz. M., Schimmelmann, A., 2007. Coalbed methane-producing microbial community in the Illinois Basin. The annual **ASM** (American Society for Microbiology) Conference, Toronto, Canada, May 2007.

Strąpoć, D., Mastalerz. M., Eble, C., **Schimmelmann, A.**, 2006. Compound-specific carbon and hydrogen stable isotope ratios of coalbed gases in southeastern Illinois Basin. **AAPG** (Association of American Petroleum Geologists), Perth, Australia, Novemebr 2006.

Strąpoć, D., Schimmelmann A, Mastalerz M., 2005. Carbon isotope fractionation of methane and CO_2 during coalbed gas desorption from coal, Illinois Basin, USA. VIII **ESIR** Meeting, Leipzig, June 2005. **<Best Poster Award for Young Scientists>**

Strąpoć, D., Beard, B., Schieber, J., 2005. What can the fingerprint of a primitive bacteria look like? A carbon and iron stable isotopic study of an iron-oxidizing bacterial community. 36th **LPSC** (Lunar and Planetary Science Conference), Houston, Texas, March, 2005.

Strąpoć, D., Schieber J, 2004. Carbon isotope characteristics of iron-oxidizing bacterial mats, Jackson Creek, Bloomington, IN, USA. VII ESIR Meeting, Graz, June 2004.

Strąpoć, D., Schieber J., 2004. Carbon Isotope Characteristics of Spring-fed Iron-precipitating Microbial Mats. 35th **LPSC**, Houston, Texas, March, 2004

SHORT COURSES

Sep 2007	**Oil biodegradation** (IMOG, 2007)
Oct 2004	**Core description** (Indiana Geological Survey)
Mar 2003	**Landmark's Stratworks** software (Indiana University)

HONORS

Jun 2007	Elected to the **Advisory Board of the European Society for Isotope Research (ESIR)**
Apr 2007	**The Graduate Student Research Grant, GSA**
Apr 2007	**The Outstanding Academic Achievement Award, Estwing Award**, Department of Geological Sciences, Indiana University
Apr 2007	**The Energy and Minerals Grant** Grants-in-Aid, **AAPG**
Mar 2007	**Best Graduate Poster Award**, Indiana University, Department of Geological Sciences, Research Day and Job Expo
Jan 2006	Selected as one of 10 students from United States outside of Arizona to participate in the **LAPLACE Astrobiology** Winter School, Tucson, Arizona
Jun 2005	**Best Poster Award** for Young Scientists, European Society for Isotope Research (**ESIR**) VIII meeting, Leipzig, Germany

EDITORIAL WORK

Reviewed two papers for *Applied Geochemistry*
Translated papers from Polish to English for Psychology Dept., IU

AFFILIATIONS

since April 2007	**American Society for Microbiology (ASM)**
since May 2006	**Sigma Psi**
since Feb 2005	**Indiana Soccer League (Referee)**
since Oct 2004	**Geological Society of America (GSA)**
since Aug 2004	**European Society for Isotope Research (ESIR), on the Advisory Board since June 2007**
since Sep 2003	**Bloomington International Futbol Club**
since 1995	**Mars Society**

LANGUAGES

Polish (native)
English (proficient)
Russian (good)

REFERENCES

Maria Mastalerz, Ph.D.
Indiana Geological Survey
Indiana University, Bloomington, IN, USA
mmastale@indiana.edu

Arndt Schimmelmann, Ph.D.
Department of Geological Sciences
Indiana University, Bloomington, IN, USA
aschimme@indiana.edu

Flynn Picardal, Ph.D.
School of Public and Environmental Affairs
Indiana University, Bloomington, IN, USA
picardal@indiana.edu

Mariusz Orion Jędrysek, Ph.D.
Department of Geological Sciences
Wrocław University, Wrocław, POLAND
morion@ing.uni.wroc.pl